



700
2016

Berichte

zur Polar- und Meeresforschung

Reports on Polar and Marine Research

The Expedition PS96 of the Research Vessel POLARSTERN to the southern Weddell Sea in 2015/2016

Edited by

Michael Schröder

with contributions of the participants

Die Berichte zur Polar- und Meeresforschung werden vom Alfred-Wegener-Institut, Helmholtz-Zentrum für Polar- und Meeresforschung (AWI) in Bremerhaven, Deutschland, in Fortsetzung der vormaligen Berichte zur Polarforschung herausgegeben. Sie erscheinen in unregelmäßiger Abfolge.

Die Berichte zur Polar- und Meeresforschung enthalten Darstellungen und Ergebnisse der vom AWI selbst oder mit seiner Unterstützung durchgeführten Forschungsarbeiten in den Polargebieten und in den Meeren.

Die Publikationen umfassen Expeditionsberichte der vom AWI betriebenen Schiffe, Flugzeuge und Stationen, Forschungsergebnisse (inkl. Dissertationen) des Instituts und des Archivs für deutsche Polarforschung, sowie Abstracts und Proceedings von nationalen und internationalen Tagungen und Workshops des AWI.

Die Beiträge geben nicht notwendigerweise die Auffassung des AWI wider.

Herausgeber

Dr. Horst Bornemann

Redaktionelle Bearbeitung und Layout

Birgit Reimann

Alfred-Wegener-Institut
Helmholtz-Zentrum für Polar- und Meeresforschung
Am Handeshafen 12
27570 Bremerhaven
Germany

www.awi.de

www.reports.awi.de

Der Erstautor bzw. herausgebende Autor eines Bandes der Berichte zur Polar- und Meeresforschung versichert, dass er über alle Rechte am Werk verfügt und überträgt sämtliche Rechte auch im Namen seiner Koautoren an das AWI. Ein einfaches Nutzungsrecht verbleibt, wenn nicht anders angegeben, beim Autor (bei den Autoren). Das AWI beansprucht die Publikation der eingereichten Manuskripte über sein Repository ePIC (electronic Publication Information Center, s. Innenseite am Rückdeckel) mit optionalem print-on-demand.

The Reports on Polar and Marine Research are issued by the Alfred Wegener Institute, Helmholtz Centre for Polar and Marine Research (AWI) in Bremerhaven, Germany, succeeding the former Reports on Polar Research. They are published at irregular intervals.

The Reports on Polar and Marine Research contain presentations and results of research activities in polar regions and in the seas either carried out by the AWI or with its support.

Publications comprise expedition reports of the ships, aircrafts, and stations operated by the AWI, research results (incl. dissertations) of the Institute and the Archiv für deutsche Polarforschung, as well as abstracts and proceedings of national and international conferences and workshops of the AWI.

The papers contained in the Reports do not necessarily reflect the opinion of the AWI.

Editor

Dr. Horst Bornemann

Editorial editing and layout

Birgit Reimann

Alfred-Wegener-Institut
Helmholtz-Zentrum für Polar- und Meeresforschung
Am Handeshafen 12
27570 Bremerhaven
Germany

www.awi.de

www.reports.awi.de

The first or editing author of an issue of Reports on Polar and Marine Research ensures that he possesses all rights of the opus, and transfers all rights to the AWI, including those associated with the co-authors. The non-exclusive right of use (einfaches Nutzungsrecht) remains with the author unless stated otherwise. The AWI reserves the right to publish the submitted articles in its repository ePIC (electronic Publication Information Center, see inside page of verso) with the option to "print-on-demand".

*Titel: Polarstern beim Entladen an der Festeiskante vor dem Ronne Depot
(76°47'S, 52°29'W, 11.01.- 14.01. 2016). Foto: Michael Schröder, AWI*

*Cover : Polarstern at the fast ice landing point in front of the Ronne depot
(76°47'S, 52°29'W, 11.01.- 14.01. 2016). Photo: Michael Schröder, AWI*

The Expedition PS96 of the Research Vessel POLARSTERN to the southern Weddell Sea in 2015/2016

Edited by

Michael Schröder

with contributions of the participants

Please cite or link this publication using the identifiers

hdl:10013/epic.48157 or <http://hdl.handle.net/10013/epic.48157> and

doi:10.2312/BzPM_0700_2016 or http://doi.org/10.2312/BzPM_0700_2016

ISSN 1866-3192

PS96

(ANT-XXXI/2)

6 December 2015 - 14 February 2016

Cape Town – Punta Arenas



**Chief scientist
Michael Schröder**

**Coordinator
Rainer Knust**

Contents

1.	Zusammenfassung und Fahrtverlauf	2
	Summary and Itinerary	4
1.1	Testphase of an operational system of radar based satellite pictures for route planning, navigation and antarctic ice monitoring	8
2.	Weather conditions during PS96 (ANT-XXXI/2)	11
2.1	Kapstadt – Neumayer	11
2.2	Neumayer – Drescher – Halley – Ronne Depot	11
2.3	Ronne Depot – Drescher – Rampen – Drescher	12
2.4	Drescher – Punta Arenas	13
3.	Scientific Programmes	17
3.1	Oceanographic, Meteorologic, and Geologic Investigations	17
3.1.1	Observations of the hydrographic conditions and water mass compositions at the Filchner Sill and in the Filchner Trough	17
3.1.2	Sea ice physics	38
3.1.3	Measurements of the atmospheric boundary layer using a wind lidar	50
3.1.4	Hydroacoustics and geology	55
3.2	Biological and Ecological Investigations	61
3.2.1	Phylogeny, phylogeography and population genetics of high Antarctic biota	61
3.2.2	Cold adaptation vs. sensitivity to climate change and pollution in Antarctic Notothenioids: Physiological plasticity, genetic regulation, immunology and reproductive traits	73
3.2.3	Suspension feeders in a biodiversity hotspot: sponge distribution and functioning on the eastern Antarctic shelf	81
3.2.4	Sponge ecology and benthic fluxes	88
3.2.5	Spatial distribution patterns of epibenthic megafauna and habitats	97
3.2.6	Tracing the effect of changing ice cover on benthic ecosystem functioning - from Meio to Macro	105
3.2.7	Pelagic-benthic processes in the Filchner Outflow area: a benthic community and particulate matter perspective	113
3.2.8	Seal research at the Drescher Inlet (SEADI)	116
A.1	Teilnehmende Institute / Participating Institutions	130
A.2	Participants / Teilnehmer	132
A.3	Schiffsbesatzung / Ship's Crew	134
A.4	Stationsliste / Station List	136

1. ZUSAMENFASSUNG UND FAHRTVERLAUF

M. Schröder

AWI

Polarstern lief am 6. Dezember 2015 mit 51 Wissenschaftlern und 44 Besatzungsmitgliedern von Kapstadt aus. Die *Polarstern* Reise PS96 war durch eine Vielzahl von logistischen Aktionen geprägt. Nach der *Neumayer-Station-III*-Versorgung, die 4.5 Tage dauerte, davon 3 Tage Eisrammen und 1.5 Tage eigentliche Versorgung, wurden 4 Robbenbiologen im Drescher Inlet mit ihrem Feldcamp ausgeflogen. Dabei wurden bei etwa 30 Flügen mehr als 9.5 Tonnen Material per Hubschrauber in das ca. 8 nm entfernte Lager verbracht. Hierfür wurde ein ganzer Tag benötigt. Auf dem Schelf vor *Halley* wurden dann die ersten intensiven Stationen für die Wissenschaft durchgeführt, um dann am 02.01. nach Westen auf etwa 75°S den Weg in Richtung Ronne-Depot zu versuchen. Es bedurfte allein 6 Tage schwerer Eisfahrt um den Westhang des Filchner-Trogs zu erreichen. Wenn möglich wurden zwischendurch Station für die Wissenschaft gefahren. Das oberste Ziel war jedoch, das Depot auf dem Ronne-Schelfeis so schnell als möglich zu erreichen, um, falls erfolgreich, danach eine verlässliche Zeitabschätzung für die wissenschaftlichen Arbeiten zu bekommen. Mit Hilfe sehr guter Satelliten Eiskarten konnte das Ronne-Depot am 10.01. abends erreicht werden und die Entladung von Gütern innerhalb von 3,5 Tagen erledigt werden. Auch hier musste etwa 1 ganzer Tag zum Eisbrechen verwendet werden, um das anliegende einjährige Eis vor dem Festeis wegzuräumen. Nach etwa 10 Tagen (07.01. – 17.01.) erreichten wir wieder den Westhang der Filchner-Schwelle bei 75°S. Jetzt blieben noch genau 10 Tage für die Forschung im Bereich des Filchner-Grabens, die im wesentlichen für eine weitere Querung der Schwelle und einem Schnitt bei 76° S mit dem Austausch von 3 Verankerungen genutzt wurde. Es wurden dabei 12 Bio/Geo Stationen gefahren, die jeweils zwischen 8 und 25 Stunden dauerten. Bedingt durch das kurze Wetterfenster, wurde das Drescher Camp innerhalb von 8 Stunden am 27.01. abgeborgen und die Kollegen zwei Tage später bei Rampen über die *Aboa-Station* nach *Neumayer III* ausgeflogen. Dort gab es drei weitere lange Stationen und 3 kurze CTD-Schnitte über den Küstenstrom. Am 02.02. verließ *Polarstern* das östliche Weddellmeer und versuchte vergeblich 2 Verankerungen der Ozeanographie am Ostrand der Antarktischen Halbinsel zu bergen, die bereits seit 5 Jahren im Wasser stehen. Mit Bodenkartierung und der Durchfahrt durch den Antarctic Sound endete die Reise am 14.02.2016 in Punta Arenas.

Hätte die Eissituation es erlaubt, wäre im Gebiet Austasen ein eintägiges Messprogramm eingeschoben worden, was eine weitere Überprüfung des BENDIX Experiments (Benthos-Störungsexperiment aus dem Jahr 2003/2004) ermöglichen hätte. Nach dem Aufbau des Drescher-Camps begab sich *Polarstern* in das eigentliche Forschungsgebiet, dem weiten Schelf vor dem Filchner-Ronne Schelfeis, um die bereits im Jahre 2013-2014 (FOS, Filchner Outflow System, PS82 (ANT-XXIX/9) begonnenen ozeanographischen und biologischen Untersuchungen fortzuführen und zu ergänzen (Abb. 1).

Dieses Meeresgebiet ist besonders im Nordteil des Filchner-Grabens geprägt durch die Interaktion von sehr kaltem Eisschelfwasser (ISW, Ice Shelf Water) aus dem Süden mit dem warmen Tiefenwasser (WDW, Warm Deep Water) des Weddellmeeres. Durch diese Vermischung werden sowohl die Tiefen- (WSDW, Weddell Sea Deep Water) als auch Bodenwassertypen (WSBW, Weddell Sea Bottom Water) des Weddellmeeres gebildet, die für die globale Ozeanzirkulation und die Belüftung des tiefen Ozeans von großer Bedeutung sind.

Diese hydrographischen Besonderheiten am Kontinentalabhang des Weddellmeeres sind sehr wahrscheinlich auch die primäre Ursache für die erhöhten biologischen Aktivitäten in diesem Gebiet.

Die Bildung von Tiefen- und Bodenwasser (WSDW/WSBW) im südlichen Weddellmeer ist sowohl qualitativ als auch quantitativ stark durch die Produktionsvorgänge von Schelfeiswasser (ISW) unter dem Filchner-Ronne Schelfeis beeinflusst. Eigene hydrographische Messungen mit *Polarstern* im Jahr 1995 entlang der Filchner-Schelfeisfront zeigen, dass der Abbruch von drei sehr großen Eisbergen im Jahr 1986 und deren Gründung auf der flachen Berkner Bank, die Zirkulation und die Wassermassenbildung im Filchner-Trog signifikant modifiziert haben. Auch die angrenzenden Seegebiete weisen auf deutliche Veränderungen in den Wassermassencharakteristika und Strömungsmustern im Vergleich zu Messungen aus den frühen 1980er Jahren hin. Neuere Messungen aus der Sommersaison 2013-2014 (PS82) ergeben ein neues Bild, das den Ausstrom von ISW am Osthang des Filchner-Grabens zeigt. Modellszenarien mit dem finiten Elemente Modell FESOM zeigen, dass klimabedingte Veränderungen des Küstenstroms zu einem erhöhten Zufluss von warmem Wasser (Modified Warm Deep Water - MWDW) ab Mitte des einundzwanzigsten Jahrhunderts in dieses Gebiet führen werden. Diese Veränderungen betreffen zunächst den Filchner-Graben und beeinflussen dann die Zirkulation unter dem Filchner-Ronne Schelfeis. Die Folge davon sind höhere Abschmelzraten des Schelfeises. Eine höhere Schelfeisdynamik mit häufigeren Eisbergstrandungen und eine Erhöhung der Wassertemperatur werden erheblichen Einfluss auf die Artenvielfalt des südlichen Weddellmeeres haben. Deshalb ist die Messung der Ist-Situation in diesem Gebiet so wichtig, auch um eventuell zukünftige Veränderungen der Wassermassen einordnen zu können.

Ergänzend zu den Messungen auf dem Schiff fand eine internationale Bohrkampagne (BAS, AWI und Norwegen) auf dem Filchner-Schelfeis statt. In den Jahren 2015 bis 2017 wird an 4 Lokationen das Schelfeis durchbohrt, um Messgeräte in der Wassersäule unter dem 400 m bis 1.200 m dicken Schelfeis zu verankern. Dazu war es nötig, dass *Polarstern* wissenschaftliches Equipment und Versorgungsgüter am Ronne-Depot an der Kante des Ronne-Schelfeises abgab, damit die Bohrungen in der kommenden Sommersaison 2016-2017 stattfinden können.

Die wichtigsten Forschungsziele der Expedition PS96 FROSN (ANT-XXXI/2) waren:

1. Charakterisierung der hydrodynamischen Prozesse und Wassermassen im Filchner-Ausfluss-System (Filchner Outflow System). Dabei sollte die Rolle der Meeresbodentopographie für die Wassermassenzirkulation ebenso erfasst werden, wie die Raten von Tiefen- und Bodenwasserbildung unter Einbeziehung der Schmelzraten des Schelfeises. Hierzu dienten die Stationen im West- und Südteil des Filchner-Grabens, die die Messungen von PS82 ergänzen.
2. Eine Abschätzung von möglichen Veränderungen dieser hydrographischen Prozesse durch rezente Veränderungen des antarktischen Klimas.
3. Untersuchungen zur biologischen Produktion im Filchner-Ausflusssystem und zu den Energieumsatzraten im trophischen Nahrungsnetz.
4. Eine Abschätzung des Einflusses von möglichen Veränderungen hydrographischer Gegebenheiten und der Schelfeisdynamik auf die Biodiversität und die Ökosystemfunktionen im Filchnergebiet.

Das wissenschaftliche Hauptprogramm wurden im Meeresgebiet vor dem Filchner-Ronne-Schelfeis durchgeführt. Mit einem intensiven CTD-Programm wurden die hydrographischen Parameter aufgenommen und Wasserproben gesammelt, um die unterschiedlichen Wassermassen zu identifizieren. Drei Langzeit-Verankerungen konnten im Gebiet von 76° S

geborgen und wieder ausgebracht werden. Leider musste der Austausch zweier norwegischer Verankerungen in der Filchner-Schwelle bedingt durch eine ungünstige Eissituation aufgegeben werden. Die Meeresbodentopographie und Sedimentcharakteristika wurden mit Hilfe des Fächersonars DS-III und mit Hilfe von Parasound untersucht. Um die Rolle des Meereises für die biologischen Prozesse zu untersuchen, wurden Meereisproben gewonnen und bioptische Messmethoden direkt auf dem Eis angewendet. Zur Bestimmung der Massen- und Energiebilanz des Meereises wurden in enger Kooperation mit den Meereisphysikern Bojen mit autonomen Messlaboratorien auf dem Eis ausgebracht und Eisbeobachtung entlang der Fahrtroute durchgeführt.

Die biologischen Untersuchungen beinhalten Wasserproben und Planktonfänge zur Bestimmung der Primärproduktion, der Verteilung von Planktonorganismen und deren Biomasse. Produktionsraten des Zooplanktons wurden anhand von Laborexperimenten an Bord bestimmt. Die Verteilung und Biomasse pelagischer Fische konnte mit Hilfe von Netzfängen ermittelt werden. Die Bestimmung der Verteilung und des Vorkommens von Benthosarten und demersalen Fischen, sowie die Bestimmung ihrer Biomasse wurde durch videogeführte Bodengreifer, Multicorer, Agassiz Trawls und mit Hilfe von Grundsleppnetzfangen durchgeführt. Zur Ermittlung der räumlichen Verteilung wurden auch HD Video Transekte mit einem Unterwasserfahrzeug (ROV) durchgeführt. Daten zu Produktionsraten des Benthos und der Fische wurden mit Hilfe der Biomassedaten anhand standardisierter Rechenverfahren bestimmt und durch Laborexperimente an Bord und in den Heimatlaboratorien unterstützt.

Die Benthopelagischen-Kopplungsprozesse werden durch *in-situ* Experimente, die mit dem ROV durchgeführt werden und durch biochemische Messungen des Sediments und der gelösten organischen Substanzen (dissolved organic matter - DOM) bearbeitet. Proben zur Untersuchung des Nahrungsnetzes (Stabile Isotope, Mageninhaltsuntersuchungen), der Bioenergetik, der Ökophysiologie und zur Genetik wurden von ausgewählten Organismen gewonnen, um werden später im Labor gemessen. Des Weiteren wurden lebende Tiere gefangen, um für Laborexperimente an Bord zur Verfügung zu stehen.

SUMMARY AND ITINERARY

Polarstern left Cape Town on 6 December 2015 with 51 scientists and 44 crew members on board. The expedition PS96 of RV *Polarstern* was characterized by a variety of logistical tasks. The task of supplying the *Neumayer Station III* station took 4.5 days and included three days of ice breaking but just 1.5 days of cargo work *sensu stricto*. Afterwards four seal biologists had to be deployed at their field camp in Drescher Inlet. This deployment took a full day because it required ca. 30 helicopter flights for transporting more than 9.5 tons of material to the camp, which was ca. 8 nm away from the fast ice edge. The first extensive station work for science was undertaken on the continental shelf near *Halley* before at about 75°S latitude on the 2nd of January an attempt was made to sail towards Ronne Depot on a western route. It took six days of intensive ice breaking alone to advance to the western flank of Filchner Trough. Whenever and wherever possible, scientific station work was carried out underway. The main objective, however, was to arrive at the depot on Ronne Ice Shelf as soon as possible and, after successful deployment, to get a reliable estimate of how much time would be available for scientific research during the rest of the cruise. With the help of excellent sea-ice maps derived from satellite data Ronne Depot could be reached in the evening of the 10th of January. The cargo unloading was completed within 3.5 days. Also here the breaking of ice took one full day in order to clear first-year sea ice from the fast ice edge. After ten days (07.01. – 17.01.) we had

returned to the eastern flank of Filchner Trough at 75°S latitude. At that time, exactly ten days remained for carrying out research in the Filchner Trough area, which was mainly used for an E-W crossing of the eastern trough flank and a transect into the trough at 76°S latitude, thereby recovering and re-deploying three oceanographic moorings. Twelve biological-geological stations, each taking between 8 and 25 hours, were undertaken. Constrained by a short-term time window with suitable weather conditions on the 27th of January, the field camp at Drescher Inlet could be recovered within eight hours. Two days later the four seal biologists were flown ashore at Rampen and returned via *Aboa base* to *Neumayer Station III*. On the East Antarctic continental margin three additional extensive interdisciplinary stations as well as three short CTD transects crossing the Antarctic Coastal Current were undertaken. On the 2nd of February *Polarstern* left the eastern Weddell Sea and unsuccessfully attempted to recover two oceanographic moorings on the eastern margin of the Antarctic Peninsula. The moorings had been deployed there for five years already. After bathymetric seafloor mapping and passage through Antarctic Sound the cruise ended in Punta Arenas on the 14th of February 2016.

Due to the sea-ice situation a one-day stay at Austasen for the benthos ecologists had to be cancelled. It would have been a continuation of the Bendex experiments that had been started in 2003/2004. After the built up of the Drescher camp *Polarstern* sailed to its main scientific region, the vast shelf areas in front of the Filchner-Ronne Ice Shelf. Here an extensive oceanographic and biological programme was done and completed the station grid, which already has started during the FOS campaign (Filchner Outflow System) in 2013/2014 on the PS82 (ANT-XXIX/9) expedition (Figs. 1.1).

The marine vicinities of the Filchner Ice Shelf have been identified as a special area in the southern Weddell Sea, where the outflow of Ice Shelf Water (ISW) of the Filchner Ronne Ice Shelf interacts with warmer deep water of the Weddell Gyre. The region is a key area for the formation of Weddell Sea Deep and Bottom Water (WSDW and WSBW) and therefore of major importance for the global ocean circulation. These hydrographical features are supposed to be the primary cause converting this region into a biological "hotspot" indicated by recent investigations. Previous investigations from the 1980's tell us that the region is characterized by high abundances of different marine endotherm species and a higher production in the pelagic system as compared to other regions of the Weddell Sea. This holds especially true for the Antarctic silverfish with its high biomass and production values, which is an important food source for marine mammals in the upper food web.

The formation of deep and bottom water (WSDW/WSBW) in the southern Weddell Sea is strongly influenced by flow of Ice Shelf Water (ISW) out of the Filchner-Ronne Ice cavity. Own hydrographic measurements along the Filchner Ice Front carried out with *Polarstern* in 1995, show that the breakout of three giant icebergs in 1986 and their grounding on the shallow Berkner Bank still modified the circulation and water mass formation in the Filchner Trough. Even the adjacent sea areas show significant changes in the water mass characteristics and flow patterns compared to measurements from the early 1980s. A recent model scenario indicates that a redirection of the coastal current into the Filchner Trough and underneath the Filchner-Ronne Ice Shelf during the twenty-first century would lead to increased inflow of warm MWDW waters (Modified Warm Deep Water) into the deep southern ice-shelf cavity accompanied by a water temperature increase of more than 2°C, with the consequence of higher melting rates of the shelf-ice, a higher shelf ice dynamic and a higher habitat water temperature. A higher shelf ice dynamic with higher numbers of iceberg scouring events and an increase in water temperature will significantly influence the biodiversity of the southern Weddell Sea.

As an add-on to the scientific ship's programme an international drilling programme (BAS, AWI and Norway) started on the Filchner ice stream to drill 4 holes through the 400 m- 1,200 m thick ice shelf in the summer seasons 2015 to 2017. At each location scientific instruments could be lowered into the cavity underneath the shelf ice to measure a variety of physical parameter in the water column. Therefore *Polarstern* had to bring scientific and logistic equipment to a depot near the edge of the Ronne Ice Shelf.

The main objectives of the PS96 (FROSN) expedition were:

1. To characterize the hydrographical features and water masses of the Filchner Outflow System (FOS), the role of bathymetry for current patterns, and the deep and bottom water formation rates with the related basal melting rates. More stations in the western and southern part of the Filchner Trough could be done to supplement the measurements of PS82.
5. To estimate possible changes in these hydrographical features induced by observed change in Antarctic climate.
6. To investigate the high productive Filchner Outflow System as a biological "hotspot", producing a high-energy turnover to subsequent trophic levels up to the seals as top predators of the food web.
7. To estimate the impact of possible changes in the hydrography and increasing shelf and sea ice dynamics on the biodiversity and ecosystem functioning of the southern Weddell Sea.

The main scientific programme was performed in the area of the Filchner Ronne Ice Shelf. An intensive CTD programme was run to record hydrographical parameters and to get water samples for identifying the different water masses. The main research area was the western part of the Filchner Trough as well the area in front of the Filchner Ronne Ice Shelf. Three long-time moorings will could be recovered and re-deployed along 76° S. Unfortunately the replacement of two Norwegian moorings in the Filchner sill has to be cancelled due to severe ice conditions. The sea floor topography and sediment characteristics were measured with a multi-beam system (DS-III) and parasound. To investigate the role of sea ice for the biological processes, ice cores were taken and bio-optical measurements in the ice were conducted. In close cooperation with the ice-physicists the mass- and energy balance of sea ice was measured by deploying autonomous observatories (ice buoys) and continuous along-track sea ice observations.

The biological investigations included water samples and plankton catches to estimate primary production, plankton species distribution and biomass. Zooplankton production rates had been in laboratory experiments on board. Distribution and biomass of pelagic fish fauna were estimated by pelagic fishing trawls. Species distribution and biomass of benthic invertebrates and demersal fishes had been measured by video guided grab samples, multi- corer, Agassiz trawls, a n d bottom trawls together with the help of HD video and photo transects operated by a ROV-system (Remotely Operated Vehicle). Data on production rates of benthos and fishes were estimated by standardized calculation methods supported by additional laboratory measurements and experiments on board and in the home laboratories.

Benthic-pelagic-coupling processes could be studied by *in-situ* experiments with the ROV, and by biochemical and molecular analyses of sediments and dissolved organic matter (DOM). Samples for the investigation of food web properties (stable isotopes, gut content), bioenergetics, eco- physiology and genetics could be taken from selected species. Live organisms for on board experiments were caught for ecophysiological experiments.

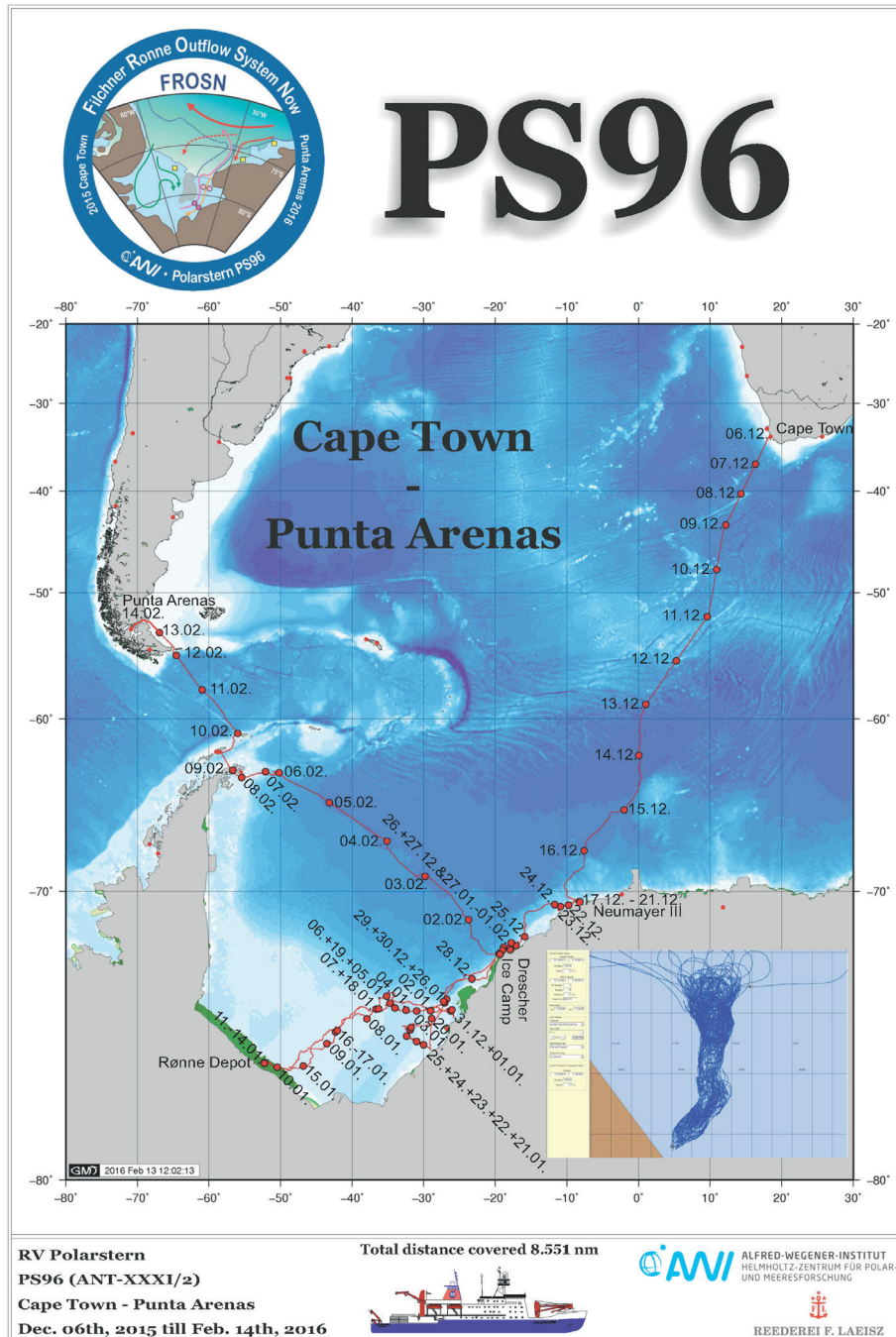


Abb. 1.1: Kursplot der Expedition PS96 (ANT XXXI/2) FROSN der FS Polarstern vom 6. Dezember 2015 bis 14. Februar 2016 (see [doi:10.1594/PANGAEA.859021](https://doi.org/10.1594/PANGAEA.859021)). Der Ausschnitt (rechts unten) zeigt den Aufwand beim Brechen des Eises an der Atka-Bucht um die Versorgung der Neumayer-Station III sicherzustellen.

Fig. 1.1: Cruise plot of the expedition PS96 (ANT XXXI/2) FROSN of RV Polarstern between 6. December 2015 – 14. February 2016 (see [doi:10.1594/PANGAEA.859021](https://doi.org/10.1594/PANGAEA.859021)). The insert (right) shows the efforts on breaking the ice at Atka Bay to ensure the supply of the Neumayer Station III.

1.1 Testphase of an operational system of radar based satellite pictures for route planning, navigation and antarctic ice monitoring

M. Schröder

AWI

This expedition was used to test near real time delivery of satellite pictures of TSX Scan SAR with a maximum of 100 to 150 km size and a resolution of maximal 18 m direct to RV *Polarstern*. These images were provided by the German Aerospace Center (DLR) within the project “TerraSAR-X for Antarctic Ice Monitoring and NRT Applications“, under supervision of Kathrin Höppner, DLR.

Here the German Antarctic Receiving Station *GARS O'Higgins* plays the key role in the short time transfer to the ship. A normal set of two pictures per day was used for the station and route planning as shown in an example near the Ronne ice front on the 10.01.2016 at around 76° 48' S, 48° 06' W (Fig. 1.1).

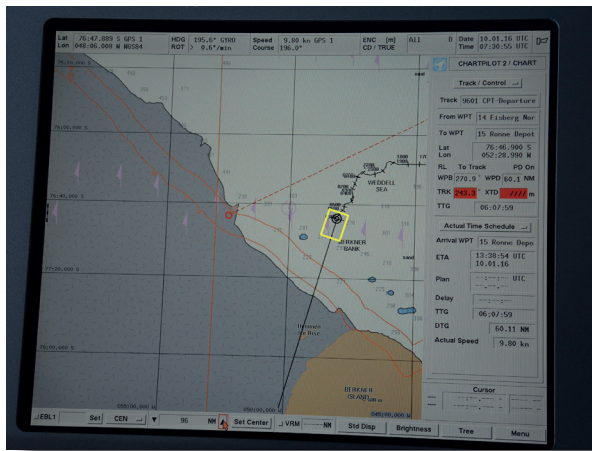


Fig. 1.1.1: Position of *Polarstern* on the 10.01.2016, 07:30 UTC shown on the electronic Chartplot. The yellow square marks the situation shown in the next figures.

The corresponding satellite image was taken on the 10.01.2016, 00:54 UTC when *Polarstern* was in the upper right corner of the image (red cross) in Fig. 1.1.2. This figure shows the far field of sea ice with leads, ponds and ice floes and the polynia in front of the Ronne Ice Shelf. The yellow square marks the situation shown in the next figures.

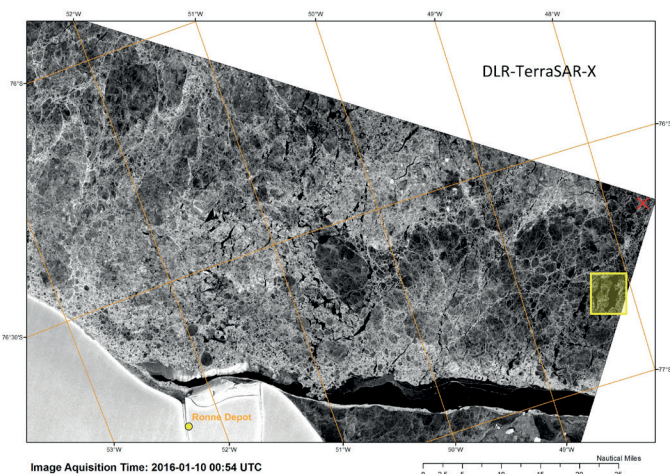


Fig. 1.1.2: TerraSAR-X wide scan image of the 10.01.2016, 00:54 UTC. Position of *Polarstern* at that time is shown as the red cross (upper right corner). The yellow square marks the situation shown in the next figures.

The next picture (Fig. 1.1.3) is a zoom up of the same image to show the near field of leads and ponds around the ship in more detail.

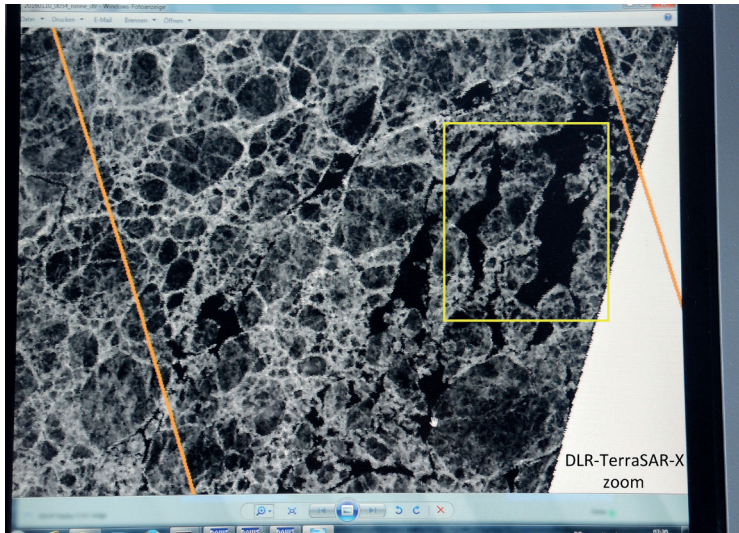


Fig.1.1.3: Zoom up of the TerraSAR-X wide scan image of the 10.01.2106, 00:54 UTC (Fig. 1.1.2). Position of Polarstern at that time is in the middle of the big pond, right dark field in the yellow square. The sea ice structure can be seen in more detail.

For comparison the two following pictures show what could be seen on the ships radar together with the ice radar on the bridge of *Polarstern* when heading south (see also Fig. 1.1.1).

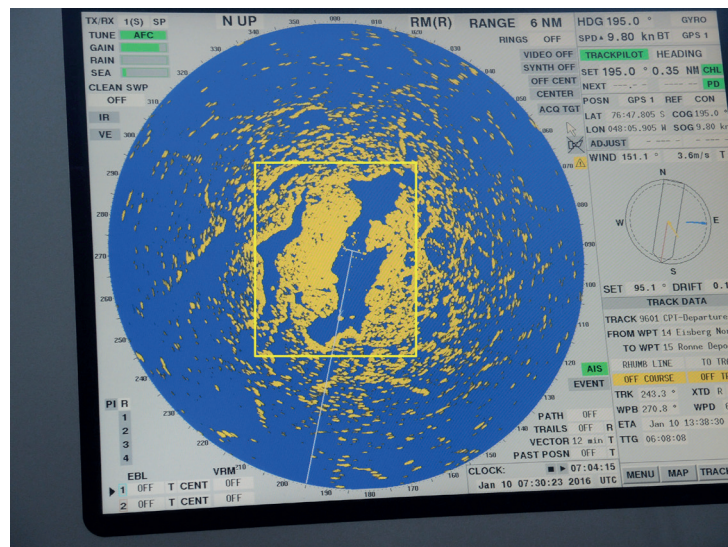
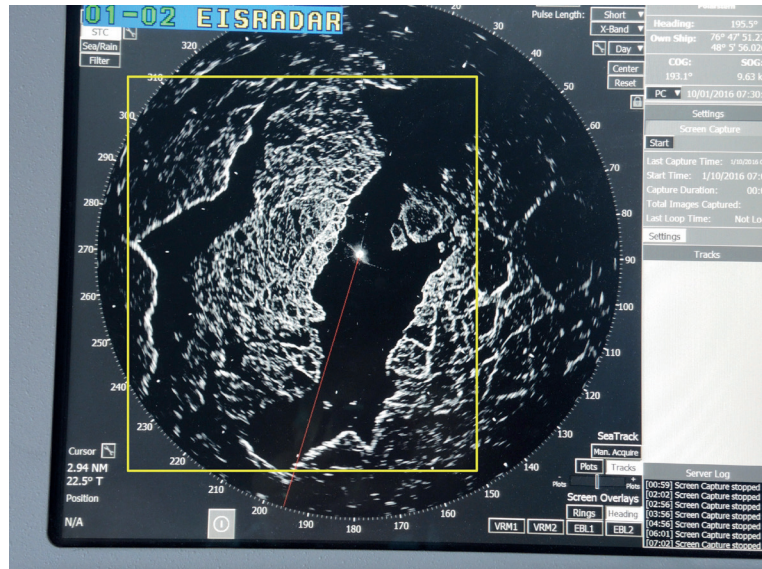


Fig. 1.1.4: Position of *Polarstern* at 07:30 on the 10.01.2016 in the middle of the big pond, right blue field in the yellow square. as shown by the ,normal' ships radar. The range is set to 6 nm.

1.1 Testphase of an operational system of radar based satellite pictures

Fig. 1.1.5: Position of Polarstern at 07:30 on the 10.01.2016 in the middle of the big pond, right dark field in the yellow square as shown by the specific ice radar of the ship. The range was set to 3 nm.



The variety of information from the near field sensors, the 'normal' radar, the ice radar and the zoom of an actual radar image together with the total satellite image with the far field information is a very helpful navigation tool in ice covered waters, especially when the weather conditions do not allow helicopter reconnaissance or the use of visual satellite images.

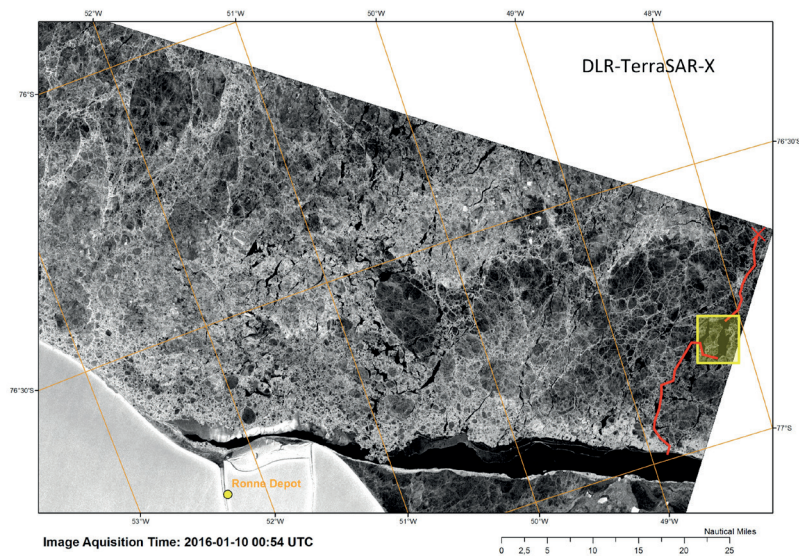


Fig. 1.1.6: Track of Polarstern on the 10.01.2016 in red out of the yellow square into the Ronne polynia. Same radar image as in Fig. 1.1.2.

In addition, whenever available, radar images from Sentinel 1a, visual images from Modis or Meteosat were taken for analysis and planning. This bunch of information made it possible to save time and fuel for transit routes and widen the possibilities for scientific work.

2. WEATHER CONDITIONS DURING PS96 (ANT-XXXI/2)

Dipl.-Met. Julia Fruntke
Juliane Hempelt

DWD

2.1 Kapstadt – Neumayer

On Sunday (Dec 6th, 2015) *Polarstern* left Cape Town while there were few clouds, mild temperatures and a light southerly wind in the harbor. Inland of South Africa a shallow low had formed. In connection with the subtropical high west of the continent just a shallow Cape Doc developed. Passing the Cape to the south the wind temporarily increased to 6 to 7 Bft.

At first *Polarstern* crossed a zone of high pressure at its weakest point. But on Tuesday and Wednesday (Dec 8th+9th, 2015) the vessel was influenced by two deep lows at Bouvet Island. The west, later northwest wind increased to 8, locally 9 Bft and the significant wave height rose to 5m. On the basis of the forecast for the following days with an intense gale on Saturday (Dec 12th, 2015) the course of *Polarstern* was slightly corrected towards the east to escape from the highest wind speeds and waves. On Saturday the upper level flow (500 hPa) changed from four to three long wave troughs. One of these troughs with a shallow amplitude stretched from the Antarctic continent across the Weddell Sea towards the South Atlantic. The flow slowed down and at the surface a trough of low pressure developed along 60S. One deep low after another influenced the weather in the sailing area. During Saturday and Sunday (Dec 12th +13th, 2015) *Polarstern* was struggling with westerly winds of 8 to 9 Bft on the northern flank of the trough. Luckily the vessel was surrounded by enough ice which damped the significant sea.

In the following high pressure was influencing the weather on *Polarstern's* way towards *Neumayer*. Several meso-scale lows passed the sailing area to the east and the west, but hardly influenced the weather.

Sunday morning (Dec 20th, 2015) the vessel berthed at the edge of the shelf ice at *Neumayer*. In the lee of the Antarctic Peninsula an intense low developed, which was weakening and moving east. Its frontal system was supposed to reach *Polarstern* during Monday (Dec 21st, 2015), but on its forward flank dry air was advected with an easterly flow of about 5-6 Bft. The frontal system reached the sailing area, but was only well developed in upper levels and further weakening.

2.2 Neumayer – Drescher – Halley – Ronne Depot

During the following days the weather at *Polarstern* was influenced by high pressure. With easterly winds between 2 and 6 Bft mild and dry air was advected. Several helicopter flights took place to scout out the ice situation and to perform first research projects on the ice.

On Saturday (Dec 26th, 2015) *Polarstern* was supposed to reach the Drescher area to build up a summer camp. Due to bad ice conditions and a damage at the machine the arrival was postponed to Sunday (Dec 27th, 2015). On Sunday a ridge of high pressure stretched from the southwestern Weddell Sea towards Drescher. On its forward flank temporarily humid air was advected causing low clouds in the sailing area. Close west of the working area the ceiling of

the low stratus clouds temporarily dropped to only 100 to 300 FT above ground level which luckily did not reach the working area. A dry easterly wind from the shelf ice ensured stable weather conditions. To build up the Drescher summer camp altogether 31 flights carrying heavy weight and people onto the shelf ice were successfully managed.

The following week started with weak pressure differences on the forward flank of a trough, which stretched along the DROMLAN-coast from *Neumayer* towards *Halley*. During New Year's Eve the southwesterly wind increased to 6-7 Bft in front of the *Halley* landing point. In the broad polynia even a fetch of about 100 km and a wind duration of about 24 hours allowed a significant sea of about 2 m.

In the first days of the new year *Polarstern* was under high pressure influence. Until Tuesday (Jan 5th, 2015) several ice reconnaissance flights as well as flights for research on ice took place due to an increasingly dry air mass and good weather conditions.

On Tuesday (Jan 5th, 2015) the flow turned to northeasterly directions and altered humid air in lower levels was advected towards the research area. Above that layer there was a very dry air mass. Although the ceiling was high enough for flights to take place the radio sounding gave hints for freezing precipitation. During the day there was no precipitation, but with the approach of a front the cloud thickness increased. In the evening a mixture of freezing drizzle and some snowflakes was registered.

During Wednesday (Jan 6th, 2016) a gale moved away from the Peninsula towards the east. At its southern flank a secondary low formed and its trough crossed the sailing area. In the following a humid and mild air mass which at first was very heterogeneous influenced the weather. Only few miles away from *Polarstern* the sun was shining while in the sailing area low clouds covered the sky, which caused light to moderate snowfall. The ceiling descended below 600 FT AGL and the visibility temporarily decreased to few kilometers. With regard to the low ceiling and the snowfall at times almost white out conditions existed which prevented any helicopter flight.

Due to low pressure differences with mostly easterly winds as well as an overall insignificant dynamic in the atmosphere a humid air mass remained in the research area until Sunday (Jan 10th, 2016). With turning wind to southerly directions the air mass began to dry and the weather conditions regarding visibility and ceiling improved.

Polarstern reached Ronne Depot on Sunday (Jan 10th, 2016). Low pressure differences and a southerly flow caused temperatures to drop during the following nights. Monday morning (Jan 11th, 2016) sea smoke developed when the air temperature decreased to -14.5°C. Also on the ice there were broad fields of fog. Although there was a very dry layer of air above 600 FT AGL the fog did not dissolve during the forenoon. On the contrary the thickness increased due to advection of humid air from the shelf ice. White out occurred on the ice which slightly influenced the work at the Ronne Depot. During the evening there was no more fog on the ice and the advection of humid air stopped. The fog disappeared within several minutes. During the following morning (Jan 12th, 2016) and the morning after (Jan 13th, 2016) the same situation occurred while the temperature dropped to -16.0°C and -17.2°C, respectively. However the air mass on the shelf ice was unmistakably drier. For that reason no advection of humid air took place and fog as well as sea smoke dissolved while the temperatures rose constantly. All the work at the Ronne Depot was successfully completed.

2.3 Ronne Depot – Drescher – Rampen – Drescher

On Thursday (Jan 14th, 2016) *Polarstern* left the Ronne Depot. Corresponding to two intense gales moving east in the polar front far north of *Polarstern* the pressure gradient increased in

the sailing area and a little bit of dynamic started to arise in the atmosphere. During Saturday (Jan 16th, 2016) a frontal system of one of those deep lows (942 hPa) west of *Neumayer* passed the sailing area with light snowfall. On the rear flank the wind turned to southeasterly directions and the clouds opened up.

During the following week mostly high pressure was present in the research area. Locally there was dense fog while few miles away the sun was shining. The boundary layer remained humid and mostly low clouds covered the area around *Polarstern* bringing some snowfall with moderate visibility. Along the shelf ice edge frequently meso-scale lows developed which usually appeared and dissolved within 24 hours. But in the surroundings of *Polarstern* there were no significant changes in wind speed regarding those lows (maximum mean wind 5 Bft).

On Wednesday (Jan 27th, 2016) *Polarstern* reached Drescher to dismantle the summer camp. Because of forecasted good weather conditions concerning helicopter flights on Wednesday *Polarstern* got there one day ahead of time. In the Weddell Sea weak high pressure was present. In a rather humid air mass without a lot of dynamic the cloud layer opened up right above the working area and the sun was shining in the morning. On the ice immediately shallow fog patches developed which luckily dissolved during the forenoon. From noon on low clouds came in which caused poor contrasts and a poor horizon. Nevertheless most of the work could be finished successfully. Only two heavy loads had to be transported to the ship during the following day when the atmosphere was rather unstable with few snow showers in the vicinity of *Polarstern*.

During Friday (Jan 29th, 2016) two long distance helicopter flights took place between *Polarstern* at Rampen and the Finnish station *Aboa*. Along the DROMLAN-coast a shallow trough of low pressure was present while high pressure influenced the weather in the Weddell Sea. In a southwesterly flow of increasingly 6 to 7 Bft humid air was advected towards the flight area. The day started with sunshine, dense fog patches on top of the ice as well as shallow sea smoke on the water. During the forenoon broken to overcast clouds came in causing increasingly poor contrasts and horizon on the ice. Nevertheless the long distance flights with both helicopters were successfully managed.

On Monday (Feb 1st, 2016) *Polarstern* was back at the Drescher site and the baptism took place while there was a ridge of high pressure influencing the weather and causing light winds up to 4 Bft from southerly directions as well as temperatures between -9°C and -7°C. In the following *Polarstern* started its transit to the northeastern tip of the Antarctic Peninsula.

2.4 Drescher – Punta Arenas

On Thursday (Feb 4th, 2016) on its way to the Antarctic Peninsula *Polarstern* was influenced by a gale, which passed the sailing area to the southeast. Since *Polarstern* had already reached more northern latitudes it was conspicuous, but by no means unusual to experience the more humid air mass that was advected with the frontal system. Temporarily moderate snowfall occurred. The wind increased to 7 Bft, but surrounded by several growlers which damped the wind sea only swell of about 3m was observed. Henceforth one gale after another interrupted by a ridge of high pressure influenced the weather. Maximum mean wind of about 8 Bft was registered. Since *Polarstern* was temporarily sailing through a lot of ice almost no significant sea was observed.

The vessel reached the Antarctic Peninsula on Sunday (Feb 7th, 2016) influenced by a frontal system of an intense gale in the Bellingshausen Sea. The wind speed increased temporarily to 8, locally 9 Bft and with freezing drizzle the visibility at times decreased below 1km. On the rear flank of the coldfront the weather conditions improved significantly. With a weak *föhn* the temperature increased to 3,9°C and several *Alto cumulus lenticularis duplicatus* were observed.

On Tuesday (Feb 08th, 2016) the vessel passed the Antarctic Sound while low clouds and drizzle diminished the visibility to just a few meters. From Wednesday to Friday (Feb 10th-12th, 2016) *Polarstern* crossed the Drake Passage. In connection with two gales the wind speed temporarily increased to 8, locally 9 Bft and a significant sea of 6 to 7 m was observed.

The vessel entered the Strait of Magellan during the night to Sunday (Feb 14th, 2016). The sky was cloudy, few showers occurred and the west to northwest wind decreased to 3 to 4 Bft until the morning. A frontal system reached the area around Punta Arenas during the afternoon. The wind increased again to 6 to 7 Bft and with the upcoming rain locally stormy gusts were observed.

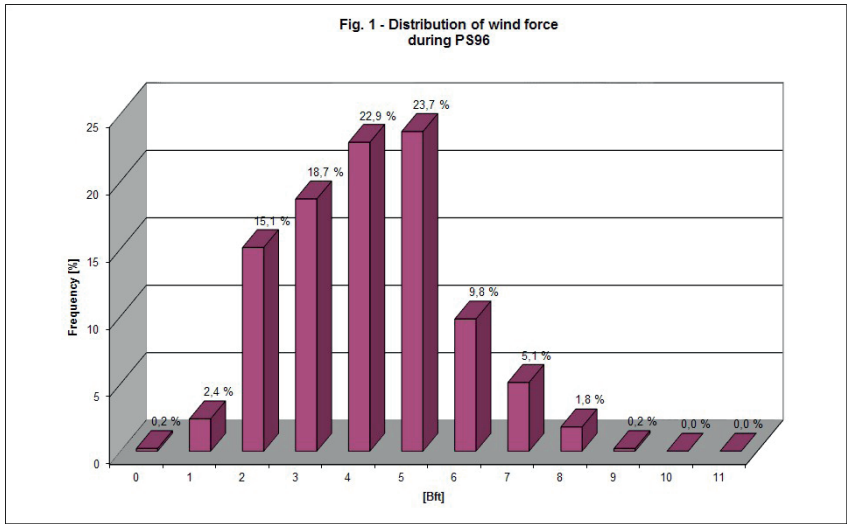
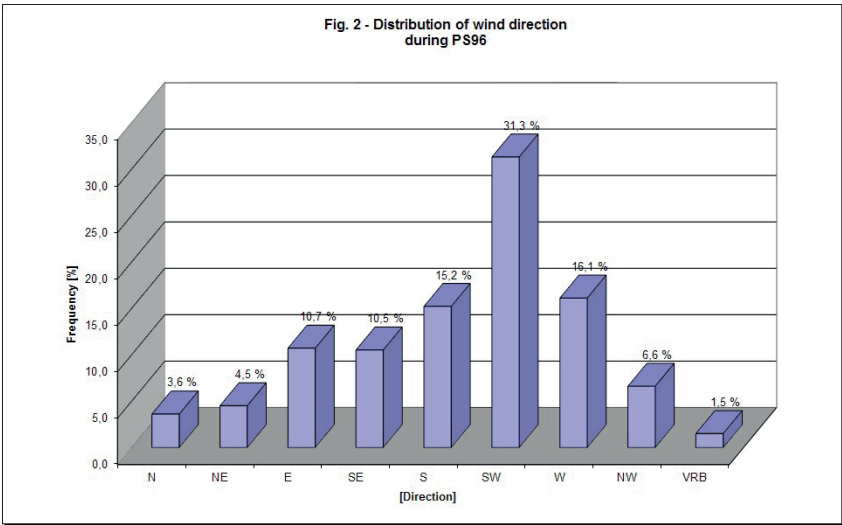


Fig. 2.1: Distribution of wind force

Fig. 2.2: distribution of wind direction



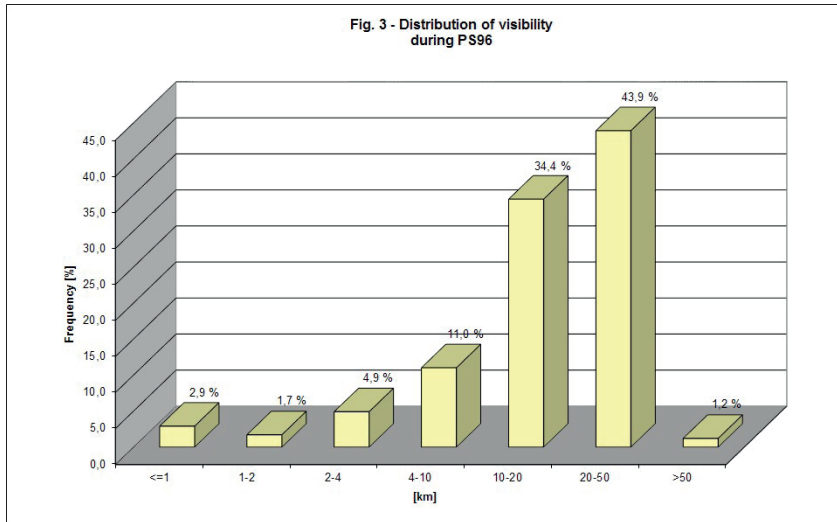


Fig. 2.3: distribution of visibility

Fig. 2.4: distribution of cloud coverage

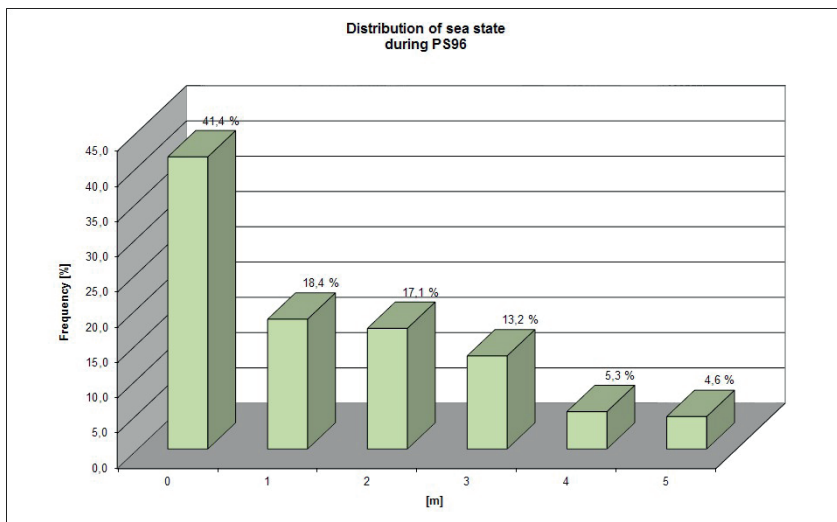
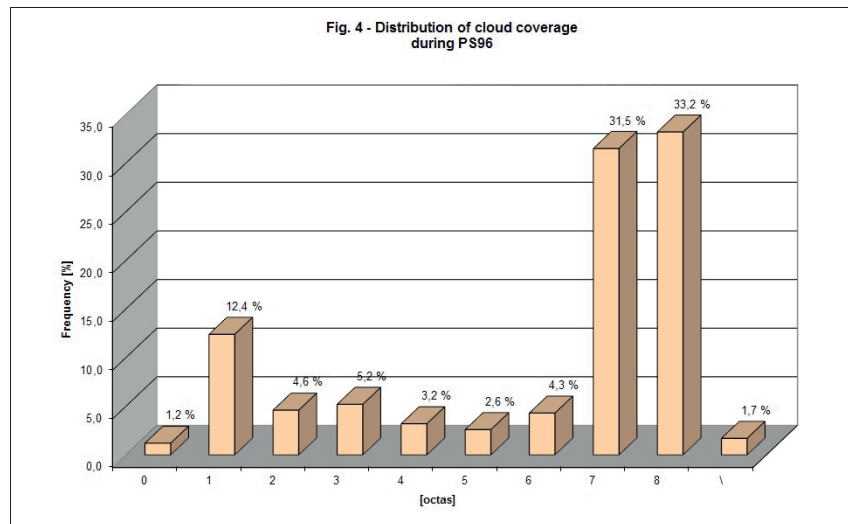
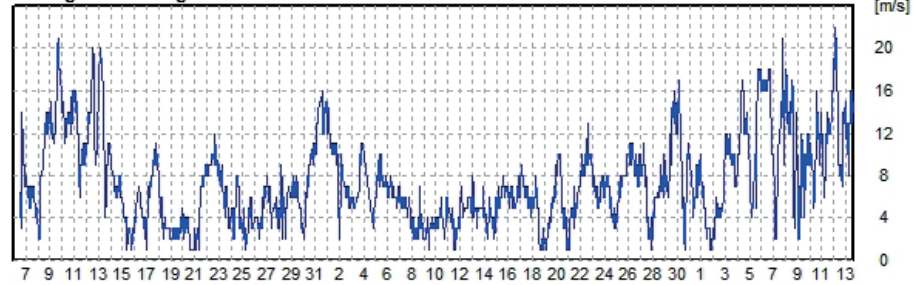


Fig. 2.5: distribution of sea state

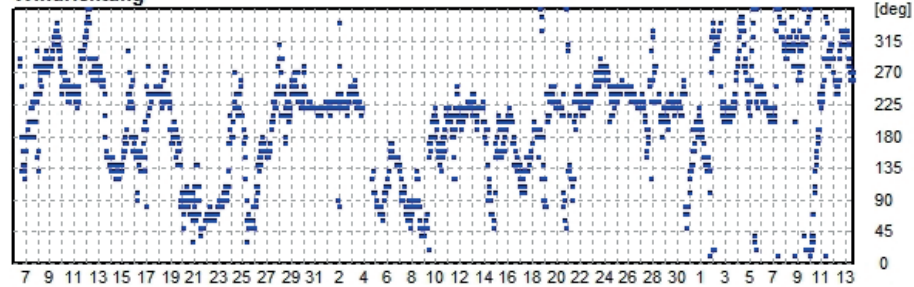
Reise PS96

vom 06.12.2015 00 UTC bis 13.02.2016 15 UTC

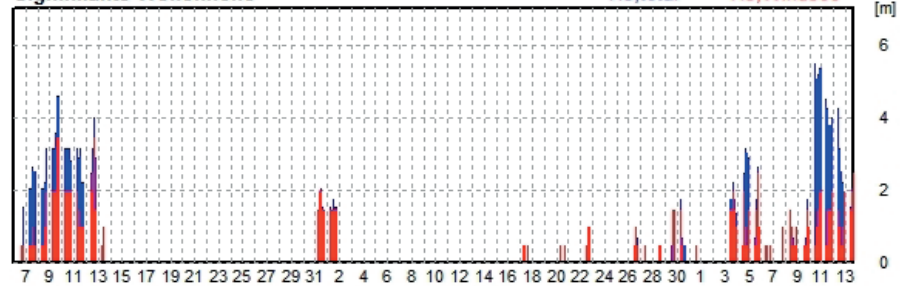
Windgeschwindigkeit



Windrichtung



Signifikante Wellenhöhe



Temperatur

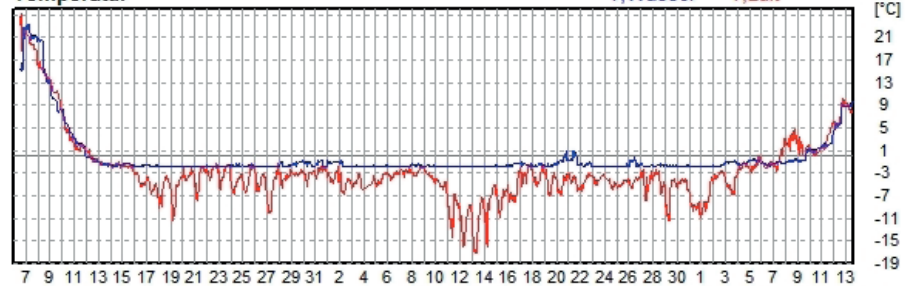


Fig. 2.6: Wetterverlauf Wind Welle Temperatur (German)

3. SCIENTIFIC PROGRAMMES

3.1 Oceanographic, Meteorologic, and Geologic Investigations

3.1.1 Observations of the hydrographic conditions and water mass compositions at the Filchner Sill and in the Filchner Trough

Michael Schröder¹, Andreas Wisotzki¹, Ralph Timmermann¹, Lukrecia Stulic¹ Svenja Ryan¹, Johanna Geilen¹, Melanie Rankl², Julia Christmann³, Svein Østerhus⁴

¹AWI,
²Uni Erlangen,
³TU Kaiserslautern,
⁴UiB-BCCR

Grant No: AWI_PS96_01

Objectives

The Filchner Trough in the southeastern Weddell Sea is considered to be the main conduit for Ice Shelf Water (ISW), defined by temperatures below the surface freezing point. ISW carries the glacial meltwater from underneath the Filchner-Ronne Ice Shelf towards the continental slope. Here, mixing with the open ocean waters forms the deep and bottom waters of the Weddell Sea. Weddell Sea Deep Water (WSDW) is the precursor of Antarctic Bottom Water (AABW) and thus one of the main contributors to the ventilation of the global abyss. Sporadically, traces of warm water of open ocean origin, called modified Warm Deep Water (mWDW), make it across the continental shelf break and flow south towards the ice shelf front along the eastern slope of the Filchner Trough. Projections based on the output of our coupled sea ice-ocean-ice shelf models indicate that in the near future the trough might become a permanent route for Warm Deep Water (WDW) into the deep Filchner-Ronne Ice Shelf (FRIS) cavity. The penetration of undiluted WDW underneath FRIS, similar to the smaller ice shelves fringing the Amundsen Sea to date, is bound to cause a dramatic increase in basal melting. The latter changes ice shelf thickness, reduces the buttressing effect of bottom topography and ultimately influences the dynamics of the ice streams draining the West and East Antarctic Ice Sheets. The resulting freshwater input will have a profound impact on the structure of the shelf water column, the sea ice cover, and the formation rate of deep and bottom waters.

General objectives:

- Specify the physical properties controlling the Filchner Trough in/outflow.
- Determine the temporal variability of the hydrography and tracer distribution in the Filchner Trough with regard to Ice Shelf Water outflow, Antarctic Bottom Water formation, and modified Warm Deep Water inflow.
- Identify temporal trends.
- Provide a comprehensive dataset for numerical model validation and initialization of coupled ocean-ice shelf – ice sheet models.
-

Specific objectives:

- Determine the course of the coastal current in the south eastern Weddell Sea and mWDW flowing towards the Filchner Ice Shelf front.

3.1.1 Observations hydrographic conditions & water mass compositions

- Specify the path of High Salinity Shelf Water (HSSW) from the Berkner Shelf into the Filchner trough.
- Produce an improved estimate of glacial melt water inventories and basal melt rates for the southern Weddell Sea (Filchner Ice Shelf) to deduce temporal trends in the future.

The combination of CTD casts from aboard *Polarstern* and long-term moorings in the Filchner Trough and underneath the Filchner Ice Shelf aims to describe the present physical environment in the southeastern Weddell Sea, and to monitor its variability and the changes, which might occur on the future. Tracer observations will help to quantify:

- Ice shelf basal melting (stable noble gas isotopes [^3He , ^4He , Ne] are used to determine basal glacial melt water inventories),
- Antarctic Bottom Water formation (transient trace gases [CFCs] to identify transit time scales and formation rates), and
- The variability of both compared to observations from previous expeditions, e.g. PS82(ANT-29/9), 2013-2014.

Work at sea

The program consisted of ship-borne measurements using a Seabird 911+ CTD (SN 937) attached to a carousel (SBE 32, SN 718) with 24 water bottles of a 12l capacity. This instrument system contains two sensor pairs of conductivity (SBE 4, SN 2325, SN 3827) and temperature (SBE 3, SN 2678, SN 5100), a high precision pressure sensor Digiquartz 410K-105 (SN 937), one oxygen sensor (SBE 43, SN 743), a transmissometer (WET Labs C-Star, SN 1120), a fluorimeter (WET Labs ECO-AFL/FL, SN 1853) and an altimeter (Benthos Model PSA-916, SN 1229). Additionally, an upward and downward looking ADCP (LADCP Workhorse Monitor WHM 300 SN 23292, SN 23293) was fixed to the carousel and coordinated by a data logger (MicroDI™ Subsea Datalogger, UDI-SI-TI-6000-1507-01). After station 110 the temperature and conductivity sensors have been changed (SN 5104 and SN 3173 respectively).

The conductivity and temperature sensor calibration was performed before the cruise at Seabird Electronics. The accuracy of the temperature sensors can be given to 2 mK. The readings for the pressure sensors are better than 1 dbar. The conductivity was corrected using salinity measurements from water samples. IAPSO Standard Seawater from the P-series P157 (K15 = 0.99985, practical salinity 34.994) was used. A total of 199 water samples were measured using an Optimare Precision Salinometer (OPS SN 006). On the basis of the water sample correction, salinity is measured to an accuracy of 0.002 (see Figure 3). The salinity still has to be corrected at home after recalibration of the sensors at the factory.

The oxygen was corrected from water samples by using the Winkler method with a Dissolved Oxygen Analyser (DOA, SIS-Kiel type). 251 water samples were measured (Figure 4). The dissolved oxygen is measured to an accuracy of 0.02 ml/l.

In total 110 CTD profiles were taken on this cruise (see Figure 3.1.1.1 and Figure 3.1.1.2). 19 profiles were taken in water depths between 1,000 m and 3,000 m, 36 in the range of 500 m to 100 m, and 56 profiles in depth less than 500 m. The deepest profile was at a water depth of 2501 m and the shallowest at 188 m. A summary of all stations is given in Table 3.1.1.1.

The whole system will be calibrated using the pre and post calibration values from Seabird. The accuracy for temperature will be better than 2 mK, for salinity it will be better than 0.002, and the pressure sensor measured with an accuracy better than 1 dbar.

3.1 Oceanographic, Meteorologic, and Geologic Investigations

To supply the ship with surface temperature and salinity values, the ship's SBE 21/ SBE 38 thermosalinograph was used in 11 m depth in the keel. The instrument was controlled by taking water samples which are measured on board with the same salinometer type as for the CTD.

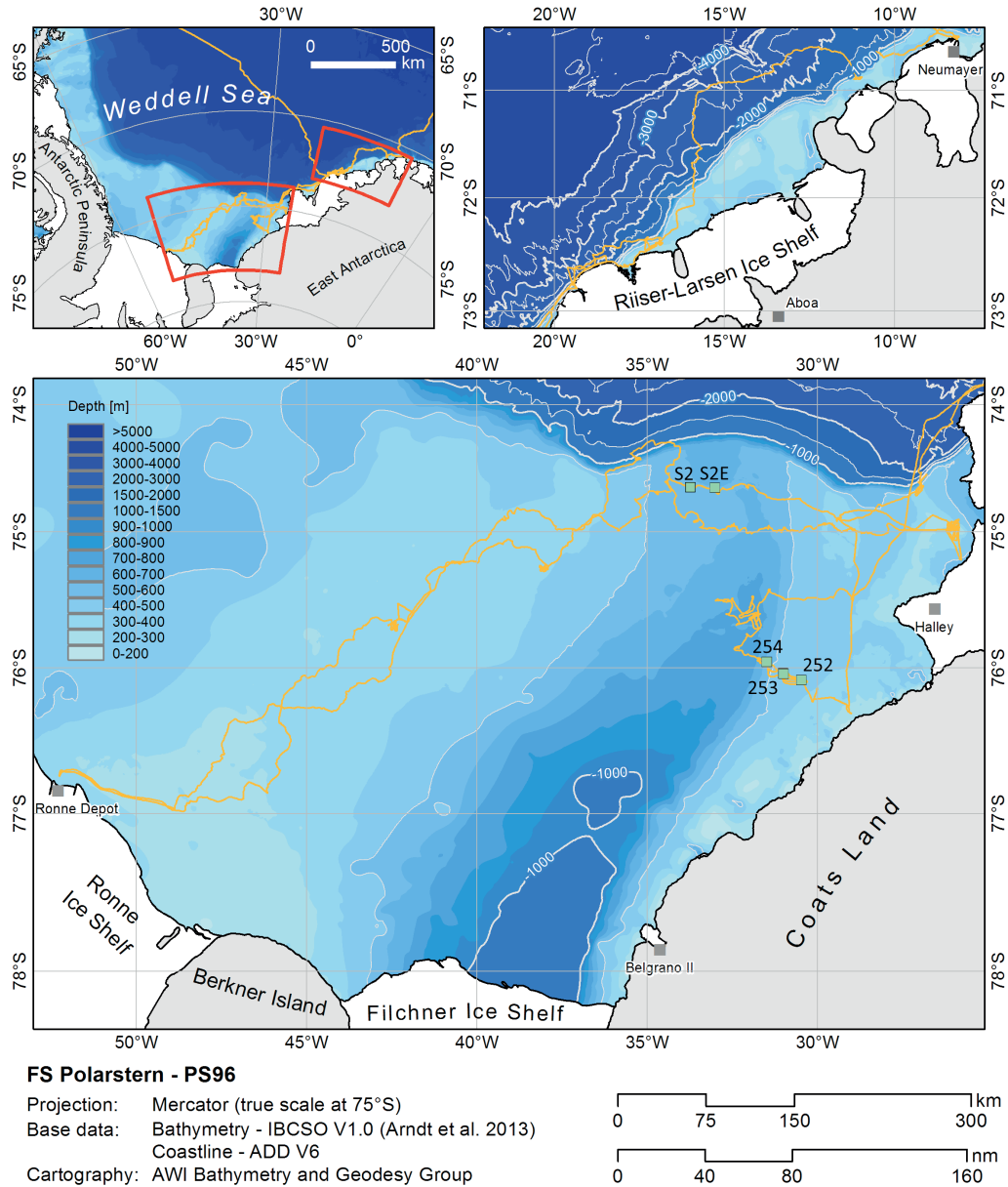


Fig. 3.1.1.1: CTD stations south eastern Weddell Sea. Numbers denote station number.

3.1.1 Observations hydrographic conditions & water mass compositions

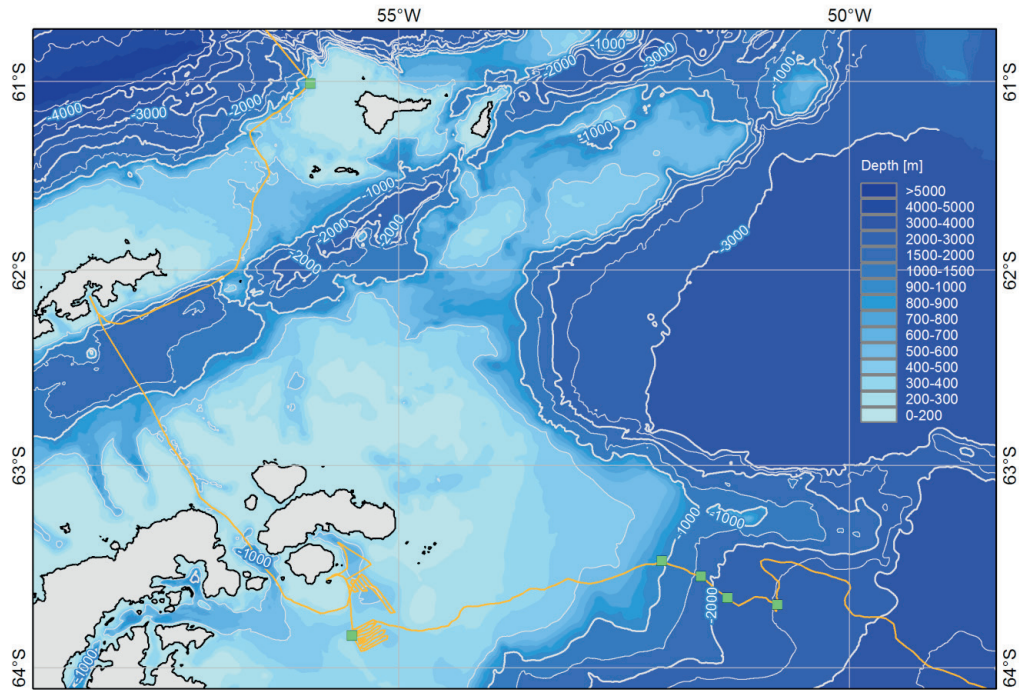


Fig. 3.1.1.2: CTD stations Antarctic Peninsula. For station numbers see table 3.1.1.1

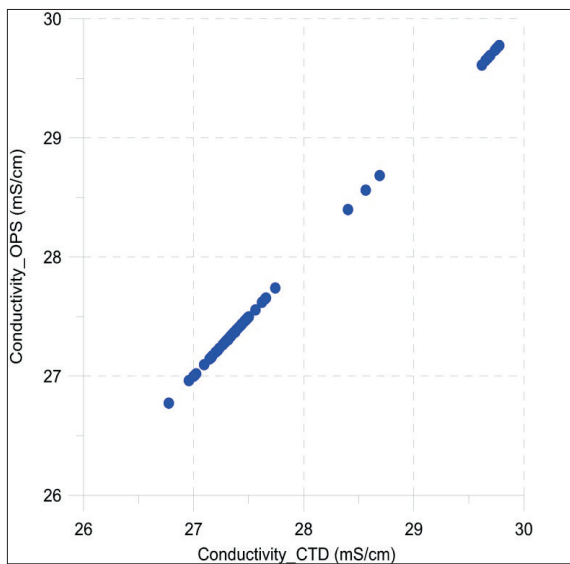


Fig. 3.1.1.3: Conductivity in mS/cm of water samples measured with OPS compared to the CTD primary conductivity sensor in mS/cm

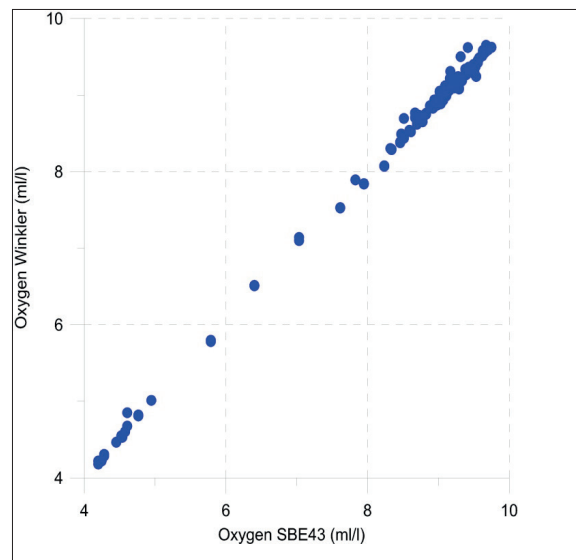


Fig. 3.1.1.4: Oxygen in ml/l of water sample measured by Winkler method compared to the CTD oxygen sensor (SBE43) values in ml/l

Preliminary (expected) results

During the cruise a closely spaced station grid has been acquired in the north eastern Filchner trough, which allows a detailed analysis of a highly variable hydrography in this area. Furthermore, measurements were taken along the western shelf all the way to the Ronne Ice Shelf front, including stations in the polynya of the big iceberg A23A, which is grounded at the eastern flank of the trough since 1986. Three short transects down the continental slope near the Drescher Inlet were done to get a picture of the coastal current carrying WDW to the south. On the way back to Chile one section consisting of 4 CTD stations was done slope-upward near the tip of the Antarctic Peninsula.

Surface properties measured with the ship's thermosalinograph between Cape Town and Neumayer Station III

Changes in the surface temperature and salinity along the cruise track can be analysed by using the data from the ship's thermosalinograph at 11 m depth. It nicely shows the latitudinal structure of the ACC (Figure 3.1.1.5). Some fronts coincide with drastic temperature and salinity changes especially the Subtropical Fronts (NSTF, SSTF) and the Subantarctic Front (SAF). Others show smaller variations at the surface as they are characterized by property changes at deeper levels such as the Polar Front. As already observed in 2013 (PS82) the Weddell Front (WF) is located further about 2° further north than its normal position. The minimum in salinity around Maud Rise (MR) is due to the melting of sea ice starting at the beginning of summer.

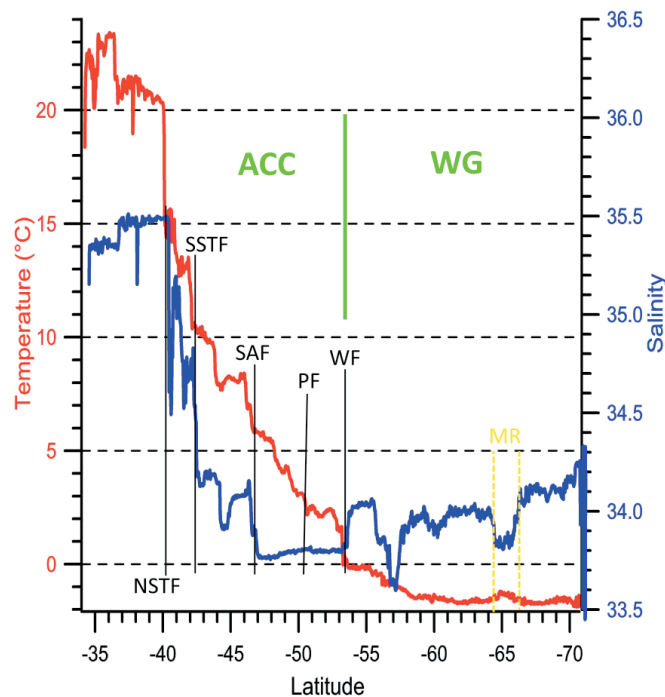


Fig. 3.1.1.5: Surface (11 m) temperature and salinity when crossing the Southern Ocean between Cape Town and Neumayer Station III over latitude. The position of fronts in the Antarctic Circumpolar Current (ACC) are shown. NSTF, SSTF – northern, southern Subtropical front, SAF – Subantarctic Front, PF – Polar Front, WF – Weddell Front, ASF – Antarctic Slope Front, WG – Weddell Gyre regime, MR – Maud Rise.

3.1.1 Observations hydrographic conditions & water mass compositions

Surface properties measured with the ship's thermosalinograph in the Filchner Ronne Area

Figures 3.1.1.6 and 3.1.1.7 show measurements of salinity and temperature recorded every minute from the thermosalinograph at 11 m depth. The temperatures have a range of -1.92°C to 1.03°C and the salinity ranges between 27.75 and 34.96. The warmest temperatures are associated with the Polynya in the eastern Filchner shelf region, where the solar radiation can directly heat the surface layer of the ocean, while the rest is mostly ice covered and shows temperatures close to the surface freezing point. In the Polynya the salinity is lowest due to a fresh surface layer, consisting of Winter Water/ Eastern Shelf Water, while it is higher in ice covered regions where sea ice formation continuously adds salt to the surface layer. Maximum values are found at the Berkner Bank south of the ice berg A23A. The region is known for intense sea ice formation and hence, production of very saline water (HSSW). Only in summer when the melting starts, a fresh surface layer can be found. However, the summer had not yet arrived when we were in the region, which explains the high surface salinity values. It can be seen nicely that as the time proceeded the temperatures increase and melting at the surface started, as the salinity values are much lower in the way back north than on the way down.

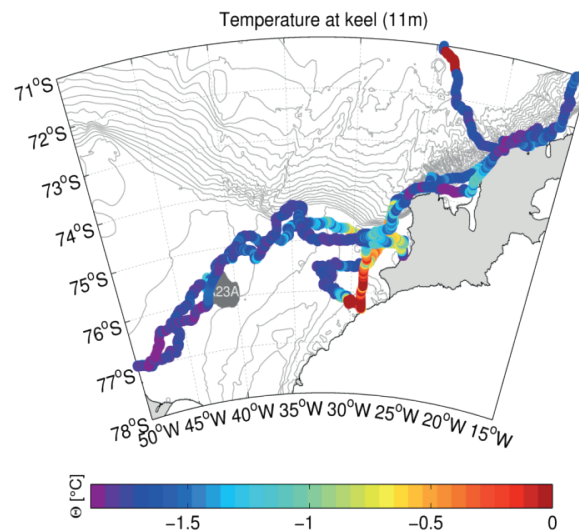


Fig. 3.1.1.6: Surface temperature (11 m) from the thermosalinograph south of 71°S .

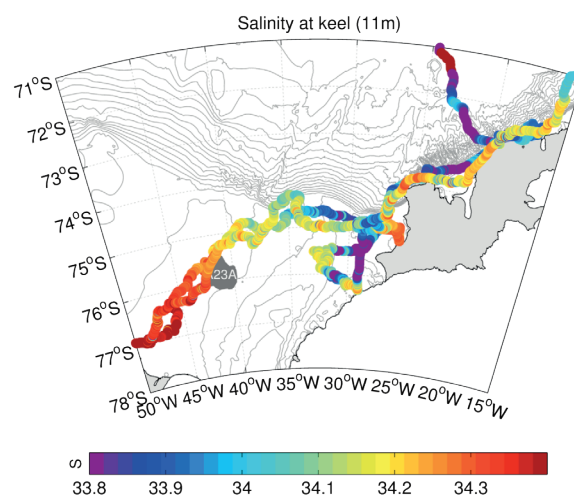


Fig. 3.1.1.7: Surface salinity (11 m) from the thermosalinograph south of 71°S .

Physical Properties of stations across the northern part of the trough and at the shelf break, showing the dominant water masses.

Figure 3.1.1.8 shows temperature – salinity properties for selected stations to describe the different water masses found in this region. The blue station at the shelf breaks covers the warm pool of the Weddell basin in the upper layer and shows the typical properties of WDW which is the warmest water mass found in the Weddell Sea and has its origin in the Antarctic Circumpolar Current (ACC). At the bottom of this station ISW is found, which spilled over the Filchner sill and is descending down the slope. Modified remnants of this WDW are found on the shelf or in the trough with temperatures between -0.5 and -1.5°C. The further west you go on the shelf the saltier and hence denser the mWDW is. This is caused by an uplift of denser water onto the shelf in the west compared to the eastern shelf. ISW is found in the deepest parts of the trough. While it is found at the eastern flank at 75°S, at 74.5°S the ISW in the middle of the trough (red and brown station). As seen at the blue station the ISW exits the trough on the western side, so it must cross the trough between 75°S and 74.2°S.

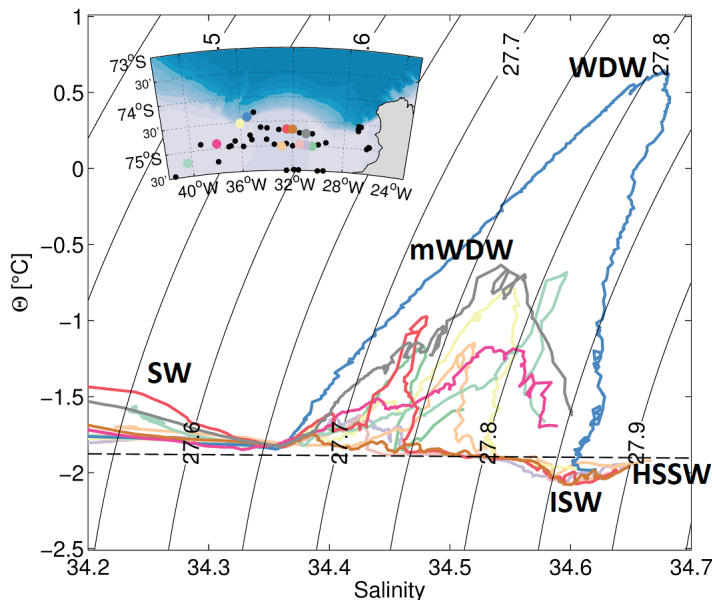


Fig. 3.1.1.8: Temperature – salinity diagram of selected stations at the northern Filchner trough and the shelf break. For better orientation the water masses are marked with their names. WDW – Warm Deep Water; mWDW – modified Warm Deep Water; ISW – Ice Shelf Water; HSSW – High Salinity Shelf Water; SW – Surface Water.

Bottom temperature and salinity from CTD measurements

Plotting the bottom properties on a lateral map (Figure 3.1.1.9 and Figure 3.1.1.10), a clear difference between the shelf regions and the trough can be found. The eastern shelf is characterized by low salinity Eastern Shelf Water (ESW) which extends all the way to the south of our measurements. The trough is governed by ISW at the bottom which has nearly the same salinity range as the warm intrusions on the shelf. The latter can be found at the eastern slope in the transitions zone of ESW to ISW. The western shelf, south of the grounded ice berg A23A shows very small variability at the bottom with salinities around 34.68 and temperatures around the surface freezing point (-1.9°C). North of the ice berg, warm water spills onto the shelf and is present as mWDW.

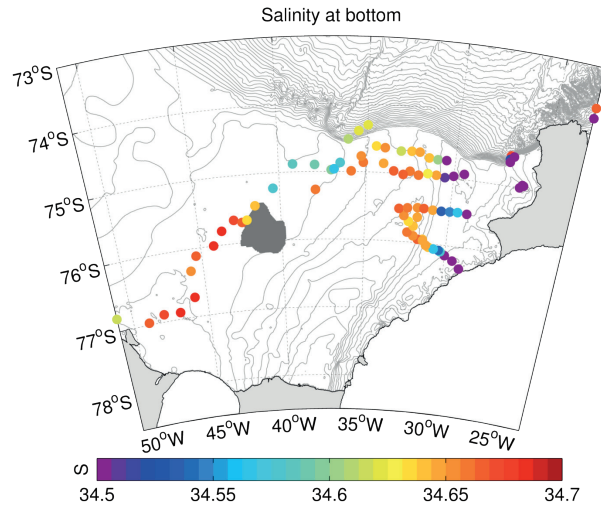


Fig. 3.1.1.9: Bottom salinity from CTD measurements in the Filchner area.

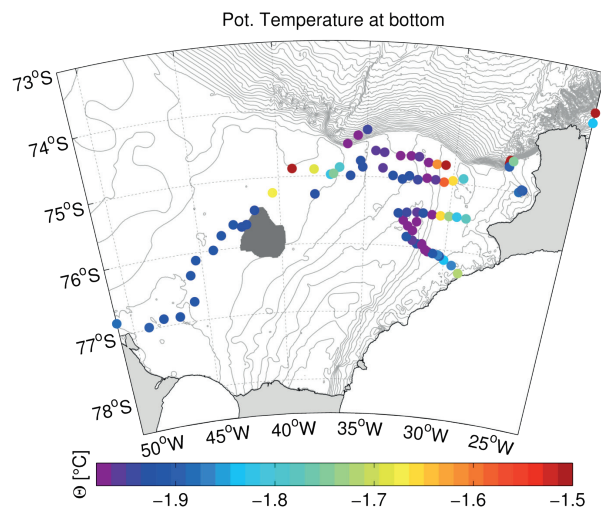


Fig. 3.1.1.10: Bottom potential temperature from CTD measurements in the Filchner area.

Physical properties found across the Filchner sill along the 74.5°S section

ISW formed beneath the Filchner Ronne Ice Shelf can only exit the shelf area via the Filchner sill which is around 600 m deep. Only the lighter ISW can cross this sill, while the other party is trapped and recirculates within the Filchner trough. The ISW which left the Filchner area is then denser than the adjacent water masses and flows downslope in form of an ISW plume. Submarine ridges and canyons enhance mixing on its way and the physical properties are altered by mixing with WDW. Figure 3.1.1.11 shows the thick layer of ISW (indicated by grey line) at the bottom in the centre of the trough. At the eastern slope warm temperatures ($T = 1.2^{\circ}\text{C}$) indicate the warm intrusions of mWDW, which is a mixture of WDW with the overlying Winter Water (WW) or the Eastern Shelf Water (ESW). Other small warm intrusions are found above the ISW layer in the trough in the density range of 27.7 kg/m^3 to 27.8 kg/m^3 . The coldest temperatures in the section are found at station 51 and 52 with temperatures of -2.1°C , while the densest water is present at station 49 at the bottom. The salinity distribution shown in Figure 3.1.1.12 reveals the highest salinity also at station 49, which is to be expected as salinity has a larger influence on density in these cold temperatures. Due to a lack of data in the centre of the trough and its western flank south of 75°S the paths of HSSW and ISW seen at the sill remain unclear.

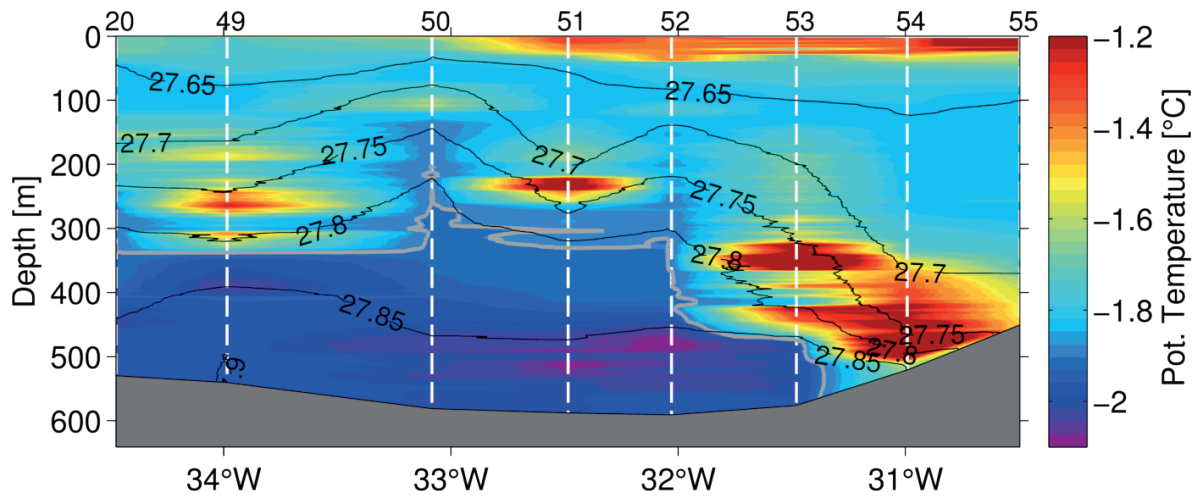


Fig. 3.1.1.11: Cross-section of potential temperature along 74.5°S crossing the Filchner trough. Stations are marked by white dashed lines. The grey line indicates the surface freezing point temperature.

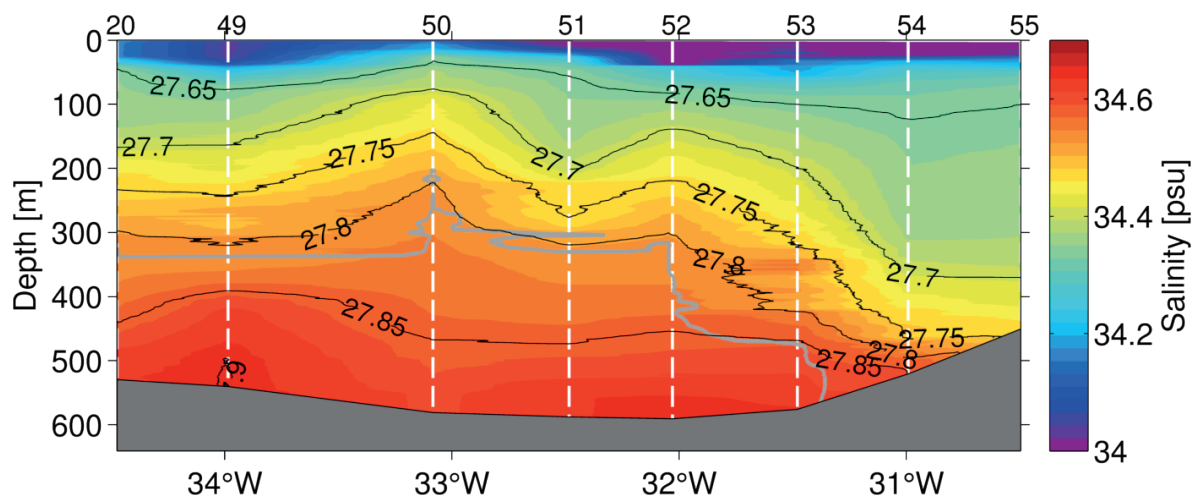


Fig. 3.1.1.12: Cross-section of salinity along 74.5°S crossing the Filchner trough. Stations are marked by white dashed lines. The grey line indicates the surface freezing point temperature.

Data management

All oceanographic data sets will be calibrated on board or after return of the sensors from the manufacturer at the Institute, quality controlled, published in a peer reviewed journal, and will then be stored in the PANGAEA Data Publisher for Earth & Environmental Science for public use.

3.1.1 Observations hydrographic conditions & water mass compositions

Table 3.1.1.1: Summary of CTD stations during PS96

Station	Cast	Date/Time	Latitude	Longitude	Water depth [m]	Pressure max. [dbar]
1	1	23-Dec-2015 13:55:00	70 52.890 S	11 6.030 W	330	337
1	5	23-Dec-2015 23:18:00	70 53.748 S	11 8.970 W	291	293
2	1	27-Dec-2015 22:10:00	72 48.222 S	19 35.928 W	1224	1209
3	1	29-Dec-2015 02:39:00	74 32.898 S	26 57.420 W	1689	1696
4	1	29-Dec-2015 04:57:00	74 36.078 S	26 59.232 W	967	949
5	2	29-Dec-2015 06:54:00	74 38.652 S	26 57.690 W	503	487
6	1	29-Dec-2015 11:14:00	74 33.468 S	26 46.998 W	0	750
8	1	30-Dec-2015 17:43:00	74 55.302 S	29 25.170 W	392	391
9	4	31-Dec-2015 12:44:00	74 59.562 S	26 11.922 W	323	321
10	2	01-Jan-2016 10:47:00	74 57.468 S	25 59.550 W	276	266
10	7	01-Jan-2016 19:46:00	74 57.012 S	26 3.930 W	274	263
11	1	03-Jan-2016 05:27:00	74 58.170 S	30 0.498 W	420	404
12	1	03-Jan-2016 08:50:00	75 0.228 S	30 29.868 W	468	451
13	1	03-Jan-2016 12:03:00	74 58.878 S	30 59.670 W	576	561
14	1	03-Jan-2016 23:43:00	74 58.200 S	31 29.358 W	619	599
15	1	04-Jan-2016 03:04:00	75 0.240 S	32 0.522 W	629	608
16	1	04-Jan-2016 10:18:00	74 57.432 S	32 30.642 W	610	586
17	1	04-Jan-2016 17:30:00	75 0.630 S	32 53.478 W	607	588
18	1	05-Jan-2016 01:16:00	74 58.092 S	33 26.370 W	589	569
19	1	05-Jan-2016 13:05:00	74 51.882 S	34 2.142 W	566	546
20	1	05-Jan-2016 21:41:00	74 36.828 S	34 28.428 W	554	536
21	1	06-Jan-2016 07:04:00	74 18.378 S	34 58.842 W	1314	1331
22	1	06-Jan-2016 09:43:00	74 23.688 S	35 29.130 W	1238	1216
23	1	06-Jan-2016 23:54:00	74 31.332 S	36 3.222 W	767	745
24	1	07-Jan-2016 11:03:00	74 52.200 S	36 29.490 W	401	386
25	1	07-Jan-2016 13:41:00	74 58.650 S	37 0.180 W	396	382
26	13	08-Jan-2016 14:23:00	75 15.972 S	37 55.170 W	413	398
27	1	14-Jan-2016 13:03:00	76 43.110 S	52 11.478 W	298	285
28	1	15-Jan-2016 01:36:00	76 58.302 S	48 59.418 W	273	260
29	1	15-Jan-2016 08:10:00	76 53.490 S	47 56.100 W	269	256
30	1	15-Jan-2016 11:04:00	76 54.120 S	46 51.582 W	288	274
31	1	15-Jan-2016 16:28:00	76 42.828 S	45 47.040 W	324	310
32	1	15-Jan-2016 21:09:00	76 19.440 S	45 47.592 W	330	316
33	1	16-Jan-2016 00:03:00	76 6.810 S	45 20.772 W	333	319
34	1	16-Jan-2016 03:25:00	75 59.952 S	44 11.808 W	344	330
35	1	16-Jan-2016 05:46:00	75 47.838 S	43 36.480 W	370	355
36	1	16-Jan-2016 09:03:00	75 39.312 S	42 49.572 W	391	376
37	2	16-Jan-2016 12:34:00	75 41.868 S	42 20.250 W	389	374

3.1 Oceanographic, Meteorologic, and Geologic Investigations

Station	Cast	Date/Time	Latitude	Longitude	Water depth [m]	Pressure max. [dbar]
40	1	17-Jan-2016 11:58:00	75 40.230 S	42 2.208 W	387	373
41	1	17-Jan-2016 14:13:00	75 28.092 S	41 29.778 W	371	362
42	1	17-Jan-2016 20:34:00	75 13.668 S	40 22.830 W	375	360
43	1	18-Jan-2016 01:31:00	74 53.010 S	39 11.490 W	391	377
44	1	18-Jan-2016 06:57:00	74 53.898 S	37 56.688 W	396	380
45	1	18-Jan-2016 10:20:00	74 57.888 S	36 50.220 W	399	383
46	1	18-Jan-2016 13:24:00	74 59.502 S	35 51.492 W	456	439
47	1	18-Jan-2016 15:44:00	74 51.618 S	35 10.950 W	501	483
48	1	18-Jan-2016 19:30:00	74 46.182 S	35 18.588 W	488	476
49	1	19-Jan-2016 16:47:00	74 37.932 S	33 59.112 W	566	547
50	2	19-Jan-2016 20:09:00	74 40.170 S	33 4.980 W	608	588
51	1	19-Jan-2016 23:01:00	74 39.678 S	32 29.070 W	615	595
52	1	20-Jan-2016 00:51:00	74 39.852 S	32 1.800 W	619	598
53	1	20-Jan-2016 03:25:00	74 44.190 S	31 28.788 W	602	583
54	1	20-Jan-2016 05:04:00	74 45.048 S	30 59.550 W	541	527
55	1	20-Jan-2016 06:33:00	74 45.018 S	30 29.832 W	473	456
56	1	20-Jan-2016 13:53:00	75 30.132 S	28 58.818 W	445	428
57	1	20-Jan-2016 21:11:00	76 19.128 S	29 2.142 W	237	238
58	1	21-Jan-2016 10:13:00	76 12.828 S	29 29.778 W	366	351
59	1	21-Jan-2016 12:17:00	76 8.910 S	30 0.420 W	411	394
61	2	21-Jan-2016 20:38:00	76 5.862 S	30 18.660 W	469	451
62	1	22-Jan-2016 06:16:00	75 56.598 S	31 27.420 W	599	579
63	1	22-Jan-2016 10:25:00	76 3.078 S	31 3.402 W	474	456
66	1	22-Jan-2016 18:09:00	76 4.908 S	30 24.858 W	462	445
67	1	22-Jan-2016 20:12:00	76 4.158 S	30 44.100 W	464	447
68	1	22-Jan-2016 21:54:00	76 1.572 S	31 13.470 W	490	471
69	1	23-Jan-2016 00:07:00	75 57.012 S	31 45.348 W	714	691
70	1	23-Jan-2016 03:13:00	75 57.552 S	31 26.208 W	569	550
71	1	23-Jan-2016 09:27:00	75 54.222 S	32 2.568 W	741	722
72	2	23-Jan-2016 14:06:00	75 51.372 S	32 25.272 W	753	729
73	1	24-Jan-2016 05:03:00	75 45.600 S	32 4.458 W	731	709
74	1	24-Jan-2016 14:53:00	75 41.760 S	32 23.142 W	716	692
75	1	24-Jan-2016 16:58:00	75 36.900 S	32 40.668 W	715	692
76	1	24-Jan-2016 20:14:00	75 30.960 S	32 59.742 W	686	663
77	1	24-Jan-2016 22:35:00	75 29.892 S	32 29.928 W	688	672
78	1	25-Jan-2016 03:08:00	75 29.112 S	31 54.222 W	756	733
79	2	25-Jan-2016 08:18:00	75 37.500 S	31 52.338 W	763	738
81	1	25-Jan-2016 14:14:00	75 29.352 S	31 31.512 W	688	689
82	1	25-Jan-2016 19:48:00	75 30.030 S	30 59.718 W	566	547
83	1	25-Jan-2016 21:23:00	75 30.210 S	30 29.460 W	449	432
84	1	25-Jan-2016 23:00:00	75 29.952 S	29 59.688 W	446	430

3.1.1 Observations hydrographic conditions & water mass compositions

Station	Cast	Date/Time	Latitude	Longitude	Water depth [m]	Pressure max. [dbar]
85	1	26-Jan-2016 00:32:00	75 29.712 S	29 31.908 W	438	421
88	1	27-Jan-2016 18:26:00	72 47.940 S	19 21.450 W	522	502
90	3	29-Jan-2016 00:49:00	72 26.010 S	17 2.280 W	280	269
90	12	29-Jan-2016 18:58:00	72 20.682 S	16 56.268 W	871	849
91	1	30-Jan-2016 01:29:00	72 23.952 S	16 56.052 W	364	350
92	1	30-Jan-2016 03:06:00	72 20.658 S	17 3.858 W	1064	1044
93	1	30-Jan-2016 04:59:00	72 17.622 S	17 12.390 W	1512	1484
94	1	30-Jan-2016 06:55:00	72 14.718 S	17 21.090 W	1756	1733
95	1	30-Jan-2016 09:12:00	72 12.498 S	17 26.772 W	1943	1917
96	1	30-Jan-2016 12:11:00	72 19.590 S	17 46.908 W	1690	1673
97	1	30-Jan-2016 14:17:00	72 21.792 S	17 40.182 W	1449	1425
98	1	30-Jan-2016 15:55:00	72 23.520 S	17 34.692 W	1236	1215
99	1	30-Jan-2016 17:22:00	72 24.912 S	17 30.018 W	752	734
100	1	30-Jan-2016 18:15:00	72 26.040 S	17 24.960 W	472	453
101	1	30-Jan-2016 19:14:00	72 28.182 S	17 19.950 W	272	260
102	1	30-Jan-2016 21:10:00	72 33.570 S	17 56.430 W	342	328
103	1	30-Jan-2016 22:10:00	72 32.628 S	18 0.378 W	594	592
104	1	30-Jan-2016 23:29:00	72 36.390 S	18 2.598 W	306	295
105	1	31-Jan-2016 05:46:00	72 31.908 S	18 3.462 W	1186	1216
106	1	31-Jan-2016 07:23:00	72 36.522 S	17 52.308 W	201	190
106	6	31-Jan-2016 16:12:00	72 36.198 S	18 4.248 W	332	319
107	1	31-Jan-2016 17:37:00	72 31.698 S	18 6.192 W	1599	1616
108	1	31-Jan-2016 21:00:00	72 31.182 S	18 9.420 W	1917	1895
109	1	31-Jan-2016 22:50:00	72 30.660 S	18 14.952 W	1946	2006
110	1	01-Feb-2016 00:49:00	72 30.018 S	18 23.940 W	2285	2298
111	1	06-Feb-2016 19:42:00	63 41.640 S	50 48.138 W	2799	2545
112	1	07-Feb-2016 00:01:00	63 39.630 S	51 21.102 W	2210	2211
113	1	07-Feb-2016 02:58:00	63 33.252 S	51 38.928 W	1724	1709
114	1	07-Feb-2016 06:03:00	63 28.650 S	52 4.980 W	963	953
115	1	08-Feb-2016 01:14:00	63 50.712 S	55 31.158 W	397	381
118	2	10-Feb-2016 12:27:00	61 00.732 S	55 58.680 W	313	300

3.1.1.1 Mooring work during PS96

Michael Schröder¹, Andreas Wisotzki¹, Ralph Timmermann¹, Lukrecia Stulic¹ Svenja Ryan¹, Johanna Geilen¹, Melanie Rankl², Julia Christmann³, Svein Østerhus⁴

¹AWI,
²Uni Erlangen,
³TU Kaiserslautern,
⁴UiB-BCCR

Grant No: AWI_PS96_01

Work at sea

In total, four moorings were successfully recovered and re-deployed with some additional sensors. Two moorings from the University of Bergen (UIB) could unfortunately not be released due to heavy ice conditions and will remain until the next summer. The positions are shown on the maps in Figure 3.1.1.1.1 and 3.1.1.1.2 and details for the recovered and deployed moorings are given in Table 3.1.1.1.1.

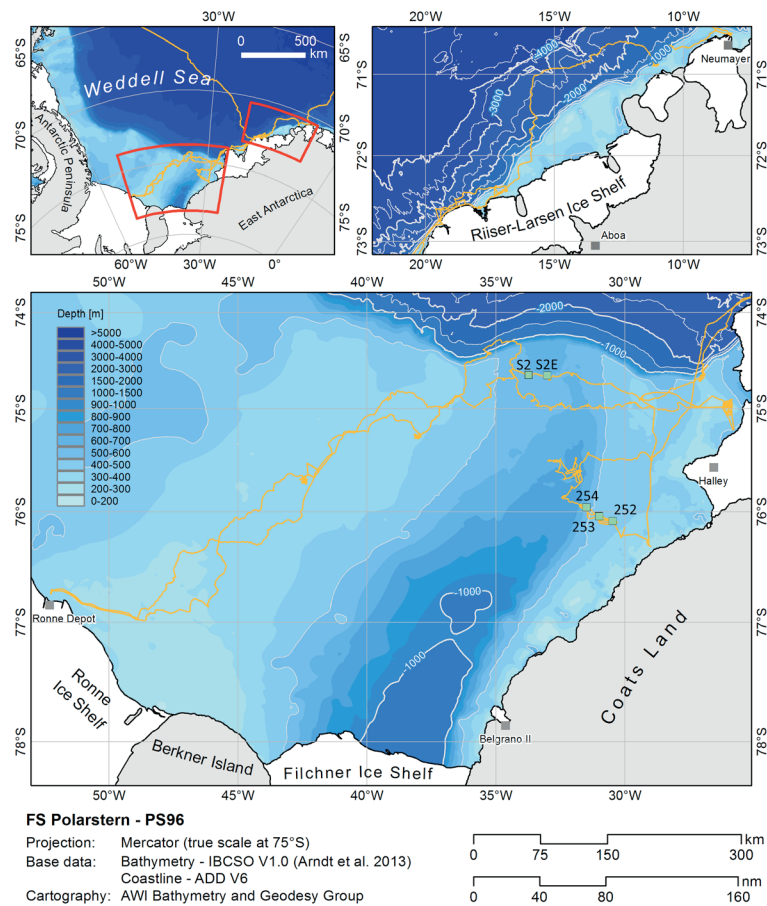


Fig. 3.1.1.1.1: Moorings Filchner trough. The moorings AWI 252-254 are located around 76°S from east to west. The moorings of the University of Bergen are located in the center of the trough near the sill. Number denote mooring number.

3.1.1 Observations hydrographic conditions & water mass compositions

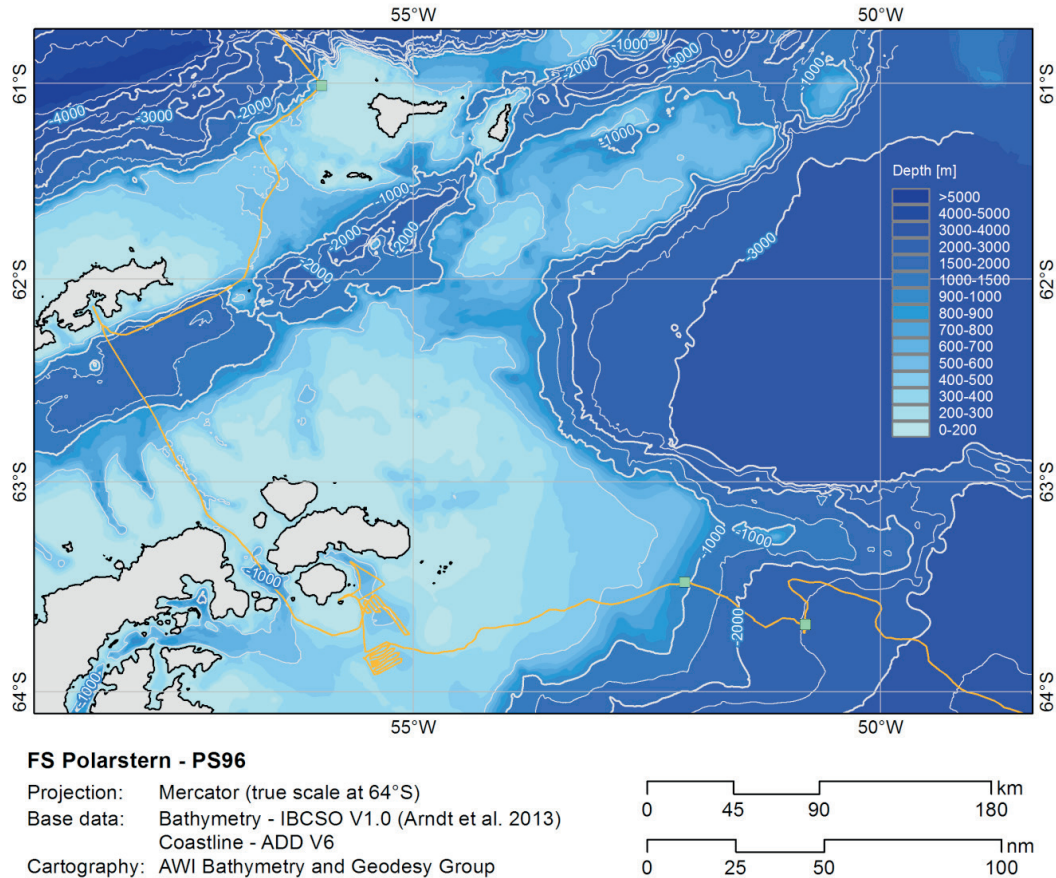


Fig. 3.1.1.1.2: Moorings at the Antarctic Peninsula. For mooring numbers see table 3.1.1.1.1

Table 3.1.1.1.1: Overview of deployed and recovered moorings

Moorings	Latitude	Longitude	Depth [m]	Status
AWI 252 - 1	76° 05.49' S	030° 28.24' W	469	recovered
AWI 253 - 1	76° 02.76' S	030° 59.72' W	473	recovered
AWI 254 - 1	75° 57.78' S	031° 29.13' W	604	recovered
AWI 252 - 2	76° 05.47' S	030° 28.19' W	465	deployed
AWI 253 - 2	76° 02.75' S	030° 59.65' W	471	deployed
AWI 254 - 2	75° 57.71' S	031° 28.92' W	598	deployed
AWI 207 - 8	63° 43.20' S	050° 49.54' W	2509	not recovered
AWI 206 - 7	63° 28.93' S	052° 05.87' W	971	not recovered
AWI 251 - 1	61° 00.88' S	055° 58.53' W	298	recovered
UNI S2	74° 40.14' S	034° 01.54' W	570	not recovered
UNI S2E	74° 39.78' S	032° 58.53' W	618	not recovered

All recovered instruments except of one current meter, which failed after one year, have recorded data for the full period of two years in the Filchner Region. Hourly time series of temperature at the mooring AWI 254-1 are shown in Figures 3.1.1.1.3 and 3.1.1.1.4 for two different depth. The upper layer (326 m) reveals a seasonal inflow of warm mWDW with temperatures around -1.6°C or warmer with a maximum in April. During winter this layer has temperatures close to the surface freezing point. Close to the bottom (558 m) ISW is the dominant water mass with a minimum temperature of -2.1°C in the middle of November, hence just before summer starts. The temperatures reached after the winter 2014 are lower compared to the year before by about 0.05°C but show a slightly higher variability. Figure 3.1.1.1.5 shows the depth over time for the upper sensor and you can nicely see the strong influence of tides at the mooring position, causing a vertical displacement of ± 1.5 m. Also some extreme events can be seen where a downward displacement of up to 6 m occurs. These predominantly happen between October and January.

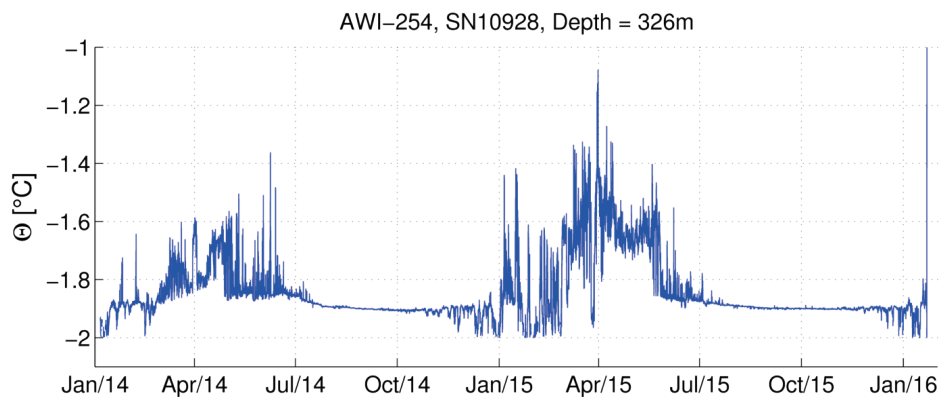


Fig. 3.1.1.1.3: Time series of temperature at 326 m depth from mooring AWI 254 -1

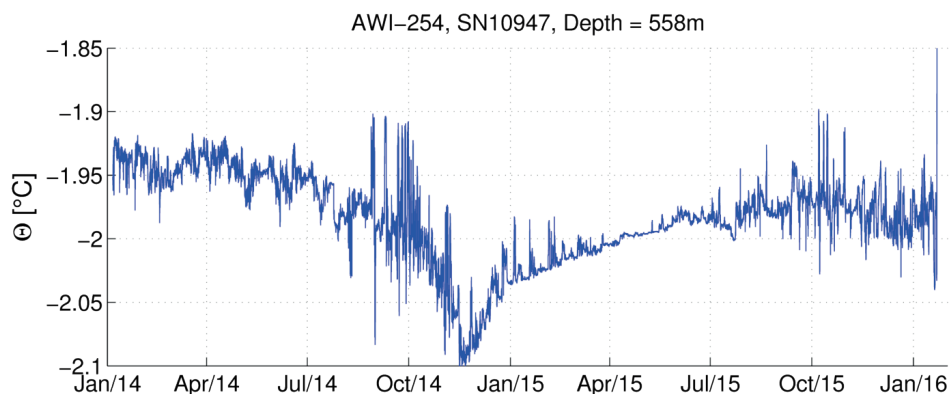


Figure 3.1.1.1.4: Time series of temperature at 558 m depth from mooring AWI 254 -1

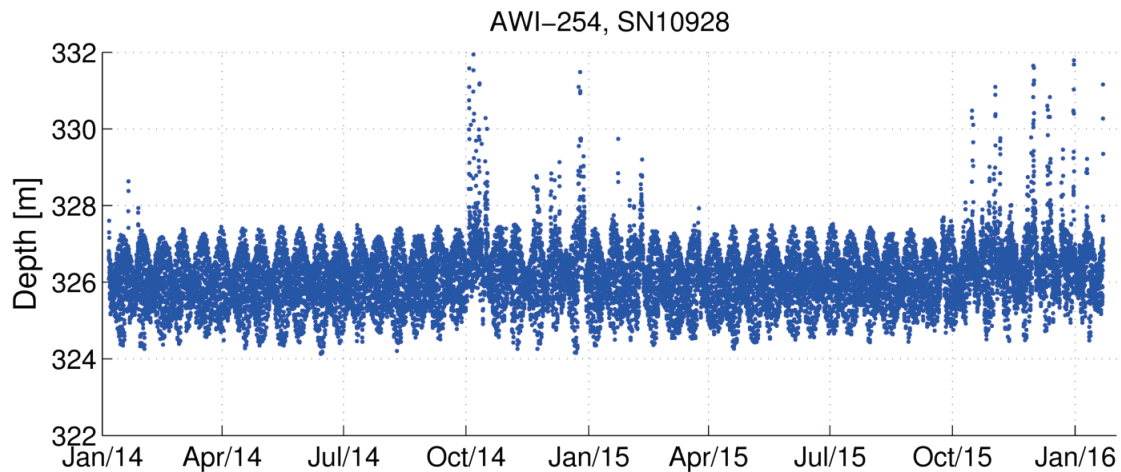


Fig. 3.1.1.1.5: Time series of depth of the upper Microcat CTD sensor at mooring AWI 254 – 1

For the redeployment of the three moorings some additional sensors (thermistors) have been added by the University of Bergen to improve the vertical resolution of temperature measurements. The set-up of the moorings is written in Table 3.1.1.1.2.

At the Filchner sill both Norwegian moorings S2 and S2E could not be serviced due to heavy ice conditions. They are part of the long term observations of the flow of dense waters from their area of formation to the abyss of the World Ocean, and the return flow of warm waters. For the Weddell Sea, an important component of such a system entails monitoring the formation of High Salinity Shelf Water (HSSW) on the continental shelf north of Ronne Ice Front, the transformation to Ice Shelf Water (ISW) beneath the floating Filchner-Ronne ice shelf, and the transport of ISW overflowing the shelf break and descending to the deep Weddell Sea. Equally important is the return flow of warm water toward the Filchner-Ronne Ice Shelf system. Uni Research in cooperation with AWI operate the long-term observatory, named S2, at the Filchner sill in the core of the ISW. Established in 1977 the S2 observatory at the Filchner sill is one of the longest existing oceanographic time series from Antarctica and situated in a key site for monitoring the ISW overflow. The S2 observatory consists of two sub-surface instrumented moorings, carrying sensors for current velocity, temperature, salinity and dissolved oxygen measurements.

The plan was to service the S2 moorings and to add on extra mooring to the system. Unfortunately due to heavy sea ice cover they could not be recovered, serviced and redeployed. We will service these two moorings next season.

In addition, a container with additional mooring equipment's did not arrive in Cape Town in time for the cruise due to failure done by the shipping company. The plan was to add one extra mooring to the S2 system, one extra mooring to the 76° S array and extra instrumentation for the AWI moorings. To the AWI moorings, we added eleven temperature sensors (SBE56). Our plan to deploy two moorings at the continental slope to study the deep/shelf sea exchanges also failed due to the missing container. All this extra moorings will be deployed next season.

Additionally, three mooring at the Antarctic Peninsula (Figure 3.1.1.1.2) have been tried to recover as they could not be recovered on previous cruises. While one has been recovered successfully (AWI 251-1), two (AWI 207-8, AWI 206-7) could be located with the ship's EK 60 fish sonar, but were not released due to critical sea ice conditions.

Table 3.1.1.1.2: Design of deployed moorings

Mooring	Latitude	Water	Date/Time	Type	Serial	Depth
	Longitude	Depth [m]			number	[m]
AWI	76° 05.47'S	465	22.01.2016	SM 37 CTD	9838	352
252 -2	30° 28.19'W		14:24			
				SBE56 Thermistor	4310	376
				SBE56 Thermistor	4232	401
				SBE56 Thermistor	1962	426
				SM 37 CTD	2391	441
				RCM 11 VT	512	
AWI	76° 02.75'S	471	22.01.2016	SM 37 CTD	9840	338
253 - 2	30° 59.65'W		16:19			
				SBE56 Thermistor	4321	383
				SBE56 Thermistor	4317	403
				SBE56 Thermistor	4313	423
				SM 37 CTD	2088	443
				RCM 11 VT	509	453
AWI	76° 57.71'S	598	23.01.2016	SM37 CTD	9834	392
254 - 2	31°38.92'W		7:50			
				SBE56 Thermistor	4333	333
				SBE56 Thermistor	4332	353
				SBE56 Thermistor	4335	373
				Develogic Sono Vault	1010	493
				SBE56 Thermistor	4327	520
				SBE56 Thermistor	4328	545
				SM 37 CTD	2091	570
				RCM 11 VT	469	580

3.1.1.2 Observation of stable noble gas isotopes (³He, ⁴He, Ne) and transient tracers (CFCs)

Oliver Huhn,
Camila Campos,
Hendrik Jechlitschek

UHB-IUP

Grant No: AWI_PS96_01

Objectives

The major aims of our stable noble gas isotope and transient tracer observations are to trace the glacial melt water (GMW) formed at the Filchner-Ronne Ice Shelf in the southern Weddell Sea and of ambient water masses, to quantify the actual GMW inventory in the Filchner outflow

area, the melt rate of the Filchner-Ronne Ice Shelf, and to assess the related Weddell Sea Bottom Water (WSBW) composition, its formation rate and export into the deep Weddell Basin. It aims to enhance our understanding how (basal) ice shelf melting, ambient water masses, and Antarctic Bottom Water (AABW) formation interact under possibly changing climate conditions.

Previous observations and model studies emphasize the complex and unique interaction of the Antarctic Ocean climate components (atmosphere – sea ice – shelf ice – ocean) and their sensitivity to changing environmental conditions and response to climate change. The WSBW formation and composition is known to be strongly related to the dynamics of the ice shelves in the southern Weddell Sea (Filchner-Ronne Ice Shelf). Recent observations show distinct variability or even trends in the WSBW properties (warming, freshening, water mass age increase, reduced ventilation and anthropogenic carbon uptake). However, the actual state of basal glacial melting, its variability and possible future trends due to changing climate conditions and its impact on the WSBW composition and formation and its variability is not yet fully understood.

Hence, investigating and quantifying glacial melting and WSBW formation as close as possible to its sources (in front of the Filchner-Ronne Ice Shelf and in the Filchner outflow area) will help to increase our understanding of the interaction of these unique Antarctic Ocean climate components.

The aims of our tracer observation based approach are the followings:

- To produce an improved actual estimate of GMW inventories, and melt rates for the ice shelves in the southern Weddell Sea (Filchner-Ronne Ice Shelf), and to be able to address temporal trends in the future.
- To trace the circulation of ambient water masses on the shelf and to trace the pathways of the GMW in the Filchner outflow area.
- To investigate how the GMW contributes to local WSBW formation and to quantify the related actual WSBW formation rates.
- To investigate, if there is evidence for local shifts of GMW circulation or temporal trends in GMW formation and discharge and the related WSBW formation. Possible changes could be related to changing properties or changing circulation of the ambient water masses due to changing environmental conditions.
- To assess, how local processes and their variability are related to basin wide or global scales (e.g. observed basin wide WSBW and AABW property changes, warming, freshening, age increase and declining ventilation, slow down anthropogenic carbon uptake, declining volumes, trends).

To reach these aims, new and spatially high resolved tracer measurements particularly near the Filchner-Ronne Ice Shelf and in the Filchner outflow area are required. Our tracer observations will help substantially to trace and to quantify basal ice shelf melting (stable noble gas isotopes [^3He , ^4He , Ne] to quantify the basal GMW), basal melt rates and the related WSBW formation (transient trace gases [CFCs] to determine transit time scales [TTDs], formation rates, and anthropogenic carbon storage) and their variability.

Approach and methods

The oceanic measurement of the low-solubility and **stable noble gases** helium (^3He , ^4He) and neon (Ne) provide a useful tool to identify and to quantify basal glacial melt water (GMW). Atmospheric air with a constant composition of these noble gases is trapped in the ice matrix

during formation of the meteoric ice. Due to the enhanced hydrostatic pressure at the base of the shelf ice, these gases are completely dissolved in the water, when the ice is melting from below. This leads to an excess of $\Delta^4\text{He} = 1280\%$ and $\Delta\text{Ne} = 890\%$ in pure glacial melt water (Loose & Jenkins, 2015; the Δ stands for the noble gas excess over the air-water solubility equilibrium). Frontal or surface melt water would equilibrate quickly and not lead to any noble gas excess in the ocean water. With an accuracy of $<0.5\%$ for He measurements performed at the IUP Bremen, basal glacial melt water fractions of $<0.05\%$ are detectable. The $^3\text{He}/^4\text{He}$ isotope ratio provides additional information. In Antarctic shelf water the ratio is low in comparison to ratios in WDW (the WDW has a maximum in $^3\text{He}/^4\text{He}$) and provide complementary information of the composition of WSBW. Finally, primordial helium (mantle helium with a far higher $^3\text{He}/^4\text{He}$ ratio, $\delta^3\text{He} \approx 800\%$) enters the ocean from spreading regions of submarine ridge systems or other hydrothermal active sites like hydrothermal vents or submarine volcanoes.

The anthropogenic transient trace gases **chlorofluorocarbons** (CFC-11 and CFC-12) allow estimating the time scales of the renewal and ventilation of inner oceanic water mass transport. They enter the ocean by gas exchange with the atmosphere. Since the evolution of these transient tracers in the ocean interior is determined on first order by their temporal increase in the atmosphere and subsequently by advection in the ocean interior, they allow quantifying the time scales of deep and bottom water transport and formation. In a higher order approach, using the so called Transit Time Distribution (TTD) method (or water mass age spectra), they allow determining the integrated advection and mixing time scale of a water mass. These CFC and TTD method based time scales of ventilated water masses integrate residence, circulation, and transport and on the shelf, slope, and deep basin and allow determining water mass ventilation and formation rates. Combined CFC based time scales with noble gas and OMP based melt water inventories allow calculating basal glacial melting rates and the basal glacial melting induced WSBW formation rates.

Additionally, the CFCs and TTD method can be used to estimate the anthropogenic carbon content in WSBW by applying the CFC based TTDs to the well known atmospheric anthropogenic carbon history. That method is very reliable particularly in deep and bottom water and it is fully independent of carbon measurements and back calculating methods, which require additional geochemical observations or linear regression methods.

Work at sea

In total we took 520 water samples for stable noble gas isotopes (^3He , ^4He , Ne) in copper tubes from 67 stations (all full bottom-surface-profiles) in the Filchner-Ronne region (violet squares in Fig. 3.2.2.1, lower panel).

For the transient tracers (chlorofluorocarbons, CFC-11 and CFC-12), we took in total 990 samples on 87 stations (all full bottom-surface-profiles). From that we took samples from 74 stations in the Filchner-Ronne region (green squares in Fig. 3.2.2.1, lower panel).

Additional we took samples from 9 stations east of the Filchner region at Rampen (green squares in Fig. 3.1.2.1, upper right panel) to investigate the inflow from the east, and from 4 stations in the northwestern Weddell Sea (not shown) to extend the CFC time series in that region.

3.1.1 Observations hydrographic conditions & water mass compositions

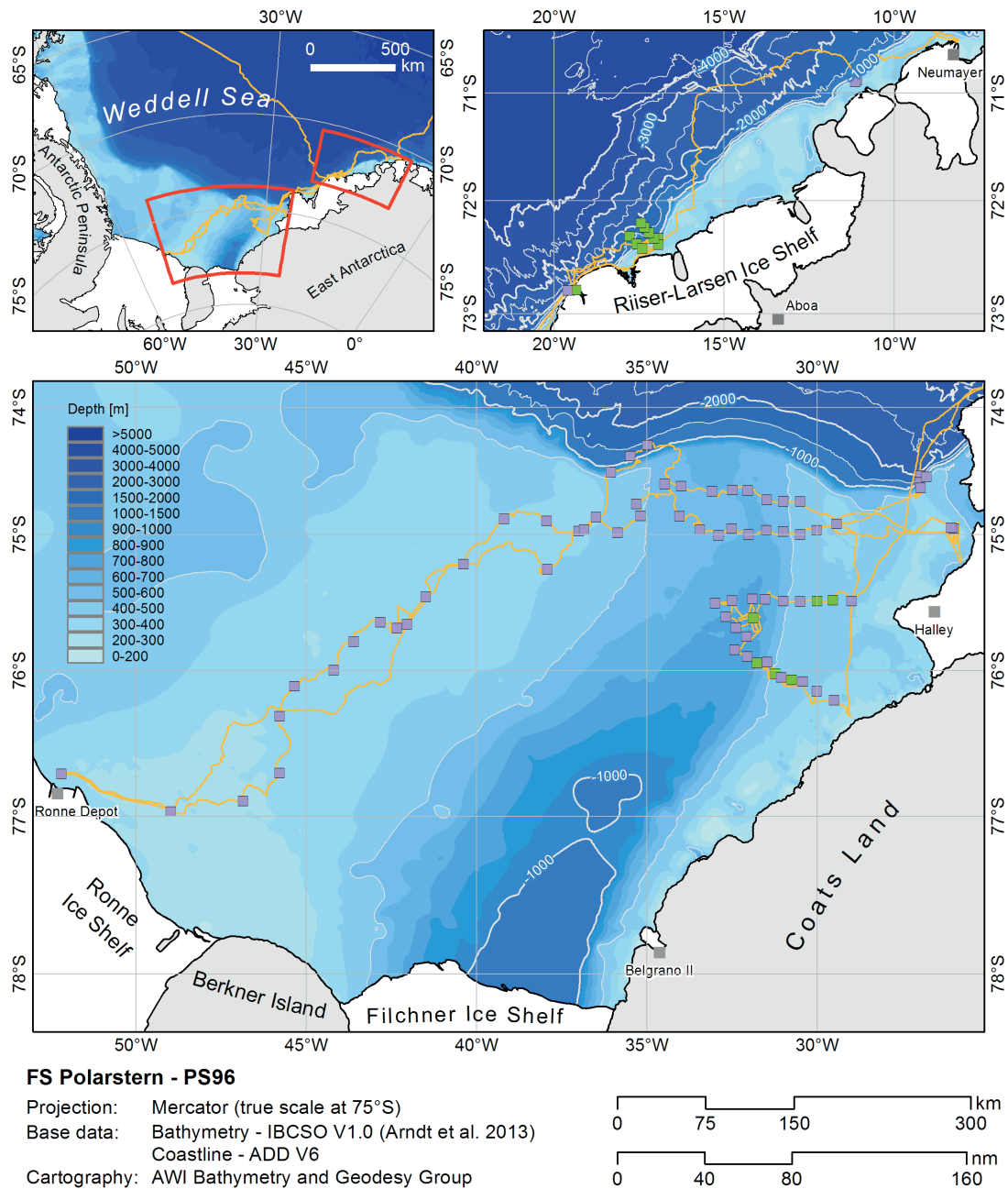


Fig. 3.1.1.2.1: Map indicating stations with noble-gas and CFC samples during PS96. Violet squares are stations with noble-gas and CFC samples, green squares are stations with CFC samples only. The orange line is the cruise track.

The water samples for helium isotopes and neon were stored from the CTD/water bottle system into gas tight copper tubes, which are clamped off at both sides. The noble gas samples are analyzed later in the IUP Bremen noble gas mass spectrometry lab. The copper tube water samples are processed in a first step with an ultra high vacuum gas extraction system. Sample

gases are transferred via water vapor into a glass ampoule kept at liquid nitrogen temperature. For analysis of the noble gas isotopes the glass ampoules are connected to a fully automated ultra high vacuum mass spectrometric system equipped with a two-stage cryogenic trap system. The system is regularly calibrated with atmospheric air standards (reproducibility better $\pm 0.2\%$). Also measurement of blanks and linearity are done.

For the transient tracers (CFC) water samples from the CTD/water bottle system were collected into 100 ml glass ampoules and are flame sealed after a CFC free headspace of pure nitrogen had been applied. The CFC samples are later analysed in the CFC-laboratory at the IUP Bremen. The determination of CFC concentration will be accomplished by purge and trap sample pre-treatment followed by gas chromatographic (GC) separation on a capillary column and electron capture detection (ECD). The amount of CFC degassing into the headspace will be accounted for during the measurement procedure in the lab. The system will be calibrated by analyzing several different volumes of a known standard gas. Additionally the blank of the system will be analyzed regularly.

All samples will be shipped home after the expedition and will be analyzed in the UHB-IUP noble gas and CFC laboratories. The measurements are expected to be completed one year after arrival in our home lab in Bremen. A careful data quality check will be carried out then.

Expected results

As soon as the measured data are available, we will use the stable noble gas data (^3He , ^4He , Ne) to trace the pathways and to quantify the GMW inventories in the Filchner outflow region and to assess the composition of newly formed WSBW. We will use the transient tracer (chlorofluorocarbon, CFC) data to determine the time scales of residence and circulation to quantify the formation rates of GMW (basal melting rates) and of WSBW formation rates. We will use CFC data to estimate the anthropogenic carbon content and uptake in the recently formed WSBW. We will extend the new data set with that obtained during PS82 (2013/14) and combine them with available historic tracer data to assess possible temporal variability of GMW pathways and inventories, basal glacial melt rates, WSBW composition, formation rates, and anthropogenic carbon uptake.

The achieved 3-dimensional spatial coverage during PS96 with noble gas and CFC samples in the Filchner outflow region is higher than from previous expedition, particularly in combination with the PS82 data (2013/2014). This spatially dense and almost synoptic station distribution is sufficient to estimate realistic contemporary GMW inventories and basal ice shelf melting rates from the Filchner-Ronne Ice Shelf and the related WSBW formation rates.

Data management

All our data will be made public on the Pangaea data base as soon as we have them available (approximately one year after the cruise), carefully quality controlled, and published in a peer reviewed journal. Our cooperation partners will receive the data as soon as the final data set is available.

Acknowledgment

We gratefully thank the master and crew of RV *Polarstern* for all support, maneuvering and running heavy gear, the oceanographic group of Michael Schröder et al. for providing water samples and hydrographic information, the bathymetry group of Jan-Erik Arndt et al. for providing detailed information about the bottom topography in the area of investigation and our station map, and AWI for the chance of participation (GrantNo PS96_01).

3.1.2 Sea ice physics

3.1.2.1 Interannual Snow, Ice and Drift experiment (InSIDE)

Stefanie Arndt¹, Leonard Rossmann¹, Marcel Nicolaus¹ (not on board), Sandra Schwegmann¹ (not on board), Kathrin Höppner² (not on board), Thomas Krumpen³ (not on board), Stefan Hendricks³ (not on board), Steve Colwell⁴ (not on board), Gareth J. Marshall⁴ (not on board)

¹ AWI,
² DLR,
³ Drift&Noise,
⁴ BAS

Grant No: AWI_PS96_01

General objectives

Sea ice and snow are key variables in the global climate system. Through its manifold interactions with the atmosphere (e.g. the ice-albedo feedback) and ocean (e.g. freshwater budgets during melt and formation) they have strong impacts on global circulation patterns extending far beyond the polar regions. To describe large-scale and inter-annual variabilities of sea-ice and snow properties, autonomous ice tethered platforms, called buoys, are deployed on representative ice floes of the area. These platforms provide information on sea ice growth (Ice Mass Balance buoys, IMB), snow accumulation (snow depth buoys) and sea ice dynamics,

as sea-ice drift and deformation, (Surface Velocity Profilers, SVP) over the entire seasonal cycle through their drift through the Weddell Sea.

Thus, the main objective of InSIDE was to deploy several sets of autonomous ice tethered platforms (buoys) to investigate the seasonal and interannual variability of sea ice thickness, snow depth, drift and deformation as a continuation of buoy deployments during previous studies on Antarctic sea ice, e.g. PS82 (ANT-XXIX/9) and PS89 (ANT-XXX/2). Additional small-scale measurements of snow properties and snow depth distribution enhance these unique data sets.

An overview of all deployed buoys and additional snow stations during PS96 is given in Figure 3.1.2.1.1.

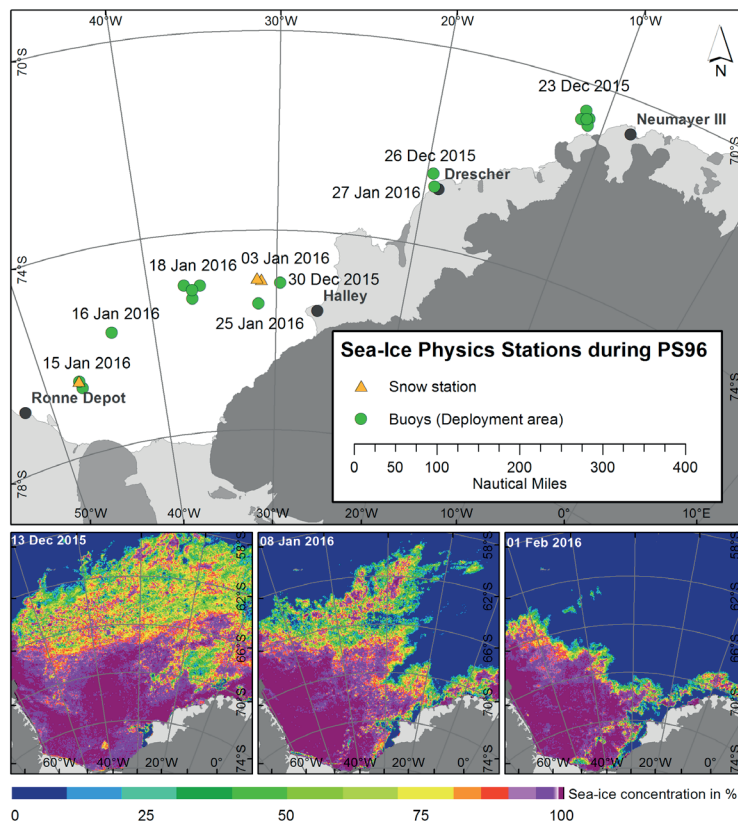


Fig. 3.1.2.1.1: Overview of all activities of the sea ice physics group during PS96. The dates in the main map indicate the respective deployment date. The three bottom panels show the sea-ice concentration from AMSR2 for the three given dates during the expedition. Not shown here: Hourly observations of sea ice conditions along the cruise track.

Tab. 3.1.2.1.1: Pangaea labels as used for sea-ice physics measurements during PS96

PANGAEA label	Description
Ship based	
ICEOBS	Ice Observations from ship bridge (along track)
Snow measurements	
SNOW	Summing-up of all snow measurements on one ice floe
SDMP	Snow Depth measured with Magna Probe
SPIT	Snow Pit
Buoys	
BUOY-IMB	Ice Mass Balance Buoy
BUOY-SNOW	Snow Depth Buoy
BUOY-SVP	Surface Velocity Profiler
BUOY-AWS	Autonomous Weather Station

3.1.2.2 Deployments of autonomous ice tethered platforms (buoys)

Grant No: AWI_PS96_01

Objectives

The investigation of physical sea-ice and snow parameters during work on one ice floe can only give a snap-shot of the sea ice conditions. In order to obtain also information about the seasonal and inter-annual variability and evolution of the observed ice floes, we deploy autonomous ice tethered platforms (buoys), which measure the sea ice and snow characteristics also beyond the cruise. Therefore, we use different kinds of buoys: Ice Mass Balance buoys (IMBs) deriving the sea ice growth; snow depth buoys measuring the snow accumulation over the course of the year; and Surface Velocity Profilers (SVPs) providing information on the local sea-ice drift. In addition, buoys are partly equipped with sensors measuring air and/or body temperature and sea level pressure. Additional information about local atmospheric parameter as temperature, humidity, wind velocity and direction, and incoming longwave and shortwave radiation are retrieved from Autonomous Weather Station, provided by the British Antarctic Survey (BAS). Combing all retrieved data, we will be able to enhance the understanding of sea-ice processes and feedback mechanisms in the ice-covered Weddell Sea.

Beyond the immediate value for our work, all SVP and snow buoys report their position together with measurements of surface temperature and atmospheric pressure directly into the Global Telecommunication System (GTS). Thus, these data may directly be used for weather prediction and numerical model applications.

Work at sea

Figure 3.1.2.2.1 and Table 3.1.2.2.1 give an overview about all deployed autonomous ice tethered platforms (buoys) during PS96 in the eastern and southern Weddell Sea.

3.1.2 Sea ice physics

In total we deployed 7 combined sets composed of an Ice Mass Balance buoy (IMB) and one snow depth buoy. The sets cover the area between Austasen (northern Weddell Sea) and the Ronne Depot (southwestern Weddell Sea). An additional IMB was deployed 10 nm in southern direction of the most southern set.

2 of these sets are surrounded by so-called drift arrays. The first drift array consists of 4 Surface Velocity Profilers (SVPs) and was deployed in the Austasen area (example picture: Figure 3.1.2.2 (a)). The second one consists of 3 SVPs. The distance between the center buoy set and the surrounding SVPs was for all buoys between 5 to 10 nm.

2 other buoy sets were combined with an Autonomous Weather Station (AWS) from the British Antarctic Survey (example picture: Figure 3.1.2.2 (b)). Due to technical issues, we were not able to align the first AWS with magnetic north. The third AWS was deployed on the fast ice in the Drescher Inlet together with an IMB.

To sum up, we deployed successfully 7 snow depth buoys, 9 IMBs, 7 SVPs and 3 AWSs. Except for the buoy deployments on the fast ice in the Drescher Inlet, all buoys were deployed by helicopter.

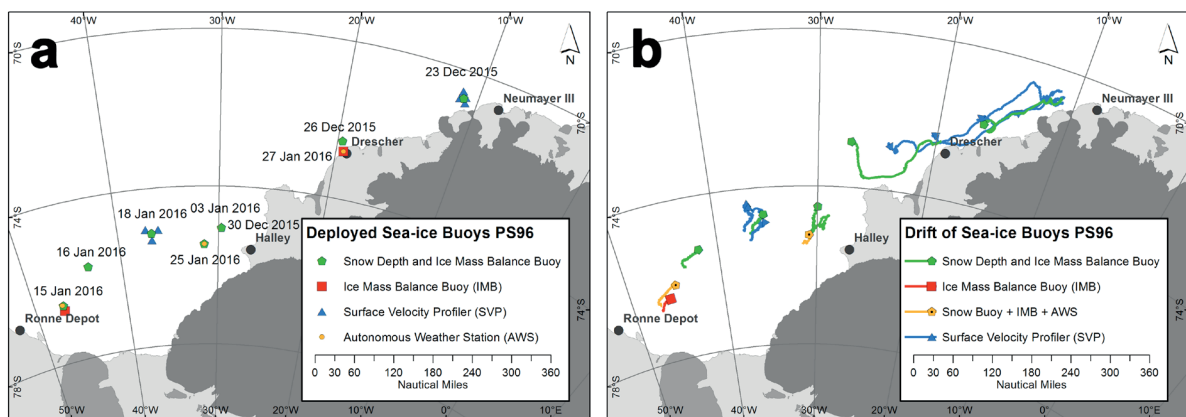


Fig. 3.1.2.2.1: (a) Overview of all deployed autonomous ice tethered platforms (buoys) during PS96. The given dates indicate the respective deployment date. (b) Drift pattern of all deployed buoys from their initial deployment position/date until 01 February 2016.



Fig. 3.1.2.2.2: (a) PS96/H009: Autonomous Weather Station (left), Ice Mass Balance buoy (middle), and snow depth buoy (right). (b) PS96/H001-BUOY-SVP-1: SVP buoy.

Tab. 3.1.2.2.1: List and initial positions of all deployed buoys during PS96. Buoy names are identical to their name in www.meereisportal.de, where all data and buoy information is available in real time, and how the buoys report into international networks.

Label	Date	Latitude	Longitude	Buoy name
PS96/H001-BUOY-IMB	2015-12-23	-70,6997	-11,0800	2015T26
PS96/H001-BUOY-SNOW	2015-12-23	-70,6988	-11,0791	2015S39
PS96/H001-BUOY-SVP-1	2015-12-23	-70,6718	-10,9314	2015P15
PS96/H001-BUOY-SVP-2	2015-12-23	-70,8090	-10,8840	2015P17
PS96/H001-BUOY-SVP-3	2015-12-23	-70,5352	-11,2634	2015P21
PS96/H001-BUOY-SVP-4	2015-12-23	-70,7310	-11,3806	2015P19
PS96/H002-BUOY-IMB	2015-12-26	-72,5452	-19,5769	2015T27
PS96/H002-BUOY-SNOW	2015-12-26	-72,5452	-19,5769	2015S42
PS96/H003-BUOY-IMB	2015-12-30	-75,0553	-29,7098	2015T28
PS96/H003-BUOY-SNOW	2015-12-30	-75,0542	-29,7071	2015S41
PS96/H005-BUOY-IMB	2016-01-15	-76,5502	-46,9345	2016T37
PS96/H005-BUOY-SNOW	2016-01-15	-76,5489	-46,9396	2016S38
PS96/H005-BUOY-IMB	2016-01-15	-76,6856	-46,9099	2016T36
PS96/H006-BUOY-AWS	2016-01-15	-76,5368	-47,0417	2016W01
PS96/H007-BUOY-IMB	2016-01-16	-75,7381	-43,4339	2016T41
PS96/H007-BUOY-SNOW	2016-01-16	-75,7378	-43,4361	2016S31
PS96/H008-BUOY-IMB	2016-01-18	-75,1420	-36,6038	2016T42
PS96/H008-BUOY-SNOW	2016-01-18	-75,1414	-36,6026	2016S37
PS96/H008-BUOY-SVP-1	2016-01-18	-75,3105	-36,6297	2016iSVP2
PS96/H008-BUOY-SVP-2	2016-01-18	-75,0378	-37,1791	2016P20
PS96/H008-BUOY-SVP-3	2016-01-18	-75,0626	-35,9549	2016P18
PS96/H009-BUOY-IMB	2016-01-25	-75,4750	-31,4081	2016T38
PS96/H009-BUOY-SNOW	2016-01-25	-75,4689	-31,3946	2016S40
PS96/H009-BUOY-AWS	2016-01-25	-75,4726	-31,4114	2016W03
PS96/087-BUOY-IMB	2016-01-27	-72,7978	-19,3448	2016T40
PS96/087-BUOY-AWS	2016-01-27	-72,7976	-19,3450	2016W02

Preliminary results

Snow depth buoys and IMBs:

The snow depth buoys measure the snow accumulation at four spots by sonar sensors whereas the main measuring device of the IMB is a thermistor string going through the ice into the water. By measuring the temperature and thermal conductivity every 2 cm, it is possible to identify the boundaries between ice and ocean, ice and snow and snow and air. Combining both data sets, information on snow depth changes, sea-ice growth and eventually estimates of flooding processes can be expected from the data.

Figure 3.1.2.2.3 gives an example for snow accumulation of the snow buoy 2016S38 for the time period from 15 January to 05 February 2016. During this time, there are barely any changes in the snow cover and meteorological data visible. End of January the local variability between the sensors increases which might be associated with the measured lower air pressure and

3.1.2 Sea ice physics

related snowdrift events. Sea-ice growth data from the IMBs will be only processed after the cruise. Finally, all data will be combined with findings of former deployments during PS82 (ANT-XXIX/9) and PS89 (ANT-XXX/2) to enhance our understanding of temporal and spatial variability in snow accumulation, sea-ice growth and eventually flooding of Antarctic sea ice.

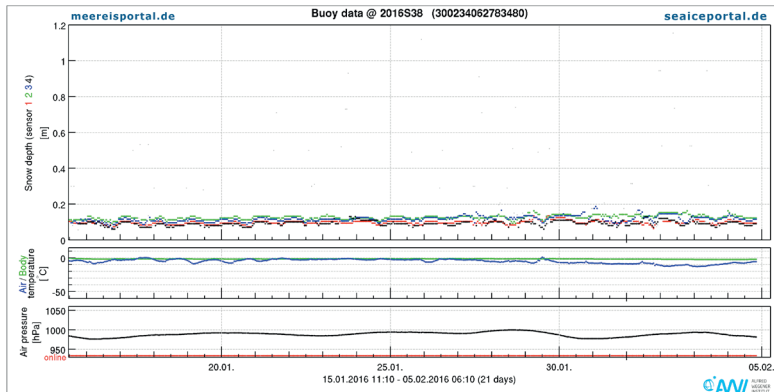


Fig. 3.1.2.2.3: Exemplary time series of snow depth along with information on meteorological conditions for snow depth buoy 2016S38, deployed on 15 January 2016.

Autonomous Weather Station (AWS):

Two AWS were deployed along with an IMB and snow depth buoy on moving sea ice. The third one was placed on the fast ice in the Drescher Inlet together with an IMB. The combination of all buoys will give the unique possibility to interpret snow accumulation and loss in terms of wind velocities and local solar radiation budgets calculated from the measurements of incoming shortwave and longwave solar radiation at each AWS.

Surface Velocity Profiler (SVP):

The SVP buoys will serve information on the sea-ice drift velocity and its seasonal behavior. As soon as the ice floe melts, the SVPs will pass over to the ocean and will measure ocean currents at the ocean surface.

Figure 3.1.2.2.4 shows the time series and histograms of drift velocities of the first drift array consisting of four SVPs from 23 December 2015 to 01 February 2016 deployed in the area of Austasen. Buoy 2015P15 stopped data transmission on the 15 January 2016 due to internal technical issues.

Although the buoys were deployed originally only 5 to 10 nm apart from each other, their drift pattern reveal obvious differences. Buoy 2015P19 shows from the beginning the highest drift velocities with a mean velocity of 0.21 m/s. The other three SVPs indicate similar drift velocities with a mean of 0.13 m/s. Associated to the variations in drift velocity, buoy 2015P19 travelled so far the longest distance of 381 nm within 41 days – compared to 228 nm (2015P17) and 267 nm (2015P21). All 3 buoys detect the strong storm in the area between the 15 and 17 January 2016.

Over the next months, the buoys will record further data from which we will calculate the sea-ice drift and deformation variability throughout the Weddell basin.

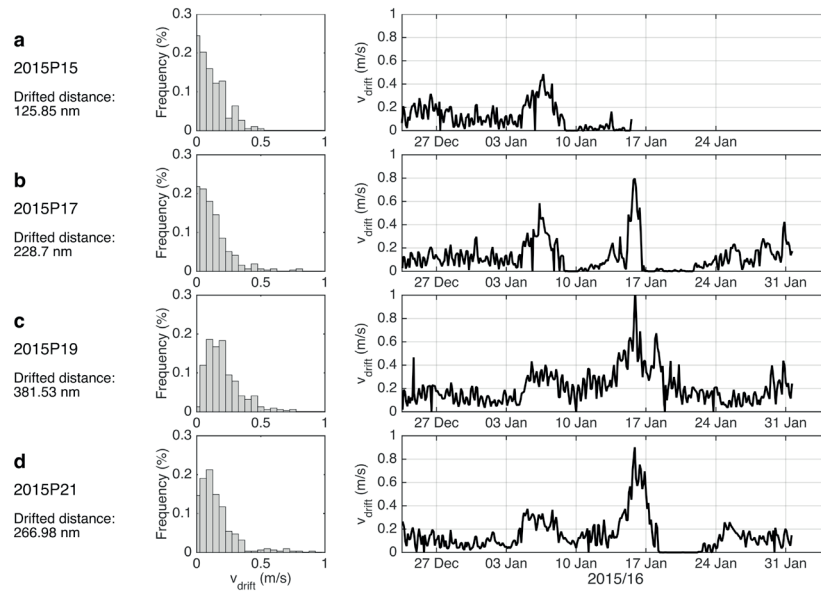


Fig. 3.1.2.2.4: Histograms and time series of drift velocities of SVPs of the first drift array deployed on 23 December 2015 until 01 February 2016. (a) PS96/H001-BUOY-SVP-1 (2015P15), (b) PS96/H001-BUOY-SVP-2 (2015P17), (c) PS96/H001-BUOY-SVP-4 (2015P19), and (d) PS96/H001-BUOY-SVP-3 (2015P21).

Data management

All buoy positions and raw data are available in near real time through the sea-ice portal www.meereisportal.de. At the end of their lifetime (end of transmission of data) all data will be finally processed and made available in PANGAEA. All SVP and snow buoys report their position and atmospheric pressure directly into the Global Telecommunication System (GTS). Furthermore, all data are exchanged with international partners through the International Program for Antarctic Buoys.

3.1.2.3 Physical properties of snow

Grant No: AWI_PS96_01

Objectives

Snow stratigraphy, physical snow properties and snow depth are highly variable even on small horizontal scales. These spatial and temporal variations in the snow pack characteristics (e.g. temperature, density, stratigraphy) and its dimension have a crucial impact on the energy and mass budget of Antarctic sea ice. Therefore, the snow pack on the different floes during PS96 is characterized in detail.

Both the snow stratigraphy and the snow depth data set will be used as ground truth for the interpretation of retrieved snow depth and snowmelt signatures from passive microwave data.

Work at sea

The work on physical snow properties and snow depth distribution was performed on two floes in the eastern Weddell Sea (Snow 01, 02) and on one floe in the southwestern Weddell Sea which was also used for sea-ice buoys deployments (Snow 03). Table 3.1.2.3.1 summarizes all snow measurements.

3.1.2 Sea ice physics

The physical snow parameters as well as the snow stratigraphy were obtained from snow pits. These were taken twice per ice floe at representative locations of the floe. The measurements were taken on the undisturbed shaded working wall of the snow pit. At first, the temperature was measured every 2 to 5 cm from the top (snow-air interface) to the bottom (snow-ice interface) with a hand-held thermometer (Testo). In a next step the different layers in the snow pack and its stratigraphic parameters were described. For each layer the snow grain size and type (e.g. rounded crystals, faceted crystals, depth hoar) is determined by the magnifying glass and a 1-to-3-mm grid card. In addition, every layer was characterized by its hardness with the following categories: fist (F), 4 fingers (4f), 1 finger (1f), pencil (p), and knife (k). Afterwards, the density of each layer was measured volumetrically by removing a defined snow block with a density cutter of snow from each layer (density cutter weight: 155 g, volume: 100 ml) and weighting it with a spring scale.

Transects of snow depth measurements on the ice were obtained on the same floe as the described snow pit measurements. These snow depth measurements were taken every 2 to 5 steps with a Magna Probe (Snow Hydro, Fairbanks, USA) in randomly chosen tracks on each floe.

All sampled ice floes were accessed via helicopter.

Preliminary results

Table 3.1.2.3.1 gives an overview about all done snow station work during P96. In total we sampled three ice floes with one transect of snow depth measurements (Magna Probe) and two snow pits at each site.

Figure 3.1.2.3.1 (a) shows the normalized histogram of snow depth on station PS96/SNOW-1. From sampled 348 snow depth measurements a mean snow depth of 26.8 ± 16.9 cm and modal snow depth of 21.7 cm is calculated. The maximum snow depth was 93 cm on that chosen floe. The snow pit PS96/H004-SPIT-1 was sampled in a representative area of the floe with a snow depth of 32 cm (Figure 3.1.2.3.1 (b)). The snow pack contained 3 different layers which were all characterized by destructive metamorphism (grain type II B1) with slightly rounded to faceted crystals which increased in size from the top layer (0.5-1mm) to lower layer (2-3 mm). This development of several layers and increasing grain size in the snow pack is also shown in the strong temperature gradient from -0.1°C (top) to -2.5°C (bottom).

Tab. 3.1.2.3.1: Overview about all snow measurements during PS96. Snow depth (zs) is given as a mean value for the snow depth transects with the Magna Probe (SDMP) and as local absolute value for the snow pit measurements (SPIT).

Label	Station	Date	Latitude	Longitude	zs (cm)
PS96/H004-SDMP-1	PS96/SNOW-01	2016-01-03	-74,9959	-31,1514	27
PS96/H004-SPIT-1	PS96/SNOW-01	2016-01-03	-74,9959	-31,1514	32
PS96/H004-SPIT-2	PS96/SNOW-01	2016-01-03	-74,9960	-31,1485	20
PS96/H004-SDMP-2	PS96/SNOW-02	2016-01-03	-74,9649	-31,4966	29
PS96/H004-SPIT-3	PS96/SNOW-02	2016-01-03	-74,9649	-31,4966	24
PS96/H004-SPIT-4	PS96/SNOW-02	2016-01-03	-74,9647	-31,4964	12
PS96/H006-SDMP	PS96/SNOW-03	2016-01-15	-76,5357	-47,0435	47
PS96/H006-SPIT-1	PS96/SNOW-03	2016-01-15	-76,5357	-47,0435	11
PS96/H006-SPIT-2	PS96/SNOW-03	2016-01-15	-76,5350	-47,0461	25

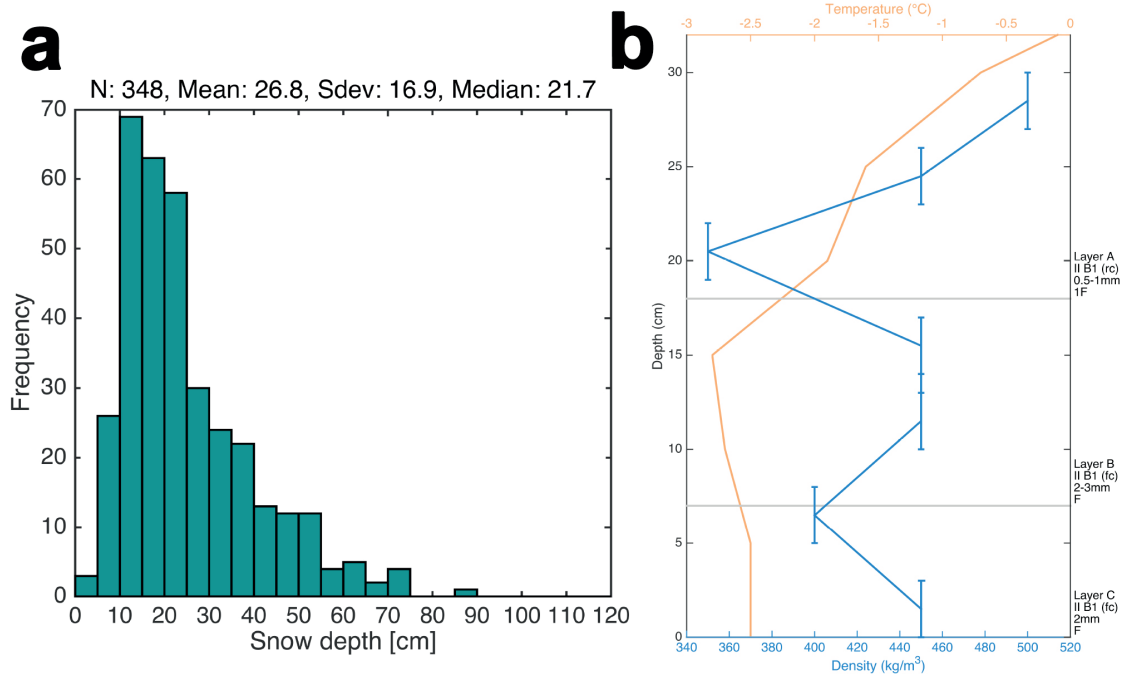


Fig. 3.1.2.3.1: First results of the example station PS96/SNOW-01 (03 January 2016): (a) Normalized histogram of snow depth (PS96/H004-SDMP-1) (b) Snow pit analysis from snowpit PS96/H004-SPIT-1. Temperature measurements are marked in orange, density measurements in blue. Grey lines indicate the interfaces between the different layers. The stratigraphy for each layer is given in the following sequence (example layer A): Layer label (A), grain type (II B1 (rc)), grain size (0.5-1mm), hardness (1F).

3.1.2.4 Along track observations of sea ice conditions

Grant No: AWI_PS96_01

Objectives

Over the last three decades, ship-based visual observations of the state of the sea ice and its snow cover have been performed over all seasons and serve the best-available observational data set of Antarctic sea ice. The recordings follow the Scientific Committee on Antarctic Research (SCAR) Antarctic Sea Ice Processes and Climate (ASPeCt) protocol and include information on sea-ice concentration, sea-ice thickness and snow depth as well as sea-ice type, surface topography and floe size. Those data are combined with information about meteorological conditions as air temperature, wind speed and cloud coverage. This protocol is a useful method to obtain a broad range of characterization and documentation of different sea-ice states and specific features during the cruise.

Work at sea

Every full hour during steaming, the sea-ice observations were carried out by trained scientists. The observations follow the ASPeCt protocol (Worby, 1999), with a software following the ASPeCt standard and being provided on a notebook on the ship's bridge. For every observation, pictures were taken in three different directions (portside, ahead, starboard).

Date, time and position of the observation were obtained from the DSHIP system, along with standard meteorological data (current sea temperature, air temperature, true wind speed, true

3.1.2 Sea ice physics

wind direction, visibility). The characterization of the ice conditions were estimated by taking the average between observations to port side, ahead and to starboard side. Ice thicknesses of tilted floes were estimated by observing a stick attached to the ships starboard side.

Preliminary results

We performed hourly sea-ice observations as soon as we passed the first sea ice on 13 December 2015 07 UTC at 58° 26.653' S and 1° 49.131' E. The ship left the sea-ice zone on 03 February 2016 09 UTC at 69° 20.823' S and 29° 12.377' W. Over the time period of 53 days, 544 individual observations were recorded. Sea-ice observations were skipped when the ship was stopped for station work (e.g. CTD, biology/ geology station) and several supplies at the shelf ice edge (*Neumayer III*, Drescher camp, Ronne Depot). Steaming west at the ice edge, we crossed small fields of drifting ice. As these fields increase in extent and volume, we restart the hourly sea-ice observations on 06 February 2016 10 UTC at 63° 42.473'S and 50° 1.586'W. The ship left sea-ice zone finally close to Paulet-Island on 08 February 2016 17 UTC at 63° 32.863'S and 55° 43.803'W. This second period of ice observations is not considered in the following statistics and plots as it was not part of the main working area.

The mean sea-ice concentration was calculated as 57.6 % with a mean level sea-ice thickness of 0.93 m and 0.45 m snow on top. Separating in ice age classes, the mean thickness of level first-year ice was 0.85 m with 0.28 m snow whereas level multi-year ice had a mean ice thickness of 1.59 m and 0.67 m snow on top. Figure 3.1.2.4.1 gives an overview about differences between the track from the marginal-ice zone to the Ronne Depot (from 13 December 2015 to 10 January 2016) and back from the Ronne Depot to the marginal-ice zone (from 14 January 2016 to 03 February 2016) for all three parameters.

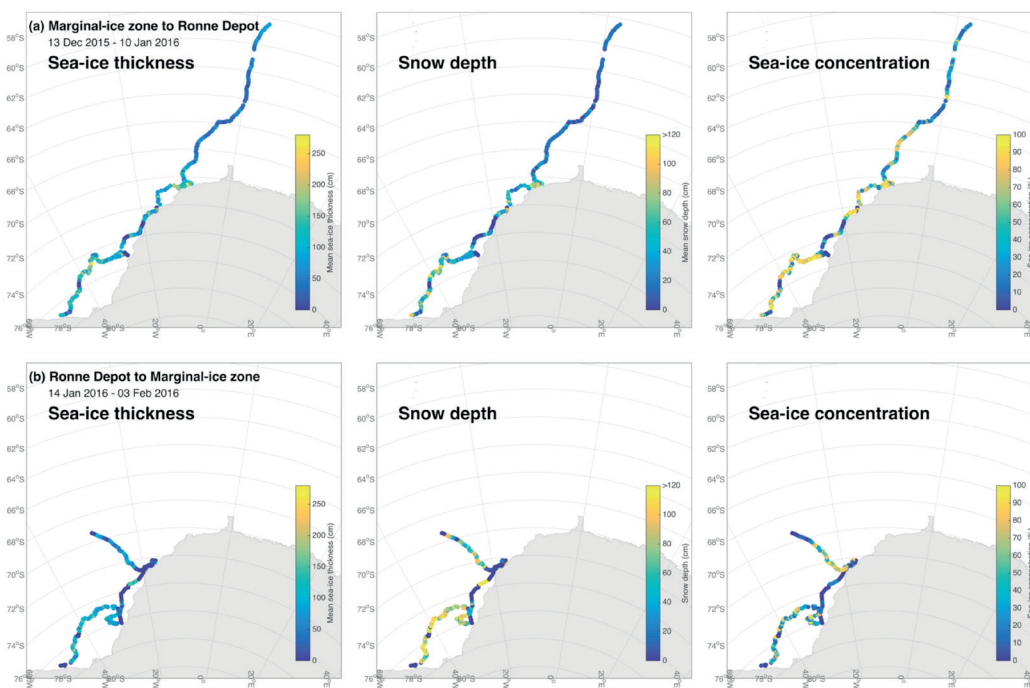


Fig.3.1.2.4.1: Sea-ice thickness, snow depth and sea-ice concentration from all ASPeCt sea-ice observations along the track separated into (a) Marginal-ice zone to Ronne depot, and (b) Ronne Depot to marginal-ice zone.

Data management

The visual sea-ice observations were already post-processed on board and will be published together with the taken pictures in PANGAEA within two months after the cruise.

References

Worby AP (1999) Observing operating in the Antarctic sea ice: *A practical guide for conducting sea ice observations from vessels operating in the Antarctic pack ice.*

3.1.2.5 Support of remote sensing data

Grant No: AWI_PS96_01

Objectives

The main objective of the planned extensive support of synthetic aperture radar (SAR) images of sea ice was to assist R/V *Polarstern* through the heavy ice conditions in the Weddell Sea, and thus give the possibility for an improved route planning during the expedition. Therefore, we defined areas of high interest with corresponding center points in advance for a better assessment of the sea-ice conditions in a time frame of days to weeks. These areas were mainly given by the planned cargo operations at *Neumayer III*, Drescher and the Ronne Depot.

The provision of Sentinel-1 images (C-Band) was coordinated and supported by Drift&Noise, whereas the data acquisition of the X-Band satellites TerraSAR-X (TSX) and TanDEM-X (TDX) were coordinated by the Earth Observation Center (EOC) of the German Aerospace Center (DLR).

Work at sea

We defined 6 main areas of interest for which we wanted to acquire as much Sentinel-1 images as possible for a successful route planning during the cruise. Figure 3.1.2.5.1 gives an overview about the defined center points.

The data acquisition of Sentinel-1 images started already mid of November 2015, before the expedition started, to track the ongoing changes in our defined areas of interest. During the expedition 3 additional center points were defined (at the marginal ice zone and two mooring positions next to the Antarctic peninsula) which were only used for a short time period. Furthermore, Sentinel-1 scenes were acquired and delivered when R/V *Polarstern* was in a Sentinel-1 scene.

During the entire acquisition time from 10 November 2015 until 07 February 2016 518 scenes were acquired and delivered via a ftp server to the ship. About a fifth of the delivered scenes were downloaded on board. The delivered scenes can be separated for the defined center points as the following: 89 scenes at center 1, 79 scenes at center 2, 58 scenes at center 3, 94 scenes at center 4, 106 scenes at center 5, 41 at center 6, 2 scenes at center 7, 3 scenes at center 8, 2 scenes at center 9, and 43 scenes centered around *Polarstern*.

The data acquisition of X-Band images from EOC started on 12 December 2015. From 12 December 2015 to 04 January 2016 R/V *Polarstern* received in total 13 stripes acquired from TanDEM-X and 1 stripe of TerraSAR-X consisting of up to 8 single scenes in order to get a general idea of the ice conditions in the area of interest. These data were delivered per mail from the EOC to the ship.

3.1.2 Sea ice physics

From 04 January 2016 onwards, the support in near-real time began. The TSX and TDX data has been received at DLR's German Antarctic Receiving Station *GARS O'Higgins* and has been locally processed to generate information products, which has been sent via email in near-real time within 1-2 hours after acquisition from *GARS O'Higgins* to the ship. Twice a day such NRT products were delivered to *R/V Polarstern*. In total, *Polarstern* obtained 47 NRT products from the TDX satellite and 8 products from the TSX satellite.

All images were geo-referenced and plotted in ArcGIS on board and were delivered to the captain and his crew to route the ship through the ice. In addition, the data were used from different working groups on board to plan the exact position of biological, geological and oceanographic stations dependent on the current ice situation.

In preparation to the cargo operations at *Neumayer III*, *Drescher* and the *Ronne-Depot* all acquired images were also provided for the AWI logistics.

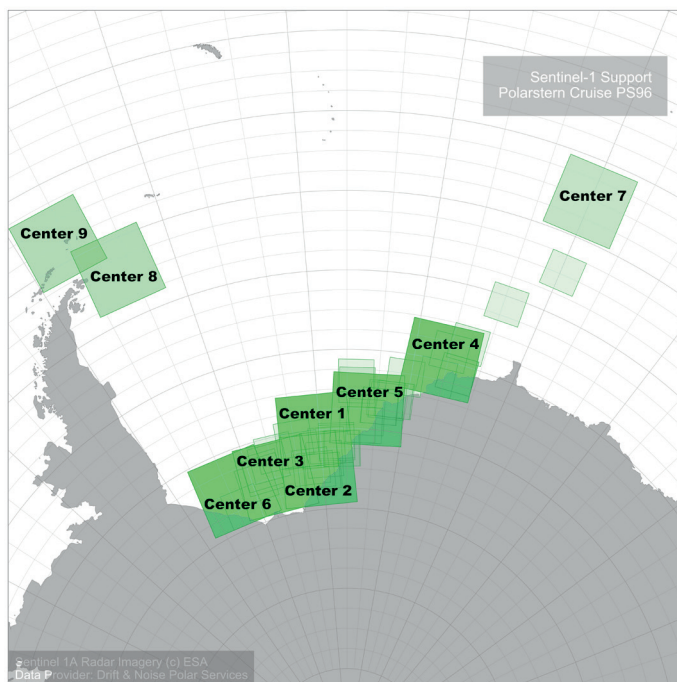


Fig. 3.1.2.5.1: Overview about the defined areas of interests (center point 1 to 9, big green squares) and all acquired and delivered scenes during PS96 (small squares in the background).

Data management

The TerraSAR-X and TanDEM-X data acquired during the cruise belongs to DLR. It will be available via the electronic EOWEB data catalogue of the DLR. Scientific users with an accepted TSX science proposal are allowed to use these data..

The Sentinel-1 data has been acquired by the European Space Agency (ESA) and were provided by Drift&Noise. The data are freely available for download from their Sentinel-1 Scientific Data Hub SciHub (<https://scihub.esa.int/>) without any retention period since the day of acquisition.

3.1.2.6 Isotope signature of water vapour

L.eonard Rossmann¹, J.-L. Bonne¹ (not on board), S. Kipfstuhl¹ (not on board), H. Meyer (not on board), B. Rabe (not on board), M. Werner (not on board), M. Behrens (not on board), L. Schönicke (not on board) ¹AWI

Grant No: AWI_PS96_01

Objectives

The CRDS instrument on board *Polarstern* in combination with surface water sampling provides a unique simultaneous data set of H₂¹⁸O and HDO in both ocean surface and the atmosphere directly above the ocean surface. Thus, the imprint of marine boundary conditions (e.g. temperature variations, circulation changes, or meltwater input) to the isotopic composition of the atmospheric water cycle can be directly measured. The results of these analyses will be of relevance for the interpretation of isotope signals found in ice cores and on terrestrial Antarctic sites in terms of past climate change.

Work at sea

During the PS96 expedition, the instrument has been continuously recording the isotopic composition of water vapour in ambient air, alternated with daily measurements of calibration standards. No troubles have been observed regarding the ambient air measurements. On the other side, several troubles have been encountered with the calibration standards delivery system since the last maintenance of the system in October 2015 in Bremerhaven. The long term heating of the oven where the vaporisation of the liquid standards takes place apparently altered the metallic ferules used to tighten the silicate capillaries, leading to the loss of several lines delivering the liquid standards. Due to the redundancy of these standards delivery lines, enough standards can still be measured to provide a calibration of the system. An adaptation of the system will be done during the next maintenance of the instrument, in May 2016 in Bremerhaven.

Preliminary results

Observations have been conducted continuously along the *Polarstern* track of the PS96 expedition, covering a transect from South Africa to *Neumayer Station III* and several weeks in the Weddell Sea.

An abrupt drop in humidity has been observed on the way from Africa to Antarctica (from 30 000 to 10 000 ppm), followed a few days later by a significant depletion of the water isotopic composition (from -10 to -30 ‰ in $\delta^{18}\text{O}$ values). From mid-December to end of January, the humidity observed in the Weddell Sea has been most of the time relatively stable (humidity around 5 000 ppm and $\delta^{18}\text{O}$ values between -20 and -30 ‰). An exception has been observed during a few days in mid-January, with an important cold synoptic event leading to very dry and isotopically depleted air. During this event, values similar to those observed in summer 2015 in the Arctic close to the North Pole have been reached (humidity of about 2000 ppm and $\delta^{18}\text{O}$ values between -40 and -50 ‰). A progressive increase of humidity and enrichment of water isotopes has been observed during the last days of transit from the Brunt ice shelf region towards the northern part of the Antarctica peninsula.

Data management

All humidity and isotope data of this project will be uploaded to the PANGAEA database after processing and post-operative calibration. Unrestricted access to the data will be granted within 2-3 years, pending analysis and publication.

3.1.3 Measurements of the atmospheric boundary layer using a wind lidar

Günther Heinemann, Rolf Zentek

Uni Trier

Grant No: AWI_PS96_01

DFG grant No: HE 2740/19 (SPP1158)

Objectives

The representation of the atmospheric boundary layer (ABL) in the Antarctic is a major challenge for numerical weather forecast models and regional climate models. Reference data sets are rare, particularly over the ocean areas. Particularly in the areas of coastal polynyas, the knowledge of wind profiles is of great interest, since the coupling of the ocean with the ABL determines sea ice production and associated formation of High-Salinity Shelf Water (Haid et al. 2015). The objectives of the group of the University of Trier were to measure vertical and horizontal profiles of wind, turbulence and aerosols in the Weddell Sea area for the verification of a regional climate model (COSMO-CLM, Ebner et al. 2014) and for process studies.

Work at sea

The main instrument was a “Halo-Photonics Streamline“ wind lidar, which is a scanner and can operate with a maximum range of 10 km, but was used only for a range up to 3600 m due to the low aerosol concentration in the Antarctic (Tab. 3.1.3.1). The operation principle of the lidar is backscattering at aerosol particles and the use of the Doppler effect. Values have been averaged for 1 to 10 seconds, depending on the signal strength. In addition to the number of pulse averages the beam focus was also adjusted in order to optimize the signal-to-noise ratio (SNR) as recommended by Hirsikko et al. (2014). The used lidar is a programmable scanner, which enables vertical scans in all directions. The main scan patterns were the vertical azimuth display (VAD), the range-height indicator (RHI) and horizontal scans with fixed azimuth (STARE). For some periods the Doppler Beam Swinging (DBS) mode was used in addition. Since the measured wind signal of a single beam is only the radial wind component (line-of-sight (LOS) wind), at least two different scan angles with respect to the wind vector are needed. We used the overlapping mode, i.e. the data are available at the original 3 m resolution of the pulses. The VAD is used for the determination of wind profiles above the lidar with eight scans with a zenith angle of 15° and 45° azimuth steps. The DBS mode is designed also for measurements of the wind profile, but uses only three directions. Some studies prefer the DBS mode compared to VAD, because it is faster (e.g. Lane et al. 2013), but the VAD is more robust (Päschke et al. 2015) particularly in the Antarctic environment with low backscatter. The STARE mode was used at two or three azimuth angles, which were adjusted to the heading of the ship and the wind direction. The RHI mode was generally applied together with the STARE mode and at the same azimuth angles. RHI scans were performed with different elevation angles up to 40°. This allows for measurements of e.g. the internal boundary layer at the sea ice edge or ice shelf front.

Wind lidar measurements on a ship have several limitations and problems. The ship's superstructure limits the available azimuth and VAD angles. The lidar was installed on the starboard side of the monkey deck at a height of 19 m above sea level (Fig. 3.1.3.1). This allows for unrestricted VAD scans as well as for STARE and RHI for 25°-170° to the starboard side. Scans to the portside were rather limited by instrument masts, stored material and the superstructure. When taking into account that the angle between two stares should be at least 20° in order to get a usable signal, only three possible azimuth angles were found for the STARE mode for the portside.

Tab.3.1.3.1: Characteristics of the lidar measurements

Wavelength	1.5 μm (eye-safe, class 1m)
Gate length	18 m
Points per gate	6 (overlapping)
Band width	± 19.4 m/s
Resolution	0.038 m/s
Threshold for signal-to-noise ratio (SNR)	variable (default -20 dB)
Measurement error	ca. 0.1 m/s (depending on SNR)
Pulse rate	15 kHz
Beam range	30-3600 m
Beam focus	variable (300-1800m)
Pulse averages	variable (15000-150000)
Scanning horizontal	0° to 360°
Scanning vertical	-15° to 90°

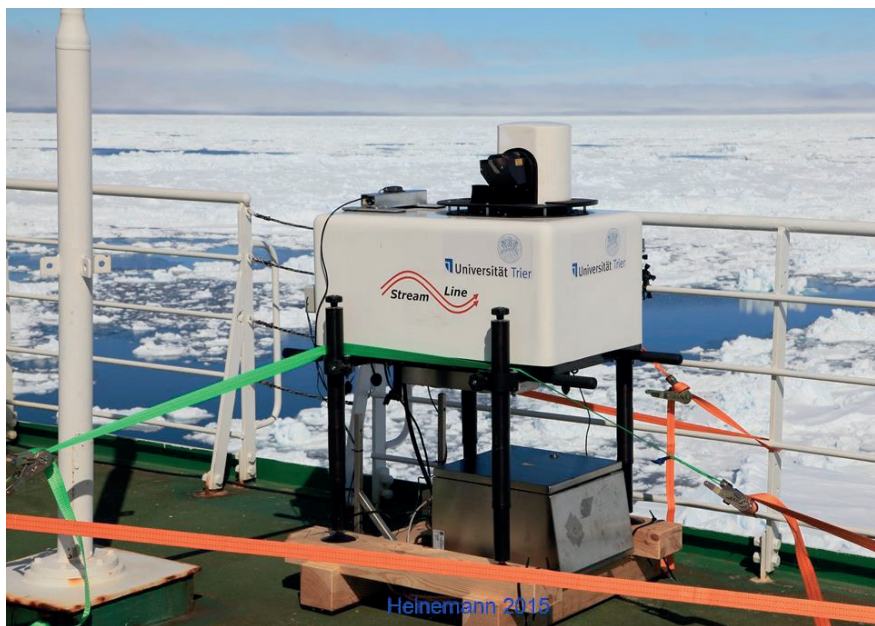


Fig. 3.1.3.1: Lidar on the starboard side

The second problem is to run a lidar on a moving ship, which requires to record the ship's heading, roll and pitch angles at exactly the same time as the measurements. This was achieved by using an Attitude Heading Reference System (AHRS, type XSENS MTi-G-700-GPS/INS), with measured position angles with up to 400 Hz. The time of the lidar computer was synchronized with an external GPS and checked against the ship's time server. Since the calibration of the magnetic field sensors of the AHRS turned out to be impossible due to the disturbance of the ship, a reliable heading could not be achieved, while roll and pitch angles were correct. We therefore used the low frequency (1 Hz) data from the ship's navigation system in addition to the AHRS data, which were found to sufficient with 10Hz. The surface and

3.1.3 Measurements of the atmospheric boundary layer using a wind lidar

weather conditions were monitored by an automatic camera (Gopro Hero 4) with photos taken every minute. In addition to the lidar measurements, the routine meteorological measurements of the ship and radiosonde data (Vaisala RS92, ascents 2-3 times daily, Vaisala 2013) were used (Tab. 3.1.3.2).

Tab. 3.1.3.2: Routine meteorological measurements on RV *Polarstern* (König-Langlo et al. 2006 with updates)

Quantity	Instrument	Height, position
Temperature and humidity	HMT 155 (Vaisala, Finland) mounted in radiation shield, not ventilated	29 m (portside and starboard)
Wind speed and direction	2D-sonic (Thies, Germany)	29 m (portside and starboard)
Cloud ceiling	cloud ceilometer CL51 (Vaisala, Finland)	20 m (portside, maximum range of 15000 m)
Water temperature	PT-100 (Thies, Germany)	-5 m (portside and starboard)
Global radiation	pyranometer (CM11, Kipp&Zonen, Netherlands)	34 m (craw's nest)
Visibility	FS11 (Vaisala, Finland)	20 m (portside, maximum range of 75000 m)
Pressure	electronic barometer (SETRA B270, Friedrichs, Germany)	16 m (reduced to sea level)
Precipitation	SRM 450 (Eigenbrodt, Germany)	34 m (craw's nest)

Preliminary (expected) results

The lidar was operated continuously between 23 December 2015 and 30 January 2016. Vertical profiles from VAD scans every 10min were the routine mode. Apart from periods of heavy ice breaking, dual STARE and RHI scans were performed adjusted for the ship's heading and wind direction. Fig. 3.1.3.2 gives an overview of the statistics of the different scanning modes

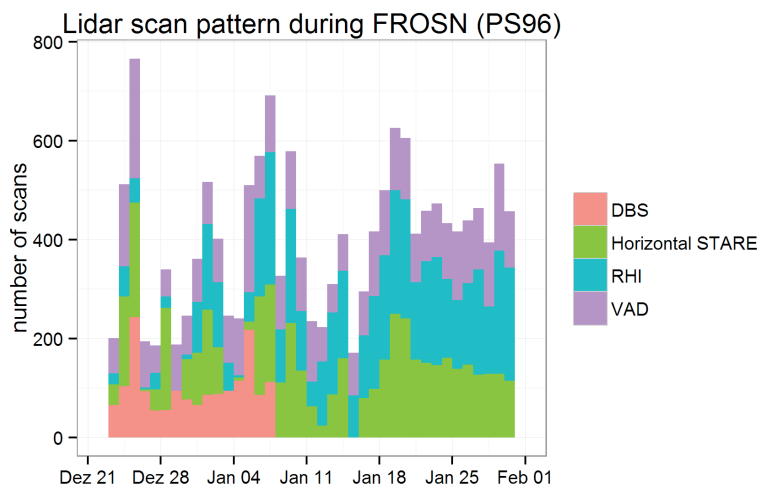


Fig. 3.1.3.2: Overview over the different scanning modes per day during FROSN

per day. As can be seen, the scan frequency was enhanced during biological stations or logistic operations, if the atmospheric conditions were suitable. The only meteorological special observation period was possible in the lee of iceberg A23A on 17 January 2016 between 0400 and 0900 UTC.

As an example of the data availability Fig. 3.1.3.3 shows VAD wind speed profiles for the

measurement period. Data gaps result from insufficient signal-to-noise ratios, which are excluded by a preliminary quality check. The vertical range is generally limited to the height of the atmospheric boundary layer of a few hundred meters, larger heights are reached, if clouds are present. A more detailed picture is shown in Fig. 3.1.3.4 for the situation in the lee of iceberg A23A on 17 January 2016. During this period, two low-level jets (wind maximum in the atmospheric boundary layer) could be measured. The next steps for data evaluation will be detailed studies of specific events, intercomparison with the radiosonde profiles and the processing of the data for the verification of the regional climate model.

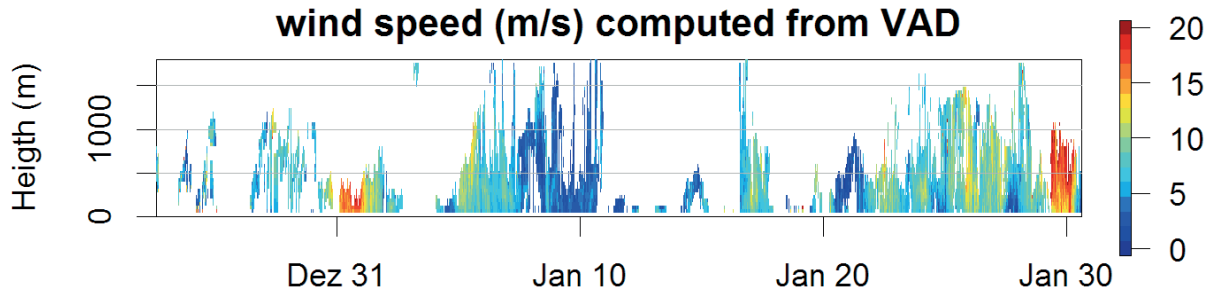


Fig. 3.1.3.3: Overview over VAD wind speed profiles during the measurement period

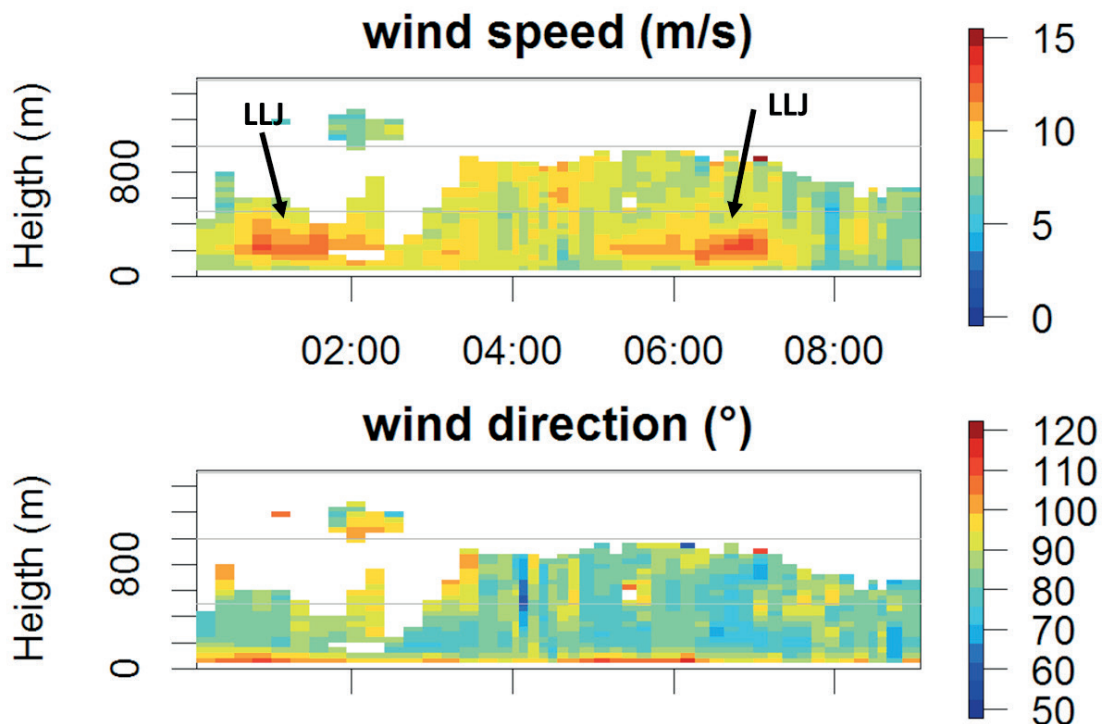


Fig. 3.1.3.4: VAD wind profiles during the period 00-09 UTC on 17 Jan. 2016. The two low-level jet events are indicated by LLJ

Data management

All lidar data will be stored at data servers of the University of Trier. After a thorough quality control, processing and publication in a peer reviewed journal, the processed data will be stored in the PANGAEA data base.

References

- Ebner L, Heinemann G, Haid V, and Timmermann R (2014) Katabatic winds and polynya dynamics at Coats Land, Antarctica. *Antarctic Science* 26:309-326, doi: 10.1017/S0954102013000679.
- Haid V, Timmermann R, Ebner L, and Heinemann G (2015) Atmospheric forcing of coastal polynyas in the southwestern Weddell Sea. *Antarctic Science* 27:388-402. doi:10.1017/S0954102014000893.
- Hirsikko A, O'Connor EJ, Komppula M, Korhonen K, Pfüller A, Giannakaki E, Wood CR, Bauer-Pfundstein M, Poikonen A, Karppinen T, Lonka H, Kurri M, Heinonen J, Moisseev D, Asmi E, Aaltonen V, Nordbo A, Rodriguez E, Lihavainen H, Laaksonen A, Lehtinen KEJ, Laurila T, Petäjä T, Kulmala M, and Viisanen Y (2014) Observing wind, aerosol particles, cloud and precipitation: Finland's new ground-based remote-sensing network. *Atmos. Meas. Tech.* 7:1351–1375, doi:10.5194/amt-7-1351-2014.
- König-Langlo G, Loose B, and Bräuer B (2006) 25 Years of Polarstern Meteorology. *WDC-Mare Reports* 0004, Alfred Wegener Institute for Polar and Marine Research, ISSN 1611-6577, 137pp.
- Lane S, Barlow JF, and Wood CR (2013) An assessment of a three-beam Doppler lidar wind profiling method for use in urban areas. *J. Wind Eng. Ind. Aerod.* 119:53–59, doi:10.1016/j.jweia.2013.05.010, 2013.
- Päschke E, Leinweber R, and Lehmann V (2015) An assessment of the performance of a 1.5 μm Doppler lidar for operational vertical wind profiling based on a 1-year trial. *Atmos. Meas. Tech.*, 8: 2251–2266, doi:10.5194/amt-8-2251-2015.
- Vaisala (2013) Radiosonde RS92-SGP, data sheet, available at: <http://www.vaisala.com/Vaisala%20Documents/Brochures%20and%20Datasheets/RS92SGP-Datasheet-B210358EN-F-LOW.pdf>, last access: 24 January 2016.

3.1.4 Hydroacoustics and geology

3.1.4.1 Bathymetry

Jan Erik Arndt¹, Jean-Guy Nistad¹, Claus-Dieter Hillenbrand², Hannes Grobe¹

¹AWI,
²BAS

Grant No: AWI_PS96_01

Objectives

Only about 15.4% of the Antarctic bathymetry has been surveyed by swath bathymetric systems (Arndt et al. 2013). High resolution data of the seafloor topography, however, has impact on various disciplines of marine research including oceanography, biology and geosciences. In geosciences, the seafloor topography can provide insights into geological processes that were active during its formation. On formerly glaciated continental shelves, submarine features produced by glacial processes can be revealed by swath bathymetric data. These submarine glacial features provide important clues for reconstructing the former extent and the retreat dynamics of ice sheets during and after past glaciations and the influences on past global sea-level changes. Studies on submarine glacial features in the Filchner Trough and the adjacent Cray Fan as well as on the shelf north of the Ronne Ice Shelf relied, so far, on limited data availability (Gales et al. 2014, Larter et al. 2012, Stollendorf et al. 2012, Hillenbrand et al. 2014) and additional swath bathymetric data is needed to improve our understanding of the past glacial system in the southern Weddell Sea embayment.

In addition, the observed high resolution bathymetric data also directly supports scientists from other disciplines on board by delivering accurate and up to date depth information for vessel positioning and decision-making.

Work at sea

Bathymetric surveying took place during the entire cruise with the hull mounted *ATLAS Hydrosweep DS3* multibeam echosounding system. The system was controlled using *ATLAS Hydromap Control*. The *Hypack* program suite was used for on the fly visualization of the acquired data. Data storage was performed with *ATLAS Parastore* and additionally with *Hypack*. Data processing and cleaning was subsequently performed in *CARIS Hips and Sips*. The cleaned data was gridded and visualized in *QPS Fledermaus* software and afterwards converted to *ArcGIS* compatible files.

Preliminary (expected) results

Preliminary investigation of the bathymetric data acquired during this cruise shows that large parts of the continental shelf seafloor have been reworked by grounded icebergs (Fig. 3.1.4.1.1). In areas of the shelf that are topographically protected from iceberg keel impacts, the seafloor is undisturbed and occasionally subglacial landforms produced by grounded ice, such as mega-scale glacial lineations and grounding zone wedges, were mapped that will provide information on the past glacial system. The bathymetric data acquired during this cruise is envisaged to be combined with other previously acquired bathymetric data to achieve a most comprehensive compilation of high resolution bathymetry. This dataset will then be systematically investigated for submarine glacial landforms that hence will improve our knowledge of the past glacial system on the shelf north of the Filchner-Ronne Ice Shelf and on parts of the East Antarctic continental shelf.

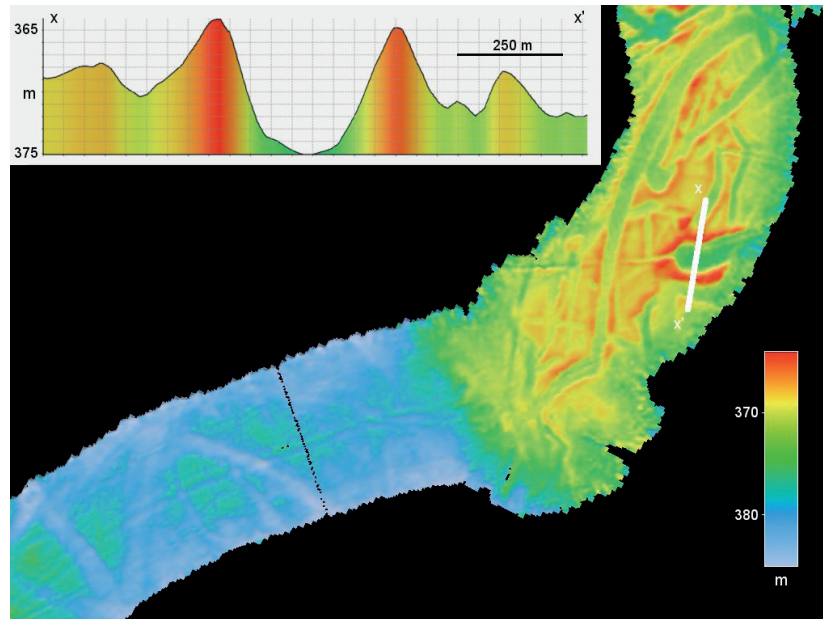


Fig. 3.1.4.1.1: Different forms and directions of iceberg ploughmarks observed in swath bathymetry (below) and bathymetric cross profile of a single ploughmark (above).

In addition, the newly acquired bathymetric data will also be incorporated in upcoming bathymetric compilations such as the International Bathymetric Chart of the Southern Ocean (Arndt, 2013) to improve the models of general seafloor morphology.

Data management

All acquired bathymetric data will be stored in PANGAEA.

3.1.4.2 Sub-bottom Profiling

Jan Erik Arndt¹, Claus-Dieter Hillenbrand²,
Hannes Grobe¹, Jean-Guy Nistad¹

¹AWI,
²BAS

Grant No: AWI_PS96_01

Objectives

The sub-bottom profiler data give information about the stratigraphy of the seabed directly underlying the seafloor. A comprehensive investigation of submarine glacial landforms strongly relies on the geological composition of the substrate to understand the processes active during their formation. In addition, the presence/absence and thickness of a sedimentary drape overlying the subglacial landforms enables an estimation of the relative timing of the different glacial and depositional processes.

Work at sea

Sub-bottom profiler data was acquired with the hull mounted *ATLAS Parasound P-70* system during the entire cruise. *Parasound* can resolve sediment layers of up to 200 m depth below seafloor by using a combination of high frequency (~20 kHz) and low frequency (~4 kHz)

signals. The system was controlled using *ATLAS Hydromap Control*. Both frequencies were acquired and displayed during the entire cruise with *ATLAS Parastore* and were used to identify suitable locations for coring devices.

Preliminary (expected) results

The features described by the swath bathymetric data are also detected in the sub-bottom profiler data. Figure 3.1.4.2.1 shows an area that has been disturbed by numerous iceberg ploughing events. Draping sediment layers up to several meters thick were identified on some submarine glacial landforms. The sub-bottom profiler data showed that morphologic wedges mapped by multibeam bathymetry consist of an acoustically transparent unit. These sedimentary features were likely formed as “grounding-zone wedges” (GZWs) at the ice margin during a stillstand of the grounding zone over hundreds or thousands of years (e.g. Batchelor & Dowdeswell 2015).

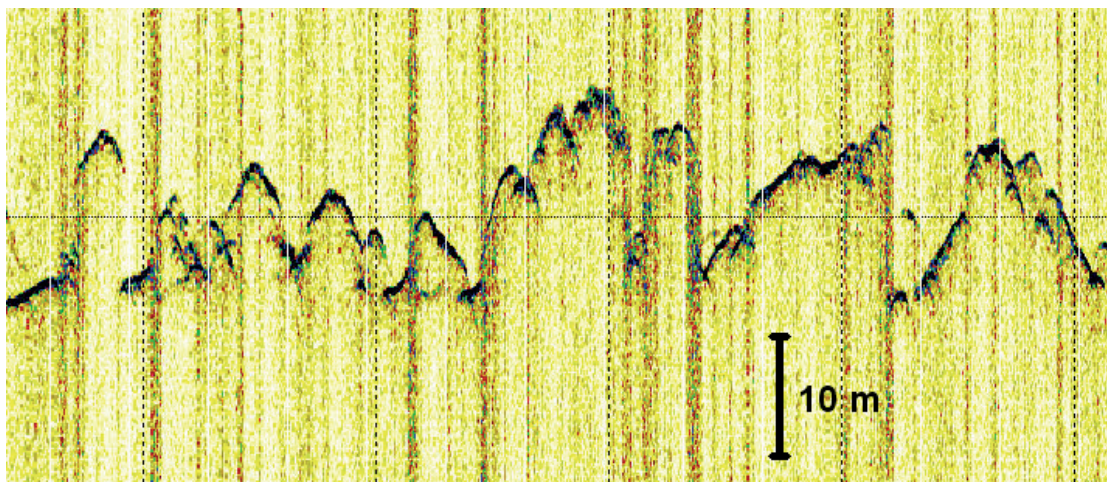


Fig. 3.1.4.2.1: Sub-bottom profiler data of an iceberg disturbed area in about 700 m water depth.

Data management

All acquired sub-bottom profiler data will be stored in PANGAEA.

3.1.4.3 Geological sampling

Hannes Grobe¹, Claus-Dieter Hillenbrand², Jan Erik Arndt¹, Jean-Guy Nistad¹

¹AWI,
²BAS

Grant No: AWI_PS96_01

Devices deployed for geological sampling were a large box corer (GKG) and a 1.5 t gravity corer (GC) equipped with a 3 m core barrel. The GKG was deployed on 14 stations, the GC was used on 12 stations with a total recovery of 15 m. The GC failed just once to recover sediment as it fell over because of the presence of a hard ground below a ca. 25 cm thick surface of soft sediment, which was washed out. Three GKGs were deployed for biological sampling.

3.1.4 Hydroacoustics and geology

In principle, the GKG was sampled with three subcores in standard PVC-liners (12 cm diameter) and three surface samples from the uppermost centimetre (0-1 cm) - as far as sufficient material was available. From five GKG stations only a bulk sediment sample was taken due to disturbance of the sediment surface, draining of seawater through the sample or insufficient sediment recovery. One surface sample was kept frozen for the investigation of biomarkers (BAS). Cores and surface samples were stored at 4°C and will partly be investigated sedimentologically at AWI or archived in the AWI core repository.

Due to initial problems with the operation of the GKG, the 20 t-swivel (Hagenuk DW50/200, 15 kg) was exchanged against a lighter 12 t-warbel (Gunnebo SKLI-18/20-B, 7.3 kg). After this change, the GKG triggered reliably.

Objectives

Marine sediment cores on cruise PS96 were collected for two main objectives. The first objective was the recovery of long sedimentary sequences by gravity coring for reconstructing the poorly known glacial history of the continental shelf in the southern Weddell Sea (e.g. Hillenbrand et al. 2014), especially the extent of grounded ice at the Last Glacial Maximum (LGM; ca. 25-19 ka before present) and the timing of subsequent ice-sheet retreat, and for identifying the geological composition of subglacial bedforms mapped by swath bathymetry (see above). The following target areas had been identified before the cruise: i) Filchner Trough, especially its western flank and subglacial bedforms mapped on previous expeditions (Larter et al. 2012, Stollendorf et al. 2012), and ii) the area north of the Ronne Ice Shelf. The second objective was the opportunistic collection of seafloor surface sediment samples by box coring for characterising the grain-size, geochemical and mineralogical composition of the seabed on the continental shelf, supplementing with these data sets previous compilations of seafloor surface sediment parameters in the Weddell Sea (Melles et al. 1995) and relating the results to environmental conditions (e.g., flow paths of deep and bottom water masses, bottom current strength, biological production, glaciological processes, etc.).

Tab. 3.1.4.3.1: Geological sampling sites with a total recovery of 15 m. (Abbreviations: SL=Schwerelot [gravity corer], GKG=Großkastengreifer [large box corer])

Station	Gear	Rec. [m]	Description	Samples	SL [m]
PS96/008-3	GKG	0,34	0-6 cm soft mud, 6-34 stiff grey gravelly mud	3 subcores, 3 kautext surface 0-1 cm, 1 seefeder for 14C	388
PS96/016-2	GKG	0,20	0-5 cm soft sandy mud, 5-20 stiff grey gravelly mud	3 subcores, 3 kautext surface 0-1 cm	582
PS96/017-2	GKG	0,05	mixed up, no sampling		591
PS96/017-3	GKG	0,15	shared with biology	1 subcore	586
PS96/017-4	GKG	0,00	failure, not released, warbel exchanged		589
PS96/017-5	GKG	0,15	tilt surface, runoff	1 surface sample	589
PS96/026-6	GKG	0,28	0-16 cm sandy mud 5Y5/2, 16-28 stiff sandy, gravelly mud	3 subcores, 3 surface samples	400
PS96/026-12	SL	0,00	20 cm penetration, tilt, core catcher washed out		407

3.1 Oceanographic, Meteorologic, and Geologic Investigations

Station	Gear	Rec. [m]	Description	Samples	SL [m]
PS96/027-5	GKG	0,20	fine sand, 5Y4/3, surface lost (leaking)	bulk surface sample	291
PS96/027-6	GKG	0,20	fine sand, 5Y4/3, surface lost (leaking)	used by biology	296
PS96/037-7	GKG	0,43	soft mud above stiff till	3 subcores, 3 surface samples	278
PS96/037-10	SL	1,10	very stiff till	0-10 cm in kautex, 10-100 core segment	385
PS96/048-6	GKG	0,30	soft mud above stiff till	1 surface sample in kautex, 0-1 cm, used by biology	468
PS96/061-3	GKG	0,35	sandy mud with dropstones, box disturbed		455
PS96/061-4	SL	1,19		0-24, 24-119 cm	458
PS96/063-2	SL	0,73	1.5 m penetration, tilt, cc did not fully work, part lost	0-73	464
PS96/066-2	SL	0,73		0-73	454
PS96/069-2	SL	1,31	penetration ab. 2.5 m, surface destroyed	0-31, 31-131, surface in kautex	706
PS96/071-2	SL	1,24	surface disturbed	0-24, 24-124, surface in kautext	730
PS96/072-6	SL	1,26		0-35, 35-126	734
PS96/079-3	SL	1,81	slightly bended but ok, next site used again	0-94, 94-181	747
PS96/080-1	SL	2,23	surface disturbed	0-23, 23-123, 123-223, surface in kautext	720
PS96/090-8	GKG	0,20	100 covered by organism fragments	test deployment after repair, sample used by biology	296
PS96/090-10	SL	0,20		tile, one segment 0-20 cm	299
PS96/104-4	GKG	0,25	90 % coverage of sponges and bryozoans	1 bulk surface sample	304
PS96/104-6	SL	0,10	fragments of sponges and bryozoans	tilt, no samples	306
PS96/115-2	MUC	0,25		1 subcore (0-25), surplus subcores preserved for biology	394
Total recovery		15,00			

Work at sea

Due to a combination of severe sea-ice conditions throughout cruise PS96 and logistical tasks, which put major constraints on the locations and the timing of both geomorphological mapping using swath bathymetry and station work involving the deployment of heavy gear, the box and gravity coring activities had to be undertaken mainly on an opportunistic basis (Fig. 1.1 location

map). A gravity coring transect across Filchner Trough near the transition from the middle to outer shelf started at the eastern flank of the trough and reached its deeper part but could not be extended further westward because of heavy sea-ice coverage. A stacked GZW mapped within Filchner Trough was targeted with two gravity cores. All other box and gravity corer deployments had to be undertaken in open leads and polynyas elsewhere on the continental shelf in the Weddell Sea embayment and offshore from Dronning Maud Land and east of the Antarctic Peninsula.

Preliminary (expected) results

Most of the gravity and box corers deployed on expedition PS96 recovered only relatively short sedimentary sequences (Table 3.1.4.3.1). The reasons for the restricted core recoveries comprise the presence of a very hard sub-bottom layer directly under the seafloor, which is either a 'stiff till' deposited and overconsolidated by slowly flowing grounded ice at some time during the past (e.g., East Antarctic shelf) or an 'iceberg turbate' resulting from the overcompaction of seafloor sediments by grounded icebergs (e.g., areas where multibeam data revealed iceberg ploughmarks), and the widespread occurrence of very coarse grained, mainly sandy seafloor sediments (e.g., shelf directly offshore from the Ronne Ice Shelf).

The sediment cores retrieved on behalf of the marine geological program of cruise PS96 were neither split nor investigated on board. Consequently, any results from sedimentological, geochemical or mineralogical analyses carried out after the cruise will be reported in future publications. It is expected that the post-cruise analyses of the collected core material will be able to achieve the first objective of the geological coring activities on cruise PS96 (as outlined above) only in part while fully achieving the second objective.

Data management

All metadata and post-cruise analytical data from sediment cores collected during expedition PS96 will be stored in the PANGAEA data repository.

References

- Arndt J E et al. (2013) The International Bathymetric Chart of the Southern Ocean (IBCSO) Version 1.0 – A new bathymetric compilation covering circum-Antarctic waters. *Geophysical Research Letters* doi:10.1002/grl.50413.
- Batchelor CL and Dowdeswell JA (2015) Ice-sheet grounding-zone wedges (GZWs) on high-latitude continental margins. *Marine Geology* 363, doi: 10.1016/j.margeo.2015.02.001.
- Gales JA et al. (2014) Large-scale submarine landslides, channel and gully systems on the southern Weddell Sea margin, Antarctica. *Marine Geology* 348:73 , doi: 10.1016/j.margeo.2013.12.002.
- Hillenbrand CD et al. (2014) Reconstruction of changes in the Weddell Sea sector of the Antarctic Ice Sheet since the Last Glacial Maximum. *Quaternary Science Reviews* 100, doi: 10.1016/j.quascirev.2013.07.020.
- Larter RD et al. (2012) Late Quaternary grounded ice extent in the Filchner Trough, Weddell Sea, Antarctica: new marine geophysical evidence. *Quaternary Science Reviews* 53:111, doi: 10.1016/j.quascirev.2012.08.006.
- Melles M et al. (1995) *Polarforschung* 64 (2), 45-74.
- Stolldorf T et al. (2012) LGM ice sheet extent in the Weddell Sea: evidence for diachronous behavior of Antarctic Ice Sheets. *Quaternary Science Reviews* 48:20, doi: 10.1016/j.quascirev.2012.05.017.

3.2 Biological and Ecological Investigations

3.2.1 Phylogeny, phylogeography and population genetics of high Antarctic biota

Kevin M. Kocot¹, Henrik Christiansen², Rebeca Zapata Guardiola³, Chester Sands⁴, Christoph Held¹ (not on board)⁵

¹ UA,
² KU Leuven,
³ ICM-CISIC,
⁴ BAS,
⁵ AWI

Grant No: AWI_PS96_02

Objectives

The objectives of the PS96 Genetics Group was to improve understanding of Antarctic animal diversity, distribution, population genetics/phylogeography, phylogeny, and genomics. Although each of the members of this team have different backgrounds and taxonomic expertise, we all share an interest in understanding how marine organisms are genetically and physically structured in the Southern Ocean.

Most members of the Genetics Group are interested in population genetics and phylogeography of Antarctic animals. Understanding the genetic diversity among populations of an organism and how this diversity is structured with respect to geography is important for understanding the effects of geographical barriers and depth as well as the possible future effects of climate change on biological diversity (e.g., Brandt et al. 2007). Samples from the southern Weddell Sea, particularly the under-sampled Ronne-Filchner region, along with samples from other regions of Antarctica will help improve understanding of the genetic diversity and large scale connectivity (or lack thereof) of diverse Antarctic animals. Samples collected during PS96 will also be important with respect to testing the hypothesis that one or more seaways previously connected the Weddell Sea to the Amundsen and/or Ross Seas (e.g., Vaughan et al. 2011). Specifically, the principle objectives for this group during PS96 were to 1) to determine whether genetic variation as identified by divergent mitochondrial cytochrome c oxidase subunit 1 (CO1) lineages is indicative of speciation or whether it is retained ancestral polymorphism, 2) to identify any genetic differentiation that may be present due to different ecological conditions (e.g. depth, substrate type, water mass), 3) compare relative divergence times between lineages to determine whether the divergence events are likely to be due to a common historical event or lineage-specific factors. We aimed to collect benthic megafauna, especially echinoderms, crustaceans, cnidarians and pycnogonids from a variety of locations maximizing the replication of depth and bottom temperature profiles.

Additionally, the Antarctic has a diverse fauna including many lineages that are endemic, have undergone major radiations within Antarctica, or are more common in the Antarctic than in the rest of the world. In addition to phylogeography and population genetics work, we also sought to collect specimens of groups of interest for various projects dealing with taxonomy, phylogeny, and comparative and evolutionary genomics. Specific goals for this work were to:

1. provide specimens for the sequencing of a scaphopod genome,
2. contribute specimens to ongoing projects addressing the phylogeny of Aplacophora, Polyplacophora, and Scaphopoda,
3. contribute specimens to an ongoing project examining the evolution of biomineralization in Mollusca using transcriptomics,

3.2.1 Phylogeny, phylogeography and population genetics of high Antarctic biota

4. contribute to projects addressing deep metazoan phylogenetics using a phylogenomic approach, and
5. description of new species of aplacophoran molluscs and documentation of species distribution.

Work at sea

Macro- and megabenthic fauna were collected with an Agassiz trawl (AGT) or a Bottom Trawl (BT). The AGT weighs 500 kg, measures 3.5 m across, and has a net with a mesh size of 10 mm in the cod end (Alvaro et al. 2013). Trawling with the AGT was conducted as previously described by Alvaro et al. (2013) and Kersken (3.2.3; this cruise report). Details on BT deployments are provided by Mark et al. (this cruise report). GPS coordinates and depths of all AGT and BT deployments are presented by Kersken (3.2.3; this cruise report). In total, we collected specimens from 10 deployments of the AGT and 6 deployments of the BT (Fig. 3.2.1.1). We were also opportunistic and additionally obtained specimens from a box corer (GKG) deployment that could not be used for subsample coring, a multicorer (MUC) core that could not be used for experiments, and even a giant hydroid growing on a mooring and a benthic ctenophore tentacle stuck to the arm of the remotely operated vehicle (ROV) were sampled.

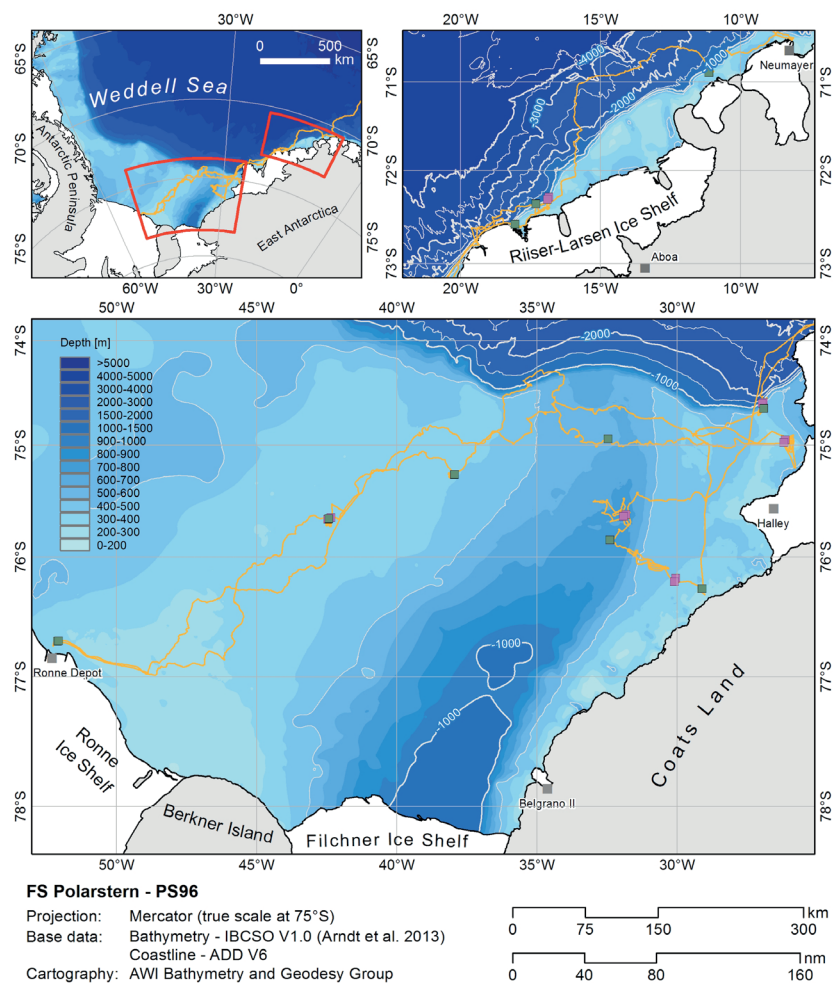


Fig. 3.2.1.1: Stations sampled by AGT (green boxes) and BT (pink boxes) during PS96

Although each researcher of the team has a taxon or select set of taxa of interest, we were opportunistic in our sampling and took advantage of the biological diversity recovered by fixing specimens or tissue samples of as many species as possible. Sufficient numbers of specimens or tissue samples for population genetics or phylogeography studies were taken whenever possible. Sorting was performed as quickly as possible keeping specimens in buckets of cold seawater on the deck as much as possible. Taxa known to possess endogenous nucleases that result in rapid degradation of DNA upon death (e.g., crustaceans and Ophiuroidea) were given top priority during sorting to ensure that the collected specimens will be suitable for any downstream nucleic acid-based studies. Most specimens were photographed with a scale and their label and identified as accurately as possible in a short amount of time. Fixation of specimens followed a standard approach where morphological vouchers were preserved using the best method for that taxon (usually fixation in 10% formalin followed by later transfer to 70% ethanol for storage) and specimens or tissue samples were fixed for molecular work using 96% ethanol (DNA-based work), RNAlater (DNA- or RNA-based work), or simply by freezing tissue samples at -80°C (DNA-, RNA-, and protein-based work as well as genome size estimation) or -20°C (DNA-based work).

Preliminary (expected) results

Sampling focused on representatives of key groups of interest. However, for all taxa except Holothuroidea, Tunicata, Bryozoa, and Pterobranchia, at least one specimen of each megafaunal species collected was saved from each station. In total 1,699 lots of specimens were collected. We define a lot as a container or vial containing one specimen, multiple specimens, or a tissue sample from a specimen. Specimens representing 17 phyla were collected (Table 3.2.1.1). Preliminary and expected results will be summarized on a taxon-by-taxon basis for key taxa of interest. Details on sponge (Porifera) sampling from the AGT and BT deployments are provided by Kersken (3.2.3; this cruise report).

Table 3.2.1.1: Higher level taxa sampled during PS96. Quantity reflects the number of lots of specimens and not the actual number of individuals sampled.

Phylum	Class	Quantity
Annelida		127
Arthropoda		
	Amphipoda	62
	Cirripedia	2
	Copepoda	7
	Cumacea	11
	Decapoda	29
	Euphausida	5
	Isopoda	70
	Mysidacea	17
	Ostracoda	4
	Pycnogonida	30
	Tanaidacea	6
Brachiopoda		
Bryozoa		
Chordata		
	Tunicata	22

3.2.1 Phylogeny, phylogeography and population genetics of high Antarctic biota

Phylum	Class	Quantity
	Craniata	2
Cnidaria		308
Ctenophora		9
Dicyemida		5
Echinodermata		
	Asterozoa	274
	Crinozoa	111
	Echinozoa	32
	Holothurozoa	30
	Ophiurozoa	104
Foraminifera		4
Hemichordata		
	Enteropneusta	3
	Pterobranchia	21
Kinorhyncha		
Mollusca		
	Aplousobranchia	22
	Bivalvia	17
	Cephalopoda	27
	Gastropoda	51
	Polyplacophora	9
	Scaphopoda	22
Nematoda		37
Nemertea		50
Platyhelminthes		4
Porifera		
	Demospongiae	34
	Hexactinellida	3

Arthropoda

Many diverse arthropods were collected during PS96. Most specimens belonged to Isopoda or Amphipoda but many specimens of Pycnogonida were also collected. Specimens of all arthropod taxa except Amphipoda and Pycnogonida were pre-sorted to species and photographed alive. Sometimes small-bodied but diverse Amphipoda collections were bulk fixed in order to avoid excessive handling time and DNA degradation. Crustaceans will be sent to Christoph Held (AWI) for phylogeographic/population genetic and/or phylogenetic work. Some isopod tissue samples fixed in RNA later will also be used for a collaborative pilot study using transcriptome data to resolve higher level isopod phylogeny. Pycnogonids will be sent to Florian Leese who is interested in the phylogeography and population genetics of these animals.

Asteroidea

Asteroids are a key taxon of the Antarctic shelf benthos (see e.g. Danis et al. 2014 or biomass estimations of cruise PS82, Knust & Schröder 2014), yet little information is available on their diversity and the distribution of species and communities. On this cruise about 150 asteroid individuals were collected, pre-sorted, photographed, and frozen whole in ziplock bags at -20° C for Prof. Bruno Danis and working group from Université Libre Bruxelles, Belgium. Sub-samples of whole individuals were preserved in 96 % ethanol and/or RNAlater, respectively. Species identification will take place in Brussels and subsequently occurrence data will be added to an Asteroidea database. Stable isotope analyses will again be conducted together with Dr. Loïc Michel of the Université de Liège (ULg), Belgium. Samples preserved for molecular analyses shall be sequenced for the mitochondrial cytochrome *c* oxidase I gene (COI) and one or two nuclear markers. A previous population genetic study of *Odontaster* resulted in the description of two new species (Janosik et al. 2011). Given the general scarcity of genetic studies on Antarctic asteroids, further analyses are expected to create new insights into the diversity of this group. To further strengthen these efforts microsatellite marker development is aspired. Comparisons of sea stars with different dispersal capacities shall help to elucidate past and present connectivity and thus diversity and distribution patterns of Antarctic asteroids. This work is part of the federal Belgian research projects vERSO and RECTO (“Ecosystem responses to global change: a multiscale approach in the Southern Ocean” and “Refugia and ecosystem tolerance in the Southern Ocean”, respectively).

Cnidaria

The cnidarian material collected during PS96 was obtained from 6 Bottom Trawls, 10 Agassiz Trawls, and one Giant Box Corer. More than 300 individuals/colonies have been preliminarily identified on board, although most are awaiting further morphological studies in the laboratory (e.g. histology, SEM). The specimens belong to 54 morphospecies, of which 2 belong to Hydrozoa, 2 to Scyphozoa and 50 to Anthozoa. This last group includes 28 species belonging to Octocorallia and 22 to Hexacorallia. The hexacoral species consisted of 14 actinarians, 4 scleractinians 2 ceriantharians, and 2 zoanthideans. The octocoral material collected consisted of 2 species of pennatulaceans, 2 bamboo corals, 1 soft coral and 23 primnoid species.

Preliminary results on the gorgonian family Primnoidae composition (Figure 3.2.1.2) showed that from the western shallow stations (~400m) only in the most southerly and westerly station primnoids were collected, a colony of *Ainigmaptilon wallini* and one colony of *Fannyella rossii*. Three stations were conducted in the Filchner Trough; primnoids were found in two of them at medium depths (620-750m). In the northerly station of the Trough only sea whips were found, while in the southerly station no sea whips were found but more ramified species (*Daystenella acanthina* and *Fannyella rossii*). From the east flank of the Filchner Trough shallowest stations (9/3 and 57/6) are more diverse than deeper ones (6/2, 59/2 and 72/1). From the stations carried out at the east Weddell Sea we can remark the high biodiversity found at the Austasen station (1/9), and the successful deepest station (90/1) at 1,097 m where 3 bottlebrush species were collected.

3.2.1 Phylogeny, phylogeography and population genetics of high Antarctic biota

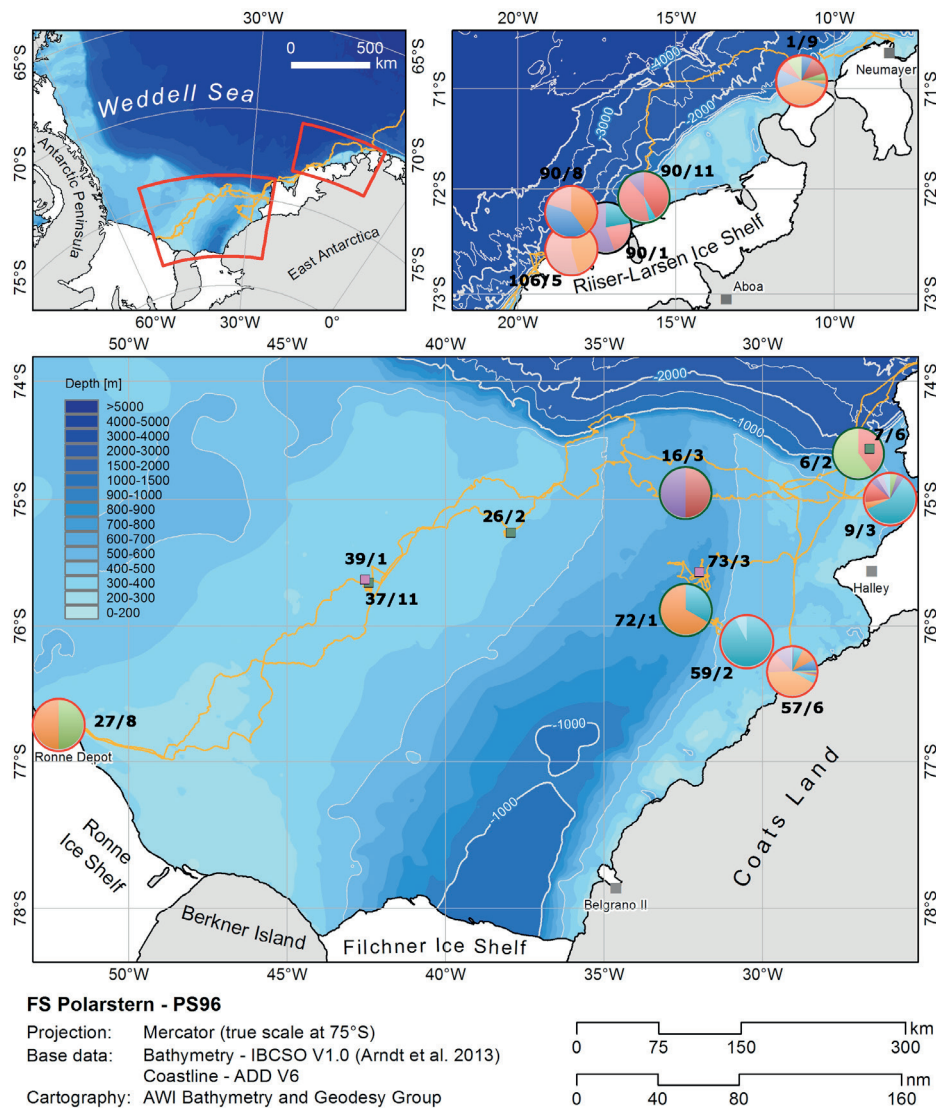


Fig. 3.2.1.2: Composition of Antarctic primnoids in the Filchner Outflow System.

All primnoid specimens were frozen at -20°C and subsamples for later identification were also taken and preserved in 70% ethanol. For each colony a subsample was also preserved in 96% ethanol and kept at -20°C for genetic analyses, and for some specimens additional subsample was taken and preserved in RNAlater.

The specimens collected in the present cruise will be analysed in conjunction with the samples from the previous cruise PS82 for the study on the gorgonian population structure and connectivity. For that purpose genomic DNA will be extracted from primnoid species once in the laboratory.

Crinoidea

Crinoids are an integral part of many Southern Ocean benthos assemblages (Eléaume et al. 2014) and are especially useful to test evolutionary hypotheses as they encompass broadcasting and brooding species. Here, more than 150 comatulid crinoids were collected for Prof. Marc

Eléaume (Muséum National d'Histoire Naturelle, Paris, France). No stalked crinoids were encountered. Most of the specimens were frozen at -20°C, with sub-samples taken either in 96 % ethanol and/or RNAlater, respectively. The last 10 individuals were fixed entirely in ethanol. Very preliminary identification suggests that *Promachocrinus kerguelensis* is with at least 40 of the collected individuals the most abundant species. Two other broadcasting spawners were also encountered: *Anthometrina adriani* and *Florometra mawsoni*. Smaller brooding crinoids, likely belonging to *Notocrinus* spp. and/or *Isometra* spp., were collected as well, but accurate identification needs to be carried out in Paris. The mitochondrial COI gene was used previously to address questions about genetic population structure and gene flow between *P. kerguelensis* from various locations around the Antarctic continent (Hemery et al. 2012). This study also showed that *P. kerguelensis* actually comprises 8 different circumpolar COI lineages. In the vERSO framework new single nucleotide polymorphism (SNP) markers will be developed to estimate effective population size and mutation rate to eventually distinguish between allopatric divergence and genetic drift. Transcriptome sequencing is another approach in order to test potential resilience of various crinoids to temperature increase of Antarctic waters.

Ctenophora

Ctenophores are of interest because recent phylogenomic studies (e.g., Whelan et al. 2015) have suggested that ctenophores and not sponges are the first branching animal phylum. This is interesting because ctenophores have nerves and muscles while sponges do not. Thus, this suggests that ctenophores independently evolved nerves and muscles or sponges secondarily lost these structures. During PS96 specimens of two species of benthic ctenophores (*Lyroctenis*?) were sampled. One species was collected using the AGT and a tentacle from one individual of a second species was sampled from the arm of the ROV. These samples will be used by Kocot and collaborators or transcriptome sequencing as part of an ongoing study investigating the evolutionary relationships within Ctenophora and placement of ctenophores in the animal tree.

Dicyemida

Dicyemids are tiny few-celled parasitic animals that are known only from the kidneys of cephalopods. Because of their small size and complex life cycle, the phylogenetic placement of Dicyemida has been debated (reviewed by Kocot 2016). During PS96 the kidneys of one specimen of *Megeledone setebos* (Octopoda) were dissected and revealed an astonishingly high density of these parasites. Samples were preserved for transcriptomic and potential genomic work to help improve understanding of the evolutionary placement of these enigmatic animals.

Mollusca

During PS96 specimens of diverse mollusc taxa were collected for various evolutionary studies. Aplacophoran molluscs along with chitons form the sister group of all other molluscs (Kocot et al. 2011). During PS96 specimens of ten species of Aplacophora were sampled. By far, the richest site in terms of aplacophoran diversity was the BENDEX site (Station 001). Here six species of aplacophorans were sampled. One of these is externally identical to *Hypomenia*, a genus that currently consists of just two species (Kocot and Todt 2013) but histological studies will be needed to confirm the identity and status of this Weddell Sea species. During a 2013 cruise on the RV *Nathaniel B. Palmer*, Kocot collected specimens of a new order of aplacophoran mollusc ("*Apodomenia enigmatica*") that lives within rossellid sponges (Kocot et al. Manuscript in preparation). During PS96, a second species of this order was found living within *Rossella racovitzae* in the eastern part of the Weddell Sea (Station 007). Further, a single specimen of a new species of *Macellomenia* was collected from Station 72. Kocot and Todt (2013) recently

summarized the global diversity of this genus and it is clear from external examination that this species represents a species that is new to science. Aplacophoran specimens collected during PS96 will be sequenced and incorporated into an ongoing large-scale phylogenetic investigation of aplacophoran evolutionary relationships. Transcriptome data generated from these aplacophoran molluscs will also be screened for biomineralization genes as part of an ongoing study comparing formation of aplacophoran spines to the shells of other molluscs.

During PS96, specimens of at least four species of Scaphopoda, including the widespread species *Polyschides dalli*, were sampled. Scaphopods are of interest because their evolutionary placement has been recalcitrant to even transcriptomic studies. Previously Kocot et al. (2014) estimated the genome size of *Polyschides dalli* and showed that it would be feasible to sequence the whole genome of this species. In order to place this species in mollusc phylogeny, specimens of *Polyschides dalli* collected during PS96 will be used by Kocot for whole genome sequencing and evolutionary genomic comparisons.

Numerous gastropods, especially representatives of the clade Caenogastropoda, were collected during PS96. Caenogastropoda is a diverse clade but relationships within this group are also ambiguous. Working with collaborators at The University of Melbourne in Australia, Kocot plans to sequence transcriptomes from key caenogastropod species collected during PS96 and use them in a large scale phylogenomic investigation of caenogastropod relationships.

Nematoda and Kinorhyncha

Nematoda is one of the most diverse animal phyla and includes many economically and medically important species that are parasites of diverse animals and plants (Baldwin et al. 2000). Additionally, many free-living taxa are of great ecological importance and *Caenorhabditis elegans* is an important research model organism. Despite the significance of nematodes to human health, agriculture, the environment, and research, higher-level evolutionary relationships within Nematoda remain unresolved. Earlier molecular investigations of nematode phylogeny relied on 18S rDNA but were unable to resolve relationships among major lineages. More recently, studies employing genomes and transcriptomes for phylogeny reconstruction (phylogenomics) have advanced understanding of nematode relationships (Blaxter et al. 2012), but taxon sampling has focused almost exclusively on parasitic species whereas most free-living lineages, especially those living in marine habitats, have been largely ignored. Further, higher-level relationships within Ecdysozoa, the clade of molting animals that includes nematodes, arthropods, priapulids, kinorhynchs, and relatives, remain unclear. During PS96, Kocot collected numerous specimens of diverse free-living nematodes and kinorhynchs. These specimens will be used for transcriptome sequencing for a phylogenomic investigation of nematode relationships that focuses on marine free-living taxa rather than economically important parasites.

Ophiuroidea

The majority of the 219 Southern Ocean ophiuroid species are small and morphologically cryptic. However, the more common, large ophiuroids are possible for a non-expert taxonomist to identify. The most widespread species collected on PS96 was *Ophiacantha antarctica*, present at most stations. Other common species include *Ophionotus victoriae*, *Ophioplinthus gelida*, *Ophiocten dubium*, *Ophioceres incipiens* and *Ophioperla koehleri*. *Ophioperla koehleri* was only found in shallower regions, (below 600 m). *Ophiacantha pentactis* was very common in the trawls near the shelf break and *Astrotopoma agassizi* was collected where there were mature sponge assemblages. Most stations were taken on the eastern slope of the trench within a few miles of previous stations and as the previous cruise (PS82) conducted a much more thorough survey of this region the biogeographic patterns are better observed from those catches and can be appreciated from that cruise report. Only catches relevant to the objectives of the cruise are taken into account here.

The main objective of our application was to sample from the western side of the Filchner Trough in order to test hypotheses regarding connectivity given strong currents and temperature variation separating the west from the well characterised eastern flank. Despite open leads north of the Ronne depot and two large polynyas to the north of this only three Agassiz trawl deployments and one bottom trawl deployment was made. All other deployments were made within a few miles of previous stations to the east or outside of the target area. Of the three AGTs to the west, the most northerly station (PS96-026_2) sampled only 8 individual ophiuroids; *Ophiocten dubium* (4), *Ophiosteira* sp. (1), *Ophionotus victoriae* (1) and an unidentified morphotype (2). The most southerly and westerly station (PS96-027_8) was in the polynya off the Ronnie Depot and consisted of seven ophiuroid morphotypes identified as follows; *Ophiacantha antarctica* (20), *Ophionotus victoriae* (3), *Ophiocten dubium* (3), *Ophioplinthus* sp. 1 (3), *Ophioplinthus* sp. 2 (2), *Ophioplinthus* sp. 3 (1). The third station (AGT PS96-037_11, BT PS96-039_1) was in the polynya to the west of the iceberg A23A, halfway between the previous two stations. Neither of these two trawls recovered ophiuroids.

On return samples will be identified by a taxonomist specializing in Antarctic ophiuroids, DNA will be extracted from all individuals and the Cytochrome c Oxidase subunit one gene amplified for molecular identification and initial phylogenetic analyses. Specific hypotheses will be tested using double digested restriction associated DNA sequencing (ddRAD).

Teleostei

Teleost fish represent the major link between plankton and smaller benthic fauna and apex predators of the ocean such as pinnipeds or toothed whales. The fish fauna of the Southern Ocean is dominated by members of the suborder Notothenioidei both in terms of abundance and biomass. Notothenioids have diversified into more than 100 extant species that occupy a diverse array of ecological niches in Antarctic waters. They are not only ecologically important, but also of commercial interest. Knowledge about their population genetics, phylogeography and trophic ecology is imperative to foster sound management and conservation of Antarctic fish.

During this cruise fish were collected predominantly by bottom trawl, but in lower numbers also by AGT. Irrespective of the gear all individuals were identified and processed following standard procedures in conjunction with the fish group (see section 3.2.2 Mark et al. for details). From a total of more than 500 teleost specimens, 396 were sampled for genetic analyses at KU Leuven (KUL). These samples consist of mainly fin clips, or rarely muscle tissue, both stored in microtubes filled with 96 % ethanol at -20°C. Another 284 specimens – largely the same as mentioned above – were sampled for isotope analysis. They are stored dry in microtubes or small ziplock bags at -20°C. Stable carbon and nitrogen isotope analyses can, for example, yield insights into the trophic ecology of selected taxa. This may be applied for instance to describe resource partitioning of certain fish communities (Stowasser et al. 2012). It has also been used to highlight the character of the diversification of notothenioids (Rutschmann et al. 2011). Stable isotope analyses may again be carried out in collaboration with Dr. Loïc Michel (ULg). Furthermore, about 60 whole specimens of *Pleuragramma antarctica* and five *Aethotaxis mitopteryx* were frozen at -20°C for potential energy content analyses (e.g. Maes et al. 2006) in collaboration with the Royal Belgian Institute of Natural Sciences (RBINS). Three specimen of different species were collected whole for teaching purposes. From all collected material especially the members of genus *Trematomus* are of particular interest to the KUL working group. Consequently additional biopsies were taken from 29 *Trematomus* sp. and preserved in RNAlater (Table 3.2.1.2). Analyses of *Notothenia coriiceps*, *N. rossii*, and *Dissostichus mawsoni* from this cruise are not possible, as they were not encountered.

3.2.1 Phylogeny, phylogeography and population genetics of high Antarctic biota

Table 3.2.1.2: Overview of trematomid fish that were sampled for KU Leuven during RV *Polarstern* cruise PS96. Number of fish (N) per station and in total is given, as well as number of samples preserved in ethanol, frozen at -20° C, and preserved in RNAlater, respectively.

Species	Station	N	Samples taken		
			Ethanol	-20° C	RNAlater©
<i>Trematomus bernacchi</i>	059-02/total	1	1	1	2
<i>Trematomus eulepidotus</i>	001-09	1	1	1	
	009-03	1	1	1	
	027-08	8	8	7	2
	039-01	5	5	5	6
	057-06	1	1	1	
	059-02	6	6	6	2
	086-02	1	1	1	
	total	23	23	22	10
<i>Trematomus hansonii</i>	059-02/total	4	4	4	8
<i>Trematomus lepidorhinus</i>	009-03	1	1	1	
	006-02	1	1	1	
	057-06	1	1	1	
	059-02	1	1	1	2
	total	4	4	4	2
<i>Trematomus loennbergii</i>	006-02	6	6	5	
	009-03	1	1	1	
	039-01	1	1	1	1
	072-01	2	2	2	4
	073-03	16	16	16	2
	090-11	7	7	7	
	total	33	33	32	7
<i>Trematomus pennellii</i>	001-09	4	4	4	6
	009-03	1	1		
	total	5	5	4	6
<i>Trematomus scotti</i>	001-09	2	2		
	007-06	1	1		
	009-03	4	4	4	2
	016-03	5	5		
	027-08	1	1	1	2
	037-11	2	2	2	
	039-01	2	2	2	1
	057-06	4	4	4	
	059-02	10	10	10	6
	total	31	31	23	11
<i>Trematomus tokarevi</i>	072-01	1	1	1	2
	073-03	4	4	4	6
	total	5	5	5	8

Species identification based on morphological characters within the Trematominae is not trivial (Van de Putte et al. 2009), and even more complicated in some members of the Artedidraconidae and Bathydraconidae. Therefore DNA barcoding shall be used to verify identifications carried

out aboard. The COI gene has been shown to differentiate many but not all notothenioid fish (Rock et al. 2008; Smith et al. 2012). For example *Trematomus loennbergii* and *Trematomus lepidorhinus* share COI haplotypes (Lautredou et al. 2010). As morphological differentiation between these species is particularly difficult, exploring other genetic markers that can be used for unambiguous species determination may be worthwhile.

Phylogeography and population genetics of *Trematomus* spp. has been investigated previously using traditional molecular markers (Damerau et al. 2012; Van de Putte et al. 2012). In order to extend these results restriction-site associated DNA (RAD) sequencing will be employed. This approach promises the cost-effective identification and genotyping of hundreds to thousands of single nucleotide polymorphisms (SNPs), thus providing information on a genome wide scale. For RAD library preparation samples from this cruise will be combined with previously obtained samples, e.g. from PS82 (Knust & Schröder 2014), but also from land-based sampling campaigns in Adélie Land, or the Antarctic Peninsula region. This will enable almost circum-Antarctic coverage, as well as spatio-temporal replication. Inferred genotypes are analysed to determine genetic population structure, demography, and adaptive potential of Antarctic fish. Fine scale connectivity and genomic variation patterns can ultimately be related to environmental predictors. All above mentioned samples will go to KUL, where they will be stored and analysed in different, partly here described studies in the framework of the federal Belgian projects vERSO and RECTO.

Data management

Sequence data generated from these specimens will be made publicly available at the time of publication. Nucleotide sequences will be released to the NCBI Nucleotide database. Raw reads generated using high throughput sequencing platforms (e.g., RAD tags, transcriptomic, and genomic data) will be uploaded to the NCBI Short Read Archive (SRA). Assembled transcriptomes and genomes will also be made publicly available via Dryad. Specimens used in taxonomic work (e.g., types, paratypes, etc.) will be archived in appropriate museum collections for that taxon. Species presence data for select taxa will be submitted to the SCAR MarBIN database (biodiversity.aq). Lists of identified species per station will be deposited in the PANGAEA database (www.pangaea.de).

References

- Alvaro M et al. (2013) *The Expedition of the Research Vessel „Polarstern“ to the Antarctic in 2013 (ANT-XXIX/3)*. pp. 16-19. J. Gutt Ed.
- Baldwin JG, Nadler SA, and Wall DH (2000) Nematodes: pervading the earth and linking all life. In P.H. Raven and T. Williams, editors, *Nature and human society: The quest for a sustainable world: Proceedings of the 2000 Forum on Biodiversity*, pages 176-191. National Academy Press, Washington, D.C.
- Blaxter M, Kumar S, Kaur G, Koutsovoulos G, and Elsworth B. (2012) Genomics and transcriptomics across the diversity of the Nematoda. *Parasite Immunology* 34(2-3):108–20.
- Brandt A et al. (2007) First insights into the biodiversity and biogeography of the Southern Ocean deep sea. *Nature* 447:307-311.
- Damerau M, Matschiner M, Salzburger W, Hanel R (2012) Comparative population genetics of seven notothenioid fish species reveals high levels of gene flow along ocean currents in the southern Scotia Arc, Antarctica. *Polar Biology* 35:1073–1086.
- Danis B, Griffiths HJ, Jangoux M (2014) Asteroidea. In: *Biogeographic Atlas of the Southern Ocean* (eds De Broyer C, Koubbi P, Griffiths HJ, et al.), pp. 200–207. Scientific Committee on Antarctic Research, Cambridge.

3.2.1 Phylogeny, phylogeography and population genetics of high Antarctic biota

- Eléaume M, Hemery LG, Roux M, Améziane N (2014) Phylogeographic patterns of the Southern Ocean crinoids. In: *Biogeographic Atlas of the Southern Ocean* (eds De Broyer C, Koubbi P, Griffiths HJ, et al.), pp. 448–455. Scientific Committee on Antarctic Research, Cambridge.
- Hemery LG, Eléaume M, Roussel V et al. (2012) Comprehensive sampling reveals circumpolarity and sympatry in seven mitochondrial lineages of the Southern Ocean crinoid species *Promachocrinus kerguelensis* (Echinodermata). *Molecular Ecology* 21:2502–18.
- Janosik AM, Mahon AR, Halanych KM (2011) Evolutionary history of Southern Ocean Odontaster sea star species (Odontasteridae; Asteroidea). *Polar Biology* 34:575–586.
- Knust R, Schröder M (2014) The Expedition PS82 of the Research Vessel POLARSTERN to the southern Weddell Sea in 2013/2014. *Berichte zur Polar- und Meeresforschung* 680:1–161.
- Kocot KM (2016) On 20 years of Lophotrochozoa. *Organisms Diversity and Evolution* in press.
- Kocot KM, Jeffery NW, Mulligan K, Halanych KM, Halanych KM (2015) Genome size estimates for aplacophora, polyplacophora, and scaphopoda: small solenogasters and sizeable scaphopods, *Journal of Molluscan Studies* in press.
- Kocot KM, Todt C (2014) Three new meiofaunal solenogaster species (Mollusca: Aplacophora) from the north-east Pacific. *Journal of Natural History* DOI: 10.1080/00222933.2014.961987.
- Lautredou AC, Bonillo C, Denys G et al. (2010) Molecular taxonomy and identification within the Antarctic genus *Trematomus* (Notothenioidei, Teleostei): How valuable is barcoding with COI? *Polar Science* 4:333–352.
- Maes J, Van de Putte A, Hecq J, Volckaert F (2006) State-dependent energy allocation in the pelagic Antarctic silverfish *Pleuragramma antarcticum*: trade-off between winter reserves and buoyancy. *Marine Ecology Progress Series* 326:269–282.
- Van de Putte AP, Van Houdt JKJ, Maes GE et al. (2009) Species identification in the trematomid family using nuclear genetic markers. *Polar Biology* 32:1731–1741.
- Van de Putte AP, Janko K, Kasparova E et al. (2012) Comparative phylogeography of three trematomid fishes reveals contrasting genetic structure patterns in benthic and pelagic species. *Marine Genomics* 8:23–34.
- Rock J, Costa FO, Walker DI et al. (2008) DNA barcodes of fish of the Scotia Sea, Antarctica indicate priority groups for taxonomic and systematics focus. *Antarctic Science* 20:253–262.
- Rutschmann S, Matschiner M, Damerou M et al. (2011) Parallel ecological diversification in Antarctic notothenioid fishes as evidence for adaptive radiation. *Molecular Ecology* 20:4707–21.
- Smith PJ, Steinke D, Dettai A et al. (2012) DNA barcodes and species identifications in Ross Sea and Southern Ocean fishes. *Polar Biology* 35:1297–1310.
- Stowasser G, Pond DW, Collins MA (2012) Fatty acid trophic markers elucidate resource partitioning within the demersal fish community of South Georgia and Shag Rocks (Southern Ocean). *Marine Biology* 159:2299–2310.
- Vaughan DG, Barnes DKA, Fretwell PT (2011) Potential seaways across West Antarctica. *Geochemistry Geophysics Geosystems* 12(10) Q1004.
- Whelan NV, Kocot KM, Moroz LL, Halanych KM (2015) Error, signal, and the placement of ctenophora sister to all other animals. *Proceedings of the National Academy of Science* 112(18):5773–5778.

Acknowledgements

This work was funded by Alfred Wegener Institute (AWI) Grant number AWI_PS96_02. We thank the officers, crew, and scientists of RV *Polarstern* cruise PS96 for making this work possible.

3.2.2 Cold adaptation vs. sensitivity to climate change and pollution in Antarctic Notothenioids: Physiological plasticity, genetic regulation, immunology and reproductive traits

Felix Mark¹, Nils Koschnick¹, Hanna Scheuffele¹, C. Papetti¹ (not on board), M. Lucassen¹ (not on board), Anneli Strobel², Patricia Burkhardt-Holm², Helmut Segner³, Emilio Riginella⁴, C. Mazzoldi⁴ (not on board), M. La Mesa⁴ (not on board), Henrik Christiansen⁵

¹AWI,
²Uni Basel,
³Uni Bern,
⁴Uni Padova,
⁵KU Leuven

Grant No: AWI_PS96_02

Objectives

Antarctic Notothenioid fishes represent more than 90% of the fish biomass on the Antarctic shelf and include more than 120 different species. They are characterized by a multitude of physiological adaptations to live in cold water. Most teleost fish inhabiting the Antarctic ecosystem are considered to be extremely stenotherm specialists, as their physiological performance is restricted to a very narrow thermal range. This thermal specialization of Antarctic fish and associated energy savings typically involve an extreme stenothermy of physiological and molecular functions, a high sensitivity to heat exposure and limited metabolic capacities to respond to changes in their abiotic environment. On the other hand, they show high reproductive investment, characterized by high gonadosomatic indexes, large eggs, prolonged gametogenesis and, in some cases, extended male parental care.

So far, high-Antarctic waters have been considered a stable environment, unaffected by climate change and chemical pollution. However, the Antarctic ecosystem is progressively exposed to anthropogenic environmental influences, such as ocean warming, ocean acidification and persistent organic pollutants.

Due to atmospheric transport and global distillation of persistent organic pollutants (POPs) including halogenated aromatic hydrocarbons (HAHs), toxic contaminants precipitate and are deposited in the Antarctic environment. It is expected that global warming will even increase levels of xenobiotics in Antarctica because they will be more available for atmospheric transport and scavenged more effectively from the atmosphere due to increased precipitation. Furthermore, as ice acts as a long-term reservoir accumulating organic pollutants, the predicted future seawater-warming and pack-ice melting in the Antarctic (Hellmer et al., 2012; Nash, 2011) may lead to increased pollutant concentrations in remote areas such as in the Filchner region. Lipophilic organic chemicals such as the HAHs bioaccumulate from the environment into biota, and can biomagnify along aquatic food chains. In fact, it has been shown that POPs bioaccumulate in Antarctic fish (Strobel et al. 2016).

Thus, the question arises if the evolutionary highly specialized Antarctic fish possess the adaptive potential to cope with these “novel” environmental stressors and xenobiotics. Environmental stress can strongly affect the energy balance of an organism due to the additional energy needed for metabolic compensation, acclimatisation and detoxification. An increase in basal metabolism can in turn lead to the reduced scope for activity, reproduction and growth due to the energetic trade-offs between basal maintenance and other essential energy requiring functions.

Our project focuses on the energy metabolism under environmental stress and the trade-offs between energetically demanding processes such as biotransformation, metabolic

compensation and immune response of high-Antarctic fish species in response to multiple stressors (temperature, pH and exposure to xenobiotics) on the one hand and the costs for reproduction and growth on the other hand.

Data on the biology of most high-Antarctic notothenioids are much less complete compared to low-Antarctic species, which have been subjected to commercial harvesting (Hubold 1992, Duhamel 1993). Indeed, pack ice characteristics make the southern Weddell Sea, in particular the Filchner Trench, an area difficult to sample. The only few data on fish distribution and reproduction collected in the southern Weddell Sea are from the early 1990s. The Filchner Outflow System is considered a biological “hotspot”, in terms of food availability and physical processes. Our integrative approach aims at assessing the level of cold adaptation and the physiological capability of high-Antarctic fish to cope with climate change and anthropogenic pollution over several levels of biological organization from the molecule to the whole organism, food availability and variation – a general constraint influencing reproductive traits. Thus we aim to contribute to develop a basis for environmental conservation efforts.

This study started with the collection of samples during previous *Polarstern* cruises and in particular the PS82 (ANT-XXIX/9) cruise, carried out between December 2014 and March 2015. The availability of samples from different years and areas will allow studying the temporal and spatial variability of the population traits. By comparing our results with previous data, we will be able to determine possible changes on their reproductive traits in relation to interannual variability of environmental factors.

Furthermore, samples coming from different sites will possibly allow an intra-specific comparison of the species life history traits in relation to environmental variables (food availability, abiotic factors) at a reduced spatial scale and highlight evidence of the potential reproductive isolation between neighbouring populations.

Work at sea

The work on board depended on fish caught by bottom trawls (BT), Agassiz Trawls (AGT) and fish traps (FT). Due to the strict logistic time schedule of this cruise and the general ice coverage, it was only possible to deploy 6 BT, 10 AGT and 4 FT. Of those, only three AGT and one BT could be realised in the intended research area on the Western Filchner Shelf (*cf.* Fig. 3.2.2.1).

The 16 hauls were located in water depths between 291 and 882 m (bottom trawls, 6 stations), and between 274 and 1113 m (Agassiz trawls, 10 stations). First of all, alive species were carefully carried to the aquarium container for further physiological analyses. Sorting and species identification were performed in the wet fish lab. Date and site of collection, together with a set of standard measurements (total and standard length, total and gutted weight and gonad weight) were recorded. Sex and maturity were macroscopically determined and assigned to each fish specimen (following the maturity scale of Kock and Kellermann, 1991). Gonads of males and females were removed and fixed in either Dietrich solution for histological analysis or 10% buffered seawater formaldehyde solutions for fecundity estimation and stored at room temperature. To estimate age, growth rate and age at first sexual maturity, otoliths were removed and stored dry.

More than 1000 tissue samples of heart, gills, liver, bile, spleen, kidney, head kidney, brain, and red and white muscle were sampled for RNA extraction from 88 individuals of 42 different species under clean conditions, snap frozen in liquid nitrogen and stored directly or in RNA later at -80°C.

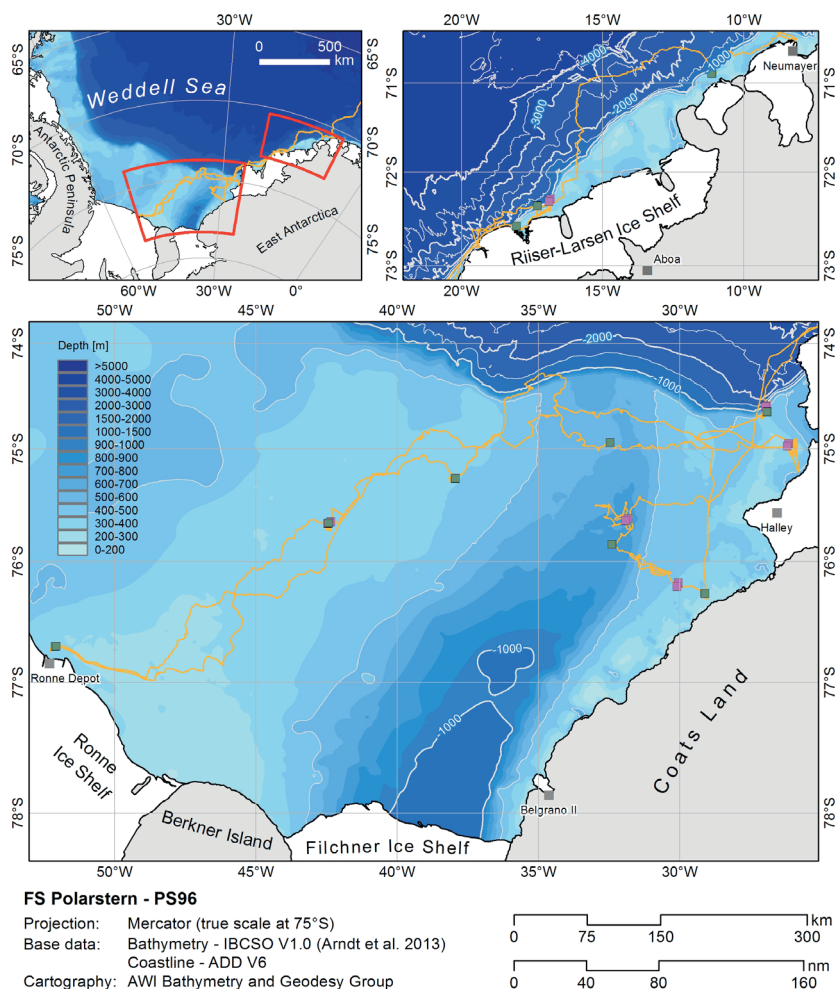


Fig. 3.2.2.1: Bottom trawls (pink squares) and Agassiz Trawls (green squares) conducted during Polarstern cruise PS96 (ANT-XXXI/2) December 2015 - February 2016

A reasonable number of further tissue samples (liver, gonad, muscle, head kidney) were collected for histological characterization (fixed and stored in buffered formaldehyde solution) and/or chemical-analytical measurements (stored at -20°C). Blood samples were taken for blood smears, partly stained with Giemsa, partly fixed in methanol.

Some whole body specimens were preserved for exposition at the University of Padova Zoological Museum. Lab procedures were performed in collaboration with Henrik Christiansen (University of Leuven) who will provide the data related to notothenioid fish population genetics of collected samples (see section 3.2.1 for more details). Furthermore, genetic samples were collected for Dr. Chiara Papetti (Alfred Wegener Institute, Bremerhaven, Germany and University of Padova, Italy) to continue the previous collaboration. Moreover, digitally recorded images of whole specimens, both from lateral and cranial perspective, were taken during sampling. They will be used for additional comparative analysis (i.e. photo and video fish identification purposes, see below). Thanks to the collaboration with Dr. Dieter Piepenburg, who kindly provided seabed photos and video footage obtained with the OFOS (Ocean Floor Observation System, see specific contributions, chapter 3.2.5), important observations about fish distribution, reproduction and parental care behaviour were recorded and will be analysed (see section 3.2.5 for more details).

Further analyses of the collected samples and images and videos will be carried out in the lab in Italy, at the University of Padova and at the Institute of Marine Science of Ancona.

Laboratory experiments on board had to be adapted to the number of individuals of a single species available. The planned incubation experiment could thus not be realised, as it would have required a stock of at least 12 individuals of one species. In the molecular biology part, we therefore only extracted RNA from a number of tissues of several individuals of *Trematomus loennbergii* and tested and optimized primer and qPCR procedures for this species.

Of the available fish species, we chose the red-blooded *Trematomus loennbergii* and the white-blooded *Chionodraco hamatus* and *Chaenodraco wilsoni* as model species for our sampling and experiments with isolated cells, muscle fibers and mitochondria on board.

The following experiments were conducted on board directly after dissection of the fish:

Hepatocyte respiration & incubation:

Cells from about 2 g liver tissue were isolated freshly every day following a protocol modified after (Mommsen et al., 1994; Segner, 1998).

Cell-respiration was measured in glass chambers (Loligo Systems, Denmark) in a chilled water bath at 0 and 6 °C. Cell metabolism was assessed in control and acutely toxicant (benzo(a)pyrene {BaP}) exposed hepatocytes.

In a second part of our experiments, cells were incubated with either benzo(a)pyrene, α -naphthoflavone and a mixture of both compounds for up to 72 hours. Cell viability was determined during and at the end of the incubation by Trypan blue exclusion and a photometric cytotoxicity assay. Samples of the toxicant incubations were frozen and stored at -80°C for further analyses at the home institute in Switzerland.

Immunopathology

Immune cells were isolated freshly every day from head kidney using Percoll density centrifugation. Respiration of isolated immune cells was assessed during exposure to the same treatments as the hepatocytes, using the same respiration setup (Loligo Systems, Denmark).

Mitochondria & heart fiber respiration

Heart and liver mitochondria were prepared from about 1g freshly excised tissue following the protocol provided in Mark et al. (2012). For preparation of permeabilised heart fibers, hearts were dissected out and the tissue was mechanically dissected in ice-cold biopsy buffer using scissors and forceps and stored in ice-cold biopsy buffer until processing for respiration assays. For each respiration experiment, a subsample of the heart fibre bundles was permeabilized for 30 min with 50 μ g/ml saponin by gentle mixing on ice for 30 min.

Respiration experiments with heart fibers and mitochondria were carried out in two Oxygraph-2k[®] respirometers (Oroboros Instruments, Innsbruck, Austria) following the substrate inhibitor (SUIT) protocol provided in Shama et al. (2014) at 0°C, 6°C and 12°C. In the mitochondrial preparations, we measured mitochondrial membrane potential simultaneously with respiration with ion selective electrodes in the presence of 5 μ M TPP⁺ (cf. Brand, 1995 for details). Via a fluorometric setup (Oroboros Instruments), ATP production was measured at the same time in the presence of 3 μ M MagnesiumGreen[®] (cf. Chinopoulos et al., 2009). To investigate the effect of rising intracellular bicarbonate concentration (ocean acidification scenario) on the mitochondrial metabolic pathways through complexes I and II of the electron transport system, heart fiber respiration under either rotenone+succinate+glutamate+malate+pyruvate+ADP (for

complex II) or malonate+glutamate+malate+pyruvate+ADP (for complex I) was titrated with bicarbonate in the range of +0.5-12mM.

A total of 111 experimental runs were conducted on 23 individuals of *Trematomus loennbergii*, 6 individuals of *Chionodracus hamatus* and *Chaenodraco wilsoni*, respectively.

Preliminary (expected) results

Fish diversity and tissue sampling

Overall, in the 16 BT and AGT hauls more than 600 specimens from 42 notothenioid species and 4 other taxa (Bathyraja, Myctophidae, Liparidae, Macrouridae) were collected (*cf.* Fig. 3.2.2.2).

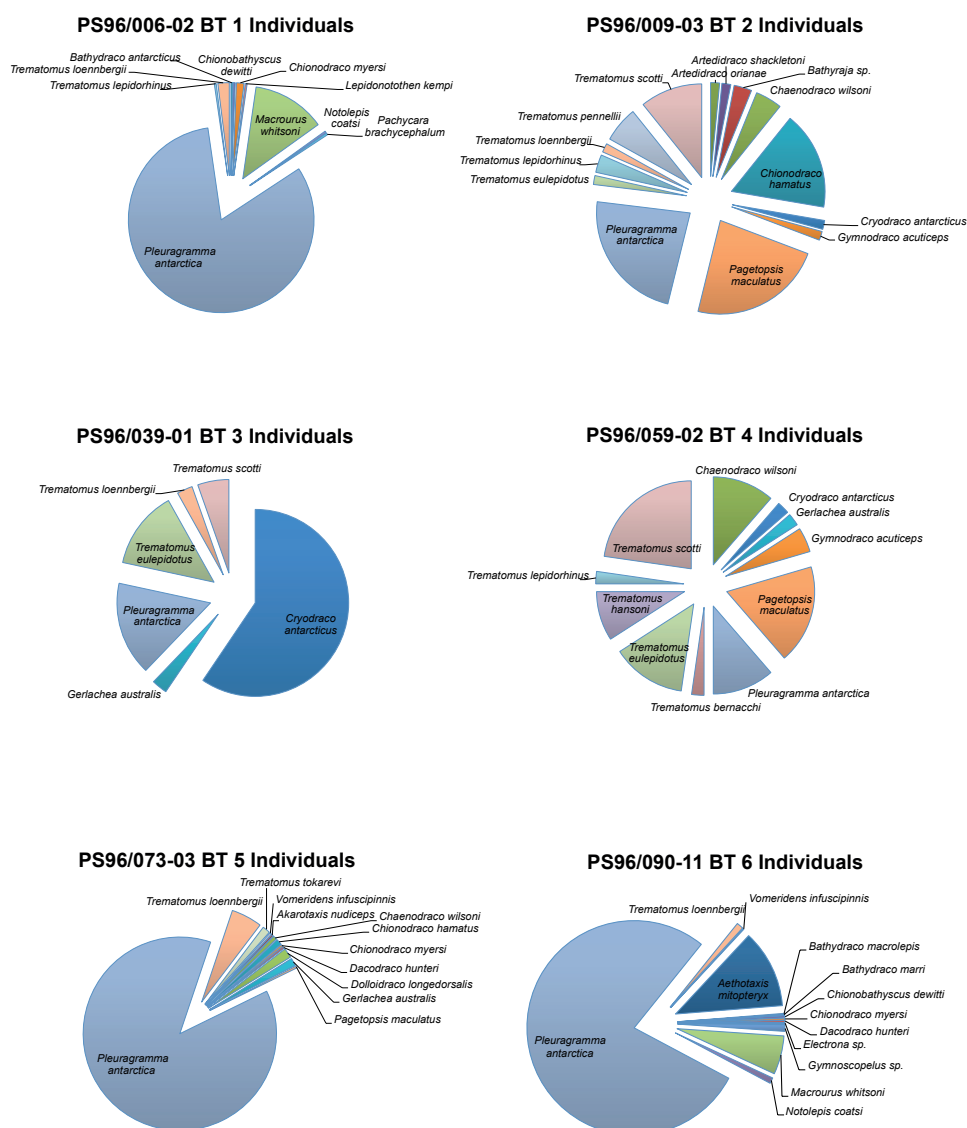


Fig. 3.2.2.2: Species composition as individuals per trawl for the six bottom trawls during Polarstern cruise PS96 (ANT-XXXI/2) December 2015 - February 2016

3.2.2 Cold adaptation vs. sensitivity to climate change and pollution in Antarctic Notothenioids

For all species, otolith and gonad samples were obtained from the whole size range of fish collected. The size range of the most abundant species (>15 specimens in total), measured as total length, was as follows:

Aethotaxis mitopteryx (15.5 – 45.0 cm), *Chionodraco hamatus* (12.0 – 42.0 cm), *Dolloidraco longedorsalis* (10.0 – 13.0 cm), *Gerlachea australis* (13.5 – 25.0 cm), *Macrourus whitsoni* (12.5 – 59.0 cm), *Pagetopsis maculatus* (15.0 – 20.0 cm), *Pleuragramma antarctica* (2.5 – 28.0 cm), *Trematomus eulepidotus* (10.5 – 28.5 cm), *Trematomus loennbergii* (14.0 – 31.0 cm), *Trematomus scotti* (7.5 – 17.0 cm).

For the reproductivity studies and age / growth rate assessment, samples from both females and males were collected for different species in this study (Table 3.2.2.1).

Table 3.2.2.1: List of samples with more than 5 specimens processed during *Polarstern* cruise PS96 (ANT-XXXI/2) December 2015-February 2016

Species	Females		Males		Total N.
	Stage 1-2	Stage 3-4-5	Stage 1-2	Stage 3-4-5	
<i>Aethotaxis mitopteryx</i>	19	20	32	3	74
<i>Akarotaxis nudiceps</i>	4	2	3	--	9
<i>Chaenodraco wilsoni</i>	1	5	2	2	10
<i>Chionodraco hamatus</i>	10	--	6	--	16
<i>Chionodraco myersi</i>	3	1	2	--	6
<i>Cryodraco antarcticus</i>	7	--	7	--	14
<i>Dolloidraco longedorsalis</i>	7	5	7	5	24
<i>Gerlachea australis</i>	4	1	10	5	20
<i>Macrourus whitsoni</i>	28	1	20	5	54
<i>Notolepis coatsi</i>	4	1	1	--	6
<i>Pagetopsis maculatus</i>	7	2	14	--	23
<i>Pleuragramma antarctica</i>	21	3	22	--	46
<i>Racovitzia glacialis</i>	2	--	1	3	6
<i>Trematomus eulepidotus</i>	10	1	6	4	21
<i>Trematomus loennbergii</i>	18	1	12	--	31
<i>Trematomus pennellii</i>	1	2	--	2	5
<i>Trematomus scotti</i>	15	--	14	--	29

Although only few specimens of rare species were obtained, they were preserved for Museum exposition, taking into account their rarity. During sampling, two low Antarctic species, namely *Trematomus tokarevi* and *Lepidonotothen squamifrons (kempi)*, were collected in the eastern part of the Filchner depression. Moreover, digitally recorded images of whole specimens, both from lateral and cranial perspective, were taken during sampling. They will be used for additional comparative analysis (i.e. photo and video fish identification purposes).

From the OFOS pictures and videos, two icefish and one bathydraconid species were observed with nesting behaviour (see specific contributions, chapter 3.2.5). Furthermore, many empty

fish nests with three different shapes were detected, indicating wide spawning areas in the eastern part of the Weddell Sea. The nests were dug some centimetres into the sediment, some of them had small stones and accumulated gravel in the centre, in others a bigger flat stone was present in the middle to which the eggs were attached. The parental presence on the nest presumably inhibits predation. Nesting and parental care appear indeed to increase the survival rate of the offspring. On the other hand, parental care has potential trade-offs as well, since the guarding fish have fewer or no chance to feed. The parental care strategy in notothenioids represents an important life history trait and appears more widespread than previously expected.

Hepatocyte & leukocyte toxicant exposure

Our first results revealed that Antarctic fish respond to acute toxicant exposure by an increase in hepatocyte and leukocyte respiration. The red-blooded fish *T. loennbergii* showed a larger increase in hepatocyte metabolism related to toxicant metabolism than the white-blooded fish *C. hamatus*. Acute temperature increase had an enhancing effect on the liver metabolism of the red-blooded species, but led to a slight depression of liver metabolism in the white-blooded species. This reflects the extreme heat-sensitivity of white-blooded Antarctic fish species, when compared to red-blooded notothenioids.

In our toxicant incubation experiments, we found no effect of BaP exposure on the viability of the hepatocytes of red- and white-blooded Antarctic fish, even not after 72 hours of toxicant exposure. Changes in metabolic enzymes, gene expression patterns or cytotoxic effects related to this chronic toxicant exposure will be analyzed in the laboratories of the home institutes in Switzerland.

Samples of the toxicant-incubated hepatocytes will be used for gene expression studies. Expression of genes involved in energy metabolism and toxicant metabolism will be determined by quantitative PCR. The results are expected to show changes in molecular pathways involved in energy metabolism and which pathways are increased or decreased in response to toxicant and exposure to increased temperature. This will give us a first idea if and how Antarctic fish will respond to future warming and pollution at the molecular level.

The histological characterization of the gonads, liver and head kidney and the analyses of blood smears will be performed in the laboratories of the University of Berne and Basel. The tissues samples for analytical studies will be analyzed at Empa, Swiss Federal Laboratories for Materials Research and Technology, Switzerland.

Mitochondria & heart fiber respiration

Experimental data will be analysed at AWI, after protein content estimation of the individual fiber and mitochondrial preparations. Prior to this analysis, only vague conclusions can be drawn from the data. It was obvious, though, that mitochondrial activity of heart fibers and mitochondria from white blooded notothenioids displayed a higher respiratory activity than those of red blooded fish, while thermal sensitivity was similar. Preliminary analysis of bicarbonate titration of heart fiber respiration indicates a slight reduction of complex II mediated respiration, while a slight boost of complex I mediated respiration was registered – in line with our hypothesis of ocean acidification effects on notothenioid cellular energy metabolism (Strobel et al., 2013).

Data management

All data will be made available by publication in scientific journals und subsequent storage in PANGAEA. The molecular data will be submitted to the respective database (NCBI; EMBL).

3.2.2 Cold adaptation vs. sensitivity to climate change and pollution in Antarctic Notothenioids

All data collected during this cruise will be provided upon request. All gonads samples will be stored and analysed at the Hydrobiological Station “Umberto D’Ancona” in Chioggia (Venice, Italy, detached facility of Biology Department, Padova University), in collaboration with C. Mazzoldi. Otoliths reading will be performed at ISMAR-CNR of Ancona (Italy) in collaboration with M. La Mesa. All data resulting from samples analyses collected during this cruise will be available through publications or reports.

References

- Brand MD (1995) Measurement of mitochondrial protonmotive force. In: *Bioenergetics: A practical approach*. eds.: Brown, G C & Cooper, C E. cpt. 3. Oxford University Press, Oxford, UK.
- Chinopoulos C, Vajda S, Csanády L, Mándi M, Mathe K and Adam-Vizi V (2009) A Novel Kinetic Assay of Mitochondrial ATP-ADP Exchange Rate Mediated by the ANT *Biophysical Journal* 96:2490–2504.
- Duhamel G, Kock KH, Baiguerias E, Hureau JC (1993) Reproduction in fish of the Weddell Sea. *Polar Biology* 13:193-200.
- Hubold G (1992) Ecology of Weddell Sea fishes. *Reports on Polar Research* 103, 157pp.
- Kock KH and Kellermann A (1991) Reproduction in Antarctic notothenioid fish. *Antarctic Science* 3:125-150.
- Mark FC, Lucassen M, Strobel A, Barrera-Oro E, Koschnick N, Zane L, Patarnello T, Pörtner HO, and Papetti C (2012) Mitochondrial function in Antarctic nototheniids with ND6 translocation. *PLoS ONE* 7(2):e31860.
- Mommsen TP, Moon TW, and Walsh PJ (1994) Hepatocytes: isolation, maintenance and utilization, in: P.W. Hochachka, T.P. Mommsen (Eds.), *Biochemistry and molecular biology of fishes, analytical techniques*, vol.3. Elsevier Science, Amsterdam, 355-372.
- Segner H (1998) Isolation and primary culture of teleost hepatocytes. *Comp Biochem Physiol A* 120: 71-81.
- Shama LNS, Strobel A, Mark FC, and Wegner KM (2014) Transgenerational plasticity in marine sticklebacks: maternal effects mediate impacts of a warming ocean. *Functional Ecology* 28(6):1482-1493.
- Strobel A, Graeve M, Pörtner HO, Mark FC (2013) Mitochondrial acclimation capacities to ocean warming and acidification are limited in the Antarctic nototheniid fish, *Lepidonotothen squamifrons* vs. *Notothenia rossii*. *PLoS ONE* 8(7): e68865
- Strobel A, Schmid P, Segner H, Burkhardt-Holm P, Zennegg M (2016) Persistent organic pollutants in tissues of the white-blooded Antarctic fish *Champscephalus gunnari* and *Chaenocephalus aceratus*. *Chemosphere*. In press.

3.2.3 Suspension feeders in a biodiversity hotspot: sponge distribution and functioning on the eastern Antarctic shelf

Daniel Kersken¹ and Dorte Janussen¹ (not on board)

¹ Senck.-F

Grant No. AWI_PS96_02

Objectives

Macro- and megabenthic communities on continental shelves in the Weddell Sea are often structured by sponge assemblages, which are in turn, dominated by representatives of the classes Demospongiae and Hexactinellida (Hogg et al. 2010, Gutt et al. 2015, Kersken et al. 2016). Their great importance for Antarctic macro- and megabenthic communities results from functional roles such as substrate formation, influence on benthic-pelagic coupling processes, association with other benthic organisms and production of bioactive secondary metabolites (McClintock et al. 2005, Bell 2008, Kersken et al. 2014).

Main objectives are:

- Expansion of the recent knowledge on sponge species occurrence and distribution patterns in the Filchner-Ronne outflow system, especially for the area west of the Filchner trough where data is scarce (Downey et al. 2012).
- Investigation of the influence of environmental variables on species composition and richness of sponge communities. One former study by Kersken et al. (2016) showed that increasing bottom water temperature significantly reduces species richness.
- Population genetics of *Rossella* spp. to study the taxonomy, systematics and evolutionary history of this genus. Recent phylogenetic data show two clades within this genus: a *Rossella antarctica* clade and a *Rossella racovitzae* clade, which is represented by a diverse species assemblage considered as species flock (Vargas et al. 2016).

Side projects are:

- A screening for bioactive secondary metabolites will be conducted with demosponge subsamples, for instance with *Latrunculia* sp. A previous study by Berne et al. (2015) shows that natural products isolated from Antarctic sponges can be used to find new pharmaceutical compounds.
- Collection of subsamples for transcriptomics of sponge species from the Filchner-Ronne outflow area. Transcriptomic data will increase the knowledge on phylogeny of Antarctic sponges and help to perform better molecular analyses in the future, for instance by the design of new universal primers for sponge rDNA marker genes.

Work at sea

Sponge samples were collected with an Agassiz trawl (AGT) and a bottom trawl (BT) (Figure 3.2.3.1) while the AGT was deployed at ten and the BT at six sample sites (Table 3.2.3.1). Specimens were cleaned, pre-sorted and transferred into buckets with cold seawater as soon as the catch was on deck. Further sorting and preliminary species identification were conducted in the laboratory. Subsamples were taken for five different types of analyses, which will be performed subsequent to the expedition: 1) Species identification, 2) DNA-Barcoding, 3) Population genetics, 4) Screening of secondary metabolites and 5) Transcriptomics.

3.2.3 Suspension feeders in a biodiversity hotspot

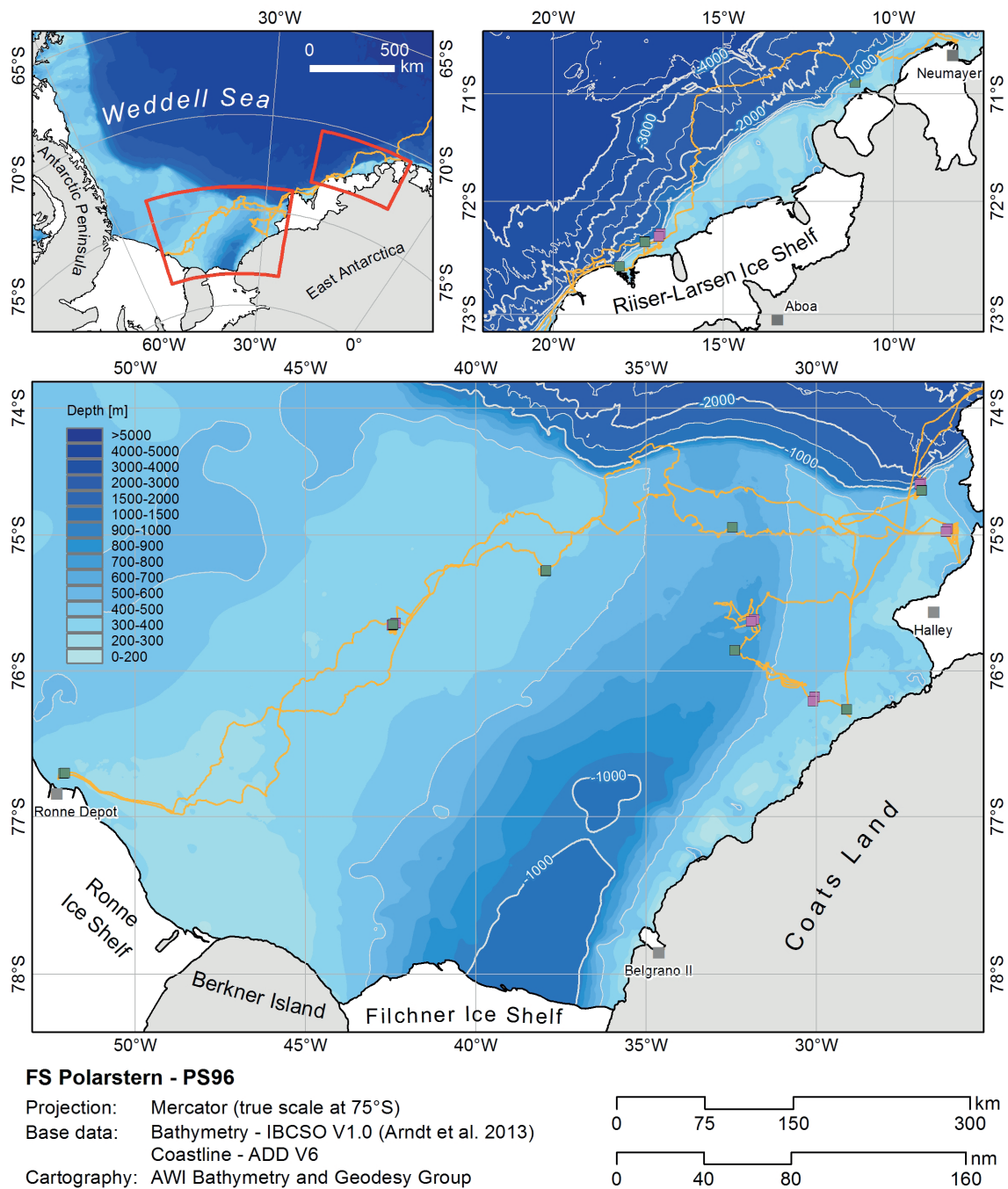


Fig. 3.2.3.1: Map with AGT (green squares) and BT (pink squares) deployments during PS96 (ANT-XXXI/2)

Table 3.2.3.1: AGT and BT deployments during PS96 (ANT-XXXI/2)

Date [dd/mm/yy]	Station	Depth [m]	Profile Start [Lat. S and Lon. W]		Profile End [Lat. S and Lon. W]	
24/12/15	AGT 001-9	303	70° 53,49' S	011° 07,78' W	70° 53,45' S	011° 08,20' W
29/12/15	BT 006-2	750	74° 36,07' S	026° 55,22' W	74° 36,79' S	026° 57,23' W
30/12/15	AGT 007-6	419	74° 39,40' S	026° 53,75' W	74° 39,58' S	026° 54,13' W
31/12/15	BT 009-3	291	74° 57,30' S	026° 08,10' W	74° 58,60' S	026° 11,12' W
04/01/16	AGT 016-3	621	74° 56,64' S	032° 27,53' W	74° 56,77' S	032° 27,85' W
07/01/16	AGT 026-2	417	75° 16,48' S	037° 56,74' W	75° 16,32' S	037° 56,39' W
14/01/16	AGT 027-8	302	76° 42,84' S	052° 06,31' W	76° 42,69' S	052° 04,61' W
17/01/16	AGT 037-1	389	75° 40,28' S	042° 25,70' W	75° 40,16' S	042° 25,34' W
17/01/16	BT 039-1	389	75° 40,49' S	042° 27,79' W	75° 39,50' S	042° 21,36' W
21/01/16	AGT 057-6	291	76° 16,41' S	029° 06,80' W	76° 16,47' S	029° 05,92' W
21/01/16	BT 059-2	396	76° 11,16' S	030° 02,90' W	76° 12,98' S	030° 05,72' W
23/01/16	AGT 072-1	752	75° 51,23' S	032° 22,91' W	75° 51,31' S	032° 23,85' W
24/01/16	BT 073-3	736	75° 37,82' S	031° 49,79' W	75° 38,83' S	031° 54,75' W
28/01/16	AGT 090-1	1104	72° 22,11' S	017° 18,61' W	72° 22,15' S	017° 19,04' W
29/01/16	BT 090-11	878	72° 17,79' S	016° 50,83' W	72° 19,24' S	016° 53,74' W
31/01/16	AGT 106-5	350	72° 35,29' S	018° 03,60' W	72° 35,37' S	018° 03,85' W

Complete specimens or subsamples of all collected sponges were preserved in denatured ethanol (96 %) and will be used for spicule preparations, which are needed to perform species identification. One specimen of each species per catch was subsampled for DNA-Barcoding. Therefore, one set of subsamples was transferred into pure ethanol (96 %) and frozen at -20°C while another set was frozen at -80°C. For population genetics, if ten or more glass sponges (class: Hexactinellida) of the same species or morphotype were collected at one sample site, each specimen was subsampled thrice. One subsample for morphology was frozen at -20°C and the other two for population genetics were processed as described for DNA-Barcoding. Sponges, which were assumed to be great producers of bioactive compounds, for instance indicated by intensive color or smell, were subsampled for a subsequent screening of secondary metabolites. Therefore, a piece of sponge material was packed with aluminum foil and frozen at -20°C. Subsamples for transcriptomics were taken each time a new species was collected, transferred into RNA-Later and stored at -80°C.

Preliminary (expected) results

Specimens, sometimes only fragments, of sponge species were collected from each catch, while species numbers per catch range from 0 (AGT 026-2) to 22 (AGT 057-6) as shown in Figure 3.2.3.2. The cumulative number of species is 127 while demosponges have the highest number with 105, followed by hexactinellids with 21 and calcareous sponges with 1 species. Table 3.2.3.2 gives a list of preliminarily identified species while representatives of three sponge classes are present: Calcarea, Demospongiae and Hexactinellida (Figure 3.2.3.3). The total number of identified species is a minimum of 33. Hidden diversity has to be considered due to species names, which cover a bunch of unidentified species, e.g. Demospongiae gen. sp. or Poecilosclerida gen. sp. sixhundred thirty-two subsamples are waiting for further analyses: 121 for morphology, 228 for DNA-Barcoding, 67 for transcriptomics, 200 for population genetics and 16 for screening of secondary metabolites.

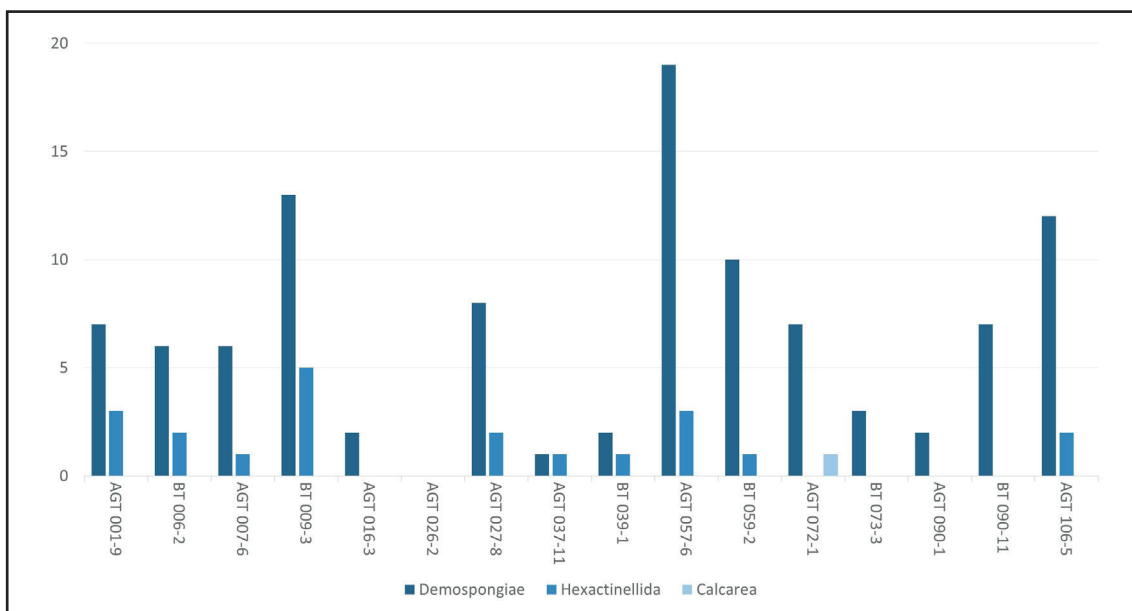


Fig. 3.2.3.2: Number of sponge species per sample site, subdivided into sponge classes

Data management

The sponges collected and investigated in the frame of our Antarctic research projects are deposited and inventoried in the Porifera collection of the Senckenberg Research Institute and Nature Museum. All identified material, including metadata, is catalogued in the SESAM Database (Senckenberg Sammlungsmanagement) and each sample is labeled with an SMF-No. SESAM data are online available immediately upon registration and approval by the collections manager. GBIF (Global Biodiversity Information Facility) and EurOBIS (European Ocean Biogeographic Information System) regularly scan and retrieve the current data of SESAM, so our data become available there as well. Data on Antarctic sponge species are furthermore registered by RAMS (Register of Antarctic Marine Species), which are available via the SCAR-MarBIN data portal. Genetic sequences will be submitted to NCBI (National Center for Biotechnology Information) prior to publication.

Table 3.2.3.2: List of preliminarily identified sponge species

Class Demospongiae	<i>Antho gaussiana</i> <i>Calyx</i> sp. <i>Cinachyra antarctica</i> <i>Cinachyra barbata</i> <i>Cinachyra</i> sp. Cladorhizidae gen. sp. <i>Clathria pauper</i> Demospongiae gen. sp. <i>Iophon</i> sp. <i>Isodictya erinacea</i> <i>Isodictya lankesteri</i> <i>Isodictya</i> sp. <i>Latrunculia</i> sp. <i>Mycale (Oxymycale) acerata</i> <i>Mycale</i> sp. <i>Myxilla (Myxilla) mollis</i> <i>Myxilla</i> sp. <i>Phorbas glaberrimus</i> <i>Phorbas</i> sp. Poecilosclerida gen. sp. <i>Sphaerotylus</i> sp. <i>Stylocordyla chupachups</i> <i>Tedania (Tedaniopsis) charcoti</i> <i>Tedania</i> sp. <i>Tentorium papillatum</i> <i>Tentorium</i> sp. <i>Tethyopsis</i> sp. <i>Tetilla</i> sp.
Class Hexactinellida	<i>Anoxycalyx (Scolymastra) joubini</i> <i>Rossella levis</i> <i>Rossella racovitzae</i> <i>Rossella</i> sp.
Class Calcarea	Calcarea gen. sp.

3.2.3 Suspension feeders in a biodiversity hotspot

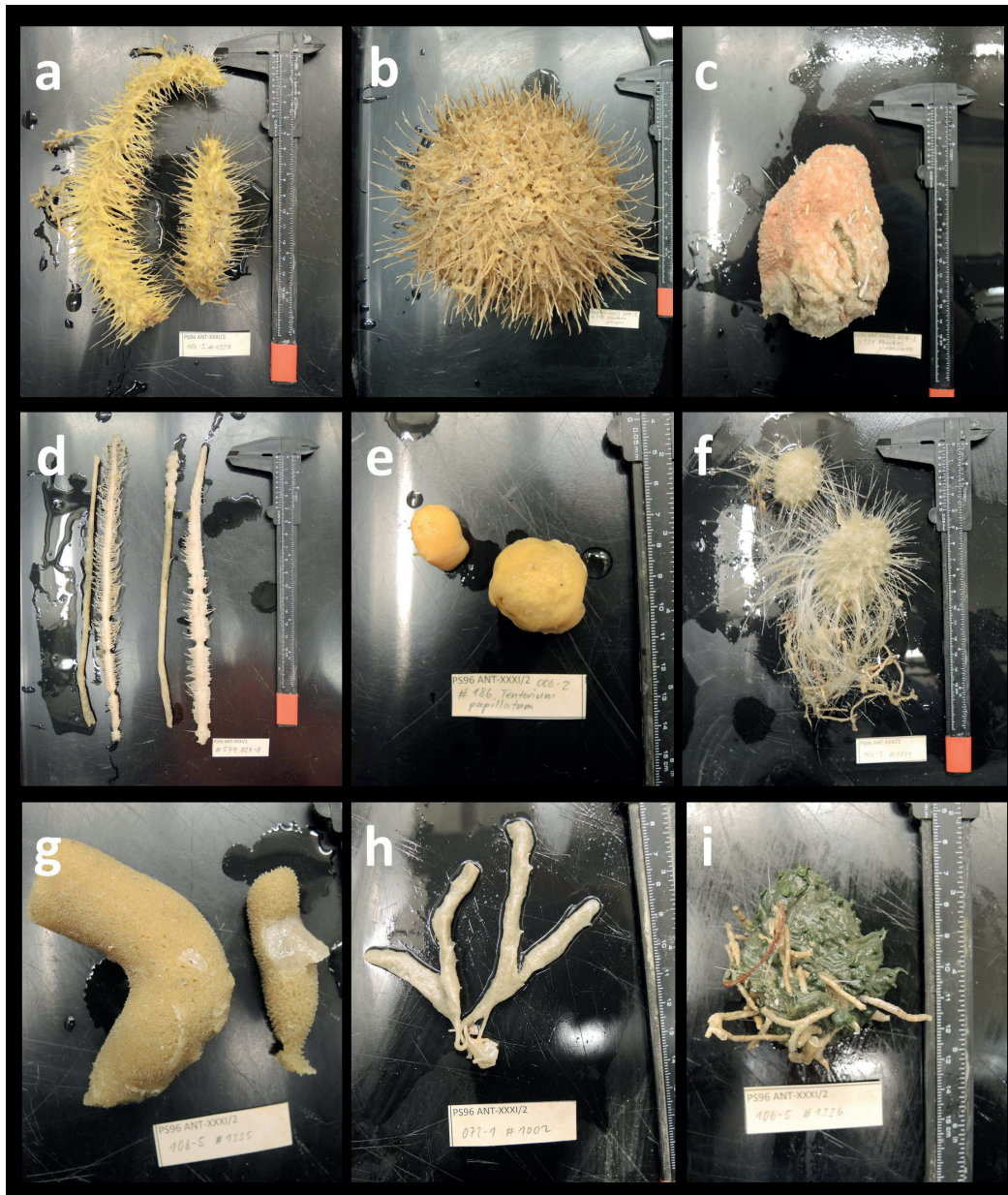


Fig. 3.2.3.3: Selection of identified sponge species: a) *Isodictya erinacea* (AGT 106-5), b) *Clathria pauper* (BT 009-3), c) *Phorbast glaberrimus* (BT 009-3), d) *Cladorhizidae* gen. sp. (AGT 027-8), e) *Tentorium papillatum* (BT 006-2), f) *Rossella levis* (AGT 106-5), g) *Demospongiae* gen. sp. (AGT 106-5), h) *Calcarea* gen. sp. (AGT 072-1) and i) *Latrunculia* sp. (AGT 106-5)

References

Arndt JA, Schenke HW, Jakobsson M, Nitsche FO, Buys G, Goleby B, Rebesco M, Bohoyo F, Hong J, Black J, Greku R, Udintsev G, Barrios F, Reynoso-Peralta W, Taisei M, Wigley R (2013) The International Bathymetric Chart of the Southern Ocean (IBCSO) Version 1.0 – A new bathymetric compilation covering circum-Antarctic waters. *Geophysical Research Letters* 40:1-7.

- Bell JJ (2008) The functional roles of marine sponges. *Estuarine Coastal and Shelf Science*. 79:341-353.
- Berne S, Kalauz M, Lapat M, Savin L, Janussen D, Kersken D, Ambrozic Avgustin J, Zemljic Jokhadar S, Jaklic D, Gunde-Cimerman N, Lunder M, Roskar I, Elersek T, Turk T, Sepcic K (2015) Screening of the Antarctic marine sponges (Porifera) as a source of bioactive compounds. *Polar Biology*, DOI: 10.1007/s00300-015-1835-4.
- Downey RV, Griffiths HJ, Linse K, Janussen D (2012) Diversity and Distribution Patterns in High Southern Latitude Sponges. *Plos One* 7(7):e41672.
- Gutt J, Alvaro MC, Barco A, Böhmer A, Bracher A, David B, De Ridder C, Dorschel B, Eléaume M, Janussen D, Kersken D, López-González PJ, Martínez-Baraldés I, Schröder M, Segelken-Voigt A, Teixidó N (2015) Macroepibenthic communities at the tip of the Antarctic Peninsula, an ecological survey at different spatial scales. *Polar Biology*, DOI: 10.1007/s00300-015-1797-6.
- Hogg MM, Tendal OS, Conway KW, Pomponi SA, van Soest RWM, Gutt J, Krautter M, Roberts JM (2010) Deep-sea Sponge Grounds: Reservoirs of Biodiversity. *UNEP-WCMC Biodiversity* 32:1-84.
- Kersken D, Göcke C, Brandt A, Lejzerowicz F, Schwabe E, Seefeldt MA, Veit-Köhler G, Janussen D (2014) The infauna of three widely distributed sponge species (Hexactinellida and Demospongiae) from the deep Ekström Shelf in the Wedell Sea, Antarctica. *Deep-Sea Research Part II* 108:101-112.
- Kersken D, Feldmeyer B, Janussen D (2016) Sponge communities of the Antarctic Peninsula: influence of environmental variables on species composition and richness. *Polar Biology*, DOI: 10.1007/s00300-015-1875-9.
- McClintock JB, Amsler CD, Baker BJ, van Soest RWM (2005) Ecology of Antarctic Marine Sponges: An Overview. *Integrative and Comparative Biology* 45:359-368.
- Vargas S, Dohrmann M, Göcke C, Janussen D, Wörheide G (2016) Nuclear and mitochondrial phylogeny of *Rossella* (Hexactinellida: Lyssacinosa, Rossellidae): a species and a species flock in the Southern Ocean. *BioRxiv* preprint, DOI: <http://dx.doi.org/10.1101/037440>.

3.2.4 Sponge ecology and benthic fluxes

Claudio Richter¹, Moritz Holtappels¹, Louisa Federwisch¹,
Hannelore Cantzler¹, Roger Johansson², Emil Anderson²

¹AWI,
²SLC Uni Gothenburg

Grant No: AWI_PS96_02

Objectives

On Antarctic shelves, sponges often dominate the megabenthic epifauna. But in spite of intensive research on epifauna community composition and distribution (Voß 1988, Gutt & Starmans 1998), the significance of sponges for Antarctic benthic processes has so far not been assessed, and much of the presumed role of sponges in carbon and silicon cycling is based on inference (Maldonado et al. 2005, Gutt et al. 2013). As deep-dwelling suspension feeders, sponges are limited by the supply of materials and energy. They have to cope with high seasonal and spatial variability in primary production and depend on the physical transport (e.g. sinking, convection) of organic matter from the productive surface layer to the benthos. The size of the phytoplankton is large, by sponge standards, where filter-feeding involves the passage of water through very narrow pores. For example, the incurrent water in hexactinellid sponges must pass the ostia and prosopyles featuring only 2-3 µm diameter (Leys et al. 2011). However, the bulk of the Antarctic phytoplankton, diatoms, are much larger, generally >10 µm in diameter involving many chain- and aggregate-building forms. Thus, an important step in the energy transfer is the conversion of the sedimented and/or convected organic matter to picoplankton (<2 µm, chiefly bacteria). Because the bulk of the dry mass of sponges consists of SiO₂ spicules (70-80%, Fillinger et al. 2013) another important step is the incorporation of dissolved Si (dSi) which may involve dissolution of diatom frustules near the seabed.

We hypothesize that diatom blooms forming in the stratified surface layers of the retreating ice edge/shelf ice polynyas sink out to the seafloor where they are decomposed near the seabed. Resuspension of this detritus may fuel a microbial loop in the benthic boundary layer supplying sponges for extended periods. The objective of this study was to test this hypothesis and close the gap in Antarctic ecological process studies relating benthic boundary layer findings to the processes in the overlying water column. Here, we combine pelagic work on plankton and benthic work on sponges, on the organismal and system level.

The main objectives were:

- to assess the diet, feeding rates and metabolism of sponge assemblages on the shelf of the southeastern Weddell Sea, providing results comparable with those from other sponge-dominated areas
- to assess the distribution of phytoplankton, bacterioplankton, C, N and Si between the surface and the seabed to infer production and re-mineralisation processes
- to assess, for the first time, the benthic oxygen flux on an Antarctic shelf, using the in situ Eddy Correlation (EC) method
- to identify spatial distribution patterns of sponges in relation to bottom-up (food, Si) and top-down factors (predators) governing sponge occurrence at local and regional scales
- to assess the abundance and size distribution of sponges investigated in previous *Polarstern* cruises to estimate growth dynamics over the scale of years to decades. Of particular interest was the recovery of sponge communities in the area of the long-

term benthic disturbance experiment (BENDEX) started in 2003 (Arntz & Brey 2005, Gerdes et al. 2008), in comparison with sponge recovery in the Larsen area (Fillinger et al. 2013).

Work at sea

Work at sea involved (1) seabed imaging for sponge abundance, size distribution and changes in sponge benthos, (2) collection of water samples from the water column, in the benthic boundary layer and the immediate vicinity of sponges, (3) assessment of sponge pumping, oxygen consumption, nitrogen excretion, dSi uptake and particle retention efficiency in situ, (4) deployment of a lander to assess oxygen fluxes in situ. A side aspect included (5) the collection of sponge tissue samples for characterisation of the sponge-associated microbiome.

Seabed imaging was carried out by the OFOS team (see ch. 3.2.5) and included one repeat transect visited during PS82 (station PS82/049).

For the collection of water samples, the CTD-rosette, a bottom water sampler (BWS) and a new custom ROV-sampling system was used. The rosette was operated by the CTD team (see ch. 3.1.1) who kindly provided Niskin samples from six standard depths: surface (2 to 10 m), the depth of the chl a maximum (20 to 70 m), 100 m, 50 m.a.b., 20 m.a.b. and 5 m.a.b. Water samples from the benthic boundary layer were collected with the BWS from six standard depths: 0.25, 0.52, 0.84, 1.21, 1.64 and 2.14 m.a.b.

Samples for dissolved organic matter (DOM) were filtered through pre-combusted GF/F filters into acid-washed plastic bottles, acidified with hydrochloric acid (HCl) to pH 2, and stored tightly sealed at 4 °C. Samples for particulate organic carbon and nitrogen (POC and PON) were filtered through pre-weighed and pre-combusted GF/F filters and stored frozen at -20°C. For ammonium, 10 ml samples were analyzed fluorometrically according to Holmes et al. (1999) directly after sampling. For dissolved silicate (dSi), 500 ml water was filtered through cellulose acetate filters and duplicate subsamples of 10 ml were stored at 4 °C until later analysis on board. The samples were analyzed photometrically according to Koroleff (1999). The filters were folded into aluminium foil and frozen at -20 °C for analysis of particulate silicate (pSi), to be carried out in Bremerhaven. Picoplankton samples (1.8 ml) were directly filled into CryoVials, fixed with glutaraldehyde and frozen at -20 °C for later flow cytometric analysis. Samples (10 ml) for bacteria and microphytoplankton were filtered through sterile 0.2 µm polycarbonate filters and frozen at -20 °C for later scanning electron microscopic (SEM) analysis. Phytoplankton samples (200 ml) were filled into brown glass bottles, fixed with Lugol's solution and stored in the dark for later Utermöhl counts. Additionally, 40 ml of water from each sampled depth were transferred to Falcon tubes and frozen at -20 °C as back-up samples or for further nutrient analyses.

To sample water directly from the osculum and from the vicinity of sponges, we used a custom-built ROV-borne water sampling system (designed by E.A.) consisting of eleven accessible 60 ml perspex cylindrical samplers mounted in the ROV's sample tray. To take a sample, the sample tray drawer was opened and the ROV's manipulator positioned above one of samplers. A connector composed of a magnetic seal matching a corresponding metal disc on the top end of the sampler ensured a temporary but snug fit between ROV arm and sampler. The ROV arm was then manoeuvred to position the sampler for the collection of paired samples of ambient and exhalant water. For the ambient water, a sample was taken next to a sponge. For the sponge exhalant water, the sampler was carefully inserted inside the sponge osculum. A hose connecting the connector to the ROV pump (a modified thruster) allowed to evacuate the sampler (filled with filtered seawater prior to the dive) and fill it with sample water. According to

3.2.4 Sponge ecology and benthic fluxes

prior tests using fluorescein tracer, the pump was turned off after 18s, corresponding to >300 ml flushing (i.e. >5-fold the sampler volume) and >99% replacement of pre-filled water with sample water. Lab and field tests showed negligible leakage of the samplers. Because of the small sample volume, subsamples were taken for dSi (10 ml), picoplankton (triplicate 1.8 ml), ammonia (10 ml) and SEM (10 ml).

To measure pumping rates of the sponges, fluorescein dye was injected at the side (greatest width) of the sponge and the time for the dye to exit the osculum was recorded on video. Frame-by-frame tracking of the dye front will allow to estimate pumping velocity.

To measure oxygen consumption, an optode (Aanderaa) attached to the manipulator was inserted into the sponge osculum and the evolution of the oxygen concentration over time recorded. Reference measurements were taken outside the sponge.

Sponge size was measured with parallel green laser lights spaced 65 mm apart.

The HD video camera of the ROV allowed us to observe sponge epifauna and sponge surroundings during the 5-10 min periods of optode measurements.

Routine deployment of the EC lander failed due to technical problems with the ROV. The combined effects of high EC payload (11 kg), ambient currents and low temperatures likely exceeded the technical specifications of the electronics causing malfunction of the ROV 's thrusters and electronics boards. The only opportunity to deploy the EC lander was at Drescher Inlet (station PS96/087) where the vessel remained in a fixed position for several hours allowing its deployment and retrieval while remaining connected via a Meteor line. The lander was lowered over the aft of the vessel and remained on the seabed at 520 m water depth for 8 h. The lander was composed of a fast sampling (64 Hz) acoustic Doppler velocimeter (Vector, Nortek), a fast sampling (5 Hz) micro-Optode (Diameter 430 µm, Pyroscience), a fast temperature sensor (Rockland Scientific), and two Aanderaa Optodes positioned at 20 cm and 120 cm above the bottom. A camera (GoPro Hero 4) in an underwater housing (GoBenthic, Group B Inc.) and a LED flashlight (Nautilux modified, Group B Inc.) in a housing (General Purpose Housing, Group B Inc.) was mounted on the frame for visual inspection of the seafloor during the first minutes of deployment. The camera/light system was also regularly mounted on the BWS to monitor closure of the sampling bottles and estimate in retrospect the percent cover of epifauna.

In addition to the work on processes and benthic fluxes, glass sponges from one particularly rich bottom trawl (station PS96/009-3) were sampled for their microbiomes, i.e. the microbial diversity in the sponge tissue. Eighteen sponges of five distinct morphotypes were selected, photographed and subsampled directly after the trawl. Three replicates of tissue from each sponge were sampled aseptically and frozen at -80 °C together with one large piece of tissue for further analyses. Another tissue subsample of each sponge was dried for later taxonomic identification. Additionally, 4 L of bottom water from the same station (CTD at PS96/009-4) were filtered through a polycarbonate filter (0.2 µm pore size) which was frozen at -80 °C, as well, to analyze the bacterial community in the water in comparison to the sponge microbiomes. The analysis of the samples will be carried out in cooperation with Ute Hentschel at GEOMAR, Kiel.

Preliminary (expected) results

Water samples were collected at 13 stations from the CTD and at 11 stations from the BWS. The ROV was deployed ten times at eight stations (Table 3.2.4.1, Fig. 3.2.4.1). Additional CTD samples were collected for a side project on dissolved organic matter (DOM) with Thorsten Dittmar at Uni Oldenburg.

Sponge distribution

Preliminary assessment of the images provided by the OFOS and the ROV shows a rich benthic epifauna in the eastern part of the shelf at Halley Bay and further south, whereas a very poor benthic epifauna was characteristic for the western part of the visited shelf area (Filchner Trough and west of it). This finding corresponds to pronounced fluorescence peaks measured by the CTD in the eastern part of the shelf, whereas low or non-detectable fluorescence peaks were found in the western waters (Fig. 3.2.4.2). Apparently, conditions for a phytoplankton bloom in the eastern areas were favorable given a large coastal polynya with relatively warm surface waters and a stratification that reduced the upper mixing depth.

Tab. 3.2.4.1: List of stations occupied by the sponge team during PS96 (ANT XXXI/2) for observations, measurements and samples collected by Remotely Operated Vehicle (ROV), Bottom Water Sampler (BWS), CTD-Rosette (including DOM-only) and Eddy Correlation (EC) Lander system

Gear	Station	Lat	Lon	Depth [m]	Remarks
CTD/RO	PS96/001-1	-70,8815	-11,1005	330	Plankton, nutrient & DOM sampling
CTD/RO	PS96/001-5	-70,89583333	-11,14833333	291	Plankton, nutrient & DOM sampling
CTD/RO	PS96/005-2	-74,64416667	-26,9615	502,6	Plankton, nutrient sampling
CTD/RO	PS96/008-1	-74,92166667	-29,4195	392,4	Plankton, nutrient & DOM sampling
CTD/RO	PS96/010-2	-74,95783333	-25,9925	275,5	Plankton, nutrient & DOM sampling
CTD/RO	PS96/026-13	-75,26616667	-37,9195	413,3	Plankton, nutrient & DOM sampling
CTD/RO	PS96/027-1	-76,7185	-52,19133333	298,3	Plankton, nutrient & DOM sampling
CTD/RO	PS96/037-2	-75,69783333	-42,3375	388,5	Plankton, nutrient & DOM sampling
CTD/RO	PS96/048-1	-74,76966667	-35,30983333	488,2	Plankton, nutrient & DOM sampling
CTD/RO	PS96/057-1	-76,31883333	-29,03566667	ca. 240	Plankton, nutrient & DOM sampling
CTD/RO	PS96/072-2	-75,85616667	-32,42116667	753,2	Plankton, nutrient & DOM sampling
CTD/RO	PS96/090-3	-72,4335	-17,038	555,6	Plankton, nutrient & DOM sampling
CTD/RO	PS96/106-1	-72,60866667	-17,87183333	200,9	Plankton, nutrient & DOM sampling
CTD/RO	PS96/051-1	-74,6613	-32,4845	614,7	DOM sampling
CTD/RO	PS96/052-1	-74,6642	-32,0300	619,3	DOM sampling
CTD/RO	PS96/062-1	-75,9433	-31,4570	599,1	DOM sampling
CTD/RO	PS96/069-1	-75,9502	-31,7558	714	DOM sampling

3.2.4 Sponge ecology and benthic fluxes

Gear	Station	Lat	Lon	Depth [m]	Remarks
CTD/RO	PS96/077-1	-75,4982	-32,4988	688	DOM sampling
CTD/RO	PS96/082-1	-75,5005	-30,9953	566,3	DOM sampling
CTD/RO	PS96/095-1	-72,2083	-17,4462	1942,5	DOM sampling
CTD/RO	PS96/096-1	-72,3265	-17,7818	1689,8	DOM sampling
CTD/RO	PS96/110-1	-72,5003	-18,3990	2285,4	DOM sampling
CTD/RO	PS96/111-1	-63,6940	-50,8023	2799	DOM sampling
BWS	PS96/001-6	-70,8950	-11,1517	319,0	Plankton, nutrient & DOM sampling
BWS	PS96/007-7	-74,6452	-26,9603	489,0	Plankton, nutrient & DOM sampling
BWS	PS96/010-5	-74,9580	-25,9998	271,7	Plankton, nutrient & DOM sampling
BWS	PS96/026-4	-75,2660	-37,9210	414,0	Plankton, nutrient & DOM sampling
BWS	PS96/027-3	-76,7195	-52,1490	301,1	Plankton, nutrient & DOM sampling
BWS	PS96/037-5	-75,6977	-42,3388	388,3	Plankton, nutrient & DOM sampling
BWS	PS96/048-4	-74,7512	-35,3473	483,7	Plankton, nutrient & DOM sampling
BWS	PS96/057-4	-76,3185	-29,0348	241,3	Plankton, nutrient & DOM sampling
BWS	PS96/072-3	-75,8558	-32,4237	751,4	Plankton, nutrient & DOM sampling
BWS	PS96/090-6	-72,4363	-17,0402	283,9	Plankton, nutrient & DOM sampling
BWS	PS96/106-4	-72,6083	-17,9063	213,9	Plankton, nutrient & DOM sampling
ROV	PS96/001-3	-70,8840	-11,1198	334,0	test station, fine tuning
ROV	PS96/007-5	-74,6583	-26,9573	415,7	sponges, first sampling tests
ROV	PS96/010-4	-74,9487	-26,0615	278,0	aborted (thruster failure, EC lander deployment unsuccessful)
ROV	PS96/037-4	-75,6978	-42,3388	388,3	no glass sponges
ROV	PS96/048-3	-74,7512	-35,3487	483,6	aborted (technical problems)

Gear	Station	Lat	Lon	Depth [m]	Remarks
ROV	PS96/057-2	-76,3185	-29,0345	241,4	"sponge station", ROV water sampling successful
ROV	PS96/057-5	-76,3187	-29,0338	244,2	"sponge station", ROV water sampling successful
ROV	PS96/090-5	-72,4357	-17,0365	282,1	sponges, ROV water sampling successful
ROV	PS96/090-13	-72,4348	-17,0360	271,7	sponges, ROV water sampling successful
ROV	PS96/106-3	-72,6087	-17,9068	213,2	sponges, ROV water sampling successful
Eddy Lander	PS96/087-1	-72,79816667	-19,35133333	524,8	

Sponge feeding, ammonium excretion and Si uptake

The new ROV-mounted water sampler was successfully deployed, yielding a total 22 samples from sponge oscula and 21 samples from ambient waters. Flow cytometric analysis of the samples will later on allow to determine retention efficiencies for picoplankton. Fluorescein dye experiments will allow to determine corresponding pumping rates. The combination of the two will hopefully provide the first *in situ* filtering rates determined so far for Antarctic hexactinellid sponges. Ammonium and dSi samples will be analyzed to assess excretion and Si uptake in the sponges.

Sponge respiration

Optode measurements in the ambient water and inside the sponge osculum revealed a measurable decrease of 0.5-4 μM oxygen in the exhalent waters (Fig. 3.2.4.3). Together with estimates of the exhalent volume flow from the fluorescein dye experiments the oxygen uptake of individual sponges can be estimated and eventually extrapolated to regional scales using the sponge abundance and sizes found in the OFOS transects.

EC Lander

Preliminary results of the deployment reveal low current velocities of 1-8 cm/s on average at 520 m water depth (Fig. 3.2.4.4). Surprisingly, wave-like current velocities with a period of 5 min were observed during ebb tide. The turbulent oxygen fluctuations were below 100 nmol/L and a preliminary turbulent oxygen flux towards the seafloor of 0.5 mmol/L/d could be calculated. The low oxygen uptake of the benthos agrees with images of a rather poor benthic epifauna taken by the camera.

3.2.4 Sponge ecology and benthic fluxes

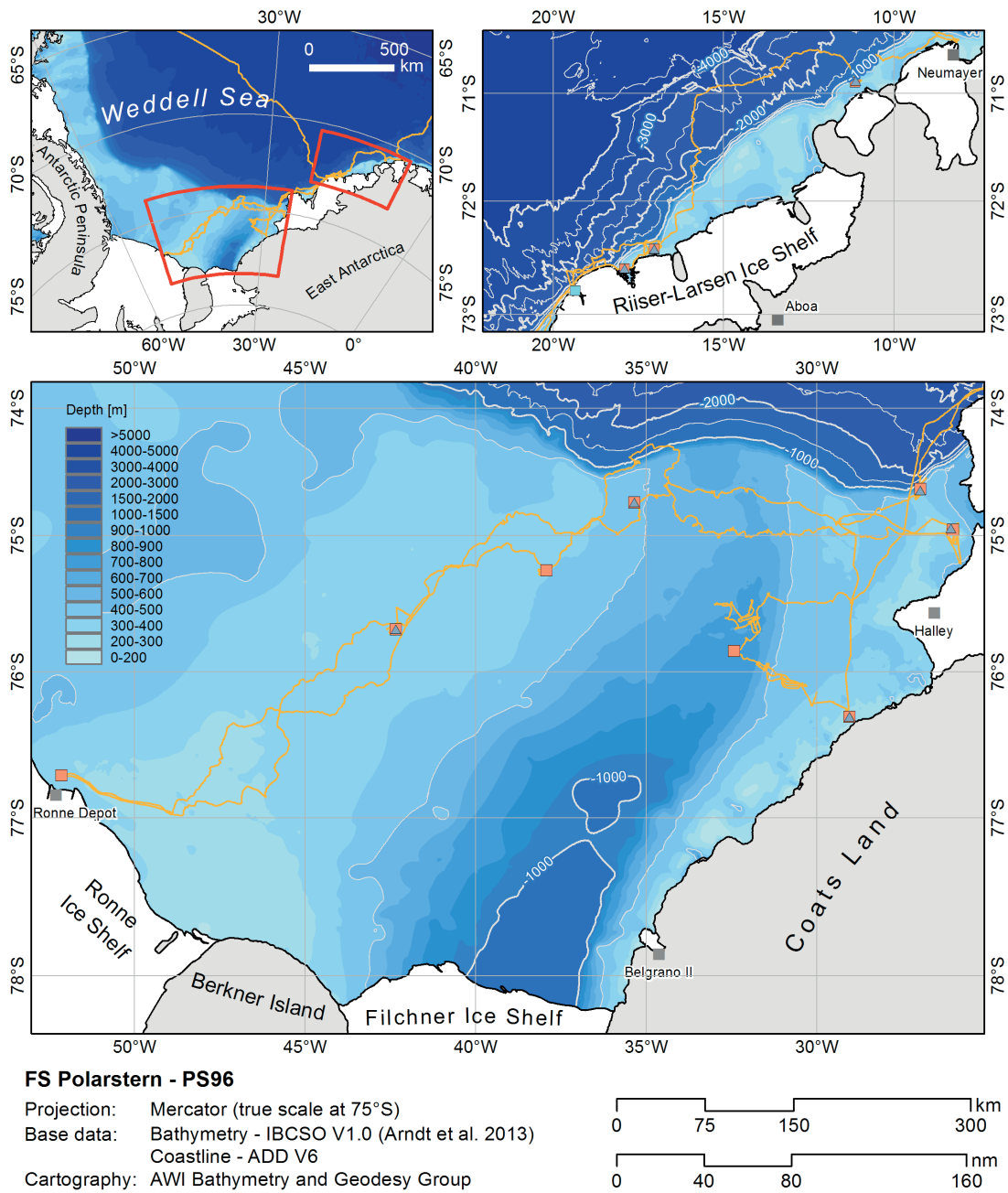


Fig. 3.2.4.1: Map of stations occupied by the sponge team during PS96 (ANT XXXI/2) for observations, measurements and samples collected by Remotely Operated Vehicle (ROV, grey triangles); CTD-Rosette and Bottom Water Sampler (BWS) (orange squares), and Eddy Correlation (EC) Lander system (turquoise square). CTD-Rosette stations for DOM only are not plotted.

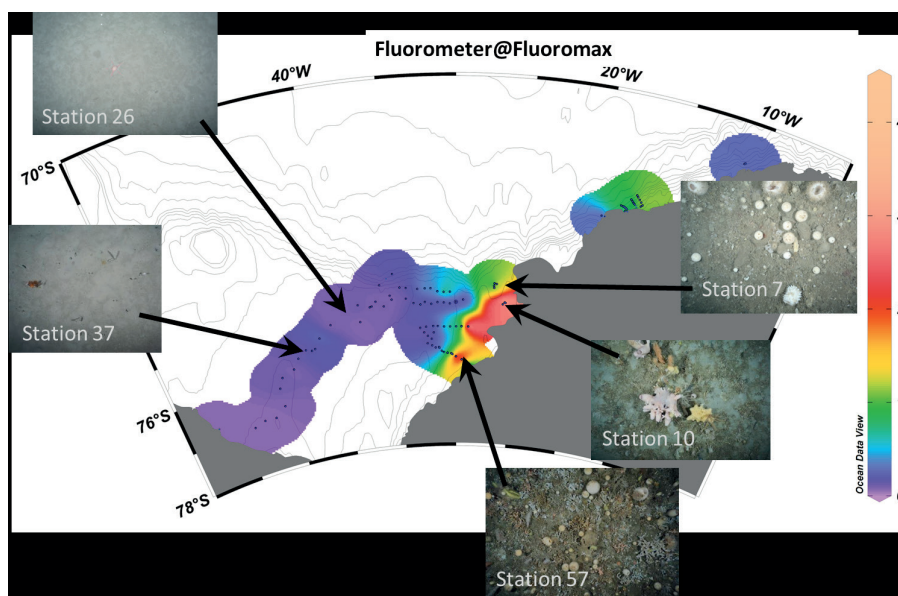


Fig. 3.2.4.2: Seabed images of benthic epifauna (by OFOS and ROV) and corresponding chlorophyll a fluorescence measurements (data courtesy oceanography team, cf. chapter 3.1.1) in CTD sampling sites during PS96 (ANT XXXI/2)

DOM

A total 118 samples for dissolved organic matter were taken. The samples were taken parallel to the nutrient samples at ROV/BWS stations, but also at several oceanographic CTD stations to be able to characterize specific water masses such as the Ice Shelf Water and Weddell Sea Deep Water for their DOM-specific molecular fingerprint.

Data management

All the data generated from this expedition will be included in Pangaea.

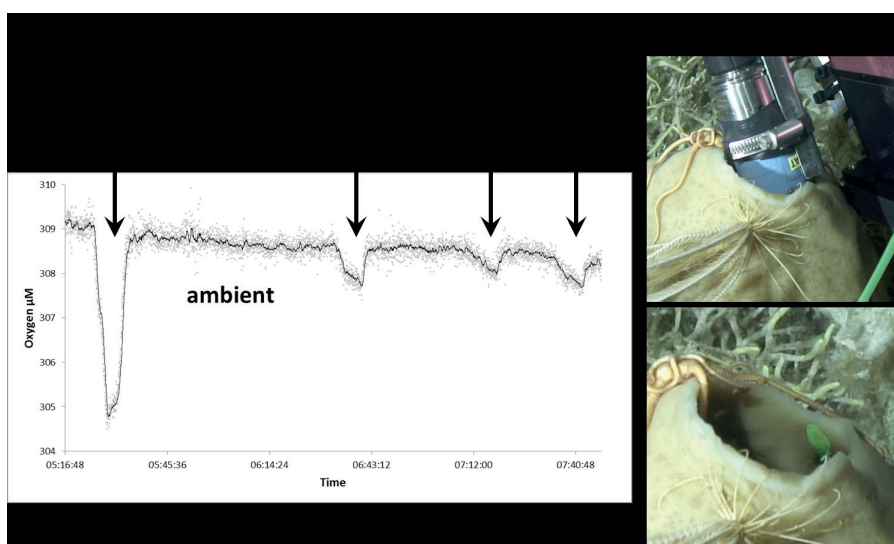


Fig. 3.2.4.3: Oxygen respiration in four sponges during PS96 (ANT XXXI/2). Optode readings (in μM , raw data: grey points, filtered data: line) show periods where the optode was immersed in sponge osculum (upper right video frame) or in ambient water. The lower right video frame shows the advancing fluorescein plume tracing the exhalant current.

3.2.4 Sponge ecology and benthic fluxes

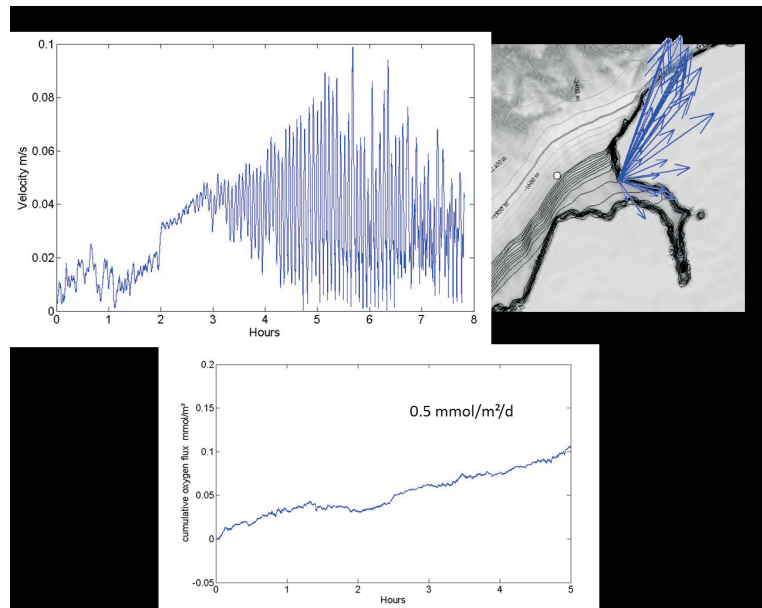


Fig. 3.2.4.4: Current velocities (cm/s), current direction (arrows) and oxygen flux (μM) of benthic epifauna after the deployment of the EC Lander at Drescher Inlet during PS96 (ANT XXI/2).

References

- Arntz WE, Brey T, eds. (2005) The Expedition ANTARKTIS XXI/2 (BENDEX) of RV "Polarstern" in 2003/2004. *Reports on Polar and Marine Research* 503, 149 pp.
- Fillinger L, Janussen D, Lundälv T, Richter C (2013) Rapid glass sponge expansion after climate-induced Antarctic ice shelf collapse. *Curr Biol* 23:1330-1334.
- Gerdes D, Isla E, Knust R, Mintenbeck K, Rossi S (2008) Response of Antarctic benthic communities to disturbance: first results from the artificial Benthic Disturbance Experiment on the eastern Weddell Sea Shelf, Antarctica. *Polar Biol* 31:1469-1480.
- Gutt J, Böhmer A, Dimmler W (2013) Antarctic sponge spicule mats shape macrobenthic diversity and act as a silicon trap. *Mar Ecol Prog Ser* 480:57-71. doi: 10.3354/meps10226.
- Gutt J, Starmans A (1998) Structure and biodiversity of megabenthos in the Weddell and Lazarev Seas (Antarctica): ecological role of physical parameters and biological interactions. *Polar Biol* 20:229-247.
- Holmes RM, Aminot A, Kérouel R, Hooker BA, Peterson BJ (1999) A simple and precise method for measuring ammonium in marine and freshwater ecosystems. *Can J Fish Aquat Sci* 56:1801-1808.
- Koroleff F (1999) Determination of dissolved inorganic silicate. In: Grasshoff K, Ehrhardt M, Kremling K (1999) *Methods of Seawater Analysis. 3rd, completely revised and extended Edition*, Wiley-VCH, Weinheim, p. 193 ff.
- Leys SP, Yahel G, Reidenbach MA, Tunnicliffe V, Shavit U, et al. (2011) The sponge pump: The role of current induced flow in the design of the sponge body plan. *PLoS ONE* 6(12): e27787. doi:10.1371/journal.pone.0027787.
- Maldonado M, Carmona MC, Velasquez Z, Puig A, Cruzado A, Lopez A, Young CM (2005) Siliceous sponges as a silicon sink: an overlooked aspect of benthic-pelagic coupling in the marine silicon cycle. *Limnol Oceanogr* 50:799-809.
- Voß J (1988) Zoogeography and community analysis of macrozoobenthos of the Weddell Sea (Antarctica). *Berichte zur Polarforschung* 45, 145 pp.

3.2.5 Spatial distribution patterns of epibenthic megafauna and habitats

Dieter Piepenburg

AWI

Grant No: AWI_PS96_02

Objectives

Megabenthic epifauna comprises the seafloor organisms that are large enough to be visible in seabed images and/or to be caught by towed sampling gear. These organisms are of very high ecological significance for Southern Ocean shelf ecosystems (Gutt, 2006), as they can strongly affect the small-scale topography of seafloor habitats and, hence, the structure of the entire benthic community (Gili et al., 2006). In addition, some megabenthic species are especially sensitive to environmental change, due to their slow growth, specific reproduction mode, high degree of environmental adaptation, and narrow physiological tolerances, and can thus serve as early indicators of ecosystem shifts in response to environmental change (Barnes et al., 2009).

The work performed during cruise PS96 on the epibenthic megafauna was a component of the main *Polarstern* cruise application S-633 titled *Dynamics of Antarctic Marine Shelf Ecosystems* (DynAMo). This project aims to assess the pace and quality of the dynamics of benthos and endotherms in stable high-Antarctic environments that are not (yet) affected by climate change. Within this context, and based on investigations performed during previous *Polarstern* cruises to the southeastern and southern Weddell Sea, comparative follow-up field studies were carried out to investigate the abundance, distribution, composition and diversity of epibenthic megafauna. The main objectives of the investigations were:

- Complement surveys of mega-epibenthic assemblages of the shelf of the southeastern and southern Weddell Sea, providing further data comparable with those gained in earlier studies (Biebow et al., 2014a)
- Identify spatial distribution patterns of epibenthic megafauna at local and regional scales
- Assess the status of the recovery of megabenthic communities in the area of the long-term benthic disturbance experiment (BENDEX) started in 2003 (Biebow et al., 2014b)
- Contribute to the standardization of the classification of Antarctic megabenthic communities (Gutt, 2007; Gutt, 2013)

Work at sea

Within the context of the overall ecological working programme of the PS96 cruise, seabed imaging surveys, providing both still photographs and video footage, were carried out by means of the Ocean Floor Observation System (OFOS).

The setup and mode of deployment of the OFOS was similar to that described by Bergmann and Klages (2012). OFOS is a surface-powered gear equipped with two downward-looking cameras installed side-by-side, a high-resolution (21 MPix), wide-angle still camera (CANON® EOS 1Ds Mark III) and high-definition color video camera (SONY® FCB-H11). The system was vertically lowered over the stern of the ship with a broadband fibre-optic cable, until it hovers 1.5 m above the seabed. Then, it was towed after the slowly sailing ship at a speed of 0.5 kn (approx. 0.25 m s⁻¹). During the casts, OFOS was kept hanging at the preferred height above the seafloor by means of the live video feed and occasional minor height adjustments

3.2.5 Spatial distribution patterns of epibenthic megafauna and habitats

with the winch to compensate small-scale bathymetric variations in seabed morphology. Information on water depth and height above the seafloor were continuously recorded by means of OFOS-mounted sensors. The ship's Global Acoustic Positioning System (GAPS), combining Ultra Short Base Line (USBL), Inertial Navigation System (INS) and satellite-based Global Positioning System (GPS) technologies, was used to gain highly precise underwater position data of the OFOS. Three lasers, which are placed beside the still camera, emit parallel beams and project red light points, arranged as an equilateral triangle with a side length of 50 cm, in each photo, thus providing a scale that can be used to calculate the photographed area in each image and/or measure the size of organisms or seabed features visible in the image. In automatic mode, a seabed photo, depicting an area of about 3.45 m² (= 1.5 m x 2.3 m; with small variations depending on the height above ground), was taken every 30 seconds to obtain series of stills distributed along transects that vary in length depending on cast duration. With a ship speed of 0.5 kn, the average distance between the seabed images was approximately 5 m. Additional photos were taken from interesting objects (organisms, seabed features, such as putative iceberg scours) when they appeared in the live video feed (which was also recorded, in addition to the stills, for documentation and possible later analysis).

During the PS96 cruise, the OFOS was deployed at a total of 13 stations at water depths between 200 and 754 m (Tab. 3.2.5.1, Fig. 3.2.5.1). During the casts of 0:54 to 2:14 hours on-ground duration, series of 110 to 293 stills (2,670 in total) were obtained along transects of 0.9 to 2.6 km length (Tab. 3.2.5.1). In addition, more than a total of 14:50 hours of video footage was recorded (Tab. 3.2.5.1).

The stations were distributed over several areas in the southeastern and southern Weddell Sea (Tab. 3.2.5.1, Fig. 3.2.5.1):

1. Off Austasen, one transect (St. 001) was positioned in close vicinity to the BENDEX sites investigated in 2003, 2011 and 2014. Unfortunately, the actual main BENDEX location, artificially disturbed in 2003, could not be revisited, since in 2015 it was under fast ice and, hence, not accessible.
2. Four stations (Sts. 026, 027, 037 and 048) were located in the main study area of the PS96 cruise, the broad shelf of the southern Weddell Sea west of the Filchner Trough.
3. Five stations (Sts. 007, 008, 010, 057 and 061) were situated on the shelf east of the Filchner Trough. Some of these station were revisits of sites that had been investigated during *Polarstern* cruise PS82 in 2014, using seabed imaging gears other than OFOS: a) St. 008 was close to the position of St. PS82-277 (74°54.3'S, 29°40.1'W), where in 2014 evidence of demersal eggs and nest-parental care behaviour (guarded fishnests) had been recorded; b) St. 057 was a revisit of a ROV track made in 2014 (from 79°19.1'S, 29°02.0'W to 79°19.3'S, 29°00.9'W), where close to the coast of Coats Land, at depths of about 240 m, a rich sponge-dominated seabed fauna had been recorded.
4. One station (St. 072) was located in the Filchner Trough itself, at about 750 m depth.
5. Two additional stations (Sts. 090 and 106) were surveyed on the southeastern Weddell Sea shelf, close to the mouths of inlets in the edge of the Riiser-Larsen Ice Shelf.

Table 3.2.5.1: List of stations where the Ocean Floor Observation System (OFOS) was deployed during *Polarstern* cruise PS96 (ANT-XXXI/2) to the Weddell Sea in December 2015-February 2016

OFOS #	PS96-#	Area	Start Transect			End Transect			Transect Data			Video Length (h)		
			Date/Time (UTC)	Lat (S)	Long (W)	D-Ship Depth (m)	Date/Time (UTC)	Lat (S)	Long (W)	D-Ship Depth (m)	Duration (h)		Length (km)	# of photos
1	001-4	Austasen	23.12.15 20:44	70°53.19'	11°06.52'	315	23.12.15 22:20	70°53.76'	11°08.79'	293	01:36	1.74	203	01:41:00
2	007-1	Filchner East	29.12.15 16:08	74°39.42'	26°56.49'	412	29.12.15 17:55	74°40.06'	26°59.91'	414	01:47	2.58	223	630 Clips
3	008-2	Filchner East	30.12.15 18:33	74°55.23'	29°25.35'	400	30.12.15 20:25	74°54.45'	29°24.58'	405	01:52	1.49	248	01:55:57
4	010-3	Filchner East	01.01.16 11:52	74°56.65'	26°02.50'	292	01.01.16 13:52	74°57.44'	26°05.13'	294	02:00	1.94	260	02:01:20
5	026-3	Filchner West	08.01.16 01:58	75°16.98'	37°55.96'	405	08.01.16 03:58	75°15.99'	37°55.17'	404	02:00	1.87	268	02:03:36
6	027-2	Rönne Depot	14.01.16 13:41	76°43.14'	52°11.30'	298	14.01.16 14:35	76°43.12'	52°09.30'	300	00:54	0.85	110	53 Clips
7	037-3	Filchner West	16.01.16 14:05	75°43.29'	42°27.65'	390	16.01.16 15:05	75°42.85'	42°26.66'	390	01:00	0.93	131	70 Clips
8	048-2	Filchner West	18.01.16 20:25	74°46.20'	35°18.63'	487	18.01.16 22:25	74°45.45'	35°21.00'	483	02:00	1.81	266	02:01:44
9	057-3	Filchner East	21.01.16 01:29	76°19.11'	29°01.97'	241	21.01.16 02:35	76°19.32'	29°00.13'	239	01:06	0.90	131	01:09:07
10	061-1	Filchner East	21.01.16 18:12	76°05.98'	30°18.04'	469	21.01.16 19:42	76°05.44'	30°20.27'	480	01:30	1.41	213	01:29:16
11	072-4	Filchner Trough	23.01.16 17:07	75°51.61'	32°22.93'	754	23.01.16 18:30	75°51.43'	32°20.30'	752	01:23	1.24	192	01:26:09
12	090-4	Rampen	29.01.16 01:29	72°26.08'	17°02.10'	271	29.01.16 03:43	72°26.66'	17°05.00'	305	02:14	1.95	293	36 Clips
13	106-2	Christmas Tree Inlet	31.01.16 08:28	72°36.54'	17°52.52'	200	31.01.16 09:28	72°36.51'	17°54.15'	210	01:00	0.90	132	01:02:25
Totals											20:22	19.60	2670	14:50:34

3.2.5 Spatial distribution patterns of epibenthic megafauna and habitats

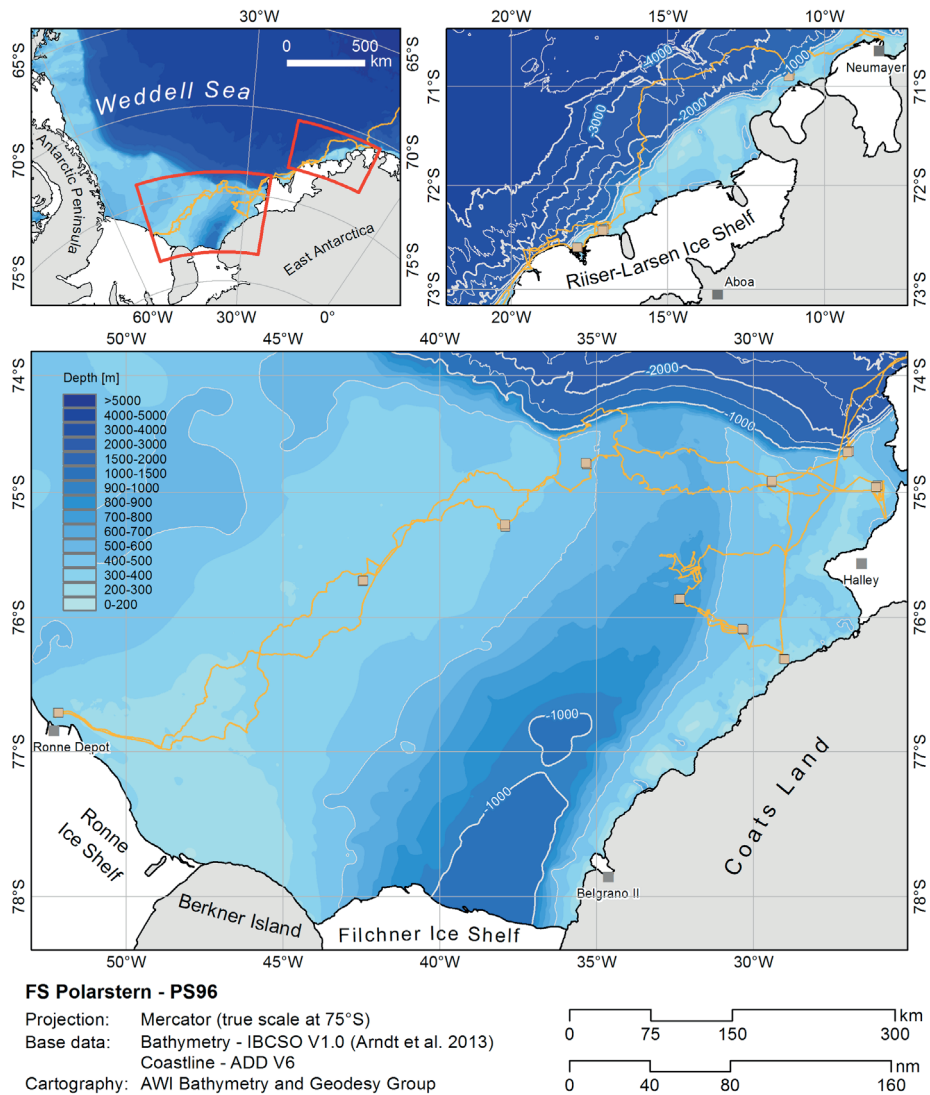


Fig. 3.2.5.1: Maps showing the geographic positions of OFOS stations visited during Polarstern cruise PS96 (ANT-XXXI/2) December 2015-February 2016. Bathymetric data acquired from IBCSO (Arndt et al. 2013).

Preliminary (expected) results

The seabed imagery (photos and videos) will be quantitatively analysed after return from the cruise. These investigations will focus on the exploration of the multi-scale distribution patterns (local = within-station, regional = among-stations) of seabed habitat features as well as abundances, composition and diversity of selected epibenthic megafaunal taxa and/or functional groups, in relation environmental seabed and water-column factors, the data on which are available through multidisciplinary collaboration with other working groups participating in the cruise.

Macro- and megabenthic fauna collected from concomitant trawl catches at the same or nearby stations will aid identification of the organisms visible in the seabed images. The combined results for the various sampling approaches, each targeting different components of the benthic

community, will contribute to developing a general standardisation scheme of Antarctic macro- and megabenthic communities (Gutt, 2013).

Already during the cruise, both seabed photos and video footage were made available to other cruise participants, who have special expertise on selected taxa (e.g., Porifera – D. Kersken and L. Federwisch, Gorgonaria – R. Zapata, Pisces – E. Riginella). This open-access approach will hopefully foster the overall quantitative analysis of the seabed images and contribute to a comprehensive coverage of the epibenthic fauna, spanning a taxonomic range as broad as possible (see also section on Data Management below).

First onboard analyses of the seabed images have provided some preliminary observations and results:

- The epifauna in the OFOS images taken at the stations on the shelf west of the Filchner Trough was clearly poorer in both abundance and diversity than that at eastern stations. Based on this evidence, we hypothesize that the western and eastern Filchner shelf regions are distinct ecological systems, characterized by pronouncedly different environmental conditions and distinct benthic communities. We hypothesize further that this difference is primarily due to the contrasting sea-ice regimes, with almost permanent ice cover in the western region vs. the formation of a recurrent summer polynya in the east. As a result, the western system lacks the typical high-Antarctic summer conditions, such as occurrence of wide open-water areas, enhanced light regime, upper water-column stratification triggering phytoplankton blooms, high primary production and particle fluxes, and, hence, strong pelagic-benthic coupling and enhanced food supply to the benthos. In addition, this east-west contrast in the general environmental setting is sustained by the isolating effect of the regional oceanographic current pattern, impeding advective exchange processes (organic matter, larvae, propagules) between the two shelf regions across the trough. As there was evidence from bathymetric – see chapter 3.1.3 – as well as seabed imaging data that iceberg scouring likewise impacts both the eastern and western shelf, we further hypothesize that this process, which is generally of high ecological significance for Southern Ocean shelf benthic systems, does not explain the striking difference in epibenthic community structures. However, as the available evidence is based on admittedly rather few point-type and snapshot-like data, further samples are required to rigorously test those hypotheses.
- In the Filchner Trough, at St. 072 at 750 m depth, one large specimen each of a tube-secreting epibenthic acorn worm (Hemichordata, Enteropneusta, Torquaratoridae) was



Fig. 3.2.5.2: Seabed photo taken by means of the OFOS during Polarstern cruise PS96 (ANT-XXXI/2) at St. 072 in the Filchner Trough at about 750 m depth, showing an epibenthic acorn worm (Hemichordata, Enteropneusta, Torquaratoridae)

3.2.5 Spatial distribution patterns of epibenthic megafauna and habitats

imaged in five of 198 photos (Fig. 3.2.5.2). A Short Note reporting this rare observation has already been submitted for publication in the journal *Marine Biodiversity* and is currently under review (Kocot and Piepenburg, submitted).

- At a number of stations, seabed habitat features were observed along the transects, which were very likely caused by grounding icebergs. These scours were most pronouncedly at St. 001 off Austasen (Fig. 3.2.5.3), but were also found at St. 026 on the western Filchner shelf.



Fig. 3.2.5.3: Seabed photo taken by means of the OFOS during Polarstern cruise PS96 (ANT-XXXI/2) at St. 001 off Austasen at about 290 m depth, showing a putative iceberg scour

- Evidence of active nest-guarding behaviour of different notothenioid fish species was found not only at St. 008, close to which similar observations were made in 2014 during cruise PS82 (Riginella, 2014), but also at six further stations (Sts. 001, 007, 010, 027, 048 and 057). These findings extend the knowledge on reproductive traits and parental care of Antarctic fish and provide evidence that active nesting behaviour is more widespread, both geographically and taxonomically, than formerly known (for more details see E. Riginella's report in chapter 3.2.2).
- At two stations, extraordinarily high abundances of (benthic)-pelagic species were detected during the descent of the OFOS in the water layer some 10 to 5 m above the seabed: At St. 010 on the northeastern Filchner shelf, there were many crustacean specimens (putatively ice krill *Euphausia crystallorophias*) recorded in the video footage, and at St. 090 off Rampen (Riiser-Larsen Ice Shelf), a very dense swarm of fish (putatively *Pleuragramma antarctica*) almost blocked the view on the seafloor (Fig. 3.2.5.4).

Data management

Seabed images and metadata will be published in due course after the cruise (approx. May 2016) at PANGAEA (www.pangaea.de), and a DOI number will be assigned for each station. When making use of the photos in scientific publications, users are asked to cite the data source as indicated in PANGAEA (for an example, search for "OFOS Piepenburg" in PANGAEA to retrieve OFOS photos from previous cruises). The video footage will be available on request.

In case it is planned to quantitatively analyze seabed photos and/or videos for a scientific study, please contact me (dieter.piepenburg@awi.de) to avoid redundant efforts and discuss opportunities of collaborative investigations.

Faunistic data will be published in AntaBIF (Antarctic Biodiversity Information Facility; www.biodiversity.aq) as soon as benthic classification, quantification and identification are finished.



Fig. 3.2.5.4: Seabed photo taken by means of the OFOS during Polarstern cruise PS96 (ANT-XXXI/2) at St. 090 off Rampen (Riiser-Larsen Ice Shelf) at about 270 m depth, showing highly abundant fish specimens (putatively *Pleuragramma antarctica*) swimming in the water layer five to ten metres above the seabed

References

- Barnes D, Griffiths H, Kaiser S (2009) Geographic range shift responses to climate change by Antarctic benthos: where we should look. *Marine Ecology Progress Series*, 393:13–26.
- Bergmann M, Klages M (2012) Increase of litter at the Arctic deep-sea observatory HAUSGARTEN. *Marine Pollution Bulletin*, 64, 2734-2741.
- Biebow H, Böhmer A, Gerdes D, Pineda S (2014a) Benthos communities and production. In: Knust R, Schröder M (ed) The expedition PS82 of the research vessel “Polarstern” to the southern Weddell Sea in 2013/14. *Ber Polarforschung Meeresforschung*, 680:64–70.
- Biebow H, Gerdes D, Isla E, Knust R, Pineda S, Sands C (2014b) The bendex experiment: follow-up 2. In: Knust R, Schröder M (ed) The expedition PS82 of the research vessel “Polarstern” to the southern Weddell Sea in 2013/14. *Ber Polarforschung Meeresforschung*, 680:94–98.
- Gili J, Arntz W, Palanques A, Orejas C, Clarke A, Dayton P, Isla E, Teixidó N, Rossi S, López-González P (2006) A unique assemblage of epibenthic sessile suspension feeders with archaic features in the high-Antarctic. *Deep-Sea Research Part II*, 53,:029–105.
- Gutt J (2006) Coexistence of macro-zoobenthic species on the Antarctic shelf: An attempt to link ecological theory and results. *Deep-Sea Research Part II*, 53:1009–1028.

3.2.5 Spatial distribution patterns of epibenthic megafauna and habitats

- Gutt J (2007) Antarctic macro-zoobenthic communities: a review and an ecological classification. *Antarctic Science*, 19(2):165–182.
- Gutt J (2013) The expedition of the research vessel “Polarstern” to the Antarctic in 2013 (ANT-XXIX/3). *Ber Polarforschung Meeresforschung*, 665:1–150.
- Kocot KM, Piepenburg D (subm) Observation of tube-secreting acorn worms (Hemichordata, Enteropneusta, Torquaratoridae) in the Weddell Sea, Southern Ocean. *Marine Biodiversity*, submitted
- Riginella E (2014) Reproductive traits in Antarctic fish: a comparative analysis of Notothenioidei. In: Knust R, Schröder M (eds) The expedition PS82 of the research vessel “Polarstern” to the southern Weddell Sea in 2013/14. *Ber Polarforschung Meeresforschung*, 680:106–109.

3.2.6 Tracing the effect of changing ice cover on benthic ecosystem functioning - from Meio to Macro

Heike Link¹, Gritta Veit-Köhler², Derya Mona Seifert¹, Yasemin Bodur²

¹ CAU,
² SaM-DZMB

Grant No: AWI_PS96_02

Objectives

Little is known, how processes at the seafloor - benthic functions - are affected by changes in ice cover. Recent studies have approached the question, how macrofauna influences benthic remineralisation fluxes (Link & Piepenburg 2013, Gutt et al. 2011), but the temporal and spatial role of meiofauna in the benthic remineralisation processes of the high Antarctic shelf is still not investigated. Pulse-chase studies on the reaction of meiofauna to enhanced food supply for a longer period have only been carried out on Antarctic meiofauna communities from the deep sea (Kapp Norvegia, 2,100 m depth, 14 days; Ingels et al. 2010) and the shelf in Bransfield Strait (227 m, 16 days; Moens et al. 2007). However, very few studies have investigated different size classes of organisms, like meio- and macrofauna, in this benthic environment simultaneously (Gutt et al. 2011). And up to now, nothing is known about the role of these benthic size compartments for benthic functions under the influence of different ice-cover regimes. Here, we jointly evaluate the response of benthic ecosystem functioning to a retreat in ice cover in the Weddell Sea using two benthic functions, namely food uptake and remineralisation of inorganic nutrients, and two benthic compartments (meio- and macrofauna).

During PS96 we studied the two complementary aspects of (A) trophic interactions and partitioning among meio- and macrobenthic communities and (B) the net remineralisation response to simulated ice retreat using pulse-chase experiments with isotopically labelled algae (U. Witte, University of Aberdeen). To disentangle the effect of local environmental conditions from regional ice cover regimes, environmental parameters need to be determined and pulse-chase experiments need to be replicated in areas of different ice cover regimes and other environmental conditions. Therefore, our objectives were to:

1. Study the effect of increased food supply on benthic ecosystem functioning (meiofauna, macrofauna, trophic pathways, remineralisation)
 - a) in areas of different ice cover in the Southern Weddell Sea
 - b) under the Filchner Outflow gradient
 - c) mitigated by Meiofauna at different time intervals
2. Study the natural variability of benthic ecosystem functioning (meiofauna, macrofauna, trophic pathways, remineralisation) along an ice-cover gradient.

Work at sea

In general, we used sediments collected by the multicorer MUC10 and water from the rosette water sampler at two depths (closest to the bottom and at the fluorescence maximum) for the work on board.

According to the objectives presented above, we conducted field experiments (incubation of sediment cores with inhabiting meio- and macrofauna, pulse-chase experiments) of three

3.2.6 Tracing the effect of changing ice cover on benthic ecosystem functioning

different types for collecting samples of faunal communities, benthic boundary fluxes and stable isotopes:

- Algae Feeding Experiments (AFEx) to answer objectives 1a-b
- Meiofauna Feeding Experiment (MeioFEx) to answer objective 1c
- Benthic Ecosystem Function Experiments (BEFEx) to answer objective 2

Further, we collected natural samples for the following parameter groups at each station:

- Habitat factors of the sediment
- Fauna natural stable isotopic composition
- Environmental factors of the water column

For this project, MUC10 deployments were carried out at all stations where bottom topography would allow safe use of the gear. We collected information on sediment composition and bottom topography from the bathymetry group (chapter 3.1.3) and by following the OFOS deployment (Ocean Floor Observing System, chapter 3.2.5).

Samples could be obtained from 8 stations (Table 3.2.6.1, Fig. 3.2.6.1). In most cases, MUC10 was used to collect up to 8 undisturbed sediment cores (inner diameter of plexiglass core liners 94 mm, surface 0.007 m²). Subsamples from the giant boxcorer (GKG) were taken with the same core liners in case conditions did not allow for safe MUC10 deployment. This was the case at station 017. At all stations, MUC sampling was accompanied by water-column sampling from the CTD-Rosette water sampler equipped with Niskin bottles.

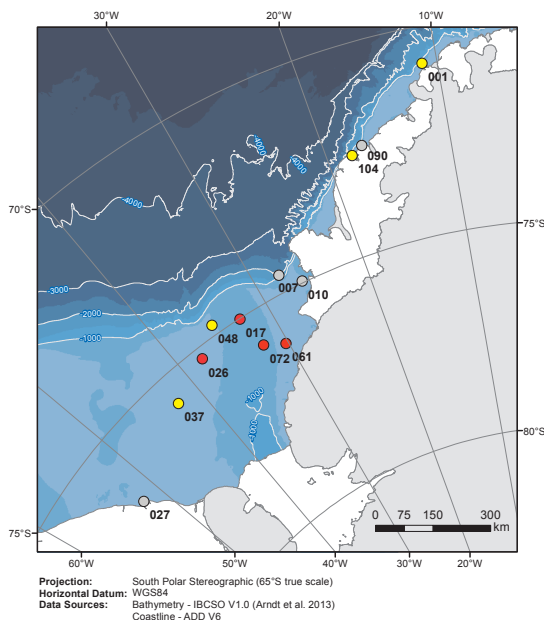


Fig. 3.2.6.1: Map of sites sampled for the benthic ecosystem functioning project. Yellow = BEFEx sites, red = AFEx sites, grey = unsuccessful deployments.

On-board experimental work and incubations

AFEx and BEFEx experiments are based on ex situ incubations of sediment cores with overlying water (Link et al. 2013). After MUC retrieval, cores were prepared in their liners as gas tight incubation chambers and transferred to the labcontainer (dark, 2°C) (Fig. 3.2.6.2). Within 6 h, chambers were topped up with water collected from other MUC cores or the CTD-Rosette bottom water, up to 3 control chambers carrying the same water (but no sediments) were filled, and all chambers were aerated for 2 h using a standard aquarium pump.

Table 3.2.6.1: Samples from 8 stations

Date	Station	Gear	Latitude	Longitude	Depth [m]	Area	Success	Experiment	Sediment Core Replicates			Water Column (CTD at Station)	SI
									Exp	Env	Profile		
24.12.15	PS96/0001-7	MUC	70°53.37' S	011°07.10' W	309,0	Eastern Shelf	yes	BEFEX	3	1	0	2	2
24.12.15	PS96/0001-8	MUC	70°53.35' S	011°07.07' W	309,0	Eastern Shelf	yes	BEFEX	2	2	0		
29.12.15	PS96/0007-3	MUC	74°39.57' S	026°57.21' W	413,4	Eastern Shelf	no	-	0	0	0	2	2
29.12.15	PS96/0007-4	MUC	74°39.51' S	026°57.79' W	415,5	Eastern Shelf	no	-	0	0	0		
01.01.16	PS96/0010-8	MUC	74°57.00' S	026°03.95' W	274,0	Eastern Shelf	no	-	0	0	0	2	2
01.01.16	PS96/0010-9	MUC	74°57.07' S	026°04.12' W	272,4	Eastern Shelf	no	-	0	0	0		
01.01.16	PS96/0010-10	MUC	74°57.46' S	026°05.11' W	293,6	Eastern Shelf	no	-	0	0	0		
01.01.16	PS96/0010-11	MUC	74°58.99' S	026°05.01' W	315,3	Eastern Shelf	no	-	0	0	0		
04.01.16	PS96/0017-3	GKG	75°00.85' S	032°52.51' W	608,2	Filchner Trough	yes	AFEX	6	2	0	2	2
04.01.16	PS96/0017-4	GKG	75°00.87' S	032°52.12' W	611,3	Filchner Trough	no	-	0	0	0		
08.01.16	PS96/0026-7	MUC	75°16.19' S	037°54.96' W	416,1	Western Shelf	yes	AFEX	3	1	0	2	2
08.01.16	PS96/0026-8	MUC	75°16.10' S	037°54.85' W	415,2	Western Shelf	yes	AFEX	3	1	0		
08.01.16	PS96/0026-9	MUC	75°16.02' S	037°54.83' W	415,0	Western Shelf	yes	-	0	0/1	1		
08.01.16	PS96/0026-10	MUC	75°15.80' S	037°54.87' W	414,3	Western Shelf	yes	AFEX	2	1	0		
08.01.16	PS96/0026-11	MUC	75°15.65' S	037°54.44' W	413,6	Western Shelf	yes	AFEX	2	1	0		
14.01.16	PS96/0027-7	MUC	76°43.11' S	052°09.14' W	298,3	Western Shelf	no	-	0	0	0	2	2
16.01.16	PS96/0037-8	MUC	75°43.30' S	042°27.71' W	390,6	Western Shelf	yes	BEFEX	3	2	0	2	2
17.01.16	PS96/0037-9	MUC	75°43.29' S	042°27.66' W	390,5	Western Shelf	yes	BEFEX	4	2	2		
19.01.16	PS96/0048-6	GKG	74°45.60' S	035°20.14' W	483,4	Western Shelf	yes	MeioFEX	0	28	0	2	2
19.01.16	PS96/0048-7	MUC	74°45.52' S	035°20.91' W	481,9	Western Shelf	yes	BEFEX	3	1	0		
19.01.16	PS96/0048-8	MUC	74°45.52' S	035°20.91' W	481,8	Western Shelf	yes	BEFEX	3	2	0		

3.2.6 Tracing the effect of changing ice cover on benthic ecosystem functioning

Date	Station	Gear	Latitude	Longitude	Depth [m]	Area	Success	Experiment	Sediment Core Replicates	Water Column (CTD at Station)
21.01.16	PS96/0061-3	GKG	76°05.85' S	030°18.69' W	469,3	Eastern Shelf	no	-	0 0 0	2
21.01.16	PS96/0061-5	MUC	76°05.93' S	030°18.23' W	467,6	Eastern Shelf	yes	AFEX	4 3 4	
22.01.16	PS96/0061-6	MUC	76°05.89' S	030°18.38' W	466,6	Eastern Shelf	yes	AFEX	5 2 5	
23.01.16	PS96/0072-7	MUC	75°51.61' S	032°17.58' W	755,4	Filchner Trough	no	-	0 0 0	2
23.01.16	PS96/0072-8	MUC	75°50.92' S	032°18.42' W	753,4	Filchner Trough	yes	AFEX	0 2 0	
24.01.16	PS96/0072-9	MUC	75°50.85' S	032°17.44' W	755,1	Filchner Trough	yes	AFEX	6 1 6	
24.01.16	PS96/0072-10	MUC	75°50.94' S	032°21.42' W	749,4	Filchner Trough	yes	AFEX	0 1 0	
29.01.16	PS96/0090-9	MUC	72°26.66' S	017°04.92' W	306,6	Western Shelf	no	-	0 0 0	2
31.01.16	PS96/0104-2	MUC	72°36.33' S	018°02.85' W	312,1	Western Shelf	yes	BEFEX	1 2 1	
31.01.16	PS96/0104-3	MUC	72°36.33' S	018°02.73' W	309,0	Western Shelf	yes	BEFEX	3 2 3	2

Then, incubations were started by closing chambers with a gas-tight lid including a magnetic stirring device (to avoid stratification in the water column). Oxygen and nutrient concentrations were measured in the overlying water column over the incubation period of 2-6 days. A Fibox-LCD optical sensor was used to determine oxygen concentration non-invasively every 4-6 h. To determine nutrient fluxes, we collected water samples at the start, during, and end of the incubations. Water samples were filtered over GF/F-filters and frozen at -80°C for nitrate, silicic acid and phosphate. For ammonia analyses, samples were treated immediately and measured using the fluorometric method proposed by Holmes et al. (1999) adapted by Link et al. (2013).

At the end of incubations - usually when oxygen concentration had decreased by 20% - sediment cores were sliced and preserved in 4% formaldehyde-seawater solution (borax-buffered) for later meio- and macrofaunal analyses.

For BEFEx, 4-5 sediment cores were incubated without any additional treatment. Water samples for nutrients were collected 3 times. Sediment cores were sliced into 1-cm slices down to 5 cm of the core and preserved in 4% formaldehyde-seawater solution (borax-buffered). A subsample of each slice was taken using a 20mL cut syringe and frozen at 80°C for chemical analyses. The remaining core was sieved over a $500\ \mu\text{m}$ sieve, and the residue was stored in 4% formaldehyde-seawater solution (borax-buffered).

For AFEx, up to 10 sediment cores and 3 water control cores were incubated (Fig. 3.2.6.2). Two hours before start of incubations, we added a pulse of cultured ^{13}C - and ^{15}N -marked, freeze-dried microalgae (*Chaetocystis* sp., 10 mg per core) to half of the cores. Microalgae were resuspended in 10 ml GF/F-filtered bottom water and pipetted directly onto the sediment surface using a sterile PS-pipette. Water samples for nutrients were taken every 24 h. After 4-6 days, sediment cores were sliced into 0-2, 2-5-cm slices and preserved in 4% formaldehyde-seawater solution (borax-buffered). A subsample sediment was taken using a 60mL cut syringe, sliced into 1-cm slices down to 5 cm and frozen at 80°C for chemical analyses. The remaining core was sieved over a $500\ \mu\text{m}$ sieve, and the residue was stored in 4% formaldehyde-seawater solution (borax-buffered). For each AFEx incubation experiment a beforehand community sampling

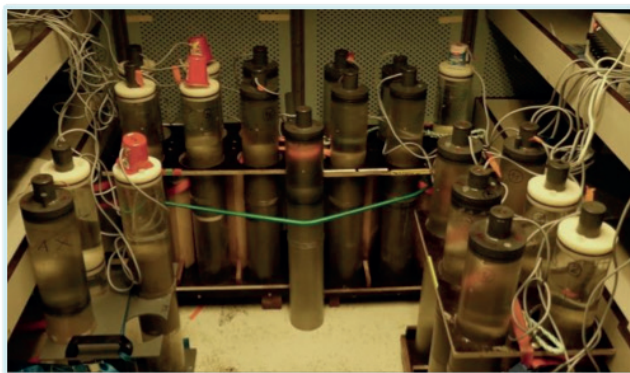


Fig. 3.2.6.2: Setup of experiments in the cold room.
Picture shows replicates of 2 AFExs

was carried out on untreated MUC cores in order to get a clear picture of community distribution (mainly depth). For that purpose cores were sliced in 1cm-layers down to 5 cm depth and stored in a 4% formaldehyde-seawater solution (borax-buffered). Later on, all fauna will be extracted, counted and identified to major taxon level in the home institutes.

The MeioFEx experiment was carried out in addition to AFEx and BEFEx to exclusively target the temporal and spatial incorporation of isotopically marked microalgae by meiofauna. The MeioFEx setup included 28 small core liners (diameter 5.4 cm, length 30 cm) that were used to subsample the GKG collected at station 048-6 (01-19-2016). Additionally, 3 20-ml syringes were collected from the GKG for each environmental analysis (pigments, grain size and sediment stable isotopic composition).

3.2.6 Tracing the effect of changing ice cover on benthic ecosystem functioning

The cores were kept in the dark at 1.1°C in a Labcontainer and aerated during the whole incubation period. MeioFEx was started on 01-21-2016 by randomly adding a pulse of cultured ¹³C- and ¹⁵N-marked, freeze-dried microalgae (*Chaetocystis* sp., 3.3 mg per core) to 15 cores. At the time of sampling, cores were sliced in 1-cm steps down to 5 cm. The rest below 5 cm was collected as bulk sample. Samples were stored in 4% formaldehyde-seawater solution (borax-buffered).

Sampling scheme:

T0: 3 control cores (01-21-2016)

From T1 on 3 treated and 2 control cores were randomly chosen per sampling date:

T1 (after 1 day), T2 (after 3 days), T3 (after 6 days), T4 (after 12 days), T5 (after 18 days). At T5, 5-ml syringes were additionally collected for Chl-a and stable isotopic composition of the sediment from control and treated cores.

Later on meiofauna will be extracted, classified to higher taxon level, counted and prepared for stable isotope analyses in the home lab.

Habitat factors of the sediment

Cores of each station were subsampled for environmental parameters (chlorophyll-a and phaeopigments, grain size, sediment stable isotopes $\delta^{13}\text{C}$ and $\delta^{15}\text{N}$) with cut-off 20 mL syringes that were pushed down to 5 cm into the core. Complete syringes/and or cut off 1-cm slices were stored at -80°C for further analyses in the home lab.

Fauna natural stable isotopic composition

Cores from which the syringes for environmental samples were taken were sliced in 1-cm steps down to 3 cm, stored in Petri dishes and frozen at -80°C. Fauna will be extracted in the home lab and their stable isotopic composition will be related to sediment and water column values.

Environmental factors of the water column

Pigment content and stable isotope signals of the benthic compartments will be compared with these parameters in the water column. For this purpose we sampled water from the CTD-Rosette water sampler at the fluorescence maximum (representing the Chl-a max) and at the bottom (5 m above ground). For both depths, water was sieved over a 100- μm sieve in order to remove larger particles and fauna and then filtered over one GF/C (for Chl-a pigment samples) and one GF/F filter (for $\delta^{13}\text{C}$ and $\delta^{15}\text{N}$ stable isotope samples) for each depth. We filtered min. 2 L and max. 5 L per filter, depending on material present. Low amounts of water were filtered if resuspended material or high amounts of microalgae lead to low filtering performance. Filtering was performed at 200 mbar to avoid rupture of cells. The filters were stored at -80°C.

Microprofile measures

In addition to incubation-based oxygen flux, we measured oxygen profiles at stations 026 - 104. After MUC retrieval, sediment cores were pushed onto a bottom lid and then pushed up with an extruder leaving a water phase of about 15 cm. In the labcontainer, oxygen microprofile measures with 200 μm resolution were conducted using optical Firesting oxygen microsensors (230 μm) mounted on a micromanipulator. Two porewater oxygen microprofiles per core have been obtained. Thereby we will assess oxygen penetration depth and the diffusive oxygen uptake of the respective sediments. The distance between profiles varied between one- and

two cm horizontally. After microprofiles were finished, cores were either used for incubations (stations 061-104), or 3 sediment samples have been taken with cut 20 mL syringes from the respective cores (stations 026-048) and frozen at -80°C .

Preliminary (expected) results

In general, we did not produce publishable results during the cruise, as the vast majority of samples taken have yet to be analysed in the lab (water samples for nutrients, isotope and pigment measures from water and sediment samples, grain size, abundance, biomass, composition and diversity of meiofauna and macrofauna assemblages in sediment cores).

As an example for one type of data to be achieved during future analyses, we show preliminary oxygen flux results from two AFEx experiments east (station 026) and west (station 061) of the Filchner Trough (Fig. 3.2.6.3). The sediment-community respiration rates of untreated cores ranged from 0.8 to to 3.3 $\text{mmol O}_2 \text{ m}^{-2} \text{ d}^{-1}$, with lower rates on the eastern shelf. Treatment with increased food (addition of microalgae) lead to a clear increase of oxygen consumption at both sites, albeit the increase was higher on the western shelf. At this preliminary stage we can only hypothesize that the smaller response to food input in the East may indicate a saturated availability of food. The higher overall oxygen flux rates on the western shelf show a high organismic activity albeit observations of epifauna (chapter 3.2.5) found higher abundance in the East. The reason for this difference has still to be investigated by the later comparative spatial analyses including other ecological parameters obtained from this cruise (e.g., sediment pigment patterns, meio- and macrofauna abundance).

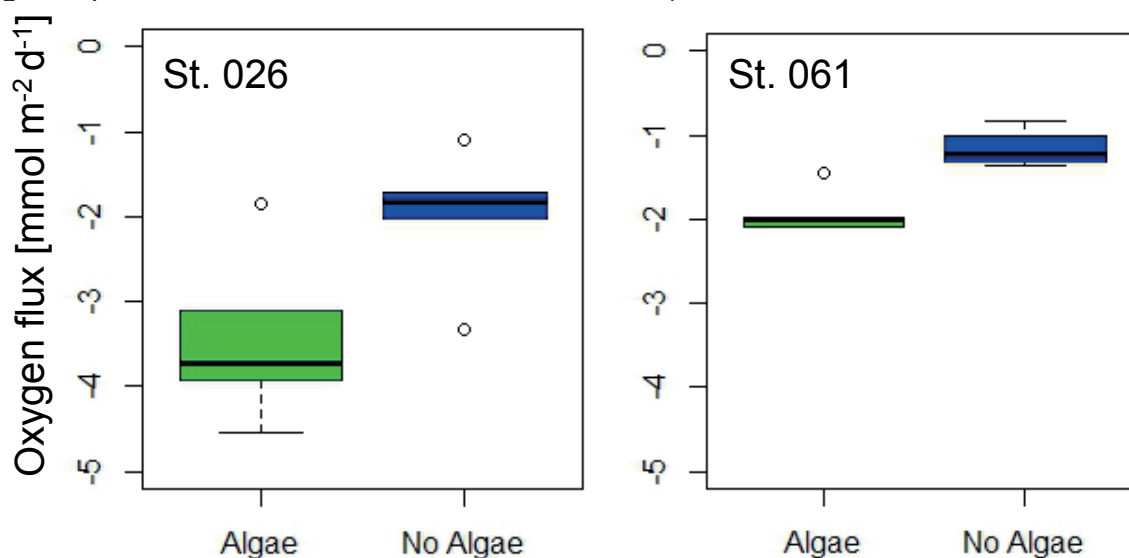


Fig. 3.2.6.3: Preliminary results of oxygen fluxes during AFEx study with 5 replicates per treatment. Blue = control sediment cores, green = sediment cores with algae pulse. Boxes = 50% confidence intervals with standard deviation, solid bold line = mean, points = outliers

Data management

Most data (see Preliminary results) will be obtained through laboratory analyses after the cruise. As soon as they have gone through quality control, processed data will be uploaded to the open-access databases PANGAEA (www.pangaea.de) and/or SCAR-MarBIN.

References

- Moens T, Vanhove S, De Mesel I, Kelemen B, Janssens T, Dewicke A, & Vanreusel A (2007) Carbon sources of Antarctic nematodes as revealed by natural carbon isotope ratios and a pulse-chase experiment. *Polar Biology* 31(1):1-13. doi: 10.1007/s00300-007-0323-x.
- Link H, & Piepenburg D (2013) 3.2 Dynamics of benthic ecosystem functioning in response to predicted environmental shifts. *Reports on Polar and Marine Research: Vol. 665. The expedition of the research vessel "Polarstern" to the Antarctic in 2013 (ANT-XXIX/3)*. (pp. 151). Bremerhaven: Alfred Wegener Institute for Polar and Marine Research.
- Link H, Chaillou G, Forest A, Piepenburg D, & Archambault P (2013) Multivariate benthic ecosystem functioning in the Arctic - benthic fluxes explained by environmental parameters in the southeastern Beaufort Sea. *Biogeosciences* 10(9):5911-5929. doi: 10.5194/bg-10-5911-2013.
- Ingels J, Van den Driessche P, De Mesel I, Vanhove S, Moens T, & Vanreusel A (2010) Preferred use of bacteria over phytoplankton by deep-sea nematodes in polar regions. *Marine Ecology Progress Series* 406:121-133. doi: 10.3354/meps08535.
- Holmes RM, Aminot A, Kerouel R, Hooker BA, & Peterson BJ (1999) A simple and precise method for measuring ammonium in marine and freshwater ecosystems. *Canadian Journal of Fisheries and Aquatic Sciences* 56(10):1801-1808.
- Gutt J, Böhmer A, & Dimmler W (2013) Antarctic sponge spicule mats shape macrobenthic diversity and act as a silicon trap. *Marine Ecology Progress Series* 480:57-71.
- Gutt J, Barratt I, Domack E, d'Acoz CD, Dimmler W, Gremare A., . . . Smith C (2011) Biodiversity change after climate-induced ice-shelf collapse in the Antarctic. *Deep-Sea Research Part II-Topical Studies in Oceanography*, 58(1-2):74-83. doi: 10.1016/j.dsr2.2010.05.024.

3.2.7 Pelagic-benthic processes in the Filchner Outflow area: a benthic community and particulate matter perspective

Santiago Pineda Metz¹, Enrique Isla²

¹AWI,

²ICM-CSIC

Grant No: AWI_PS96_03

Outline

The marine vicinities of Filchner Ice Shelf are the main area of deep and bottom water formation in the southern Weddell Sea, where the outflow of cold and fresh water from below the ice shelf mixes with the oceanic Weddell Sea Gyre waters. The resulting physical fronts presumably convert the region in a biological hotspot. This characteristic gives the study area great interest for multidisciplinary scientific research given its global influence on climate and the fact that Polar Regions are especially sensitive to the ongoing global warming and climate change. On this basis, it is likely that this biological hotspot may be undergoing rapid transformations linked to environmental changes. Analyzing how the productive processes in the pelagic zone couple with the benthic realm offers the possibility to investigate how the actual environmental conditions are reflected in the status of the local benthic communities and the chemical characteristics of the sediment providing a baseline for a region where this information is scarce. We expect to identify how the region reacts to environmental changes and the effect of these reactions on the local biogeochemical cycles, especially those of the carbon and silicon, and the Antarctic benthos. We will compare the expected results with other areas of the Weddell Sea, where climate change already produced dramatic changes (e.g., the Larsen continental shelf –results from PS77) and others where these effects are less evident (e.g., results obtained in the previous expedition PS82 to the Filchner area and the regions off Austasen and Kapp Norvegia). This approach opens the door to contrast the actual situation at the spatial extremes of the Weddell Sea basin. Concerning the benthic communities, the results obtained from the expedition PS82 have shown that the benthic community patterns in the hydrographically diverse Filchner Overflow System are more heterogeneous than previously thought. With the sampling effort achieved during the present expedition, we filled the gap of PS82, when heavy sea ice conditions did not allow sampling the western flank– a region of high ecological interest, because it is totally covered by heavy sea ice for most of the time even during consecutive years, and also the complete axis of the Filchner Depression. Therefore, sea ice may make this area of special interest for the benthic studies given that pelagic conditions differ among flanks.

We completed the set of samples with multicorer and multi-grab stations in the region called "Tannenbaum" located at the north of the Drescher Inlet.

Overall, the sampled collection obtained during PS96 will provide good basis to examine to which extent the effects of climate change in Antarctica and the influence of ice shelves and sea ice determines the intensity of biological development in polar areas.

The present expedition is a component of the project, Dynamics of Antarctic Marine Shelf Ecosystems (DynAMo – S-633).

The aim of the present proposal was to identify characteristics of the pelagic-benthic coupling in the marine vicinities of Filchner Ice Shelf through the analysis of:

- the abundance and distribution of benthic communities and function of selected species
- biochemical and geochronological characteristics of the sediment

Specific questions were:

- Is the Filchner outflow area a benthic-pelagic hotspot, i.e. a local enrichment in plankton and benthos relative to surrounding areas? What is the actual status of the diversity, abundance and biomass of the local benthic communities?
- To what extent is the biological enrichment related to particular bathymetric (ridge, canyon) and hydrographic features (vertical currents)?
- What is the quality and quantity of the organic matter incorporated into the sediment along a latitudinal and longitudinal gradients on the continental shelf in the Filchner Trough and its vicinities?
- Which are the main species structuring the benthic communities in the area?

Objectives

The particular objectives of our group were:

- To analyze the distribution of the particulate silicon and organic matter (e.g., proteins, lipids, carbohydrates, phytopigments, amino acids, fatty acids) in the sediment column
- To identify local characteristics of sediment fluxes and organic matter distribution and dynamics in the sediment column in a short-scale (km) in a presumably highly productive polar setting through the analysis of ^{14}C , ^{210}Pb .
- To identify the composition of macrobenthic communities by means of combined image and benthic sample analyses.

Work at sea

A total of 19 multicorer (8 sts.) and multi-grab (11 sts.) stations were developed in the Filchner Outflow System and its vicinities. Due to sea ice conditions most of them were located on the continental shelf on the eastern flank of the Filchner Trough; however, valuable stations were also visited on the western flank and along the axis of the Filchner Trough.

Preliminary results

Sediment cores

Sediment cores were subsampled on board in slices 0.5 cm (the uppermost 10 cm), 1 cm (from cm 10 to 20) and 2 cm (from cm 20 to 30) thick to a maximum core length of 30 cm. Overall, approximately 400 multicorer samples were obtained after slicing. First observations showed that the sediment was mainly constituted by mud and sandy mud. The stations at the continental shelf showed a sandy and even gravely mud layer in the upper 8 cm; below this layer the sediment was muddy. The color varied from dark green and brownish in the upper 10 cm to grey towards the base of the cores. The continental slope stations and those in the axis of the Filchner Trough presented only greenish to grey mud.

In total, 80 multi-grab cores were obtained during PS96. The three stations from the continental shelf east of the Filchner Trough were repetitions of PS82 stations, and they did not appear to differ in terms of fauna. Within the continental shelf west of the Filchner Trough, five deployments were made, but only four were successful; the first impression is that the fauna of this shelf is rather poor compared to the eastern continental shelf of the Filchner region, and it is mainly dominated by polychaetes, however other groups like scaphopods and ophiuroids

were also present within the cores. Within the "Tannenbaum" region there were two stations, in both a rich fauna was present, within the corers sponges and sponge spicules were the most conspicuous discovery.

Once back in the lab, the cores will be analyzed for abundance and biomass of the different groups of the benthos.

Data management

All the data generated from this expedition will be included either in Pangaea (www.pangaea.de) or in the Spanish Polar Database located in the Spanish Polar Committee's National Polar Data Center, <http://hielo.igme.es/index.php/en/>.

3.2.8 Seal research at the Drescher Inlet (SEADI)

Horst Bornemann¹, Christoph Held¹ (not on board), Dominik Nachtsheim^{1,2}, Nils Owsianowski¹, Claudio Richter¹, Richard Steinmetz¹

¹AWI,
²Uni Bremen



Grant No AWI_PS96_02

Objectives

SEAls and ROV at the *Drescher Inlet* (SEADI) represents a follow-up study of seal investigations carried out during RV *Polarstern*'s expedition PS82 at the Filchner Outflow System and at the Drescher Inlet in 2014 (Bornemann et al. 2014). It also complements earlier investigations at these locations initiated in 1986. Though SEADI is primarily an ANT-Land 2015/2016 activity carried out via *Neumayer Station III*, it was conducted in liaison with the research expedition *Filchner Ronne Outflow System Now* (FROSN) of RV *Polarstern* (PS96). FROSN also integrated SEADI as part of its research programme and served as a logistic platform for this campaign.

SEADI focuses on the foraging ecology of Weddell seals (*Leptonychotes weddellii*). Data obtained from seal-borne 3D-multi-channel data loggers and cameras during an earlier expedition to the Drescher Inlet in 2003/2004 (PS65) documented that Weddell seals dived along the steep cliffs of the shelf ice and made foraging excursions under the ice shelf (Liebsch et al. 2007; Watanabe et al. 2006). The seal-borne images and dive data led to the discovery of a hitherto unknown cryo-benthic community of marine invertebrates, presumably isopods (Antarcturidae, Austrarcturellidae, Aegiidae), and potentially anthozoans (*Edwardsiella* spp., cf. Daly et al. 2013), being attached head-down to the underside of the floating ice shelf at depths of around 130-150 m (Watanabe et al. 2006). These "hanging gardens" may represent an attractive food horizon, where seals could benefit from a local hotspot of high biological activity. This particular finding could also explain the bimodal distribution of dive depths of Weddell seals known from earlier investigations during PS65, PS48, PS34, PS20, PS17 (Plötz et al. 2005, 1999, 1997, 1994, 1991). A synoptic field study at Atka Bay (*Neumayer Station II*) during austral spring 2008 also showed a bimodal distribution in dive depths and feeding events of Weddell seals with an increased feeding rate likely on smaller prey items in the pelagic realm (Naito et al. 2010). A number of seals undertook dives to shallower depths between 60 and 80 m close to the ice shelf edge and along an iceberg stranded inside the Atka Bay, and supported our hypothesis of shelf ice associated foraging (Naito et al. 2010).

The question whether or not these findings are representative for the far-ranging Antarctic ice shelves in general still remains open. Though the seals' diving behaviour at the Drescher Inlet indicates active foraging in a locally attractive feeding spot, the factors contributing to this hotspot of enhanced food availability and its stability over time are largely unexplored. In particular questions towards species composition, horizontal extent and nutrient supply of the fauna inhabiting the underside of the ice shelf are still open and call for additional investigations to further our understanding of benthic-pelagic coupling processes.

Physical environment

The Drescher Inlet is a 25 km long and 1 – 2 km wide crack in the Riiser-Larsen Ice Shelf, located at -72.83667 (LAT) -19.15300 (LON). A recent radar scan of the shelf ice edge by RV *Polarstern* during PS82 indicated a shift of the inlet contour of about 20 km to the north-west

during a period of 10 years due to the continuous flow of the shelf ice (unpubl. data). The seabed under the ice shelf extends for over 100 km to the nearest grounding line of Dronning Maud Land (Arndt et al. 2013; Schenke et al. 1998). Bathymetric surveys reveal seafloor depths inside the inlet ranging between 400 m in the inner section and 520 m at the inlet mouth (Graffe & Niederjasper 1997); however these bathymetric data do not match with the current situation due to the aforementioned shift. The depth outside the inlet gradually increases, reaching the 1,000 m isobath about 3.5 km beyond the inlet mouth. Fast ice remains in the entire inlet from its mouth to the inner parts, where it can pile up to some meters over several years. Beneath the fast ice, platelet ice can also aggregate to layers of several meters (Thomas et al. 2001; Günther et al. 1999). The hydrography within the inlet is characterised by a stable thermo(pycno)cline between 130 and 230 m coinciding with the depth of the floating shelf ice (Thomas et al. 2001).

Biological environment

An estimated aggregation of about 200 - 300 Weddell seals (*Leptonychotes weddellii*) is regularly associated with the area of the Drescher Inlet. A count along the main tidal cracks during noon on 24 January 2016 revealed a total of 119 adult seals and 13 pups. The seals haul out along these tidal cracks in the fast ice and adjacent to the cliffs of the ice shelf during summer. By mid-December their offspring is weaned and mainly (non-lactating) adult female and male Weddell seals in the moult and weaned pups and yearlings are present on the inlet's fast ice. Strong wind and gales may initiate a break-up of the formerly consolidated fast ice towards the end of summer. When the ice cover recedes, also other pack ice seals, mainly crabeater seals (*Lobodon carcinophaga*), but also leopard (*Hydrurga leptonyx*) and Ross seals (*Ommatophoca rossii*) were observed during earlier research campaigns, as well as Antarctic minke whales (*Balaenoptera bonaerensis*), Arnoux's beaked whales (*Berardius arnuxii*), and killer whales (*Orcinus orca*) patrolling in the leads of the disintegrating fast ice of the inlet. An emperor penguin colony consisting of approx. 7,000 breeding pairs is resident in the inlet (cf. Fretwell et al. 2012; Wöhler 1993; Reijnders et al. 1990; Klages & Gerdes 1988; Plötz et al. 1987; Hempel & Stonehouse 1987; Plötz et al. 1987). Their chick rearing period comes to an end towards the end of January (Pütz & Plötz 1991), and only moulting (sub)adult birds and chicks are present on the sea ice afterwards. The pelagic and demersal fish fauna in the inlet is dominated by the nothotheniid *Pleuragramma antarcticum* (Plötz et al. 2001); abundance and biomass of other species of the families Nototheniidae (cf. Gutt 2002), Channichthyidae, Bathydraconidae, Artedidraconidae, and others seem to be much lower (Plötz et al. 2001). However, krill (*Euphausia* spp.), gelatinous plankton and amphipods seem to be abundant in considerable amounts (Plötz et al. 2001; Günther et al. 1999). The epibenthic community, in so far as it is known, is in comparison with other areas along the east coast of the Weddell Sea, especially north of the Drescher Inlet, relatively poor in life forms and biomass (J. Gutt, pers. comm.).

Work at sea and on ice

The four SEADI participants used the Dronning Maud Land Air Network (DROMLAN) via Cape Town and *Neumayer Station III* to embark on RV *Polarstern* on 22 December 2015. The return was facilitated via a helicopter shuttle between RV *Polarstern* and *Aboa Station* (FIN) near Rampen Inlet on 29 January 2016, combined with an immediate connecting flight of the AWI's research aircraft *Polar 5* back to *Neumayer Station III*, and again back to Cape Town via DROMLAN. SEADI complemented earlier studies on Weddell seals and their prey in a season that was characterized by stable fast ice within the inlet and permanent daylight. Research was facilitated by means of a temporary *field camp*. Weddell seals were instrumented with digital still camera loggers (Naito et al. 2013) in order to obtain *seal-borne image data* of the under

3.2.8 Seal research at the Drescher Inlet (SEADI)

shelf ice fauna, and to document encounters of zooplankton, krill and fish, both in the pelagial and benthal. Ross seals were considered to be instrumented upon their presence in liaison with a concurrent research study undertaken by collaborating scientists of the Mammal Research Institute (University of Pretoria, RSA) on RV SA *Agulhas II*. However, only one juvenile Ross seal was encountered but not considered for instrumentation. The Remotely Operated Vehicle (ROV) V8Sii (Ocean Modules®) equipped with twin high-resolution cameras was deployed to provide *ROV-borne footage* and samples of the “hanging garden” biota with accuracy unavailable to seal-mounted cameras. Seals were furthermore tagged with *CTD satellite relay data loggers* to provide data on dive depth, spatial movement and *in situ* hydrography under the sea ice. *Additional sampling* of whiskers provided material for post hoc analyses of stable isotopes. All *animal handling* procedures required chemical immobilisation.

Field camp

Research on the ice was conducted via a temporary field camp that was located on the Riiser-Larsen Ice Shelf in the immediate vicinity of the Drescher Inlet at -72.83106 (LAT) -19.13091 (LON) from 27 December 2015 to 27 January 2016 (Fig. 3.2.8.1). A reconnaissance flight allowed identifying a suited location for the camp on 25 December, requiring 1:16 hrs flight time. All field equipment was flown onto the ice shelf (27. December) and returned (27./28. January) by the two *Polarstern* helicopters *Polarheli 1* and 2. The total weight of the equipment to be flown out and in was 9,740 kg plus PAX. Transportation of the equipment for establishing the camp including staff required 31 shuttle flights of which 23 contained sling load (nets). The camp was completely equipped within 14 hours, requiring 9:44 hrs of helicopter flight operation over a distance of 7.5 nm between RV *Polarstern* and the camp site. *Polarstern*'s positions at the eastern side of the Drescher Inlet were -72.77667 (LAT) -19.46000 (LON) on 27 December 2015, and -72.79833 (LAT) -19.77667 (LON) on 27 and 28 January 2016. Dismantling of the camp and returning of the cargo on 27 and 28 January was done within six hours and required 8:35 hrs of helicopter time by the 2 helicopters during 26 flights in total. Since a break-off of sea ice in the inlet mouth shortened the flight distance to 4.3 nm, and skidoos and sledges were driven directly to the ship over the ice, the operational time to reload all equipment was much shorter than during the set-up of the camp.

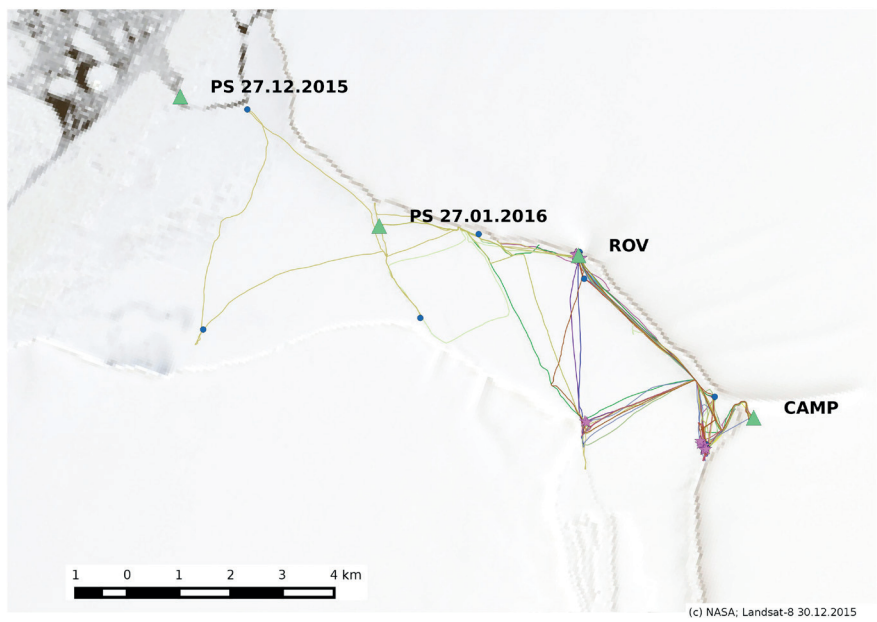


Fig. 3.2.8.1: Overview of locations relevant for the field work, highlighting the positions of RV *Polarstern*, the camp, the ROV installation, and the deployment and retrieval sites, respectively, of cameras and satellite transmitters on moulted adult Weddell seals (pink stars). See table 3.2.8.1a and b for the individual seal instrumentations. Image NASA Landsat-8, 30.12.2015.

Facilities of the Drescher ice camp (Fig. 3.2.8.2) comprised of two fiberglass igloo satellite cabins (Wallhead), with one igloo serving as living quarters and the other igloo for kitchen and provisions, one Polarhaven tent (Weatherhaven) as workshop and living quarter, a canopy-covered sledge (Wallhead), and a Scott tent as toilet facility. In order to guard against strong snowdrifts, the igloos and tents were lined-up across the main easterly wind direction (Figs. 3.2.8.2 and 3.2.8.3). For the power supply two Knurtz generators of 8 and 5 kW, and two Elektra Bekum 1 kW-generators were used alternately, and another 6.5 kW and 2 kW Honda generators to supply the ROV. Main consumers of electricity were two snowmelts for producing water, a deep fryer, fan heaters to dry the working clothes and snow boots, and the ROV. Cooking and basic heating was done with propane gas. An ice ramp in the immediate vicinity of the field camp allowed commuting between the camp site and the inlet's fast ice. Three skidoos and four Nansen-sledges provided the necessary mobility for the fieldwork. Two pop-up tents sheltered equipment on the ice. Depending on weather conditions, the maximum daily energy consumption amounted up to 25 litres of fuel and approx. 1.5 kilograms of gas. A total of 823 km was driven by two of the skidoos, while the third one was not used. The overall consumption of fuel comprised 5 of the 7 barrels of fuel (1,000 L) and 6 out of 8 bottles of propane (60 kg). Two-stroke oil consumption amounted to 7 L. A safety depot of 3 barrels of kerosene (600 L) for potential emergency evacuation flights remained untouched, and was brought back together with all of the equipment. With the exception of the kitchen sewage, all wastes of glass (0.03 m³), plastic (0.3 m³), metal (0.12 m³), paper (0.3 m³), as well as organic (0.15 m³) and human waste (0.33 m³) were kept in separate 30 L Septicont-buckets or sacks, which were then brought back to RV *Polarstern* and *Neumayer Station III* respectively, and its takeover documented according to MARPOL regulations.

Alternative camp sites as a result of potentially unfavourable weather or sea ice conditions were envisaged at Atka Bay with a direct liaison and support via *Neumayer Station III*, and at another inlet in the vicinity of the research station *Halley VI*. As a result of our early arrival via DROMLAN, locations of seals along tidal cracks within the Atka Bay could be identified in the beginning of the campaign prior to the arrival of RV *Polarstern*. However, at the time of arrival of RV *Polarstern* the weather forecast was favourable and thus active research was carried out only at the Drescher Inlet. Communication with the German Field Operation Manager at *Neumayer Station III* was ensured by a daily call via Iridium, which also provided access by email to the daily weather information and forecast provided by the flight weather forecaster at *Neumayer Station III*.



Fig. 3.2.8.2: Aerial photo of the Drescher ice camp upon deployment of the igloos and tents on 27 December 2015. Photo: Michael Schröder, AWI

3.2.8 Seal research at the Drescher Inlet (SEADI)

Fig. 3.2.8.3: Facilities of the Drescher ice camp. In order to guard against strong snowdrifts, igloos, tents, and generators were lined-up across the main easterly wind direction. Photo: Horst Bornemann, AWI



Seal-borne image data and ROV footage

Four Weddell seals were instrumented with Infrared (IR) still picture camera loggers (Little Leonardo, Japan; cf. Naito et al. 2013) in order to track their foraging behaviour visually during the course of the study and to investigate the seals' under shelf ice foraging excursions (Fig. 3.2.8.4). Two of the data sets could be retrieved. In addition, a video camera system was



Fig. 3.2.8.4: Weddell seal with IR Digital Still Picture Logger (DSL). Photo: Richard Steinmetz, AWI

deployed twice; however, this and two of the still picture camera loggers could not be retrieved from the instrumented seals. The camera systems are provided and used in collaboration with scientists from the National Institute of Polar Research and the Biologging Institute (Tokyo, J). The units were retrieved four to eight days after deployment in order to download the images. Seals were immobilized (see below) to achieve a reliable attachment of the devices and concurrent sampling of whiskers, and for the retrieval of the archival tags.

Particular attention was paid to extend earlier findings on the foraging behaviour under the shelf ice. Thus, animals were instrumented preferentially in the proximity of the shelf ice edge.

The establishment of an 1.5 to 1.5 m hole in the fast ice at -72.80279 (LAT) -19.23379 (LON) to allow the deployment of the ROV was by far the most time-consuming and physically exhausting labour (Fig. 3.2.8.5). Opening of the 1.20 m thick sea ice close to a tidal crack and removing of a 6 m thick platelet ice layer beneath required more than five days. In addition, a full day after each of the two snow drift events was required to re-open the ice hole, and further daily maintenance of between one and four hours required to remove new platelet ice out of the hole.

The V8Sii ROV (Ocean Modules) is equipped with two High Definition (HD) video cameras (Kongsberg oe14-502) in the front and one wide-angle camera (Bowtech L3C-550) in the rear. Both HD cameras were complemented with three parallel red lasers providing reference scales of 10 by 10 cm on the videos. The lighting is ensured by four LED lights (Bowtech LED-2400 aluminium) in the front and one in the back. The ROV has a compass, an orientation sensor, an altimeter (Tritech Micron Echo Sounder), an obstacle avoidance sonar (Tritech Micron), and an Ultra Short Baseline (USBL) system (Easytrak Lite USBL, Applied Acoustics) to determine its exact underwater position relative to a GPS being installed on top of a crane over the ice hole.

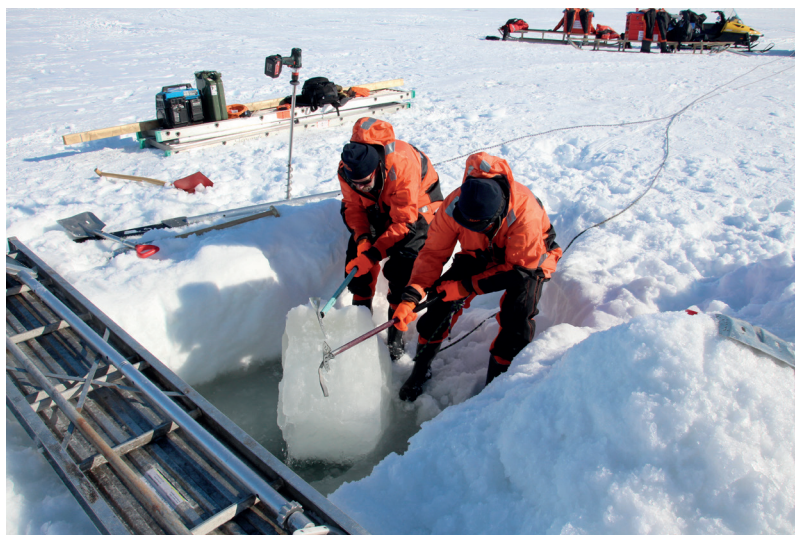


Fig. 3.2.8.5: Establishment of an ice hole to launch the ROV at -72.80279 (LAT) -19.23379 (LON). Photo: Dominik Nachtsheim, AWI

The USBL transducer was installed at the end of a six meter aluminium pole inside the ice hole. A sledge module bearing a CTD (SeaBird SBE19 plus) and sensors for pH, oxygen, light, fluorescence, as well as a Doppler Velocity Logger (Doppler Velocity Log (DVL) Teledyne RDI Instruments, Explorer PA) for bottom tracking and current measurements was mounted to the underside of the ROV. A mini-dredge and sampling box called Rowski's Bucket Broom (RBB) attached to the upper side of the ROV was available to obtain invertebrate specimens for post hoc morphological and genetic investigations (Fig. 3.2.8.6). Setting out and retrieval of the ROV was achieved by an A-framed crane over the hole, and coiling of the ROV cable was done by a hand winch, which was placed on a sledge next to the ice hole. All steering equipment was sheltered by a pop-up tent, and the navigation screens additionally shaded by blue insulation mats. See Fig. 3.2.8.7 for the complete ROV set-up at the ice hole. A passive

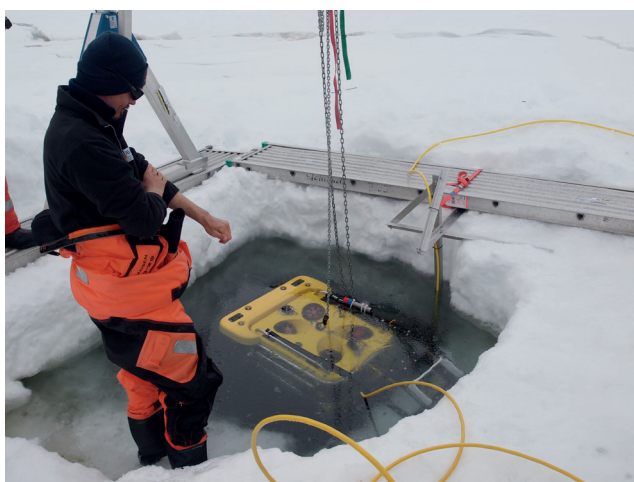
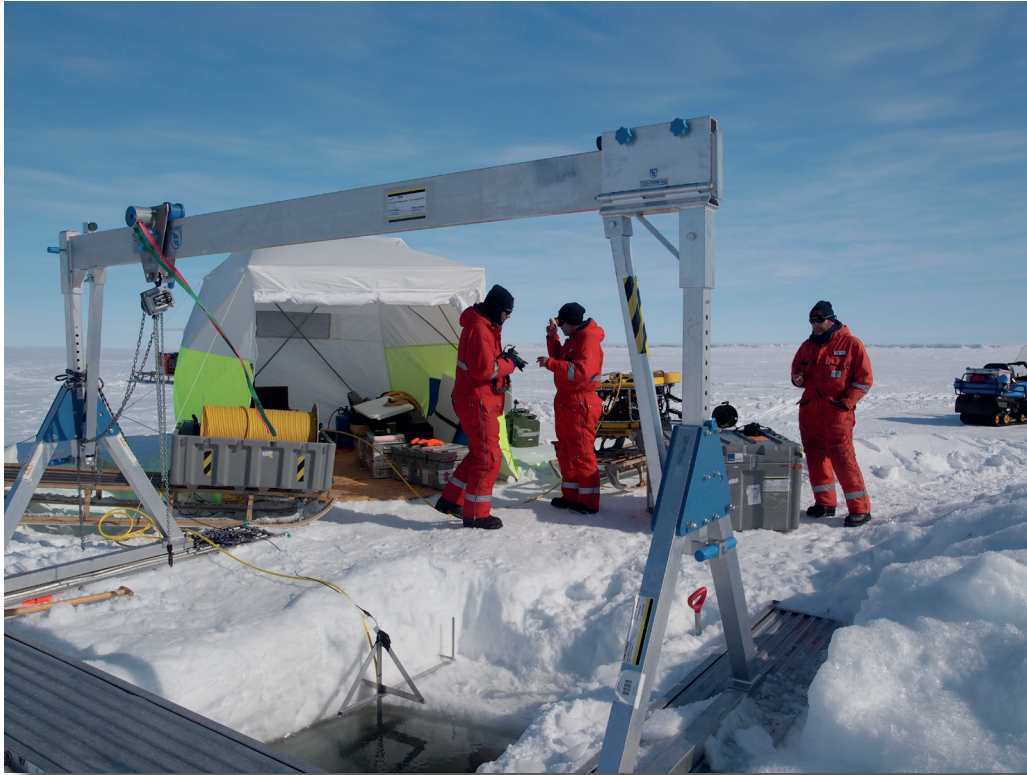


Fig. 3.2.8.6: The ROV V8Sii (Ocean Modules®) equipped with RBB prior to its launch at the ice hole. Photo: Horst Bornemann, AWI

icListen Smart Hydrophone (S/N 1212, Model SB2-EHT) was deployed during three of the ROV dives to record data on sound pressure levels of the navigation devices. Dives of the ROV turned out to be close or even beyond its operational technical specifications, and hence required intensive technical support and maintenance before and after each dive (Fig. 3.2.5.8). As a result five dives needed to be aborted prematurely due to various technical malfunctions. Two successful dive operations under the ice shelf provided high resolution footage and samples of the under shelf ice community at depths of around 80 m. Tab. 3.2.8.1 provides all data on the deployments of ROV.

3.2.8 Seal research at the Drescher Inlet (SEADI)



*Fig. 3.2.8.7: The set-up to launch the ROV V8Sii (Ocean Modules®) at the ice hole.
Photo: Horst Bornemann, AWI*



Fig. 3.2.8.8: Platelet ice covers the entire ROV. Photo: Nils Owsianowski, AWI

Tab. 3.2.8.1: Deployments of the Ocean Modules V8Sii ROV, Drescher Inlet, Antarctic, 2016

Dive Nr	Date yyyy-mm-dd	Duration [h:mm]	Depth [m]	Measurements/Recordings							
				CTD	DVL	NAVII	Sonar	USBL	Video	icList.	Samp
1	2016-01-10	1:25	1	x	x	x	x	x	x	x	
2	2016-01-11	0:17	1	x	x	x	x	x	x		
3	2016-01-12	0:17	1	x	x	x	x	x	x		
4	2016-01-13	1:40	81	x	x	x	x	x	x		
5	2016-01-19	0:17	1	x	x	x	x	x	x		
6	2016-01-20	0:33	70	x	x	x	x	x	x	x	x
7	2016-01-20	0:52	301	x	x	x	x	x	x	x	

CTD SBE19 plus CTD including, pH, Oxygen, Light, Fluorescence, SeaBird

DVL Doppler Velocity Log (DVL), Explorer PA, Teledyne RDI Instruments

NAVII Heading, Roll, Pitch, Depth

SONAR Micron DST Sonar / Micron Echosounder Altimeter, Tritech

USBL Easytrak Lite Ultra Short Baseline (USBL), Applied Acoustics

Video 2 HD Video cameras, Kongsberg oe14-502, 1 wide angle camera, Bowtech L3C-550

icList. icListen Smart Hydrophone, Model S/N 1212, Model SB2-EHT

Samp. Sampling with Rowski's Bucket Broom

Micron Nav USBL, Tritech was considered as backup, and was not used

CTD satellite relay data loggers

Four Weddell seals were instrumented with CTD Satellite Relay Data Loggers (CTD-SRDL; Valport, Sea Mammal Research Unit, UK) in order to obtain information about the seals' foraging and migratory behaviour as well as concurrent *in situ* hydrography within and beyond the area of the Drescher Inlet (Fig. 3.2.8.9). Long-distance tracking of marine mammals in the Southern Ocean by satellite relies on the ARGOS system. ARGOS satellite transmitters for marine mammal applications (e.g. CTD-SRDLs) are designed to provide the animals' at-sea locations and transmit these data to polar-orbiting satellites when the seals surface. Beside logging data about each dive (dive depth, dive duration, post-dive surface interval) CTD-SRDLs have the capabilities to record also *in situ* water temperature and conductivity for the entire migrations of tracked seals. Such data are of suitable quality to characterise the oceanographic settings utilised by the seals (e.g. Meredith et al. 2011; Boehme et al. 2009; Nicholls et al. 2008), and are complementary to the oceanographic investigations to be carried out during FROSN (PS96). Two CTD-casts have been taken on board RV *Polarstern* on 27 December 2015 and 27 January 2016 at -72.80317 (LAT) -19.59683 (LON) and -72.79867 (LAT) -19.35700 (LON) down to depths of 1,238 m (Stat. No. 002/01) and 521 m respectively (Stat. No 088/01) in order to calibrate the seal-borne CTD-data. The reconciliation of data on the seals' diving behaviour and on the hydrographic features with information on the occurrence and biomass of the seals' prey aims to contribute to the understanding of the upper trophic level interactions at the

3.2.8 Seal research at the Drescher Inlet (SEADI)

Drescher Inlet. So far only three publications provide data about satellite-tracked Weddell seals within the Weddell Sea (McIntyre et al. 2013; Årthun et al. 2012; Nicholls et al. 2008). Adult Weddell seal males (*Leptonychotes weddellii*) should be preferably instrumented with CTD-SRDLs, since they can be expected to remain in the investigation area throughout the year due to their “maritorial” behaviour. Weddell seals, furthermore, dive to depths of up to 900 m (Årthun et al. 2012), and their foraging dives can yield information on both potential pelagic and demersal or benthic prey in the investigation area. The deployments of CTD-SRDLs took place during the Weddell seals’ annual moult. Only seals were selected, which had already completed moulting their hair on the head and upper neck. The devices were then glued to the new hair of the anaesthetized seals using a two component, quick setting Araldite epoxy resin. During the next annual moult the units will be shed, and thus tracks and concurrent behavioural as well as hydrographic data can be collected over a period of one year at maximum.



*Fig. 3.2.8.9: Weddell seal with CTD satellite relay dive logger.
Photo: Dominik Nachtsheim, AWI*

Additional sampling

On top of the deployments two whiskers (vibrissae) were sampled from each of the instrumented seals. Whiskers will be used to get retrospective information on the prey spectra on intermediate time scales up to a couple of months by means of component-specific isotope analyses (*cf.* Hückstädt et al. 2012a, 2012b; Newsome et al. 2010; Lewis et al. 2006).

Animal handling

For the purpose of instrumentation, the seals needed to be anaesthetized following the methods as described in Bornemann et al. (1998) and Bornemann & Plötz (1993). Drugs were initially administered intramuscularly by remote injection using blowpipe darts. Follow-up doses were usually given intramuscularly by direct manual injection or in rare cases intravenously. The dose regime involved the drugs as listed below (Tab. 3.2.8.2a & b) and dosages or respectively dose ranges varied depending on initial or follow-up injections. The seals were immobilized with ketamine/xylazine (Weddell seals) combinations. Depending on the course of the immobilisation, dosages were individually adjusted and complemented by the same drugs to maintain or extend the immobilisation period on demand. Atipamezol was used to reverse the xylazine component in the xylazine/ketamine immobilisation. Doxapram was exclusively reserved for the necessity to stimulate breathing in a case of a finally irreversible apnoea, where mechanical obstructions of the upper airways could be excluded. The length and girth of each seal was measured. All procedures were carried out pursuant to the SCAR Code of Conduct for Animal Experiments, and were approved by the German Federal Environmental

3.2 Biological and Ecological Investigations

Agency (Umweltbundesamt) and the Federal Agency for Nature Conservation (Bundesamt für Naturschutz) under the German acts implementing the Protocol of Environmental Protection to the Antarctic Treaty and the Convention for the Conservation of Antarctic Seals.

Tab. 3.2.8.2a: Data on immobilisations and dose regimes of 18 adult Weddell seals (*Leptonychotes weddellii*), at Drescher Inlet, Antarctic, 2016

Weddell seal		Location		Date	Time	Length	Girth	
<i>Animal.Narcosis</i>		LAT	LON					
<i>No.No</i>	<i>Alter</i>	<i>Sex</i>	[°]	[°]	<i>yyyy-mm-dd</i>	<i>hh:mm</i>	[mm]	[mm]
1.1	adult	F	-72.80279	-19.23379	2016-01-01	11:30	*	*
2.1	adult	F	-72.80329	-19.23229	2016-01-02	10:30	*	*
3.1	adult	F	-72.80329	-19.23229	2016-01-02	14:30	2490	1820
3.2	adult		-72.80277	-19.23381	2016-01-08	15:34		
4.1	adult	M	-72.83623	-19.15999	2016-01-03	11:07	*	*
5.1	adult	F	-72.83623	-19.15999	2016-01-03	12:10	2760	2000
6.1	adult	F	-72.83626	-19.16007	2016-01-10	13:25	2490	1930
7.1	adult	M	-72.83180	-19.22918	2016-01-11	11:20	2340	1910
7.2	adult		-72.83163	-19.23026	2016-01-21	15:40		
8.1	adult	F	-72.83080	-19.13175	2016-01-14	12:03	2690	1780
8.2	adult		-72.80285	-19.23428	2016-01-18	11:00		
9.1	adult	M	-72.83575	-19.15971	2016-01-21	11:40	2540	1900
10.1	adult	F	-72.83648	-19.16012	2016-01-21	13:10	2870	2220
11.1	adult	M	-72.80267	-19.23400	2016-01-22	11:40	*	*
12.1	adult	M	-72.83071	-19.13169	2016-01-22	13:40	*	*
13.1	adult	F	-72.83644	-19.15894	2016-01-22	14:10	2850	1850
14.1	adult	F	-72.83656	-19.15997	2016-01-22	15:50	2610	1730
15.1	adult	M	-72.83504	-19.16238	2016-01-23	14:50	2630	1850
16.1	adult	M	-72.80143	-19.27574	2016-01-24	11:15	*	*
17.1	adult	M	-72.83626	-19.16007	2016-01-25	11:05	*	*
18.1	adult	F	-72.83273	-19.16045	2016-01-25	12:05	2540	1890

F = Female

M = Male

* Narcosis not deep enough

3.2.8 Seal research at the Drescher Inlet (SEADI)

Tab. 3.2.8.2b: Data on immobilisation, sampling and tagging procedures of 18 adult Weddell seals (*Leptonychotes weddellii*) at Drescher Inlet, Antarctic, 2016

Weddell seals <i>Animal.Narcosis</i>	Duration	Full procedure	Sampling/Instrumentation			
			Blood	Whiskers	Hair	Logger type
No.No	[h:mm]	[h:mm]				
1.1	*	*				
2.1	*	*				
3.1	1:18	1:48		X		DSL 1 d
3.2	0:43	1:13				DSL 1 r
4.1	*	*				
5.1	0:55	1:25		X		DSL 2 d
6.1	1:00	1:30		X		DSL 3 d
7.1	0:45	1:15		X		DSL 4 d
7.2	0:35	1:05				DSL 4 r
8.1	0:47	1:17		X		DVL 1 d
8.2	0:35	1:05				DVL 1 r
9.1	1:05	1:35		X		SRDL 1 d
10.1	1:10	1:40		X		SRDL 2 d
11.1	*	*				
12.1	*	*				
13.1	0:55	1:25		X		SRDL 3 d
14.1	1:00	1:30		X		DVL 2 d
15.1	0:50	1:20		X		SRDL 4 d
16.1	*	*				
17.1	*	*				
18.1	0:55	†		X		
Mean	0:53	1:23				

* incomplete immobilisation † seal died in narcosis x sample taken

DSL Digital Still Picture Logger

DVL Digital Video Logger

SRDL Satellite Relay Dive Logger

d Instrumentation

r Retrieval

Preliminary and expected results

Two still picture camera data sets could be retrieved providing a total of 3,454 and 15,027 images. Some of the exposed seal-borne images confirmed shelf ice associated pelagic foraging, and showed isopods under the ice shelf. Another fraction of images exposed during dives to the sea floor showed the benthic community deep in the Drescher Inlet. The video camera and two of the still picture camera loggers could not be retrieved from the instrumented seals. The ROV provided 161 and 91.5 GByte of footage of the two successful dives under the shelf ice (dives 4 & 6), and another 34 GByte of the pelagic dive (dive 7). For all dives concurrent *in situ* hydrographic data are available, and samples of several specimen of isopods of different size (*Antarcturus* spp.) were collected underneath the shelf ice at about 80 m, where they were found in dense aggregations (Tab. 3.2.8.1). The successful retrieval of invertebrate samples by the ROV will enable the first genetic investigation of the species inventory of

the “hanging garden” community. The species identity, molecular barcodes, phylogenetic and population genetic connections of the under-ice fauna to epibenthic communities will be studied, suitably preserved material for a comparative study is already available in the collection of C. Held. The interpretation of the seal borne images, the ROV footage and post hoc genetic analyses of the under-ice samples is expected to provide insights into the species composition and density of the fauna inhabiting the underside of the ice, and may trigger further investigations of the ecological processes under ice shelves in the future. Deployment of ARGOS satellite transmitters on four post-moulting adult Weddell seals augments earlier projects on post-breeding adult males and females satellite-tagged within the region of the outflow of the Filchner Trough (Bornemann et al. 2014; Årthun et al. 2012; Nicholls et al. 2008) and in the Atka Bay (McIntyre et al. 2012). From each of the four CTD-SRDL tagged seals we expect per day about four temperature, salinity and depth profiles almost in real time, which will allow us to study how changes in the underwater environment alter prey distribution beneath the ice as indicated by the seals’ individual diving and foraging behaviour. We furthermore expect that these key physical oceanographic variables collected from hitherto under-sampled near coastal shelf regions may support the refinement of computer models of the Southern Ocean circulation. Sampling of whiskers will provide information on the seals’ prey spectrum in subsequent laboratory analyses. The combination of the data obtained from the different systems allows us to characterise the foraging strategies of the Weddell seals and to quantify their pelagic and benthic foraging. A synthesis of the expected findings is considered to provide new insights into the complexity of intermediate and upper level trophic interactions and energy flows in the high Antarctic pelagic and benthic food webs.

Data management

All data and related meta-information will be made available in open access via the Data Publisher for Earth & Environmental Science PANGAEA (www.pangaea.de/), and will be attributed to a consistent project label denoted as “Marine Mammal Tracking” (MMT, see <http://www.pangaea.de/search?q=project:label:mmt>). Species barcodes derived from genetic analyses will be deposited in the barcode of life database (www.barcodeoflife.org).

References

- Arndt JE, Schenke HW, Jakobsson MN, Frank-Oliver Buys G, Goleby B, Rebesco M, Bohoyo F, Hong JK, Black J, Greku RKh, Udintsev GB, Barrios F, Reynoso-Peralta W, Taisei M & Wigley R (2013) The International Bathymetric Chart of the Southern Ocean Version 1.0 - A new bathymetric compilation covering circum-Antarctic waters. *Geophysical Research Letters* 40(9):1-7.
- Årthun M, Nicholls KW, Makinson K, Fedak MA & Boehme L (2012) Seasonal inflow of warm water onto the southern Weddell Sea continental shelf, Antarctica. *Geophysical Research Letters* 39:L17601.
- Boehme L, Lovell P, Biuw M, Roquet F, Nicholson J, Thorpe SE, Meredith MP & Fedak M (2009) Technical Note: Animal-borne CTD-Satellite Relay Data Loggers for real-time oceanographic data collection. *Ocean Science* 5:685-695.
- Bornemann H, Oosthuizen WC & Bester MN (2014) Seal research at the Filchner Outflow System (SEAFOS), pp 115-136 in Knust R & Schröder M (eds) The Expedition PS82 of the Research Vessel POLARSTERN to the southern Weddell Sea in 2013/2014, *Berichte zur Polar- und Meeresforschung = Reports on polar and marine research*, Bremerhaven, Alfred Wegener Institute for Polar and Marine Research 680, 155 p.
- Bornemann H, Mohr E, Plötz J & Krause G (1998) The tide as *zeitgeber* for Weddell seals. *Polar Biology* 20:396-403.
- Bornemann H & Plötz J (1993) A field method for immobilizing Weddell seals. *Wildlife Society Bulletin* 21:437-441.

3.2.8 Seal research at the Drescher Inlet (SEADI)

- Daly M, Rack F & Zook R (2013) *Edwardsiella andrillae*, a New Species of Sea Anemone from Antarctic Ice. *PLoS ONE* 8(12):e83476.
- Fretwell PT, LaRue MA, Morin P, Kooyman GL, Wienecke B, Ratcliffe N, Fox AJ, Fleming AH, Porter C & Trathan PN (2012) An emperor penguin population estimate: the first global, synoptic survey of a species from space. *PLoS ONE* 7(4):e33751.
- Graffe D & Niederjasper F (1997) Meeresbodenkartierung mit dem HydrosweepSystem. In: Jokat W & Oerter H (eds) Die Expedition Antarktis XII mit FS „Polarstern“ 1992. *Berichte zur Polarforschung* 219:37-44.
- Günther S, Gleitz M & Dieckmann G (1999) Biogeochemistry of Antarctic sea ice: a case study on platelet ice layers at Drescher Inlet, Weddell Sea, *Marine Ecology Progress Series* 177:1-13.
- Gutt J (2002) The Antarctic ice shelf: an extreme habitat for notothenioid fish. *Polar Biology* 25(4):320-322.
- Hempel G & Stonehouse B (1987) Aerial counts of penguins, seals and whales in the eastern Weddell Sea. *Berichte zur Polarforschung* 39:227–230.
- Hückstädt LA, Burns JM, Koch PL, McDonald BI, Crocker DE & Costa DP (2012a) Diet of a specialist in a changing environment: the crabeater seal along the Western Antarctic Peninsula. *Marine Ecology Progress Series* 455:287-301.
- Hückstädt LA, Koch PL, McDonald BI, Goebel ME, Crocker DE & Costa DP (2012b) Stable isotope analyses reveal individual variability in the trophic ecology of a top marine predator, the southern elephant seal. *Marine Ecology Progress Series* 455:287-301.
- Klages N & Gerdes D (1988) A little known colony of emperor penguins on the coast of the eastern Weddell Sea. *South African journal of Polar Research* 18(1):18-20.
- Lewis R, O'Connell TC, Lewis M, Campagna C & Hoelzel AR (2006) Sex-specific foraging strategies and resource partitioning in the southern elephant seal (*Mirounga leonina*). *Proceedings of the Royal Society B-Biological Sciences* 273:2901-2907.
- Liebsch, N., Wilson, R.P., Bornemann, H., Adelung, D. & Plötz, J (2007) Mouthing off about fish capture: jaw movements in pinnipeds reveal the real secrets of ingestion. *Deep Sea Research II* 54:256-269.
- McIntyre T, Stansfield LS, Bornemann H, Plötz J & Bester MN (2013) Hydrographic influences on the summer dive behaviour of Weddell seals (*Leptonychotes weddellii*) in Atka Bay, Antarctica, *Polar Biology* 36:1693-1700.
- Meredith MP, Nicholls KW, Renfrew IA, Boehme L, Biuw M & Fedak M (2011) Seasonal evolution of the upper-ocean adjacent to the South Orkney Islands, Southern Ocean: Results from a “lazy biological mooring”. *Deep-Sea Research II* 58:1569-1579.
- Naito Y, Costa DP, Adachi T, Robinson PW, Fowler M, & Takahashi A (2013) Unravelling the mysteries of a mesopelagic diet: a large apex predator specializes on small prey. *Functional Ecology* 27(3):710–717.
- Naito Y, Bornemann H, Takahashi A, McIntyre T & Plötz J (2010) Fine scale feeding behaviour of Weddell seals measured by mandible accelerometer. *Polar Science* 4(2):309-316.
- Newsome SD, Clementz MT & Koch PL (2010) Using stable isotope biogeochemistry to study marine mammal ecology. *Marine Mammal Science* 26:509-572.
- Nicholls KW, Boehme L, Biuw M & Fedak MA (2008) Wintertime ocean conditions over the southern Weddell Sea continental shelf, Antarctica. *Geophysical Research Letters* 35:L21605.
- Plötz J, Bornemann H, Liebsch N & Watanabe Y (2005) Foraging Ecology of Weddell seals. In: Arntz W & Brey T (eds) The expedition ANTARKTIS XXI/2 (BENDEX) of RV “Polarstern” in 2003/04. *Reports on Polar and Marine Research* 503:63-67.

- Plötz J, Bornemann H, Knust R, Schröder A & Bester M (2001) Foraging behaviour of Weddell seals, and its ecological implications. *Polar Biology* 24:901-909.
- Plötz J & Bornemann H (1999) Diving and foraging behaviour of Weddell seals. In: Arntz W & Gutt J (eds) The expedition ANTARKTIS XV/3 (EASIZ II) of RV "Polarstern" in 1998. *Reports on Polar Research* 301:95-98.
- Plötz J, Bornemann H, Gleitz M & Günther S (1997) Biological investigations at the Drescher Inlet – sea ice communities and Weddell seals. In: Jokat W & Oerter H (eds) Die Expedition Antarktis XII mit FS „Polarstern“ 1992. *Berichte zur Polarforschung* 219:61-66.
- Plötz J, Bornemann H, Pütz K, Steinmetz R & Ulbricht J (1994) Investigations in penguins and seals at the Drescher Inlet, Vestkapp. In: Miller H & Oerter H (eds) Die Expedition Antarktis X mit FS „Polarstern“ 1992. *Berichte zur Polarforschung* 152:112-118.
- Plötz J, Bornemann H, Pütz K & Steinmetz R (1991) Investigations in penguins and seals at the Drescher Inlet, Riiser-Larsen ice shelf In: Miller H & Oerter H (eds) Die Expedition Antarktis VIII mit FS „Polarstern“ 1989/90. *Berichte zur Polarforschung* 86:41-46.
- Plötz J, Gerdes D, Gräfe M, Klages N, Reijnders R, Steinmetz R & Zegers K (1987) Weddell seals and emperor penguins in Drescher Inlet. *Berichte zur Polarforschung* 39:222–227.
- Plötz J, Dubbels R, Graefe M & Limberger D (1985). Studies on seals and seabirds. In: Hempel G (ed) *Berichte zur Polarforschung* 25:133–137.
- Pütz K & Plötz J (1991) Moulting and starvation in emperor penguins (*Aptenodytes forsteri*) chicks. *Polar Biology* 11:253-258.
- Reijnders HP, Plötz J, Zegers K & Gräfe M (1990) Breeding biology of Weddell seals *Leptonychotes weddellii* at Drescher Icelet, Riiser Larsen Ice Shelf. *Polar Biology* 10:301-306.
- Schenke HW, Dijkstra SJ, Niederjasper F, Schöne T, Hinze H & Hoppmann B, (1997) The new bathymetric charts of the Weddell Sea: AWI BCWS. In: Jacobs, S., Weiss, R. (Eds.), *Antarctic Research Series*. American Geophysical Union, Washington, p. 75; See Hinze H, Schenke HW, Schöne T (1997) AWI Bathymetric Chart of the Weddell Sea, Antarctica (BCWS). Alfred Wegener Institute for Polar and Marine Research, Bremerhaven doi:10.1594/PANGAEA.708081.
- Thomas DN, Kennedy H, Kattner G, Gerdes G, Gough C & Dieckmann G (2001) Biogeochemistry of platelet ice: its influence on particle flux under fast ice in the Weddell Sea, Antarctica. *Polar Biology* 24(7):486-496.
- Watanabe Y, Bornemann H, Liebsch N, Plötz J, Sato K, Naito Y & Miyazaki N (2006) Seal-mounted camera detect invertebrate fauna underneath Antarctic ice shelf. *Marine Ecology-Progress Series* 309:297-300.
- Woehler E (1993) The distribution and abundance of Antarctic and Subantarctic penguins. *SCAR Publication*, Cambridge, UK 76 pp.

A.1 TEILNEHMENDEINSTITUTE/PARTICIPATINGINSTITUTIONS

	Address
AWI	Alfred-Wegener-Institut Helmholtz-Zentrum für Polar- und Meeresforschung Postfach 120161 27515 Bremerhaven/Germany
BAS	British Antarctic Survey Natural Environment Research Council High Cross, Madingley Road Cambridge CB3 0ET/United Kingdom
CAU	Christian-Albrechts-Universität Kiel Institut für Ökosystemforschung 24098 Kiel/Germany
DWD	Deutscher Wetterdienst Geschäftsbereich Wettervorhersage Seeschiffahrtsberatung Bernhard-Nocht-Str. 76 20359 Hamburg/Germany
HELISERVICE	HeliService international GmbH Am Luneort 15 27572 Bremerhaven/Germany
ICM-CISIC	Institut de Ciencies del Mar-CSIC Passeig Maritim de la Barceloneta 37-49 08003 Barcelona/Spain
KU Leuven	Katholieke Universiteit Leuven Laboratory of Biodiversity and Evolutionary Genomics Ch. Deberiotstraat 32, box 2439 B-3000 Leuven/Belgium
LAEISZ	Reederei F.Laeisz Zweigniederlassung Bremerhaven Bartelstraße 1 27570 Bremerhaven/Germany
SaM-DZMB	Senckenberg am Meer Wilhelmshaven -Deutsches Zentrum für Marine Biodiversitätsforschung Südstrand 44 26382 Wilhelmshaven/Germany
Senck.-F	Senckenberg Forschungsinstitut u. Naturkundemuseum Marine Zoologie Senckenberganlage 25 60325 Frankfurt a. M./Germany

	Address
SLC Uni Gothenburg	Sven Lovén Centre for marine Sciences at University of Gothenburg, The Lovén Centre Tjärnö SE - 452 96 Strömstad/Sweden
TU Kaiserslautern	Technische Universität Kaiserslautern Postfach 3049 67653 Kaiserslautern/Germany
UA	The University of Alabama Department of Biological Sciences 307 Mary Harmon Bryant Hall Tuscaloosa, AL 35487/USA
UiB-BCCR	Universitetet i Bergen Berknes Centre for Climate Research and Geophysical Institute Postboks 7800 5020 Bergen/Norway
UHB-IUP	Universität Bremen Institut für Umweltphysik Otto-Hahn-Alle 1 28359 Bremen/Germany
Uni Basel	MGU, DUW, Uni Basel Vesalgasse 1 CH-4051 Basel/Switzerland
Uni Bern	Universität Bern Postfach 8466 CH-3001 Bern/Switzerland
Uni Erlangen	Friedrich-Alexander Universität Inst. f. Geographie Wetterkreuz 15 91058 Erlangen/Germany
Uni Padova	Università degli Studi di Padova Via 8 Febbraio 2 35122 Padova/Italy
Uni Trier	Universität Trier Umweltmeteorologie Behringstr. 21 54296 Trier/Germany

A.2 PARTICIPANTS / TEILNEHMER

Name	First Name	Institute	Profession	
Andersson	Emil	SLC Uni Gothenburg	Engineer	biology
Arndt	Stefanie	AWI	Scientist,	physics
Arndt	Jan Erik	AWI	Scientist,	geo sciences
Bodur	Yasemin	SaM-DZMB	Student,	biology
Bornemann	Horst	AWI	Scientist,	biology
Brauer	Jens	HELISERVICE	Pilot	shipping company
Campos	Camila Pinheiro	AWI	Scientist,	oceanography
Cantzler	Hannelore	Uni Bremen	Student,	biology
Christiansen	Henrik	KU Leuven	Scientist,	biology
Christmann	Julia	TU Kaiserslautern	Scientist,	oceanography
Federwisch	Luisa	AWI	Scientist,	biology
Frontke	Julia	DWD	Scientist,	shipping company
Geilen	Johanna	AWI	Student,	oceanography
Grobe	Hannes	AWI	Scientist,	geo sciences
Heckmann	Hans	HELISERVICE	Pilot	shipping company
Heinemann	Günther	Uni Trier	Scientist,	physics
Hempelt	Juliane	DWD	Technician,	shipping company
Hillenbrand	Claus-Dieter	BAS	Scientist,	geo sciences
Holm	Patricia	Uni Basel	Scientist,	biology
Holtappels	Moritz	AWI	Scientist,	biology
Huhn	Oliver	UHB-IUP	Scientist,	oceanography
Isla	Enrique	ICM-CISIC	Scientist,	biology
Jechlitschek	Hendrik	UHB-IUP	Student,	oceanography
Johansson	Roger	SLC Uni Gothenburg	Engineer	biology
Kersken	Daniel	Senck .-F	Scientist,	biology
Kocot	Kevin	UA	Scientist,	biology
Koschnick	Nils	AWI	Technician,	biology
Link	Heike	CAU	Scientist,	biology
Mark	Felix	AWI	Scientist,	biology
Möllendorf	Carsten	HELISERVICE	Technician,	shipping company
Nachtsheim	Dominik	AWI	Scientist,	biology
Nistad	Jean-Guy	AWI	Technician,	geo sciences
Østerhus	Svein	UiB-BCCR	Scientist,	oceanography
Oswianowski	Nils	AWI	Engineer	biology
Piepenburg	Dieter	AWI	Scientist,	biology
Pineda Metz	Santiago	AWI	Scientist,	biology
Rankl	Melanie	Uni Erlangen	Scientist,	oceanography
Richter	Claudio	AWI	Scientist,	biology
Riginella	Emilio	Uni Padova	Scientist,	biology
Rossmann	Hans Leonard	AWI	Scientist,	physics
Ryan	Svenja	AWI	Scientist,	oceanography
Sands	Chester	BAS	Scientist,	biology
Scheuffele	Hanna	UHB-IUP	Student,	biology
Schröder	Michael	AWI	Chief Scientist	oceanography

Name	First Name	Institute	Profession	
Schröter	Thomas	HELISERVICE	pilot	shipping company
Segner	Helmut	Uni Bern	Scientist,	biology
Seifert	Derya Mona	CAU	Student,	biology
Steinmetz	Richard	AWI	Technician,	biology
Strobel	Anneli	Uni Basel	Scientist,	biology
Stulić	Lukrecia	AWI	Scientist,	oceanography
Timmermann	Ralph	AWI	Scientist,	oceanography
Veit-Köhler	Gritta	SaM-DZMB	Scientist,	biology
Wisotzki	Andreas	AWI	Scientist,	oceanography
Zapata Guardiola	Rebeca	ICM-CISIC	Scientist,	biology
Zentek	Rolf	Uni Trier	Scientist,	physics

A.3 SCHIFFSBESATZUNG / SHIP'S CREW

	Name	Rank
01	Wunderlich, Thomas	Master
02	Grundmann, Uwe	1. Offc
03	Westphal, Henning	ChEng
04	Lauber, Felix	2.Offc
05	Kentges, Felix	2.Offc
06	Peine, Lutz	2.Offc
07	Scholl, Thomas	Doctor
08	Hofmann, Jörg	Comm.Offc
09	Schnürch, Helmut	2.Eng
10	Buch, Erik-Torsten	2.Eng
11	Rusch, Torben	2. Eng
12	Brehme, Andreas	ElecTech
13	Ganter, Armin	Electron
14	Dimmler, Werner	Electron
15	Winter, Andreas	Electron
16	Feiertag, Thomas	Electron
17	Schröter, Rene	Boatsw
18	Neisner, Winfried	Carpenter
19	Glaser, Nils	AB
20	Winkler, Michael	AB
21	Schröder, Norbert	AB
22	Scheel, Sebastian	AB
23	Hartwig-Labahn, Andreas	AB
24	Kretzschmar, Uwe	AB
25	Müller, Steffen	AB
26	Brickmann, Peter	AB
27	Sedlak, Andreas	AB
28	Beth, Detlef	Storekeep
29	Plehn, Markus	Mot-man
30	Klein, Gert	Mot-man
31	Krösche, Eckard	Mot-man
32	Dinse, Horst	Mot-man
33	Watzel, Bernhard	Mot-man
34	Meißner, Jörg	Cook
35	Tupy, Mario	Cooksmate
36	Möller, Wolfgang	Cooksmate
37	Wartenberg, Irina	1 Stwdess
38	Schwitzky-Schwarz, Carmen	Stwdss/KS

	Name	Rank
39	Hischke, Peggy	2 Stwdess
40	Duka, Maribei	2 Stwdess
41	Chen, Tingdong	2 Steward
42	Hu, Guo Yong	2 Steward
43	Chen, Quan Lun	2 Steward
44	Ruan, Hui Guang	Laundrym

A.4 STATIONSLISTE / STATION LIST

Station	Date	Time	Gear Abbr.	PositionLat	PositionLon	Depth [m]	Comment
PS96/001-1	2015-12-23	13:55:00	CTD/RO	70° 52.89' S	011° 06.03' W	330,0	
PS96/001-2	2015-12-23	14:19:00	HS_PS	70° 52.86' S	011° 06.42' W	330,9	
PS96/001-2	2015-12-23	15:45:59	HS_PS	70° 53.04' S	011° 06.77' W	329,2	
PS96/001-3	2015-12-23	17:32:01	ROV	70° 53.14' S	011° 07.55' W	324,0	
PS96/001-3	2015-12-23	17:32:59	ROV	70° 53.14' S	011° 07.55' W	324,0	
PS96/001-4	2015-12-23	20:43:00	OFOS	70° 53.21' S	011° 06.63' W	313,0	
PS96/001-4	2015-12-23	22:21:00	OFOS	70° 53.79' S	011° 08.89' W	290,0	
PS96/001-5	2015-12-23	23:18:00	CTD/RO	70° 53.75' S	011° 08.97' W	291,0	
PS96/001-6	2015-12-24	00:27:00	BWS	70° 53.70' S	011° 09.10' W	319,0	
PS96/001-7	2015-12-24	01:29:00	MUC	70° 53.37' S	011° 07.10' W	309,0	
PS96/001-8	2015-12-24	02:07:00	MUC	70° 53.35' S	011° 07.07' W	309,0	
PS96/001-9	2015-12-24	03:25:00	AGT	70° 53.49' S	011° 07.78' W	305,0	
PS96/001-9	2015-12-24	03:30:00	AGT	70° 53.45' S	011° 08.20' W	314,0	
PS96/002-1	2015-12-27	22:10:00	CTD/RO	72° 48.22' S	019° 35.93' W	1224,3	
PS96/003-1	2015-12-29	02:39:00	CTD/RO	74° 32.90' S	026° 57.42' W	1688,6	
PS96/004-1	2015-12-29	04:57:00	CTD/RO	74° 36.08' S	026° 59.23' W	966,5	
PS96/005-1	2015-12-29	06:16:59	TRAPF	74° 38.89' S	026° 55.97' W	431,1	fish trap deployed
PS96/005-2	2015-12-29	06:54:00	CTD/RO	74° 38.65' S	026° 57.69' W	502,6	
PS96/005-3	2015-12-29	07:40:00	HS_PS	74° 40.24' S	026° 57.97' W	390,6	
PS96/005-3	2015-12-29	08:59:59	HS_PS	74° 40.95' S	026° 55.66' W	391,0	
PS96/006-1	2015-12-29	11:14:00	CTD/RO	74° 33.47' S	026° 47.00' W	745,0	
PS96/006-2	2015-12-29	12:53:01	BT	74° 36.07' S	026° 55.22' W	750,0	
PS96/006-2	2015-12-29	13:08:00	BT	74° 36.79' S	026° 57.23' W	750,0	
PS96/007-1	2015-12-29	16:04:01	OFOS	74° 39.43' S	026° 56.34' W	413,7	
PS96/007-1	2015-12-29	17:55:00	OFOS	74° 40.06' S	026° 59.89' W	414,4	
PS96/007-2	2015-12-29	19:46:00	TRAPF	74° 39.06' S	026° 55.91' W	421,2	fish trap recovered
PS96/007-3	2015-12-29	20:41:00	MUC	74° 39.57' S	026° 57.21' W	413,4	
PS96/007-4	2015-12-29	21:41:00	MUC	74° 39.51' S	026° 57.79' W	415,5	
PS96/007-5	2015-12-29	23:27:01	ROV	74° 39.50' S	026° 57.44' W	415,7	
PS96/007-5	2015-12-30	00:35:00	ROV	74° 39.50' S	026° 57.47' W	415,6	
PS96/007-5	2015-12-30	04:38:00	ROV	74° 39.40' S	026° 57.67' W	418,5	
PS96/007-6	2015-12-30	06:59:00	AGT	74° 39.40' S	026° 53.75' W	421,8	
PS96/007-6	2015-12-30	07:10:00	AGT	74° 39.58' S	026° 54.13' W	415,4	
PS96/007-7	2015-12-30	09:06:00	BWS	74° 38.71' S	026° 57.62' W	489,0	
PS96/008-1	2015-12-30	17:43:00	CTD/RO	74° 55.30' S	029° 25.17' W	392,4	
PS96/008-2	2015-12-30	18:30:01	OFOS	74° 55.23' S	029° 25.37' W	399,4	
PS96/008-2	2015-12-30	20:25:00	OFOS	74° 54.45' S	029° 24.58' W	404,8	
PS96/008-3	2015-12-30	21:04:00	GKG	74° 54.22' S	029° 23.85' W	401,4	
PS96/008-4	2015-12-30	22:35:00	MG	74° 53.70' S	029° 22.77' W	405,2	
PS96/009-1	2015-12-31	05:14:00	HS_PS	74° 52.46' S	026° 35.88' W	315,3	
PS96/009-1	2015-12-31	07:00:59	HS_PS	74° 54.81' S	026° 12.96' W	300,9	
PS96/009-2	2015-12-31	08:05:59	TRAPF	74° 58.82' S	025° 53.65' W	196,2	fish trap deployed
PS96/009-3	2015-12-31	11:02:00	BT	74° 57.30' S	026° 08.10' W	294,4	

A.4 Stationsliste/Station List

Station	Date	Time	Gear Abbr.	PositionLat	PositionLon	Depth [m]	Comment
PS96/009-3	2015-12-31	11:43:00	BT	74° 58.60' S	026° 11.12' W	313,0	
PS96/009-4	2015-12-31	12:44:00	CTD/RO	74° 59.56' S	026° 11.92' W	322,8	
PS96/010-1	2016-01-01	00:45:00	HS_PS	75° 06.60' S	025° 49.51' W	398,6	
PS96/010-1	2016-01-01	10:25:59	HS_PS	74° 57.32' S	025° 58.04' W	283,9	
PS96/010-2	2016-01-01	10:47:00	CTD/RO	74° 57.47' S	025° 59.55' W	275,5	
PS96/010-3	2016-01-01	11:52:00	OFOS	74° 56.65' S	026° 02.49' W	292,0	
PS96/010-3	2016-01-01	13:52:00	OFOS	74° 57.44' S	026° 05.14' W	293,6	
PS96/010-4	2016-01-01	14:59:01	ROV	74° 56.92' S	026° 03.69' W	278,0	
PS96/010-4	2016-01-01	15:10:00	ROV	74° 56.92' S	026° 03.69' W	277,8	
PS96/010-5	2016-01-01	16:49:00	BWS	74° 57.48' S	025° 59.99' W	271,7	
PS96/010-6	2016-01-01	18:24:00	MG	74° 56.69' S	026° 02.66' W	289,2	
PS96/010-6	2016-01-01	19:03:00	MG	74° 56.75' S	026° 02.87' W	286,8	
PS96/010-7	2016-01-01	19:46:00	CTD/RO	74° 57.01' S	026° 03.93' W	273,6	
PS96/010-8	2016-01-01	20:52:00	MUC	74° 57.00' S	026° 03.95' W	274,0	
PS96/010-9	2016-01-01	21:26:00	MUC	74° 57.07' S	026° 04.12' W	272,4	
PS96/010-10	2016-01-01	22:08:00	MUC	74° 57.46' S	026° 05.11' W	293,6	
PS96/010-11	2016-01-01	22:58:00	MUC	74° 58.99' S	026° 05.01' W	315,3	
PS96/010-12	2016-01-01	23:54:00	TRAPF	74° 59.07' S	025° 53.91' W	263,7	fish trap recovered
PS96/011-1	2016-01-03	05:27:00	CTD/RO	74° 58.17' S	030° 00.50' W	420,3	
PS96/012-1	2016-01-03	08:50:00	CTD/RO	75° 00.23' S	030° 29.87' W	467,5	
PS96/013-1	2016-01-03	12:03:00	CTD/RO	74° 58.88' S	030° 59.67' W	576,1	
PS96/014-1	2016-01-03	23:43:00	CTD/RO	74° 58.20' S	031° 29.36' W	618,5	
PS96/015-1	2016-01-04	03:04:00	CTD/RO	75° 00.24' S	032° 00.52' W	629,2	
PS96/016-1	2016-01-04	10:18:00	CTD/RO	74° 57.43' S	032° 30.64' W	609,7	
PS96/016-2	2016-01-04	10:58:00	GKG	74° 57.30' S	032° 30.64' W	605,9	
PS96/016-3	2016-01-04	13:08:00	AGT	74° 56.64' S	032° 27.53' W	620,5	
PS96/016-3	2016-01-04	13:24:01	AGT	74° 56.77' S	032° 27.85' W	623,5	
PS96/017-1	2016-01-04	17:30:00	CTD/RO	75° 00.63' S	032° 53.48' W	606,7	
PS96/017-2	2016-01-04	18:08:00	GKG	75° 00.75' S	032° 53.04' W	607,5	
PS96/017-2	2016-01-04	18:11:00	GKG	75° 00.76' S	032° 53.00' W	608,2	
PS96/017-3	2016-01-04	18:41:00	GKG	75° 00.85' S	032° 52.51' W	608,2	
PS96/017-4	2016-01-04	19:20:00	GKG	75° 00.87' S	032° 52.12' W	611,3	
PS96/017-5	2016-01-04	19:45:00	GKG	75° 00.86' S	032° 52.06' W	610,8	
PS96/018-1	2016-01-05	01:16:00	CTD/RO	74° 58.09' S	033° 26.37' W	589,3	
PS96/019-1	2016-01-05	13:05:00	CTD/RO	74° 51.88' S	034° 02.14' W	566,1	
PS96/020-1	2016-01-05	21:41:00	CTD/RO	74° 36.83' S	034° 28.43' W	553,9	
PS96/021-1	2016-01-06	07:04:00	CTD/RO	74° 18.38' S	034° 58.84' W	1313,9	
PS96/022-1	2016-01-06	09:43:00	CTD/RO	74° 23.69' S	035° 29.13' W	1238,3	
PS96/023-1	2016-01-06	23:54:00	CTD/RO	74° 31.33' S	036° 03.22' W	767,2	
PS96/024-1	2016-01-07	11:03:00	CTD/RO	74° 52.20' S	036° 29.49' W	400,5	
PS96/025-1	2016-01-07	13:41:00	CTD/RO	74° 58.65' S	037° 00.18' W	396,3	
PS96/026-1	2016-01-07	20:11:00	HS_PS	75° 15.05' S	037° 51.07' W	399,8	
PS96/026-1	2016-01-07	22:37:59	HS_PS	75° 16.48' S	038° 08.86' W	394,9	
PS96/026-2	2016-01-07	23:21:00	AGT	75° 16.48' S	037° 56.74' W	416,6	
PS96/026-2	2016-01-07	23:32:01	AGT	75° 16.32' S	037° 56.39' W	415,5	
PS96/026-3	2016-01-08	01:57:01	OFOS	75° 16.98' S	037° 54.94' W	415,0	
PS96/026-3	2016-01-08	03:59:00	OFOS	75° 15.98' S	037° 55.19' W	414,0	
PS96/026-4	2016-01-08	05:03:00	BWS	75° 15.96' S	037° 55.26' W	414,0	
PS96/026-5	2016-01-08	05:55:00	MG	75° 16.01' S	037° 55.16' W	414,0	
PS96/026-5	2016-01-08	06:15:00	MG	75° 16.17' S	037° 55.09' W	415,0	

Station	Date	Time	Gear Abbr.	PositionLat	PositionLon	Depth [m]	Comment
PS96/026-6	2016-01-08	07:11:00	GKG	75° 16.19' S	037° 55.07' W	415,0	
PS96/026-7	2016-01-08	08:24:00	MUC	75° 16.19' S	037° 54.96' W	416,1	
PS96/026-8	2016-01-08	09:33:00	MUC	75° 16.10' S	037° 54.85' W	415,2	
PS96/026-9	2016-01-08	10:48:00	MUC	75° 16.02' S	037° 54.83' W	415,0	
PS96/026-10	2016-01-08	11:49:00	MUC	75° 15.80' S	037° 54.87' W	414,3	
PS96/026-11	2016-01-08	12:49:00	MUC	75° 15.65' S	037° 54.44' W	413,6	
PS96/026-12	2016-01-08	13:36:00	GC	75° 15.74' S	037° 53.97' W	414,0	
PS96/026-13	2016-01-08	14:23:00	CTD/RO	75° 15.97' S	037° 55.17' W	413,3	
PS96/027-1	2016-01-14	13:03:00	CTD/RO	76° 43.11' S	052° 11.48' W	298,3	
PS96/027-2	2016-01-14	13:42:00	OFOS	76° 43.14' S	052° 11.31' W	298,7	
PS96/027-2	2016-01-14	14:35:00	OFOS	76° 43.12' S	052° 09.30' W	299,4	
PS96/027-3	2016-01-14	15:20:00	BWS	76° 43.17' S	052° 08.94' W	301,1	
PS96/027-4	2016-01-14	15:57:00	MG	76° 43.17' S	052° 08.82' W	302,1	
PS96/027-4	2016-01-14	16:04:00	MG	76° 43.17' S	052° 08.55' W	301,7	
PS96/027-5	2016-01-14	17:11:00	GKG	76° 43.17' S	052° 08.55' W	301,4	
PS96/027-6	2016-01-14	17:43:00	GKG	76° 43.17' S	052° 08.56' W	301,3	
PS96/027-7	2016-01-14	18:38:00	MUC	76° 43.11' S	052° 09.14' W	298,3	
PS96/027-8	2016-01-14	20:04:00	AGT	76° 42.84' S	052° 06.31' W	302,8	
PS96/027-8	2016-01-14	20:21:01	AGT	76° 42.69' S	052° 04.61' W	299,0	
PS96/028-1	2016-01-15	01:36:00	CTD/RO	76° 58.30' S	048° 59.42' W	273,0	
PS96/029-1	2016-01-15	08:10:00	CTD/RO	76° 53.49' S	047° 56.10' W	268,8	
PS96/030-1	2016-01-15	11:04:00	CTD/RO	76° 54.12' S	046° 51.58' W	288,3	
PS96/031-1	2016-01-15	16:28:00	CTD/RO	76° 42.83' S	045° 47.04' W	323,5	
PS96/032-1	2016-01-15	21:09:00	CTD/RO	76° 19.44' S	045° 47.59' W	329,9	
PS96/032-2	2016-01-15	21:42:00	MG	76° 19.36' S	045° 47.17' W	330,2	
PS96/033-1	2016-01-16	00:03:00	CTD/RO	76° 06.81' S	045° 20.77' W	332,8	
PS96/034-1	2016-01-16	03:25:00	CTD/RO	75° 59.95' S	044° 11.81' W	344,3	
PS96/035-1	2016-01-16	05:46:00	CTD/RO	75° 47.84' S	043° 36.48' W	369,9	
PS96/036-1	2016-01-16	09:03:00	CTD/RO	75° 39.31' S	042° 49.57' W	391,1	
PS96/037-1	2016-01-16	10:00:00	HS_PS	75° 39.48' S	042° 30.07' W	374,8	
PS96/037-1	2016-01-16	12:05:59	HS_PS	75° 42.07' S	042° 20.04' W	372,8	
PS96/037-2	2016-01-16	12:34:00	CTD/RO	75° 41.87' S	042° 20.25' W	388,5	
PS96/037-3	2016-01-16	14:04:00	OFOS	75° 43.30' S	042° 27.66' W	390,7	
PS96/037-3	2016-01-16	15:05:00	OFOS	75° 42.84' S	042° 26.65' W	390,1	
PS96/037-4	2016-01-16	16:39:01	ROV	75° 41.87' S	042° 20.33' W	388,3	
PS96/037-4	2016-01-16	18:28:00	ROV	75° 41.87' S	042° 20.33' W	388,2	
PS96/037-5	2016-01-16	19:55:00	BWS	75° 41.86' S	042° 20.33' W	388,3	
PS96/037-6	2016-01-16	21:23:00	MG	75° 43.27' S	042° 27.49' W	389,1	
PS96/037-7	2016-01-16	22:20:00	GKG	75° 40.49' S	042° 26.36' W	389,1	
PS96/037-8	2016-01-16	23:18:00	MUC	75° 43.30' S	042° 27.71' W	390,6	
PS96/037-9	2016-01-17	00:12:00	MUC	75° 43.29' S	042° 27.66' W	390,5	
PS96/037-10	2016-01-17	01:20:00	GC	75° 40.49' S	042° 26.35' W	389,2	
PS96/037-11	2016-01-17	02:27:00	AGT	75° 40.28' S	042° 25.70' W	389,1	
PS96/037-11	2016-01-17	02:40:01	AGT	75° 40.16' S	042° 25.34' W	389,1	
PS96/038-1	2016-01-17	03:49:00	LIDAR	75° 40.21' S	042° 03.19' W	372,5	
PS96/038-1	2016-01-17	08:22:00	LIDAR	75° 38.55' S	042° 17.56' W	372,8	
PS96/039-1	2016-01-17	09:45:00	BT	75° 40.49' S	042° 27.79' W	388,4	
PS96/039-1	2016-01-17	10:22:00	BT	75° 39.50' S	042° 21.36' W	388,2	
PS96/040-1	2016-01-17	11:58:00	CTD/RO	75° 40.23' S	042° 02.21' W	387,0	
PS96/041-1	2016-01-17	14:13:00	CTD/RO	75° 28.09' S	041° 29.78' W	371,4	
PS96/042-1	2016-01-17	20:34:00	CTD/RO	75° 13.67' S	040° 22.83' W	374,6	

A.4 Stationsliste/Station List

Station	Date	Time	Gear Abbr.	PositionLat	PositionLon	Depth [m]	Comment
PS96/043-1	2016-01-18	01:31:00	CTD/RO	74° 53.01' S	039° 11.49' W	390,8	
PS96/044-1	2016-01-18	06:57:00	CTD/RO	74° 53.90' S	037° 56.69' W	395,7	
PS96/045-1	2016-01-18	10:20:00	CTD/RO	74° 57.89' S	036° 50.22' W	398,6	
PS96/046-1	2016-01-18	13:24:00	CTD/RO	74° 59.50' S	035° 51.49' W	455,7	
PS96/047-1	2016-01-18	15:44:00	CTD/RO	74° 51.62' S	035° 10.95' W	501,0	
PS96/048-1	2016-01-18	19:30:00	CTD/RO	74° 46.18' S	035° 18.59' W	488,2	
PS96/048-2	2016-01-18	20:24:00	OFOS	74° 46.21' S	035° 18.63' W	486,7	
PS96/048-2	2016-01-18	22:25:00	OFOS	74° 45.44' S	035° 21.00' W	482,9	
PS96/048-3	2016-01-18	23:14:01	ROV	74° 45.07' S	035° 20.92' W	483,6	
PS96/048-3	2016-01-18	23:14:02	ROV	74° 45.07' S	035° 20.92' W	483,6	
PS96/048-4	2016-01-19	00:30:00	BWS	74° 45.07' S	035° 20.84' W	483,7	
PS96/048-5	2016-01-19	01:58:00	MG	74° 45.53' S	035° 20.61' W	481,9	
PS96/048-6	2016-01-19	02:49:00	GKG	74° 45.60' S	035° 20.14' W	483,4	
PS96/048-7	2016-01-19	04:14:00	MUC	74° 45.52' S	035° 20.91' W	481,9	
PS96/048-8	2016-01-19	05:14:00	MUC	74° 45.52' S	035° 20.91' W	481,8	
PS96/049-1	2016-01-19	16:47:00	CTD/RO	74° 37.93' S	033° 59.11' W	566,2	
PS96/050-1	2016-01-19	19:21:00	MOR	74° 39.77' S	033° 00.18' W	618,1	S2 not recovered
PS96/050-2	2016-01-19	20:09:00	CTD/RO	74° 40.17' S	033° 04.98' W	608,1	
PS96/051-1	2016-01-19	23:01:00	CTD/RO	74° 39.68' S	032° 29.07' W	614,7	
PS96/052-1	2016-01-20	00:51:00	CTD/RO	74° 39.85' S	032° 01.80' W	619,3	
PS96/053-1	2016-01-20	03:25:00	CTD/RO	74° 44.19' S	031° 28.79' W	601,8	
PS96/054-1	2016-01-20	05:04:00	CTD/RO	74° 45.05' S	030° 59.55' W	540,9	
PS96/055-1	2016-01-20	06:33:00	CTD/RO	74° 45.02' S	030° 29.83' W	472,9	
PS96/056-1	2016-01-20	13:53:00	CTD/RO	75° 30.13' S	028° 58.82' W	444,5	
PS96/056-2	2016-01-20	14:24:59	TRAPST	75° 30.29' S	028° 58.67' W	446,3	fish trap deployed
PS96/056-3	2016-01-20	14:41:59	TRAPST	75° 30.35' S	028° 56.76' W	441,6	fish trap deployed
PS96/056-4	2016-01-20	15:10:00	MG	75° 31.02' S	028° 57.18' W	453,8	
PS96/057-1	2016-01-20	21:11:00	CTD/RO	76° 19.13' S	029° 02.14' W	243,0	
PS96/057-2	2016-01-20	22:16:01	ROV	76° 19.11' S	029° 02.07' W	241,4	
PS96/057-2	2016-01-21	00:10:00	ROV	76° 19.11' S	029° 02.14' W	237,4	
PS96/057-3	2016-01-21	01:29:00	OFOS	76° 19.10' S	029° 01.97' W	240,7	
PS96/057-3	2016-01-21	02:36:00	OFOS	76° 19.33' S	029° 00.11' W	250,4	
PS96/057-4	2016-01-21	03:24:00	BWS	76° 19.11' S	029° 02.09' W	241,3	
PS96/057-5	2016-01-21	04:25:01	ROV	76° 19.12' S	029° 02.03' W	244,2	
PS96/057-5	2016-01-21	06:49:00	ROV	76° 19.12' S	029° 02.04' W	244,4	
PS96/057-6	2016-01-21	08:27:00	AGT	76° 16.41' S	029° 06.80' W	289,1	
PS96/057-6	2016-01-21	08:41:01	AGT	76° 16.47' S	029° 05.92' W	293,7	
PS96/058-1	2016-01-21	10:13:00	CTD/RO	76° 12.83' S	029° 29.78' W	366,2	
PS96/059-1	2016-01-21	12:17:00	CTD/RO	76° 08.91' S	030° 00.42' W	410,7	
PS96/059-2	2016-01-21	13:28:00	BT	76° 11.16' S	030° 02.90' W	394,6	
PS96/059-2	2016-01-21	14:03:01	BT	76° 12.98' S	030° 05.72' W	392,5	
PS96/060-1	2016-01-21	16:36:59	MOR	76° 05.47' S	030° 27.80' W	469,0	AWI 252-1 recovered
PS96/061-1	2016-01-21	18:12:01	OFOS	76° 05.98' S	030° 18.02' W	469,1	
PS96/061-1	2016-01-21	19:42:00	OFOS	76° 05.45' S	030° 20.27' W	480,0	
PS96/061-2	2016-01-21	20:38:00	CTD/RO	76° 05.86' S	030° 18.66' W	469,1	
PS96/061-3	2016-01-21	21:09:00	GKG	76° 05.85' S	030° 18.69' W	469,3	
PS96/061-4	2016-01-21	22:52:00	GC	76° 05.95' S	030° 18.30' W	467,6	

Station	Date	Time	Gear Abbr.	PositionLat	PositionLon	Depth [m]	Comment
PS96/061-5	2016-01-21	23:38:00	MUC	76° 05.93' S	030° 18.23' W	467,6	
PS96/061-6	2016-01-22	00:36:00	MUC	76° 05.89' S	030° 18.38' W	466,6	
PS96/062-1	2016-01-22	06:16:00	CTD/RO	75° 56.60' S	031° 27.42' W	599,1	
PS96/062-2	2016-01-22	07:18:00	MOR	75° 57.67' S	031° 28.84' W	604,0	AWI 254-1 recovered
PS96/063-1	2016-01-22	10:25:00	CTD/RO	76° 03.08' S	031° 03.40' W	474,2	
PS96/063-2	2016-01-22	11:00:00	GC	76° 02.96' S	031° 03.16' W	473,7	
PS96/063-3	2016-01-22	11:54:00	MOR	76° 02.54' S	031° 00.27' W	473,0	AWI-253-1 recovered
PS96/064-1	2016-01-22	14:24:59	MOR	76° 05.47' S	030° 28.19' W	465,1	AWI 252-2 deployed
PS96/065-1	2016-01-22	16:19:59	MOR	76° 02.75' S	030° 59.65' W	471,3	AWI 253-2 deployed
PS96/066-1	2016-01-22	18:09:00	CTD/RO	76° 04.91' S	030° 24.86' W	462,0	
PS96/066-2	2016-01-22	18:48:00	GC	76° 04.94' S	030° 24.88' W	462,1	
PS96/067-1	2016-01-22	20:12:00	CTD/RO	76° 04.16' S	030° 44.10' W	463,0	
PS96/068-1	2016-01-22	21:54:00	CTD/RO	76° 01.57' S	031° 13.47' W	489,9	
PS96/069-1	2016-01-23	00:07:00	CTD/RO	75° 57.01' S	031° 45.35' W	714,0	
PS96/069-2	2016-01-23	00:53:00	GC	75° 56.79' S	031° 44.92' W	715,0	
PS96/070-1	2016-01-23	03:13:00	CTD/RO	75° 57.55' S	031° 26.21' W	569,1	
PS96/070-2	2016-01-23	07:50:59	MOR	75° 57.71' S	031° 28.92' W	598,3	AWI 254-2 deployed
PS96/071-1	2016-01-23	09:27:00	CTD/RO	75° 54.22' S	032° 02.57' W	741,1	
PS96/071-2	2016-01-23	10:09:00	GC	75° 54.17' S	032° 02.32' W	744,7	
PS96/072-1	2016-01-23	12:43:00	AGT	75° 51.23' S	032° 22.91' W	747,8	
PS96/072-1	2016-01-23	13:04:00	AGT	75° 51.31' S	032° 23.85' W	747,3	
PS96/072-2	2016-01-23	14:06:00	CTD/RO	75° 51.37' S	032° 25.27' W	753,2	
PS96/072-3	2016-01-23	15:22:00	BWS	75° 51.35' S	032° 25.42' W	751,4	
PS96/072-4	2016-01-23	17:06:01	OFOS	75° 51.61' S	032° 22.95' W	752,1	
PS96/072-4	2016-01-23	18:30:00	OFOS	75° 51.43' S	032° 20.30' W	751,7	
PS96/072-5	2016-01-23	19:33:00	MG	75° 51.47' S	032° 20.03' W	749,8	
PS96/072-5	2016-01-23	19:36:00	MG	75° 51.47' S	032° 20.01' W	749,9	
PS96/072-6	2016-01-23	20:32:00	GC	75° 51.56' S	032° 19.39' W	751,4	
PS96/072-7	2016-01-23	21:53:00	MUC	75° 51.61' S	032° 17.58' W	755,4	
PS96/072-8	2016-01-23	23:01:00	MUC	75° 50.92' S	032° 18.42' W	753,4	
PS96/072-9	2016-01-24	00:11:00	MUC	75° 50.85' S	032° 17.44' W	755,1	
PS96/072-10	2016-01-24	01:47:00	MUC	75° 50.94' S	032° 21.42' W	749,4	
PS96/073-1	2016-01-24	05:03:00	CTD/RO	75° 45.60' S	032° 04.46' W	731,3	
PS96/073-2	2016-01-24	05:35:00	HS_PS	75° 45.61' S	032° 03.89' W	708,3	
PS96/073-2	2016-01-24	09:15:59	HS_PS	75° 37.16' S	031° 46.37' W	734,8	
PS96/073-3	2016-01-24	11:41:00	BT	75° 37.82' S	031° 49.79' W	736,3	
PS96/073-3	2016-01-24	12:11:00	BT	75° 38.83' S	031° 54.75' W	763,2	
PS96/074-1	2016-01-24	14:53:00	CTD/RO	75° 41.76' S	032° 23.14' W	715,8	
PS96/075-1	2016-01-24	16:58:00	CTD/RO	75° 36.90' S	032° 40.67' W	714,6	
PS96/076-1	2016-01-24	20:14:00	CTD/RO	75° 30.96' S	032° 59.74' W	685,5	
PS96/077-1	2016-01-24	22:35:00	CTD/RO	75° 29.89' S	032° 29.93' W	688,0	
PS96/078-1	2016-01-25	03:08:00	CTD/RO	75° 29.11' S	031° 54.22' W	755,5	
PS96/079-1	2016-01-25	06:05:00	HS_PS	75° 37.11' S	032° 12.37' W	736,1	
PS96/079-1	2016-01-25	07:38:59	HS_PS	75° 36.30' S	031° 43.53' W	721,9	
PS96/079-2	2016-01-25	08:18:00	CTD/RO	75° 37.50' S	031° 52.34' W	763,0	
PS96/079-3	2016-01-25	09:19:00	GC	75° 37.50' S	031° 52.33' W	763,1	

A.4 Stationsliste/Station List

Station	Date	Time	Gear Abbr.	PositionLat	PositionLon	Depth [m]	Comment
PS96/080-1	2016-01-25	10:30:00	GC	75° 41.34' S	031° 47.90' W	739,4	
PS96/081-1	2016-01-25	14:14:00	CTD/RO	75° 29.35' S	031° 31.51' W	687,5	
PS96/082-1	2016-01-25	19:48:00	CTD/RO	75° 30.03' S	030° 59.72' W	566,3	
PS96/083-1	2016-01-25	21:23:00	CTD/RO	75° 30.21' S	030° 29.46' W	449,2	
PS96/084-1	2016-01-25	23:00:00	CTD/RO	75° 29.95' S	029° 59.69' W	445,8	
PS96/085-1	2016-01-26	00:32:00	CTD/RO	75° 29.71' S	029° 31.91' W	437,8	
PS96/086-1	2016-01-26	02:44:00	TRAPST	75° 30.19' S	028° 56.74' W	422,7	fish trap recovered
PS96/086-2	2016-01-26	04:38:00	TRAPST	75° 30.10' S	028° 58.66' W	443,9	fish trap recovered
PS96/087-1	2016-01-27	09:05:00	LANDER	72° 47.89' S	019° 21.08' W	524,8	
PS96/088-1	2016-01-27	18:26:00	CTD/RO	72° 47.94' S	019° 21.45' W	521,6	
PS96/089-1	2016-01-28	14:01:00	HS_PS	72° 36.36' S	018° 04.03' W	312,4	
PS96/089-1	2016-01-28	19:35:59	HS_PS	72° 26.97' S	017° 10.26' W	278,1	
PS96/090-1	2016-01-28	21:39:00	AGT	72° 22.11' S	017° 18.61' W	1097,7	
PS96/090-1	2016-01-28	22:02:01	AGT	72° 22.15' S	017° 19.04' W	1092,2	
PS96/090-2	2016-01-28	22:59:00	HS_PS	72° 24.61' S	017° 19.56' W	517,2	
PS96/090-2	2016-01-29	00:23:59	HS_PS	72° 25.40' S	017° 03.79' W	295,4	
PS96/090-3	2016-01-29	00:49:00	CTD/RO	72° 26.01' S	017° 02.28' W	555,6	
PS96/090-4	2016-01-29	01:28:00	OFOS	72° 26.08' S	017° 02.09' W	282,3	
PS96/090-4	2016-01-29	03:43:00	OFOS	72° 26.65' S	017° 04.98' W	306,0	
PS96/090-5	2016-01-29	05:05:01	ROV	72° 26.14' S	017° 02.19' W	282,1	
PS96/090-5	2016-01-29	07:43:00	ROV	72° 26.20' S	017° 02.48' W	283,8	
PS96/090-6	2016-01-29	08:53:00	BWS	72° 26.18' S	017° 02.41' W	283,9	
PS96/090-7	2016-01-29	09:53:00	MG	72° 26.63' S	017° 05.00' W	306,0	
PS96/090-8	2016-01-29	10:41:00	GKG	72° 26.64' S	017° 04.99' W	306,6	
PS96/090-9	2016-01-29	12:34:00	MUC	72° 26.65' S	017° 04.96' W	306,7	
PS96/090-9	2016-01-29	12:35:00	MUC	72° 26.65' S	017° 04.96' W	306,6	
PS96/090-9	2016-01-29	12:42:00	MUC	72° 26.66' S	017° 04.92' W	306,6	
PS96/090-10	2016-01-29	13:35:00	GC	72° 26.64' S	017° 05.08' W	307,0	
PS96/090-11	2016-01-29	17:00:01	BT	72° 17.79' S	016° 50.83' W	878,3	
PS96/090-11	2016-01-29	17:30:01	BT	72° 19.24' S	016° 53.74' W	881,6	
PS96/090-12	2016-01-29	18:58:00	CTD/RO	72° 20.68' S	016° 56.27' W	870,7	
PS96/090-13	2016-01-29	21:07:00	ROV	72° 26.09' S	017° 02.16' W	271,7	
PS96/090-13	2016-01-29	23:37:00	ROV	72° 26.08' S	017° 02.14' W	281,7	
PS96/091-1	2016-01-30	01:29:00	CTD/RO	72° 23.95' S	016° 56.05' W	363,8	
PS96/092-1	2016-01-30	03:06:00	CTD/RO	72° 20.66' S	017° 03.86' W	1063,9	
PS96/093-1	2016-01-30	04:59:00	CTD/RO	72° 17.62' S	017° 12.39' W	1511,7	
PS96/094-1	2016-01-30	06:55:00	CTD/RO	72° 14.72' S	017° 21.09' W	1756,2	
PS96/095-1	2016-01-30	09:12:00	CTD/RO	72° 12.50' S	017° 26.77' W	1942,5	
PS96/096-1	2016-01-30	12:11:00	CTD/RO	72° 19.59' S	017° 46.91' W	1689,8	
PS96/097-1	2016-01-30	14:17:00	CTD/RO	72° 21.79' S	017° 40.18' W	1448,7	
PS96/098-1	2016-01-30	15:55:00	CTD/RO	72° 23.52' S	017° 34.69' W	1235,7	
PS96/099-1	2016-01-30	17:22:00	CTD/RO	72° 24.91' S	017° 30.02' W	752,0	
PS96/100-1	2016-01-30	18:15:00	CTD/RO	72° 26.04' S	017° 24.96' W	471,9	
PS96/101-1	2016-01-30	19:14:00	CTD/RO	72° 28.18' S	017° 19.95' W	272,1	
PS96/102-1	2016-01-30	21:10:00	CTD/RO	72° 33.57' S	017° 56.43' W	341,9	
PS96/103-1	2016-01-30	22:10:00	CTD/RO	72° 32.63' S	018° 00.38' W	593,6	
PS96/104-1	2016-01-30	23:29:00	CTD/RO	72° 36.39' S	018° 02.60' W	305,6	
PS96/104-2	2016-01-31	01:02:00	MUC	72° 36.33' S	018° 02.85' W	312,1	
PS96/104-3	2016-01-31	02:05:00	MUC	72° 36.33' S	018° 02.73' W	309,0	

Station	Date	Time	Gear Abbr.	PositionLat	PositionLon	Depth [m]	Comment
PS96/104-4	2016-01-31	02:41:00	GKG	72° 36.34' S	018° 02.75' W	308,8	
PS96/104-5	2016-01-31	03:41:00	MG	72° 36.34' S	018° 02.64' W	307,5	
PS96/104-6	2016-01-31	04:12:00	GC	72° 36.31' S	018° 02.71' W	309,1	
PS96/105-1	2016-01-31	05:46:00	CTD/RO	72° 31.91' S	018° 03.46' W	1186,1	
PS96/106-1	2016-01-31	07:23:00	CTD/RO	72° 36.52' S	017° 52.31' W	200,9	
PS96/106-2	2016-01-31	08:28:00	OFOS	72° 36.54' S	017° 52.51' W	200,4	
PS96/106-2	2016-01-31	09:30:00	OFOS	72° 36.51' S	017° 54.15' W	209,8	
PS96/106-3	2016-01-31	10:41:00	ROV	72° 36.52' S	017° 54.42' W	213,2	
PS96/106-3	2016-01-31	13:03:00	ROV	72° 36.51' S	017° 54.35' W	213,7	
PS96/106-4	2016-01-31	13:49:00	BWS	72° 36.50' S	017° 54.38' W	213,9	
PS96/106-5	2016-01-31	15:15:00	AGT	72° 35.29' S	018° 03.60' W	350,8	
PS96/106-5	2016-01-31	15:26:01	AGT	72° 35.37' S	018° 03.85' W	351,1	
PS96/106-6	2016-01-31	16:12:00	CTD/RO	72° 36.20' S	018° 04.25' W	332,4	
PS96/107-1	2016-01-31	17:37:00	CTD/RO	72° 31.70' S	018° 06.19' W	1598,7	
PS96/108-1	2016-01-31	21:00:00	CTD/RO	72° 31.18' S	018° 09.42' W	1917,3	
PS96/109-1	2016-01-31	22:50:00	CTD/RO	72° 30.66' S	018° 14.95' W	1945,9	
PS96/110-1	2016-02-01	00:49:00	CTD/RO	72° 30.02' S	018° 23.94' W	2285,4	
PS96/111-1	2016-02-06	19:42:00	CTD/RO	63° 41.64' S	050° 48.14' W	2588,0	AWI 207-8 not recovered
PS96/112-1	2016-02-07	00:01:00	CTD/RO	63° 39.63' S	051° 21.10' W	2195,0	
PS96/113-1	2016-02-07	02:58:00	CTD/RO	63° 33.25' S	051° 38.93' W	1723,7	
PS96/114-1	2016-02-07	06:03:00	CTD/RO	63° 28.65' S	052° 04.98' W	963,0	
PS96/114-2	2016-02-07	10:00:00	MOR	63° 28.95' S	052° 05.80' W	969,5	AWI 206-7 not recovered
PS96/115-1	2016-02-08	01:14:00	CTD/RO	63° 50.71' S	055° 31.16' W	397,3	
PS96/115-2	2016-02-08	02:03:00	MUC	63° 50.56' S	055° 31.72' W	400,1	
PS96/116-1	2016-02-08	03:22:00	HS_PS	63° 55.44' S	055° 24.74' W	337,7	
PS96/116-1	2016-02-08	14:25:59	HS_PS	63° 49.01' S	055° 30.13' W	383,8	
PS96/117-1	2016-02-08	21:39:00	HS_PS	63° 29.61' S	055° 18.33' W	211,1	
PS96/117-1	2016-02-09	06:13:59	HS_PS	63° 32.92' S	055° 22.99' W	583,3	
PS96/118-1	2016-02-10	11:07:00	MOR	61° 00.76' S	055° 58.81' W	285,8	AWI 251-1 recovered
PS96/118-2	2016-02-10	12:27:00	CTD/RO	61° 00.73' S	055° 58.68' W	313,3	

Die **Berichte zur Polar- und Meeresforschung** (ISSN 1866-3192) werden beginnend mit dem Band 569 (2008) als Open-Access-Publikation herausgegeben. Ein Verzeichnis aller Bände einschließlich der Druckausgaben (ISSN 1618-3193, Band 377-568, von 2000 bis 2008) sowie der früheren **Berichte zur Polarforschung** (ISSN 0176-5027, Band 1-376, von 1981 bis 2000) befindet sich im electronic Publication Information Center (**ePIC**) des Alfred-Wegener-Instituts, Helmholtz-Zentrum für Polar- und Meeresforschung (AWI); see <http://epic.awi.de>. Durch Auswahl "Reports on Polar- and Marine Research" (via "browse"/"type") wird eine Liste der Publikationen, sortiert nach Bandnummer, innerhalb der absteigenden chronologischen Reihenfolge der Jahrgänge mit Verweis auf das jeweilige pdf-Symbol zum Herunterladen angezeigt.

The **Reports on Polar and Marine Research** (ISSN 1866-3192) are available as open access publications since 2008. A table of all volumes including the printed issues (ISSN 1618-3193, Vol. 377-568, from 2000 until 2008), as well as the earlier **Reports on Polar Research** (ISSN 0176-5027, Vol. 1-376, from 1981 until 2000) is provided by the electronic Publication Information Center (**ePIC**) of the Alfred Wegener Institute, Helmholtz Centre for Polar and Marine Research (AWI); see URL <http://epic.awi.de>. To generate a list of all Reports, use the URL <http://epic.awi.de> and select "browse"/ "type" to browse "Reports on Polar and Marine Research". A chronological list in declining order will be presented, and pdf icons displayed for downloading.

Zuletzt erschienene Ausgaben:

Recently published issues:

700 (2016) The Expedition PS96 of the Research Vessel POLARSTERN to the southern Weddell Sea in 2015/2016, edited by Michael Schröder

699 (2016) Die Tagebücher Alfred Wegeners zur Danmark-Expedition 1906/08, herausgegeben von Reinhard A. Krause

698 (2016) The Expedition SO246 of the Research Vessel SONNE to the Chatham Rise in 2016, edited by Karsten Gohl and Reinhard Werner

697 (2016) Studies of Polygons in Siberia and Svalbard, edited by Lutz Schirrmeister, Liudmila Pestryakova, Andrea Schneider and Sebastian Wetterich

696 (2016) The Expedition PS88 of the Research Vessel POLARSTERN to the Atlantic Ocean in 2014, edited by Rainer Knust and Frank Niessen

695 (2016) The Expedition PS93.1 of the Research Vessel POLARSTERN to the Arctic Ocean in 2015, edited by Ruediger Stein

694 (2016) The Expedition PS92 of the Research Vessel POLARSTERN to the Arctic Ocean in 2015, edited by Ilka Peeken

693 (2015) The Expedition PS93.2 of the Research Vessel POLARSTERN to the Fram Strait in 2015, edited by Thomas Soltwedel

692 (2015) Antarctic Specific Features of the Greenhouse Effect: A Radiative Analysis Using Measurements and Models by Holger Schmidthüsen

691 (2015) Krill in the Arctic and the Atlantic Climatic Variability and Adaptive Capacity by Lara Kim Hünlerlage

690 (2015) High latitudes and high mountains: driver of or driven by global change? 26th Intern. Congress on Polar Research, 6 – 11 September 2015, Munich, Germany, German Society for Polar Research, edited by Eva-Maria Pfeiffer, Heidemarie Kassens, Christoph Mayer, Mirko Scheinert, Ralf Tiedemann and Members of the DGP Advisory Board



ALFRED-WEGENER-INSTITUT
HELMHOLTZ-ZENTRUM FÜR POLAR-
UND MEERESFORSCHUNG

BREMERHAVEN

Am Handelshafen 12
27570 Bremerhaven
Telefon 0471 4831-0
Telefax 0471 4831-1149
www.awi.de

